

AD-A262 581



1



AMPLIFICATION OF SHOCK OVERPRESSURE
BY REFLECTION WITHIN CONCAVE CORNERS

THESIS

John E. Loftis, Captain, USAF

AFIT/GNE/ENP/93M-4

DTIC
SELECTED
APR 05 1993
S B D

DISTRIBUTION STATEMENT A

Approved for public release;
Distribution Unlimited

DEPARTMENT OF THE AIR FORCE
AIR UNIVERSITY
AIR FORCE INSTITUTE OF TECHNOLOGY

Wright-Patterson Air Force Base, Ohio

20001013184

AFIT/GNE/ENP/93M-4

AMPLIFICATION OF SHOCK OVERPRESSURE
BY REFLECTION WITHIN CONCAVE CORNERS

THESIS

John E. Loftis, Captain, USAF

AFIT/GNE/ENP/93M-4

93-06901
 2058

Approved for public release; distribution unlimited

98 4 02 060

AFIT/GNE/ENP/93M-4

**AMPLIFICATION OF SHOCK OVERPRESSURE
BY REFLECTION WITHIN CONCAVE CORNERS**

THESIS

**Presented to the Faculty of the School of Engineering
of the Air Force Institute of Technology
Air University
In Partial Fulfillment of the
Requirements for the Degree of
Master of Science in Nuclear Engineering**

John E. Loftis, B. S.

Captain, USAF

March 1993

Accession For	
NTIS GRA&I	<input checked="checked" type="checkbox"/>
DTIC TAB	<input type="checkbox"/>
Unannounced	<input type="checkbox"/>
Justification	
By _____	
Distribution /	
Availability Codes	
Dist	Special
A-1	

Approved for public release; distribution unlimited

DTIC QUALITY INSPECTED 1

Preface

The purpose of this study was to evaluate the utility of an existing hydrodynamics code (CTH) in modeling the reflection of air shocks within concave corners of buildings, and to determine the degree to which the dimensions and vertex angle of V-shaped buildings affect the peak reflected overpressure at the vertex. The production code CTH, produced by Sandia National Laboratories, was identified as having the desired capabilities. It was obtained and installed on AFIT's SUN computer system. Installation to ensure both proper operation and export control was challenging, and familiarization with the use of the code came slowly despite the good documentation provided. After this phase, I developed models to simulate an air shock representative of one from a nuclear burst and then modeled its interaction with several buildings. I modeled twelve cases to make comparisons of buildings with various "V" depth or width, or vertex angles. The data also provided information that will be useful in any more-detailed modeling that may be considered in the future.

I am deeply indebted to many others for their assistance during this effort. First, I am indebted to my faculty advisor, Dr Kirk Mathews, for his assistance and keen knowledge, and interest in this problem. I also thank Lt Col Mark Byers of the Defense Nuclear Agency for

sponsoring this project and serving on my thesis committee. I am also indebted to Dr Gene Hertel of Sandia National Laboratories, who provided the code, and much assistance with using it. The AFIT computer system administrator, Tony Schooler, also deserves credit for his valuable assistance and responsiveness to my needs. Finally, I thank my wife, Mary, for her support and understanding, and my children for their patience during my work on this project.

John E. Loftis

Table of Contents

	Page
Preface	ii
List of Figures	vi
Abstract	viii
I. Introduction	1
Background	1
Problem	2
Scope	2
Approach and Presentation	4
II. Theoretical Development	7
The Blast Wave	7
Fluid Dynamics	9
Numerical Methods	11
The Ideal Shock Front	12
III. Computational Code	16
CTH Hydrodynamics Code System	16
System Application	19
IV. Shock Front Generation	20
Geometry	20
Physical Dimensions and Mesh	21
Other Problem Definition Requirements	24
Wave Initiation	25
V. Buildings	29

	Page
VI. Results and Discussion	34
Shock Wave Generation	34
Interaction with Buildings	40
VII. Conclusions and Recommendations	49
The CTH Code	49
Shock Amplification	49
Future Studies	50
Bibliography	53
Appendix A: Input Data Files	54
Appendix B: Output Data Plots	82
Vita	193

List of Figures

Figure	Page
1. Illustration of Building Orientation	6
2. Merging of Incident and Reflected Waves to Form Mach Stem . .	7
3. Variation of Overpressure with Time as an Ideal Shock Front Passes a Fixed Point	12
4. Problem Dimensions in the Vicinity of a Building	22
5. Initial Problem Area Setup	23
6. Pressure Plot of Near-Ideal Shock Wave Generated	27
7. Diagram of Building Set at Coordinate Point Twelve	31
8. Tracer Positions and Wall Placement Near the Vertex	32
9. Time History of Free-Field Shock Front Passing the Point Eighty Meters to the Left of the Vertex	34
10. Rate of Decay of Overpressure with Time for Several Values of the Peak Overpressure	36
11. Peak Overpressures on the Ground for 1-kiloton Burst	37
12. Positive Phase Duration on the Ground of Overpressure and (Dynamic Pressure) for 1-kiloton Burst	39
13. Time History of Pressure Three Meters from Vertex of Building Twelve	43
14. Shock Wave Flowing into Building Twelve (Time = 0.15 sec) . . .	45
15. Shock Wave Flowing into Building Twelve (Time = 0.175 sec) . . .	46

Page

16. Shock Wave Flowing into Building Twelve (Time = 0.2 sec) 47

17. Shock Wave Flowing into Building Twelve (Time = 0.225 sec) . . . 48

Abstract

In this study, CTH, a production hydrodynamics code developed and provided by Sandia National Laboratories, modeled the interaction of a shock wave with tall V-shaped buildings with various wall lengths and vertex angles. The purpose of this study was to determine the degree to which the length and vertex angle affect the peak overpressure at the vertex. CTH performed two-dimensional Eulerian-Lagrangian computations to obtain solutions of this problem. The models were cast in two-dimensional rectangular geometry on a horizontal plane because of the computational costs of three-dimensional calculations. This geometry simulates tall buildings exposed to a tall Mach stem blast.

The free-field shock increased sharply to a peak overpressure of 6.2 psi and returned to ambient conditions after about one second. This incident shock amplified significantly in the building vertices. Peak overpressures measured as high as 8.7 times the incident free-field overpressure of 6.2 psi, or 3.9 times the peak reflected overpressure of 14 psi due to reflection at normal incidence. The amplification was greatest with narrow vertex angles, but was significant (2.7 times that at normal incidence) even with right-angle vertices. The amplification of the peak overpressure due to reflection within concave corners is important

in determining the vulnerability of structures to blast damage. This is particularly important because many buildings and other structures are constructed with square concave corners.

THE AMPLIFICATION OF SHOCK OVERPRESSURE BY REFLECTION WITHIN CONCAVE CORNERS

I. *Introduction*

Background

Shock overpressure amplifies when a shock wave reflects from a rigid boundary. At normal incidence, the shock stagnates and dynamic pressure converts to static overpressure as kinetic energy converts to internal energy. Far from normal incidence, complex flow patterns develop, resulting in less pressure against the reflecting surface. In an interior (concave) corner, however, the flow converges into the corner, then stagnates. This focuses the energy near the corner, with the possibility of very large stagnation pressure. Interior corners are likely to be weak points in many structures. With focussing, this could result in mechanical failure even if the free-field overpressure of the shock is below the threshold for failure under normal incidence.

Survivability tests of structures are usually conducted with the structure placed face on to the blast wave (normal incidence), since this is worst-case with respect to loading of the front face. However, other

orientations may be more limiting due to the focussing described above. Unfortunately, there has been no systematic investigation or modeling of the effect of different orientations. We need to investigate this effect and look for empirical fits that could aid in estimating the vulnerability of structures.

Problem

The objective of this research is to obtain an existing hydrodynamics code package and determine its utility for modeling the reflection of air blast waves within concave corners. The code will be used to examine the reflection of an air shock into several different interior corners, varying the angle of the corner, or vertex, and the "V" depth and width.

Scope

Computational Code. The identification of an existing code involved making inquiries with several contacts in the field. The CTH code, developed by Sandia National Laboratories, was selected for examination and use in this study. CTH is a hydrodynamics code that performs a variety of Lagrangian-Eulerian computations for various types of material and energy flow problems. The code handles a wide array of dimensions up to three-dimensional rectangular grids. This effort involved identifying the requirements and limitations of using this code with the SUN system for modelling the air blast effect on inside corners.

Air Blast Wave. The type of blast wave of interest is one similar to that expected in the Mach reflection region at some distance from a nuclear air burst. This may be approximated by a planar shock front of modest overpressure, and a positive phase duration measured in seconds. The overpressure should not change appreciably over the range of the building dimensions.

Buildings. The Models examined several buildings for comparison of the effect of varying the vertex angle and the "V" width and depth. The assumption of perfectly smooth, rigid walls simplified the modeling and analysis. I modeled buildings as solid steel blocks with smooth walls. The choice of solid steel ensures rigidity, and provides high inertia to prevent bulk building motion over the time required for the completion of the interesting phase of the shock interaction. Since the problems were cast in two dimensions, they modeled buildings that are tall compared to their length and width.

Mesh and Dimensions. The computations in this study used the highest spacial dimension and finest mesh possible, given the limitations of the code, and the speed and storage capacity of the computer system. Two-dimensional rectangular geometry and a mesh of 2-meter square cells resulted in acceptable computational costs. The computations were performed using the finite-difference analogs of the Lagrangian mass, momentum, and energy conservation equations with rezoning after each

time step to construct Eulerian differencing. Eulerian differencing results in a fixed mesh in space, which material flows through. This is the desired result, because of the fixed mesh, but is difficult or impossible to obtain directly. CTH applies the simpler Lagrangian equations, which maintain the same material in a cell, with the cell walls moving with the material, and reconstructs the mesh after completing the computations for all the cells for each time step.

Approach and Presentation

Theory. This study is based on the theory of fluid dynamics. A variety of phenomena (blast effects, sound propagation, flow simulation, etc.) are described by this broad field, but this study is focussed on the development of propagation of a shock wave, and its reflection at rigid boundaries. Section II presents the theory applied to this problem.

Code Selection. The CTH code was identified as a very likely candidate to be fully capable of the desired computations, and was installed on the SUN system at AFIT for use in this study. This phase was time consuming and involved not only the proper installation, but also learning to use the program. This step involved both learning the capabilities of the code, and how to invoke these capabilities by the proper selection and use of options in the creation of input files. The study of several example models provided with the package, and the

development and use of several original trial models served to examine the capabilities, requirements, and limitations of both the code and the computer system. This phase overlapped with the next step of attempting to generate a representative shock wave. Section III provides a description of the CTH code.

Shock Front Generation. Several attempts were made to generate the desired shock front. This was largely a trial-and-error process because of the many parameters of the problem that impact on computational time, storage requirements and accuracy of results. These parameters include default values employed by the code for various physical quantities, mesh size and problem area, treatment of boundary conditions, and the physical behavior of the shock wave itself. The shock wave developed had a peak (free field) overpressure of 6.2 pounds per square inch over the region where it interacted with the various structures, and had a positive phase duration of 0.89 seconds. Section IV presents the details of the generation of, and the physical characteristics of the free-field shock.

Interaction With Buildings. The shock front interacted separately with several building arrangements. The buildings were oriented as illustrated in Figure 1. The upper part of the building reflected about a symmetry boundary along the bisector ("x" axis) produced the "V." The shock front for each case was oriented parallel to the vertex bisector, and

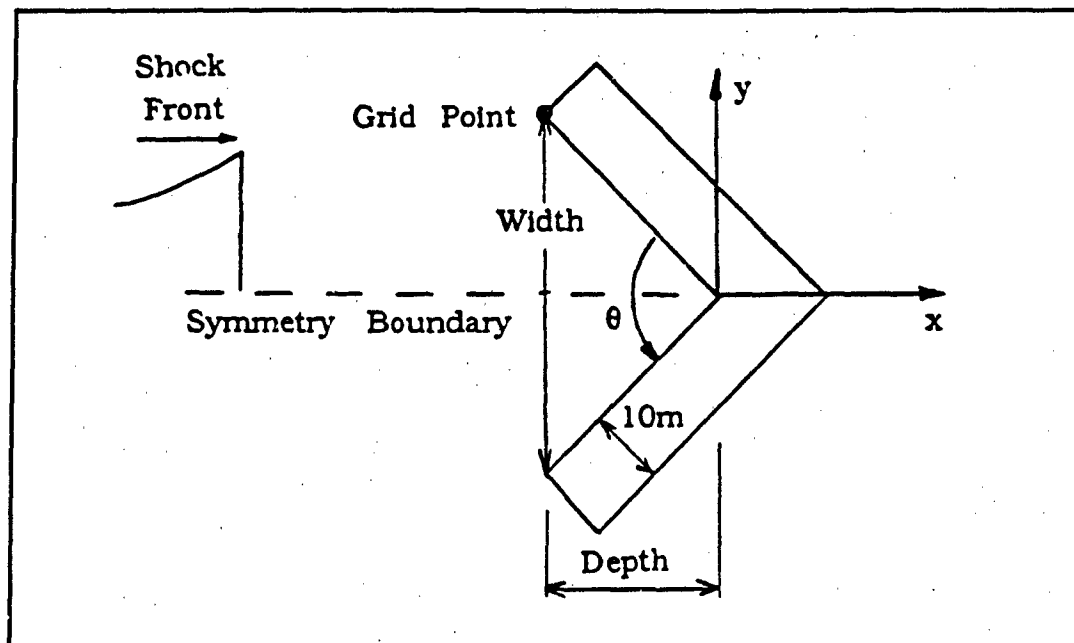


Figure 1. Illustration of Building Orientation

started at the same point relative to the vertex of each building. The models investigated twelve test cases with various values for the width, depth, and vertex angle, as described in Section V. Section V also gives details of the CTH modeling steps required. The results and data evaluation are presented in Section VI, and conclusions and recommendations are given in Section VII. The input data files for the execution of the models and for the creation of plots are presented in Appendix A. The resulting plots are presented in Appendix B.

II. Theoretical Development

The Blast Wave

The air blast wave generated following a nuclear explosion produces most of the structural damage caused to buildings by a nuclear burst at or near the ground. The rapid expansion of intensely hot gasses at extremely high pressures in the fireball shortly after the explosion drives the formation of the air blast or shock wave. An air blast with peak overpressures of only one-half pound per square inch will cause damage to many structures (4:80). The goal of this study is to model the reflection of such a shock wave within concave corners of buildings, and to quantify the effect of the focussing on the peak reflected overpressure experienced in the corner.

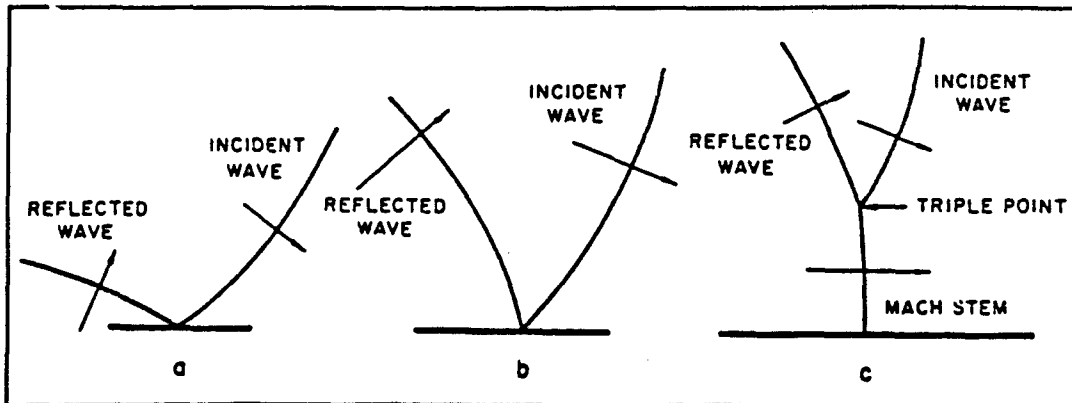


Figure 2. Merging of Incident and Reflected Waves to Form Mach Stem (4:89)

In air bursts, the shock wave reflects off the ground. The reflected wave travels in air heated by the passage of the initial shock front, and thus moves faster than the initial wave front. The reflected wave overtakes and merges with the initial wave near the surface producing the Mach region or Mach stem. Figure 2 shows the merging of the two waves (4:87-89). This Mach stem portion of the advancing shock front may be approximated by a planar wave at distances where the dimensions of the building with which the wave is interacting are small compared to the range from the burst point. The spherical nature of the advancing front becomes approximately cylindrical in the Mach stem region, and then becomes nearly planar over relatively small regions of interest at long ranges.

A blast wave with characteristics typical of those in a blast formed by a nuclear burst is desired for investigation in this study. The positive phase of the blast wave from a 20-kiloton air burst, for example, lasts roughly 1.0 second to 1.4 seconds at slant ranges of one to two miles. The arrival time for the shock front at one mile from a 20-kiloton detonation is about three seconds (4:83). These characteristics are compared to those of the wave modeled by the CTH code described in the following section. This study uses CTH to apply the theory of fluid dynamics, or hydrodynamics, to model the behavior of the advancing shock front, and its interaction with various buildings.

Fluid Dynamics

The study of fluid dynamics is based on the conservation of mass, momentum, and energy. These three relationships, in their generalized three-dimensional Eulerian forms, are

$$\begin{aligned}\frac{\partial \rho}{\partial t} + (\vec{u} \cdot \nabla) \rho + \rho \nabla \cdot \vec{u} &= 0 \\ \frac{\partial \vec{u}}{\partial t} + (\vec{u} \cdot \nabla) \vec{u} + \frac{1}{\rho} \nabla p &= 0 \\ \frac{\partial E}{\partial t} + (\vec{u} \cdot \nabla) E + \frac{1}{\rho} \nabla \cdot (p \vec{u}) &= 0\end{aligned}\tag{1}$$

where ρ is density, u is particle velocity, p is pressure, and E is total energy per unit mass. The ∇ operator represents the spatial derivatives and the "t" represents time. Thus there are three equations for the four unknown functions ρ , u , p , and E . The total energy, E , may be separated into internal and kinetic energy components and expressed as

$$E = I + \frac{1}{2} \vec{u} \cdot \vec{u}\tag{2}$$

giving a total of four equations in five unknowns. The above Eulerian equations describe the behavior of the material at a fixed point, or from the viewpoint of flux at a point.

The final equation needed, the equation of state, describes the properties of the material. Several simplified equations of state are

available for specific materials, but the Grüneisen equation of state is one with general application to several materials, and describes the properties of many gasses and metals. The Grüneisen equation of state is written

$$p = p_H + \frac{\gamma_s}{V} (I - I_H) \quad (3)$$

where

$$p_H = \frac{c_0^2 (V_0 - V)}{[V_0 - s(V_0 - V)]^2}$$

$$I_H = \frac{1}{2} \left[\frac{c_0 (V_0 - V)}{V_0 - s(V_0 - V)} \right]^2$$

$$s = \frac{\gamma_s + 1}{2}$$

$$V = 1/\rho$$

The three basic parameters of this equation of state are ρ_0 , the ambient density of the material, c_0 , the speed of sound in the unshocked (ambient) material, and γ_s , the Grüneisen ratio. The Grüneisen ratio lies between 1.0 and 2.0 for most metals, but is less than 1.0 for a few. In the polytropic gas equation of state, $\gamma_s = \gamma - 1$ where γ is the ratio of the specific heats of the material, and $\gamma = 1.4$ for air. The above system of five equations in five unknown functions can be solved, but in practice,

the solutions of these Eulerian conservation equations can be very difficult to obtain.

To reduce the difficulty of solution, the three conservation equations may be manipulated, by applying the Lagrangian time derivatives, into equivalent expressions that describe the rate of change along the general three dimensional motion of the fluid instead of at a fixed point, as with the Eulerian forms. The generalized Lagrangian forms of the three conservation equations may be written (5:2-8)

$$\begin{aligned}\frac{d\rho}{dt} + \rho \nabla \cdot \vec{u} &= 0 \\ \frac{d\vec{u}}{dt} + \frac{1}{\rho} \nabla p &= 0 \\ \frac{dE}{dt} + \frac{1}{\rho} \nabla \cdot (p\vec{u}) &= 0\end{aligned}\tag{4}$$

The solutions of these equations and the equation of state are more easily obtained.

Numerical Methods

Since the time and space derivatives cannot be calculated precisely, they must be approximated by finite differences. This requires that the smallest possible time and space steps be taken to enhance accuracy. The smaller the steps, the more calculations that have to be solved. This is possible with the speed of computers, but is not without limitation.

Time and space step sizes present a trade-off of accuracy with the limitations of real computational time and storage space in memory and on disk in the computer. Numerical methods involve other issues such as numerical instabilities and evaluation of the accuracy of results; both are influenced by the magnitude of the time and space steps. There is an extensive literature on this topic; I found the exposition by Harlow and Amsden (5:81-103) to be particularly useful, since they specifically address the fluid dynamics computations.

The Ideal Shock Front

The overpressure of an ideal shock front rises sharply to a peak, decays gradually to zero, and then undergoes a relatively small drop below zero, before settling back to ambient pressure (see Figure 3).

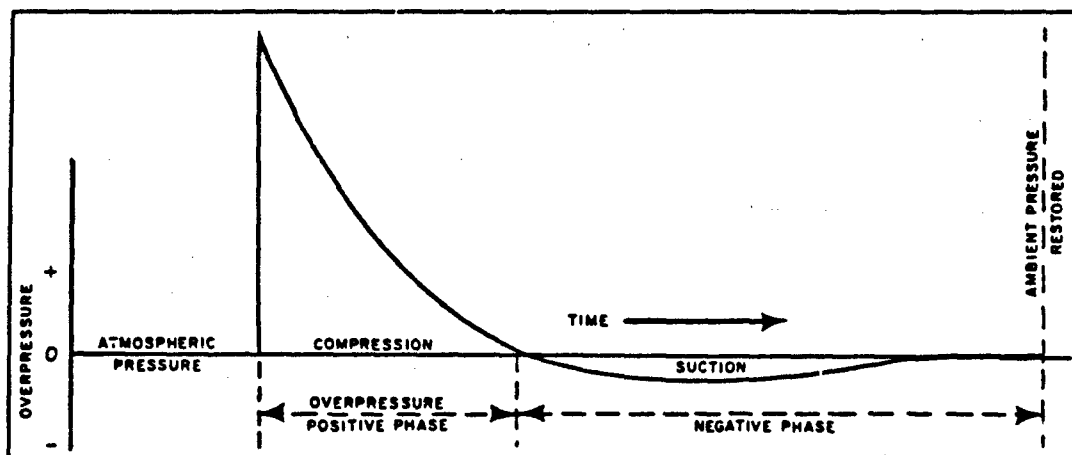


Figure 3. Variation of Overpressure with Time as an Ideal Shock Front Passes a Fixed Point (4:84)

The Rankine-Hugoniot conditions, also based on the conservation of mass, momentum, and energy, provide the relationships among the thermodynamic properties of an ideal shock front. These conditions with the equation of state for air, permit the derivation of the relations involving the shock velocity, the overpressure, the dynamic pressure, and the density of the air at the ideal shock front. These relations provide useful approximations for comparison of results obtained by numerical methods, as shown on page 40.

The following equations are applicable within the Mach reflection region (below the triple point) of a reflected shock front or for a surface burst where there is only one shock front. The shock velocity, U , is expressed by

$$U = c_0 \left(1 + \frac{\gamma + 1}{2\gamma} \cdot \frac{p}{P_0} \right)^{1/2} \quad (5)$$

where c_0 is the speed of sound in ambient air, p is the peak overpressure, P_0 is ambient pressure, and γ is the ratio of the specific heats (c_p / c_v) of the air. For air at moderate temperatures, $\gamma = 1.4$. Applying this value for γ , Eq (5) simplifies to

$$U = c_0 \left(1 + \frac{6p}{7P_0} \right)^{1/2} \quad (6)$$

Again, for air at moderate temperature, the particle velocity, or peak wind velocity, u , behind the shock front is given by

$$u = \frac{5p}{7P_0} \cdot \frac{c_0}{(1+6p/7P_0)^{1/2}} \quad (7)$$

The density, ρ , of the air behind the shock front is related to the ambient density, ρ_0 , by

$$\frac{\rho}{\rho_0} = \frac{2\gamma P_0 + (\gamma+1)p}{2\gamma P_0 + (\gamma-1)p} = \frac{7+6p/P_0}{7+p/P_0} \quad (8)$$

With the last two equations, the kinetic energy per unit volume of the air immediately behind the shock front, i.e., the dynamic pressure, q , is defined by

$$q = \frac{\rho u^2}{2} = \frac{5}{2} \cdot \frac{p^2}{7P_0 + p} \quad (9)$$

When a blast wave strikes a flat surface at normal incidence, the peak value of the reflected overpressure, p_r , is given for air at moderate temperature by

$$p_r = 2p + (\gamma+1)q = 2p \frac{7P_0 + 4p}{7P_0 + p} \quad (10)$$

which shows that the value of the reflected overpressure approaches

eight times incident for very large incident overpressure, and twice incident for small incident overpressure. Shock fronts of the strength of interest in this study should produce reflected overpressures of just over twice incident when reflecting off a flat wall at normal incidence. The expected amplification effect of reflection of a shock into corners is not predicted by these equations.

Another important blast damage parameter is impulse, which is the positive overpressure integrated over the positive phase duration time (t_p^+). The positive phase overpressure impulse (per unit area), I_p^+ , is represented mathematically by (4:96-99)

$$I_p^+ = \int_0^{t_p^+} p(t) dt \quad (11)$$

This study did not evaluate impulse because of computational constraints on problem dimensions and problem run times, which prevented the collection of sufficient data to measure the impulse. The computation of impulse requires data for the entire positive phase. The incident shock front has a positive phase duration of 0.89 seconds, but the large computational time and required storage space limited simulation times to only 0.5 seconds after the shock arrival. The models terminated before the entire positive phase duration was over.

III. Computational Code

CTH Hydrodynamics Code System

CTH is a software system designed to treat a wide range of shock propagation and material motion phenomena in one, two, or three dimensions, and has models suited for most conditions encountered in shock physics. Models provide capability for computations of material strength, fracture, distended materials, high explosives, and a variety of boundary conditions. The material equation of state (EOS) models allow description of most states of matter normally encountered in shock physics. CTH provides two EOS packages, an analytic EOS package, and a newer package that offers vectorized Sesame tabular EOS.

The program employs the finite-difference analogs of the Lagrangian conservation equations and rezones to the original mesh to produce an equivalent to Eulerian differencing. As discussed in the previous section, we desire a fixed mesh, but the Eulerian conservation equations are too difficult to use. The simpler Lagrangian forms provide results that include the movement of mesh cell boundaries with the material, causing a distortion of the original mesh. After each time step, CTH rezones the new conditions to the original mesh boundaries. The CTH system is available for a variety of computer systems, including CRAY

UNICOS, CRAY CTSS, SUN OS4, and VAX VMS systems. CTH has been under continuing development by Sandia National Laboratories and is still evolving rapidly.

The system has two primary processing programs, CTHGEN and CTH. CTHGEN sets up the problem definition. This includes definition of the initial parameters that describe the problem, namely geometry, mesh size, number of cells, active cells, material insertion, tracers, and equation of state. CTH integrates the problem through time to a predetermined completion time, writing parameter values to storage files at specified time intervals. CTH also handles the definition of boundary conditions. These two programs together take the problem from initial definition through completion, and handle the creation of all necessary output data files for later use with post-processors.

CTH stores computed data in two types of files. CTH keeps a complete set of values for all parameters for every computational cell in the problem at user-determined time intervals. These files are referred to as dump files. They are snapshots of the problem data in time and are very large (tens of megabytes or more, depending on the number of computational cells), and thus are kept infrequently. CTH also keeps much smaller history files of selected data at specific points in the problem area. These are also kept at user-determined time intervals, and because of their small size, can be kept at more frequent intervals.

Appendix A gives examples of the input files used by these programs for the modeling done in this study.

The CTH system includes powerful post-processing programs. Two graphics post-processors provide for a variety of one, two, and three-dimensional black and white or color spatial plots, and time history plots of thermo-mechanical data at "Eulerian tracer points" (fixed in spatial location) and "Lagrangian tracer points" (moves with the material). The graphics post-processor, CTHPLT, provides spatial data display in several one, two, and three-dimensional formats. CTHPLT produces black and white or color shaded band, dot density, and contour plots of up to 50 variables. CTHPLT uses the large data files to produce these plots. The post-processor, HISPLT, produces history plots of up to 50 point variables for up to 100 points, 12 material variables for up to 20 materials, and 14 global variables. HISPLT uses the data stored in the smaller history files to create the time-history plots.

Another valuable post-processor is CTHREZ, which allows for manual rezoning and/or problem modification. CTHREZ uses data available for any user-determined time at which data were dumped to the dump file. CTHREZ allows information in the CTHGEN input deck to be altered, and allows the problem to be restarted from any point in time at which data were kept in the data dump file. The CTH processing program can be manually terminated at any time step, and a data dump

at that time is appended to the dump file. CTHREZ can thus be used to rezone or make input parameter modifications at any time step of the simulation (2:1, 10-11;3:1-1;6:1, 9;7:1). Appendix A contains the plotting input files used in this study, and Appendix B gives examples of the plots produced by the plotting programs.

System Application

The CTH system was used to simulate the interaction of shock waves in air with V-shaped buildings with various sizes and vertex angles. CTHGEN set up a two-dimensional rectangular coordinate system, which included a region of compressed air and a region of ambient air. The compressed air was released from a rectangular area at the left end of the problem domain. The problem domain was bound by a transmitting boundary on the right side, and by symmetry boundaries on the remaining three sides. CTH modeled the release and hydrodynamic flow of the compressed air into the ambient air until the desired shock front developed. CTHREZ allowed the repeated use of this shock front for modeling the interaction with the various buildings, without requiring the regeneration of the front each time, thus saving time. The graphics post-processors, CTHPLT, and HISPLT, plotted the pressure, density, and temperature of the air in the region around the buildings, and at Eulerian tracer points near the vertex.

IV. Shock Front Generation

The development of a shock front similar to that experienced at long range after a nuclear burst proceeded by trial-and-error, with respect to the initial conditions needed to produce the desired shock. The idea was to release a region of compressed air into a region of ambient air, and let the computation proceed until the shock wave formed, much like what happens when the hot gasses of a fireball expand and develop a shock front. The initial parameters addressed were geometry, physical problem dimensions, mesh size, number of cells, initial pressure in compressed region, size of the compressed region, active cells, material insertion, tracers, equation of state, and boundary conditions. These will be discussed in turn.

Geometry

Options for the geometry were limited. Although CTH can process problems in many geometries, in up to three dimensions, some geometries were simply not applicable to this problem. For example, one-dimensional cylindrical geometry (1DC) could model the expanding Mach stem, but building layout would be impossible. The building layout is best done in two-dimensional rectangular geometry (2DR). The rezone capability of CTH does not allow for rezone of 1DC to 2DR, so the

initial air shock must be created in 2DR geometry also. Since the shock front in this geometry will be planar, it will vary only in one dimension, thus, the same result is then obtained for the developing shock front in one-dimensional rectangular (1DR) or 2DR geometries. The second dimension is needed only for the region where the shock interacts with the buildings. Although CTH would not rezone from 1DR to 2DR, the desired shock front characteristics were developed in 1DR. Once the required initial conditions, run time, and data recording frequency, etc. were established the problem was recast in 2DR geometry. Since the length along the direction of the shock front was 120 meters or 60 cells, this reduced the computational time for determining the necessary conditions and producing the desired shock by about a factor of 60.

Physical Dimensions and Mesh

The distance required for the advancing wave to develop into a near-ideal shock front and the size of the widest building modeled determine the problem dimensions for this shock-generation phase. The distance in the direction of the shock propagation ("x" direction) is set by the time required for the shock front to form and its speed during the formation process. The distance in the perpendicular direction ("y" direction) is driven by the maximum building "V" width to be modeled. The dimensions changed as trials were run and requirements developed. The

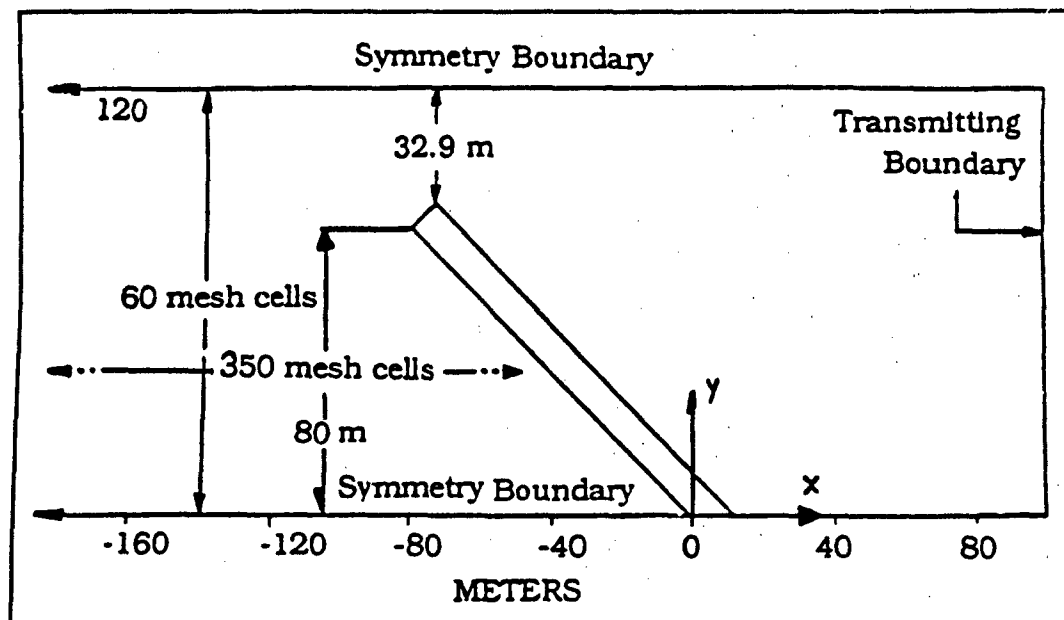


Figure 4. Problem Dimensions in the Vicinity of a Building

shock front required nearly 1700 meters to develop, and the largest building "V" half-width was 80 meters, as shown in Figure 4.

The modeling required additional space in both directions for other reasons. Additional space in the "y" direction above the widest point of the building allowed for the wave to flow around the end of the building without reflecting from the boundary and affecting the peak reflected overpressure in the corner. The 400-meter depth of the shock, and space for it to pass beyond the building required additional space in the "x" direction. Figure 4 shows the end gap of 32.9 meters for the largest building. It is greater for the others. The final dimensions for the 2DR model were 1900 meters in the "x" and 120 meters in the "y" directions.

In CTH, the mesh is limited to 1000 cells in each of the first two dimensions, and 500 in the third. So this determines the minimum cell size, once the problem dimensions are established. The final 1DR problem dimension was 2,000 meters which gave 1,000 2-meter cells in one dimension. The dimension along the "x" direction has the largest minimum cell size of 1.9 meters. Although not required, it is desired to have the cells as nearly square as possible to minimize computational instabilities, and to improve accuracy. For the purpose of using convenient numbers and to keep the original cell size of the 1DR model for comparison, the cell size is thus set at 2.0 meters square, giving a mesh of 950 cells in the "x" direction, and 60 cells in the "y" direction, as shown in Figure 5. This mesh will move with the material in each cell

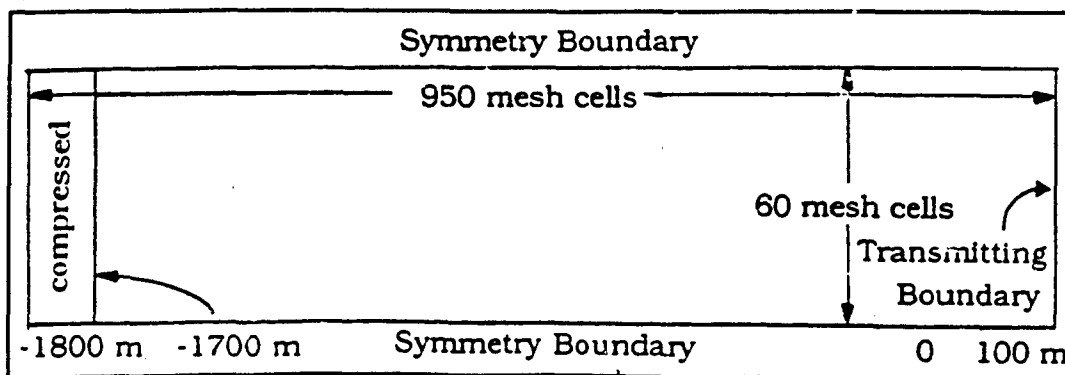


Figure 5. Initial Problem Area Setup

during each Lagrangian time step, and will then be rezoned to its original configuration before the next time step to maintain an Eulerian mesh, as discussed in Section III.

Other Problem Definition Requirements

The remaining requirements to fully define the problem for modeling are the assignment of active cells, insertion of materials and tracers, selection of an equation of state package, and the selection of boundary conditions. The definition of an active cell region allows the computation to proceed more quickly by eliminating calculations for cells that have no material velocity. As cells become influenced and are needed in the calculations, they are included. The active cell region for the shock wave generation was initially only the compressed region. As the shock wave moved away from the starting point, more of the mesh became active and each computational cycle (time step) took longer. Material insertion is used to define the material type and its physical parameters at the initial starting time. These include the dimensions of each block of material and the physical properties such as temperature, pressure, and density. Tracers are inserted as either Eulerian (fixed) points or as Lagrangian points, which flow as a particle with the material. Data for temperature, pressure, and up to 70 other variables (see Section III) are tracked in time through the progress of the calculations providing time histories at the defined points. The SESAME table equation of state package was used in the models run in this study. Boundary conditions are shown in Figure 5 on page 23. The modeling required that the left (x_{\min}) top (y_{\max}) and bottom (y_{\min})

boundaries be symmetry boundaries, and that the right (x_{\max}) boundary be a sound speed-based absorbing or transmitting boundary which allows material to flow into and out of the mesh. The initial pressurized region of air is against the left boundary, and the generated wave propagates toward the right.

Wave Initiation

Several combinations of initial pressure and size of the pressurized region produced shock fronts with shapes similar to the ideal shock front shape described in Section II, and shown in Figure 3 on page 12. The initial trials produced shocks that were shaped correctly, but had pressure, temperature, or density values that did not approximate those expected from the formation of a blast wave by a nuclear explosion. Another problem was very short duration of the positive phase of the shocks. Shock fronts formed quickly when high initial pressures and small compressed regions were used to initiate the waves, but the shocks exhibited the problems cited above. None of the shocks generated precisely matched the ideal front; they all lacked the smooth drop below and subsequent return to ambient pressure. Most had good shape at the front, but did not drop back to ambient. The generated shock fronts approached the desired characteristics as the initial pressure was reduced and the depth of the pressurized region was increased.

The initial condition of 10 centimeters (cm) of compressed air at 100 atmospheres (atm) produced a shock front of peak overpressure of 72 pounds per square inch (psi), with about 0.005 seconds positive phase duration after (coincidentally) 0.005 seconds of flow simulation, and did not return to ambient pressure behind the front. Starting with 10 cm at

Table 1. Comparison of Shock Fronts Generated by Releasing Various Pressurized Regions.

<i>Initial Compression</i>		<i>Developed Shock Front</i>	
<i>Pressure</i>	<i>Depth</i>	<i>Peak Overpressure</i>	<i>Positive Phase Duration</i>
100 atm	10 cm	72 psi	0.005 s
50 atm	10 cm	29 psi	0.006 s
2 atm	100 m	6 psi	1 s

50 atm increased the duration to about 0.006 seconds, reduced the peak overpressure to about 29 psi, with only slightly closer return to ambient conditions, after 0.007 seconds of flow simulation. The shock fronts developed quickly in both these cases. Releasing 100 meters of air compressed to only two atmospheres generated the shock front used for modeling with the buildings. As shown in Table 1, the shock wave has a positive phase duration of nearly one second and a peak overpressure of 0.43 atm or 6.3 psi, after 2.5 seconds of flow simulation. This shock

front was at 1580 meters from the original leading edge position when it became fully developed into a near-ideal shock front.

The characteristics of this shock front closely resemble those expected from a 20 kiloton nuclear burst at about one mile range, as presented in Section II. The shock front traveled 1580 meters or 0.98 miles in 2.5 seconds, and the arrival time for the shock front at one mile from a 20-kiloton nuclear burst is about three seconds. The positive phase duration is consistent with that of the blast wave from a 20 kiloton air burst, which lasts roughly one second at a slant range of one mile. The shock front is described here as near ideal because, although it has a sharp increase to peak overpressure followed by a gradual return to ambient pressure, the pressure did not smoothly dip below and

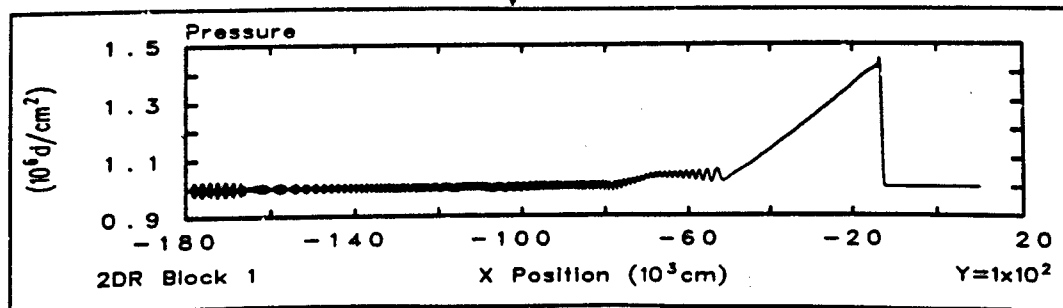


Figure 6. Pressure Plot of Near-Ideal Shock Wave Generated

then settle to ambient conditions. Instead, it oscillated above and below ambient with high frequency and decreasing magnitude, as shown in Figure 6. This deviation was accepted since the primary interest is in the propagation and eventual reflection of the shock front into the

building corners, and not the entire history of the passage of the shock wave. The input file for the generation of the shock wave is presented in Appendix A, on page 55.

V. Buildings

The advancing shock front is parallel to the "y" axis and propagates in the positive "x" direction from the left. The modeling invoked CTHREZ to rezone a portion of the fully developed shock wave and combine it with each individual steel building. The modeling used 500 meters of the developed shock wave at the time step at 2.5 seconds. The section between -600 and -100 meters, as shown in Figure 6 on page 27, includes essentially all the 400-meter thick positive phase of the wave. Using the smallest portion possible cuts down the computer resources and the computation time required. The shock wave generation and interaction phases of the modeling share a common coordinate system and origin, which simplifies the rezoning process. The rezoned problem region lies between the values -600 and 100 meters in the "x" direction, and between zero and 120 meters in the "y" direction.

Material insertion provides for the addition of the building material. The first step in the addition of buildings is the insertion of a rectangular piece of steel ten meters wide and of the appropriate length, oriented lengthwise in the "y" direction with the left edge along the "y" axis. Rotation of this piece about the origin to the desired coordinate point results in the desired orientation, and the symmetry boundary along the

"x" axis produces the effect of a "V," as described below. The building walls are solid steel and are ten meters thick to provide a smooth, flat, rigid wall with high inertia to prevent or reduce movement when hit by the advancing shock front.

Each building vertex is at the origin of the rectangular coordinate system, with the "V" opening toward the negative "x" direction. The placement of the inside end corner at one of twelve coordinate points fixes the size and vertex angle of a building. The twelve points chosen allow comparisons of data from buildings with the same "V" width or depth, or vertex angle. The points are at 20, 40, and 80 meters in the "y" direction, and 0, 20, 40, and 80 meters in the negative "x" direction, indexed 1 to 12, as shown in Figure 7. This arrangement and a symmetry boundary along the "x" axis model the V-shaped buildings oriented with the "V" opening to the left, and straight buildings with their left sides along the "y" axis. The "x" axis is the building vertex bisector. Several input files (see page 55) provide the information required by CTHREZ to set up the various buildings.

For example, Figure 7 shows the building with its inside end corner at coordinate point twelve (-80,80). The length required for this case is 113.14 meters (the distance from the origin to point twelve). CTHREZ inserts the steel piece by defining the position of the lower left corner

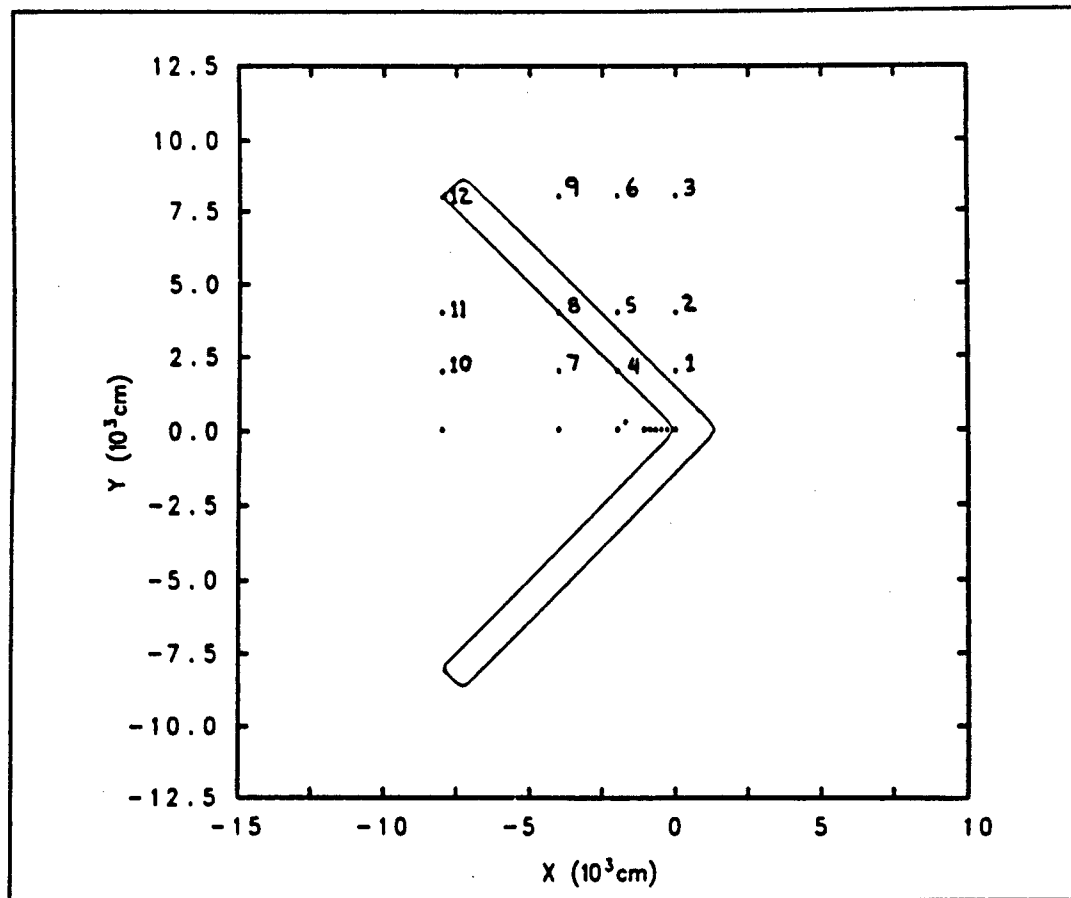


Figure 7. Diagram of Building Set at Coordinate Point Twelve

and the upper right corner. For this case the lower right corner is placed at the point (0, -40), and the upper right corner is placed at the point (10, 113.14). The program then rotates the piece through 45 degrees to set the upper left corner to point twelve. The lower left corner is below the "x" axis to provide extra material so that, when rotated, the point of the "V" (right end of the building) will be closed. CTHREZ will truncate the building along the "x" axis after the insertion is complete,

since the problem exists only in the positive "y" region. The amount (40 meters) of extra length below the "x" axis is minimum extra length needed to keep the "V" closed with the largest rotation angle of 75.964° to point ten. The input instructions for this insertion are in the material insertion section of the input file "rez8.8.2" on page 69 in Appendix A.

Tracers identify points in the material where the time histories of selected physical parameters will be kept. Due to cell averaging, cells that contain more than one material will not have physical properties representative of any individual material, but will be averaged values. This requires the placement of tracers in the nearest cell to the point of interest that contains only the material of interest. The intended use of tracers in this study is to obtain data on the behavior of the air, so they need to be placed in the cells that contain only air. Buildings with

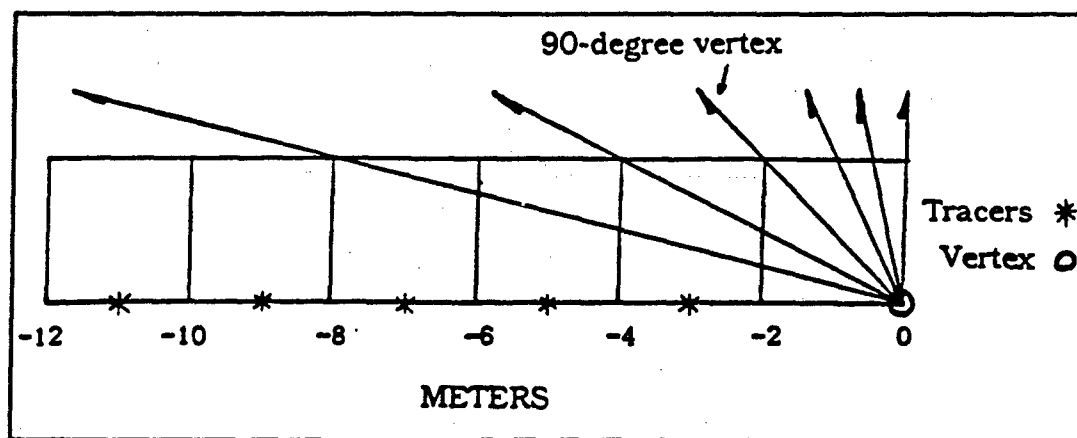


Figure 8. Tracer Positions and Wall Placement Near the Vertex

vertex angles greater than 90 degrees allow the use of the second cell to the left of the vertex for tracer placement in only air. The tracers must be placed farther out for buildings with smaller vertex angles. Tracer locations are along the "x" axis at three, five, seven, nine, and eleven meters left of the "y" axis, as shown in Figure 8. These represent points centered in the "x" direction, on the lower "y" boundary of the second, third, fourth, fifth, and sixth cells from the vertex, respectively. The tracers at nine and eleven meters are the only two that are in cells containing only air for all of the vertex angles. Additional fixed tracers placed ten centimeters left of the coordinates used to set the buildings, and at the same intervals along the negative "x" axis, provide pressure data as the advancing front moves through the building layout area. The tracers were offset to the left so they would not be in a region of mixed air and steel. The tracers at these points, without a building in place, record the free-field shock wave as it passes through the region. All the tracers are marked by asterisks in Figure 7 on page 31.

VI. Results and Discussion

Shock Wave Generation

The shock wave generated by CTH is a good approximation of one expected from a nuclear air burst. The computer-generated shock front, shown in Figure 9 by the pressure history at 80 meters to the left of the

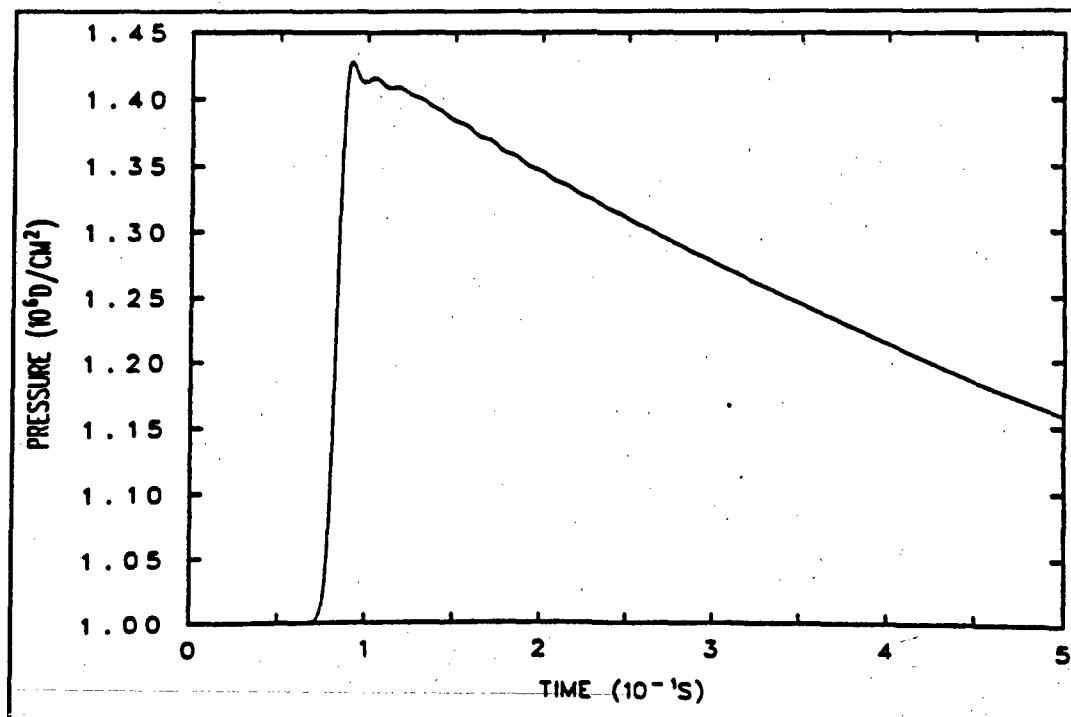


Figure 9. Time History of Free-Field Shock Front Passing the Point Eighty Meters to the Left of the Vertex

vertex point on the "x" axis, has the desired shape. As demonstrated below, the positive phase duration is consistent with the value of the peak overpressure at the same distance (1800 meters) from ground zero

of a 27.7 kiloton nuclear air burst at 922 meters altitude. The entire positive phase is not shown since the computations terminated at 0.5 seconds after the rezoning. The positive phase duration of this wave may be estimated, however, by applying the plots of Figure 10 to the pressure history in Figure 9.

The overpressure at 0.5 seconds normalized to the peak overpressure is 0.37 (from Figure 9). This value with a peak overpressure of 6.2 psi gives a normalized time of 0.46, from Figure 10. The time after reaching the peak to reach the normalized overpressure of 0.37 is 0.41 seconds, which divided by 0.46 gives a positive phase duration of 0.89 seconds.

For comparison, this and other values may be estimated for a nuclear burst by applying the techniques described by Glasstone and Dolan (4:114 - 119). Key to these estimates is the scaling law given by

$$\frac{d}{d_1} = \frac{h}{h_1} = \frac{t}{t_1} = W^{1/3} \quad (12)$$

where d, h, and t are the distance from ground zero, the height of burst, and the positive phase duration, respectively, and W is the explosion energy in kilotons. The values with subscripts are those for a reference yield of one kiloton.

Figure 11 may be used to find the size of a nuclear burst required to

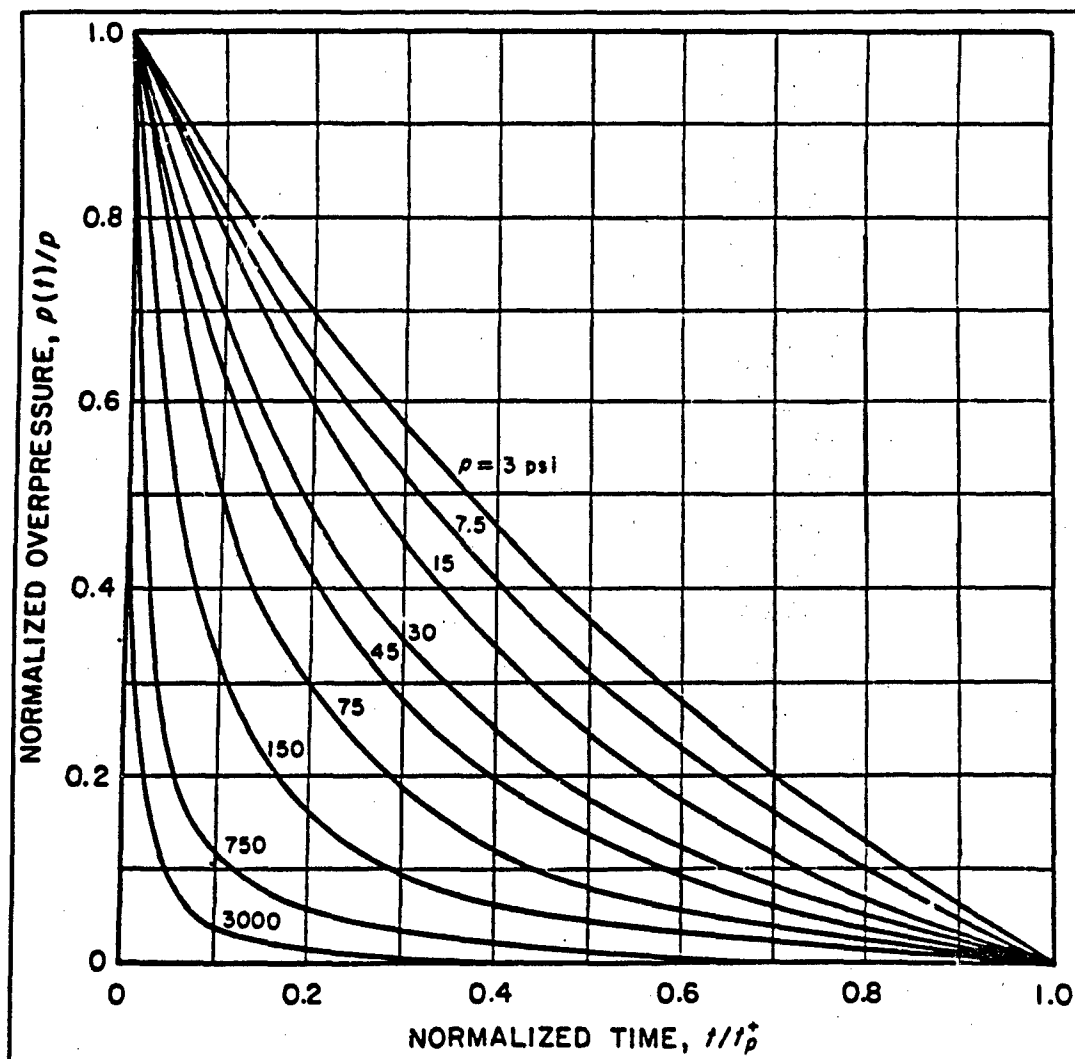


Figure 10. Rate of Decay of Overpressure with Time for Several Values of the Peak Overpressure (4:100)

produce a peak overpressure of 6.2 psi at a range similar to the distance the buildings are from the origination point of the shock wave (about 5900 feet). The figure shows that the peak overpressure of 6.2 psi could be expected on the ground at 1950 feet from ground zero below a one kiloton air burst at 1000 feet altitude. The scaling law of Eq (12) gives a

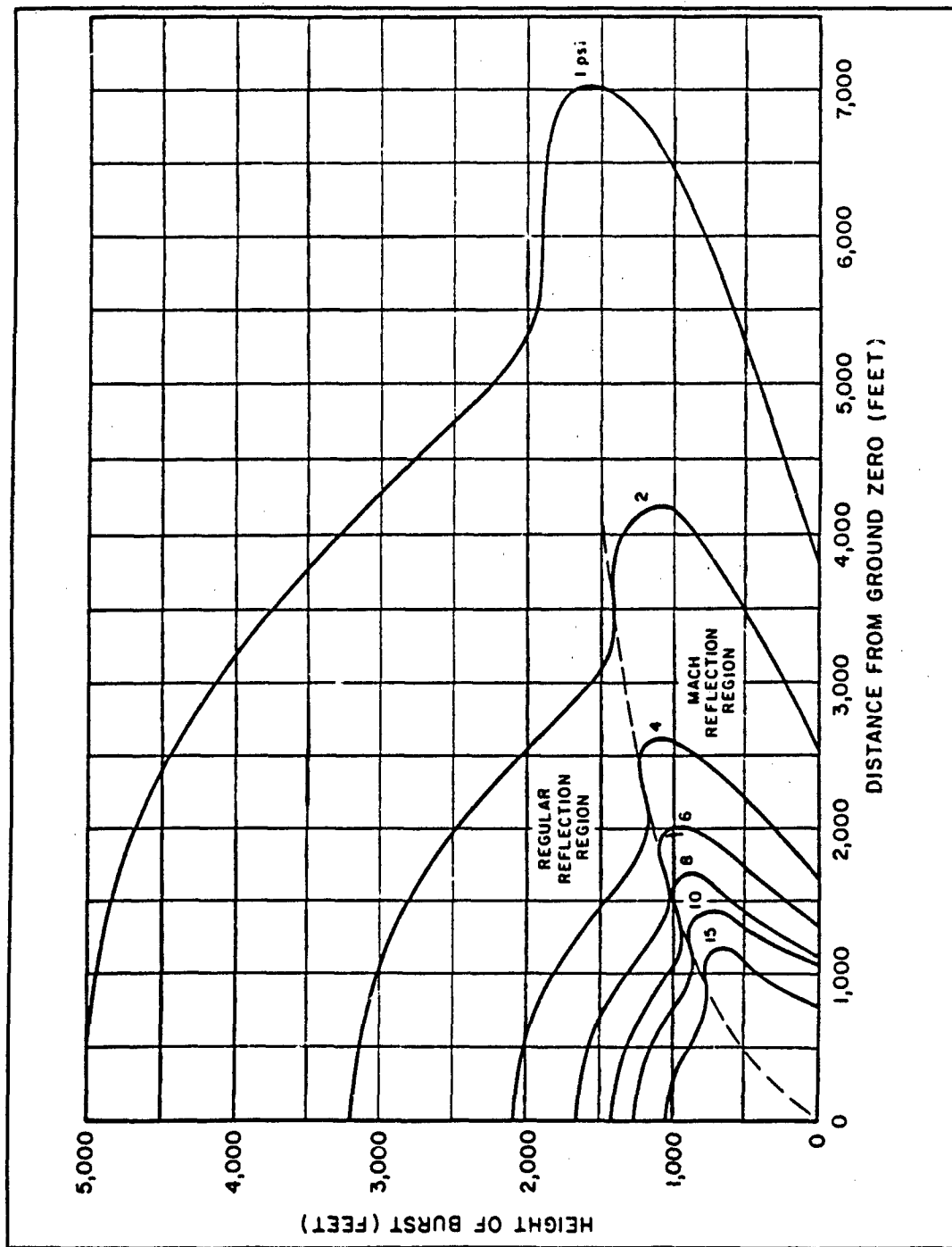


Figure 11. Peak Overpressures on the Ground for 1-kiloton Burst (4:115)

yield of 27.7 kilotons detonated at 3025 feet altitude. This value and Figure 12 can be used to get another estimate of the positive phase duration expected at 5900 feet from a 27.7 kiloton nuclear detonation at the same altitude. The distance (1950 feet) and height of burst (1000 feet) values for a one kiloton burst give a duration of about 0.29 seconds, which when scaled for the 27.7 kiloton case gives a positive phase duration of 0.893 seconds, which is essentially identical with 0.89 seconds found using Figure 10.

The free-field overpressures were constant at 0.42 atmospheres, or 6.2 psi, across the 80-meter distance through the region where the buildings would be placed. The histories at other points are identical, with the exception that the shock front arrives later at points closer to the "y" axis. The steady value of the peak overpressure across this region is reasonable since even a shock wave diverging in space would change very little over a short distance relative to its overall radius (80 meters versus a nearly 2000-meter radius). This is consistent with Figure 11, which shows that a spherically diverging shock wave would pass through about another 600 meters before its peak overpressure reduces to four psi overpressure (scaling to the 27.7 kiloton case). As mentioned in the previous section, the shock wave had a depth or thickness of 400 meters at the time it became fully formed. This is the starting point (time zero) for the rezoned interaction phase.

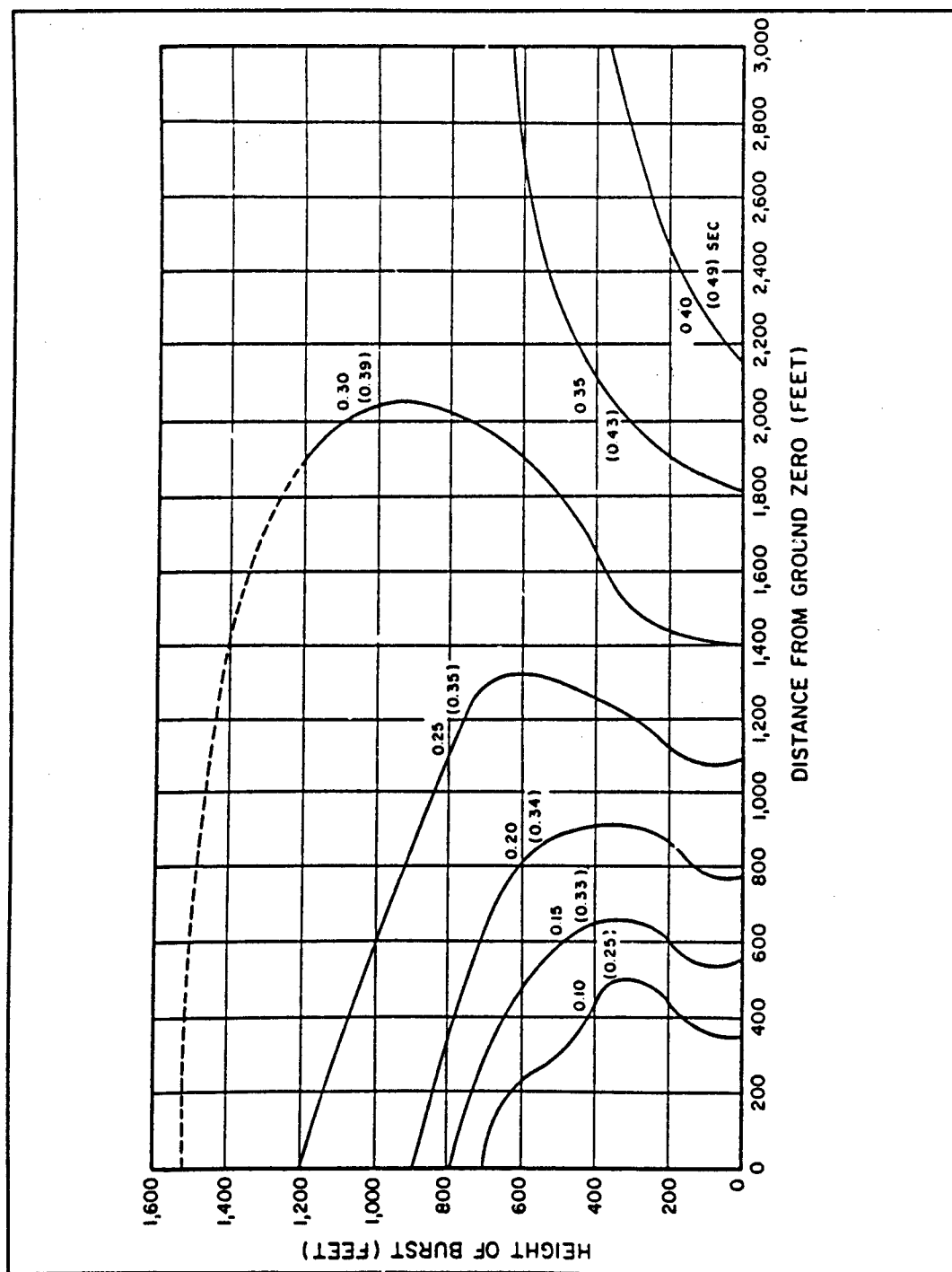


Figure 12. Positive Phase Duration on the Ground of Overpressure and (Dynamic Pressure) for 1-kiloton Burst (4:119)

The planar shock front is also a reasonable approximation. Since the angle subtended by 80 meters of arc length on a circle of 2000-meter radius is only 2.3 degrees, the arc would diverge from its tangent by only 1.6 meters at 80 meters from the intersection point of the tangent and the arc. Figure 11 also shows that for the height of burst and range found for the one kiloton case that mach reflection is occurring. These two points, when taken together, support the planar approximation of the shock front.

Interaction with Buildings

Table 2, on the following page, gives the peak overpressures at the tracers near the building vertices. All three face-on walls (20, 40, and 80-meter half-lengths) produced the same peak reflected overpressure near the vertex point. The peak overpressures were 0.95 atm, 0.95 atm, 0.94 atm, 0.93 atm, and 0.92 atm, for the five tracer points at 3, 5, 7, 9, and 11 meters, respectively. The value of 0.95 atmospheres at the point nearest the wall compares well with the peak reflected overpressure of 1.0 atmosphere predicted by Eq (10) on page 14 for an incident shock with a peak overpressure of 0.42 atm.

Several observations are made from the data in Table 2. The use of the twelve coordinate point reference numbers, described earlier, will simplify the discussion of these observations in the following

paragraphs. For example, the building defined by setting the inside end corner to the coordinate point (-80,40), will be called simply "case eleven," as shown in the table.

The peak reflected overpressure increases with decreasing vertex

Table 2. Peak Overpressures Near the Vertices of the Twelve Buildings

Tracer Positions (meters)	Building Number, End Corner Coordinates (meters) and Approximate Vertex Angle (degrees)			
	Peak Overpressures at the Indicated Tracers (atm)			
	12 (-80, 80) 90	9 (-40, 80) 127	6 (-20, 80) 152	3 (0, 80) 180
-3.00	2.52	1.38	1.12	0.95
-5.00	2.52	1.38	1.12	0.95
-7.00	2.42	1.38	1.13	0.94
-9.00	2.37	1.38	1.14	0.93
-11.0	2.22	1.38	1.15	0.92
	11 (-80, 40) 53	8 (-40, 40) 90	5 (-20, 40) 127	2 (0, 40) 180
-3.00	-	2.27	1.38	0.95
-5.00	3.65	2.17	1.38	0.95
-7.00	3.21	2.07	1.38	0.94
-9.00	2.76	1.83	1.38	0.93
-11.0	2.57	1.68	1.38	0.92
	10 (-80, 20) 28	7 (-40, 20) 53	4 (-20, 20) 90	1 (0, 20) 180
-3.00	-	-	1.88	0.95
-5.00	-	2.52	1.68	0.95
-7.00	-	2.32	1.53	0.94
-9.00	2.86	2.02	1.38	0.93
-11.0	2.81	1.88	1.33	0.92

angle in each case for which a valid pressure is available for the tracer nearest the vertex (vertex angles of 90 degrees or more). This is true even when comparing case nine, which is 89.4 meters long, with case four, which is only 28.3 meters long. These two cases have vertex angles of 126.9 and 90.0 degrees, respectively. Case four only captures one quarter the length of the incident wave front that case nine does, but the peak reflected pressure near the corner in case four is 1.36 times greater. The same trend holds for the tracer five meters from the vertex, except in case twelve (113 meters long) compared to case seven (44.7 meters long), which both result in the same overpressure of 2.52 atmospheres at that point. The building of case seven only captures one quarter the length of the incident wave front that case twelve does, but the peak reflected pressure near the corner is the same.

Another observation involves the comparison of the vertex overpressures for the buildings of cases nine and five. These two both represent the same vertex angle of 126.9 degrees, but case five is 44.7 meters long, or one half the length of case nine, and captures one half as much of the wave front. Although the angle remains constant, while the length decreases by half, the peak reflected overpressure at all five tracers is the same 1.38 atmospheres for both cases. This did not occur in any other cases. The peak overpressure at each tracer decreases with wall length for constant angle for each of the other angles.

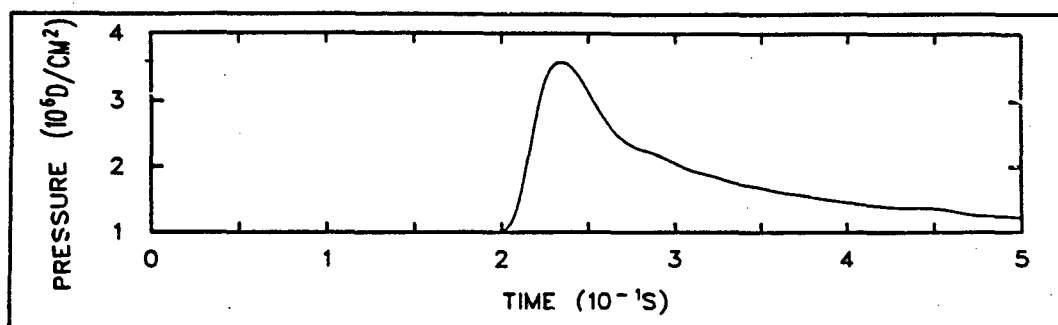


Figure 13. Time History of Pressure Three Meters from Vertex of Building Twelve

The plots of the data were the best way to determine the values of the peaks given the time constraints. The time history plot of pressure for case twelve is presented in Figure 13 as an example of the history plots generated with HISPLT. The Eulerian tracers near the vertex and the Eulerian and Lagrangian tracers placed at the grid points are marked by asterisks. Note the rightward shift of the leftmost Lagrangian tracers due to their movement with the air as the shock front passed them.

The general trend shows that the vertex angle has a greater effect than the building wall length on the amplification of the peak overpressure near the vertex or concave corner. Case ten produced the greatest peak overpressures at the fourth and fifth tracers out from the vertex, but it captures less of the wave front. The evidence supports the existence of a critical angle of incidence (vertex angles of 180° correspond to normal incidence) where the shock reflection becomes

more forward-directed, as opposed to reflecting back out of the "V," but the data in this study are too coarsely spaced to identify this angle accurately. The critical angle of incidence may occur near 26.6° , as in cases five and nine, since the length had no effect on the peak overpressure near the vertex in these cases.

The following sequence of four diagrams are pressure contour plots generated by CTHPLT. These figures show the advancement of the shock wave from a point at a reference time of 0.15 seconds through three steps of 0.025 seconds to the reference time of 0.225 seconds, just after reaching the vertex. As the shock wave enters the "V," and begins reflecting off the walls, the pressure begins to build along the wall, and a reflected front moves toward the vertex bisector of the building. When the reflected waves converge at the bisector, they are amplified, and the flow retains a component in the positive "x" direction. The pressure is further amplified as the air is forced tighter into the vertex, until the flow stagnates and is then redirected back out of the "V." In narrow vertices, the flow is reflected in a more forward direction, allowing more of the wave's kinetic energy to be transmitted to the vertex region, where it is converted to internal energy, increasing the temperature, density, and pressure there. The pressure contour legend shown on the first plot applies to all four plots. Appendix B contains contour plots of the wave's interaction with building cases 6 and 12.

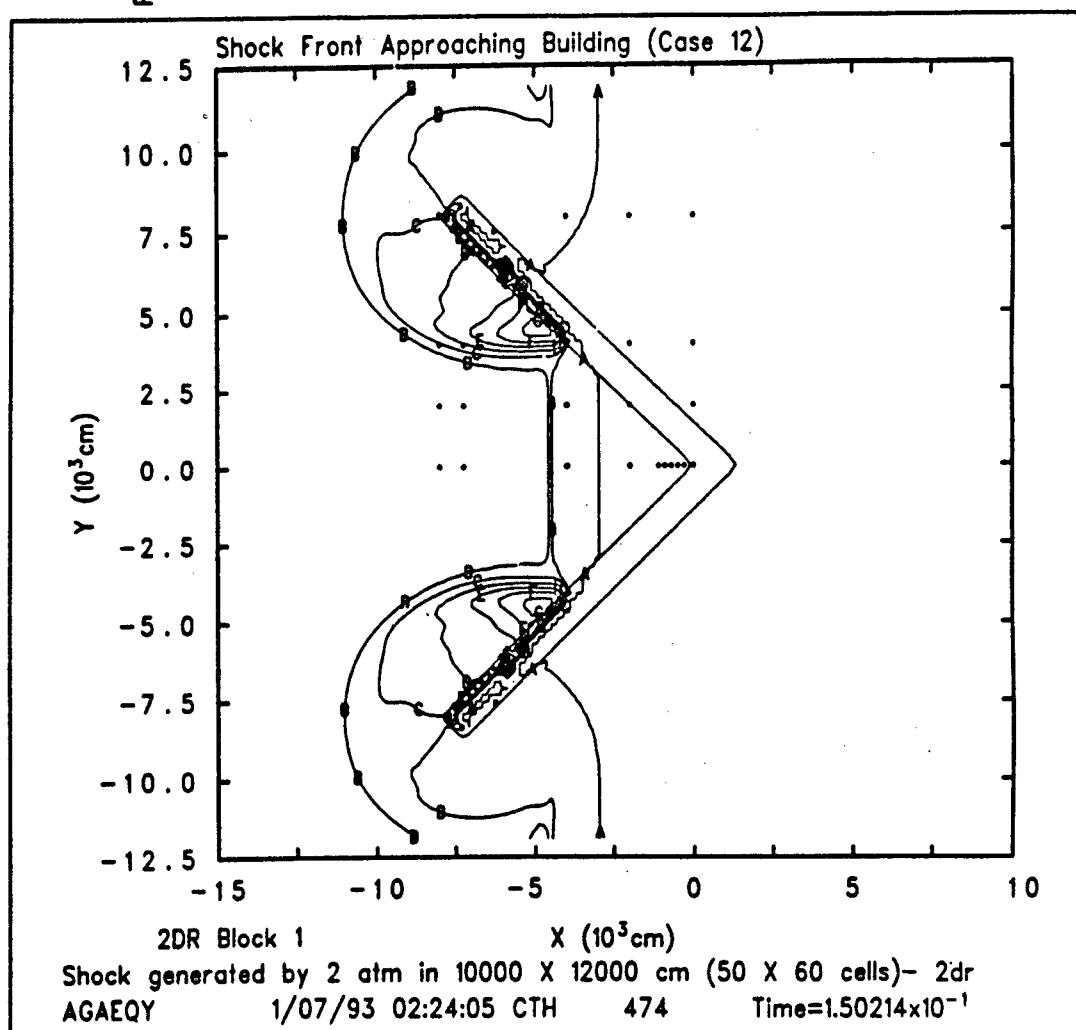
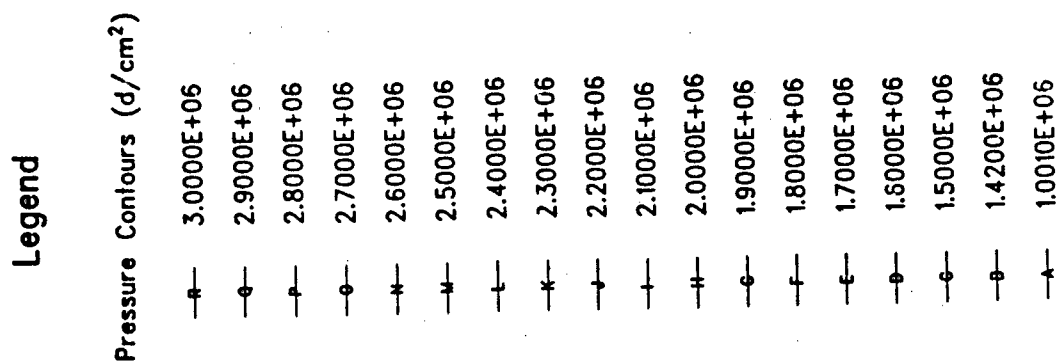


Figure 14. Shock Wave Flowing into Building Twelve (Time = 0.15 sec)

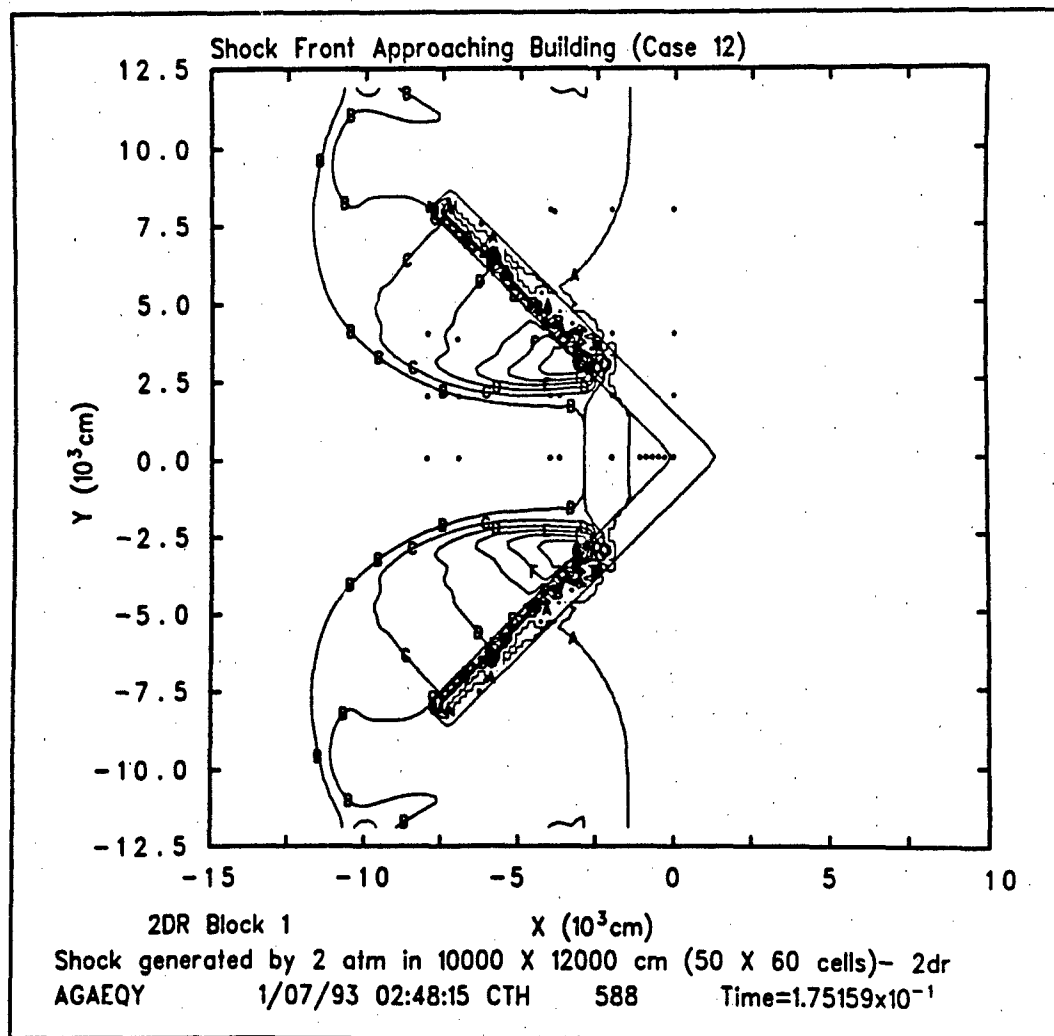


Figure 15. Shock Wave Flowing into Building Twelve (Time = 0.175 sec)

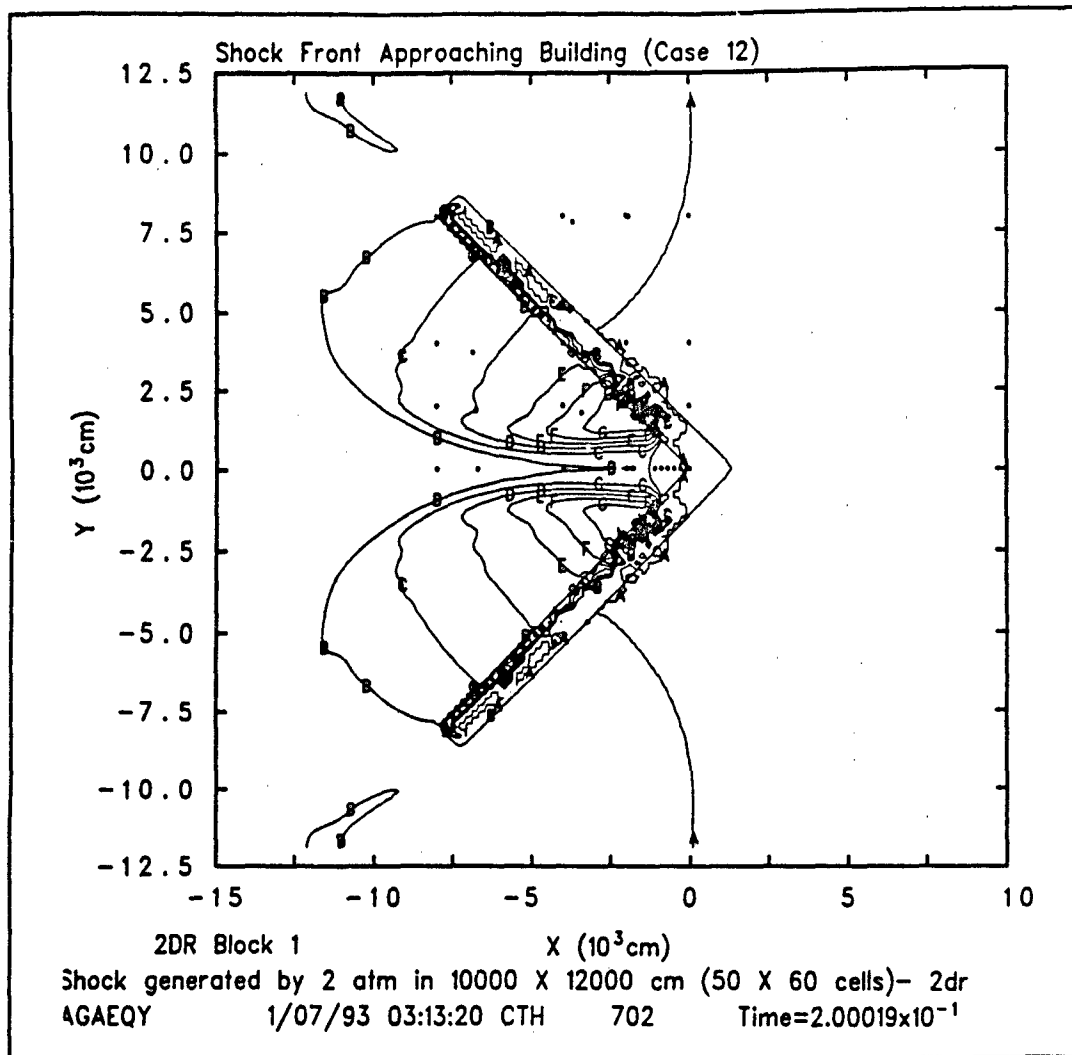


Figure 16. Shock Wave Flowing into Building Twelve (Time = 0.2 sec)

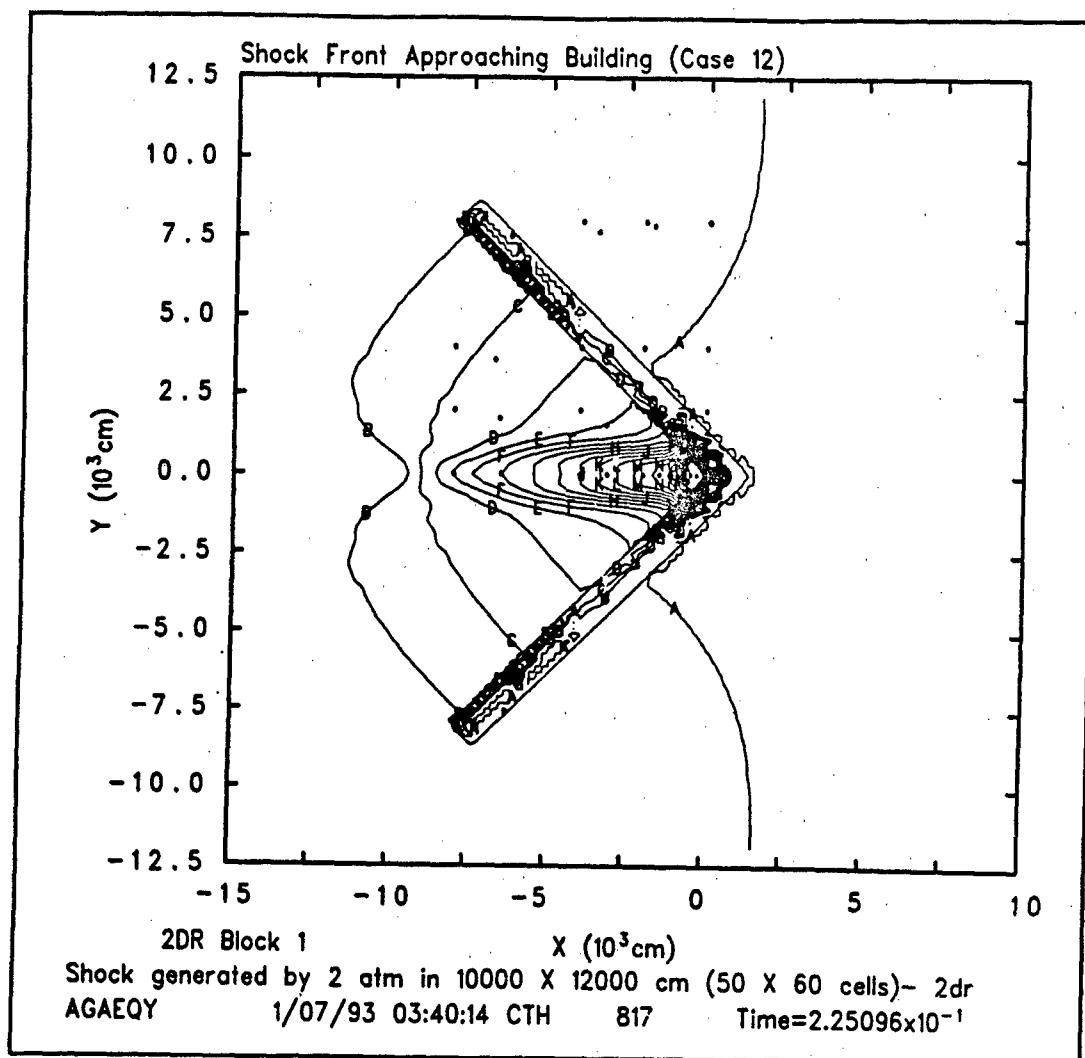


Figure 17. Shock Wave Flowing into Building Twelve (Time = 0.225 sec)

VII. *Conclusions and Recommendations*

The CTH Code

The CTH fluid hydrodynamics code is an excellent tool for this type of study. It is easy to implement and provides an excellent approximation of the desired incident shock front. The code has applicability to a wide variety of studies of shock propagation and reflection phenomena. The computational time and storage capacity of the computer system are the primary limitations encountered in this study - not the code. While the computational aspects are limited, we have gained some valuable information, and this study provides the groundwork for serious consideration of more difficult hydrodynamics problems in future studies.

Shock Amplification

This study has shown that shock amplification by reflection into concave corners occurs and can be significant even at shallow angles of incidence (wide vertex angles). The peak reflected overpressure observed with normal incidence was about 2.2 times the incident overpressure, while at the next larger angle investigated, 26.6° , which corresponds to a vertex angle of 127° , the reflected overpressure was about 2.7 times incident. Most importantly, the three cases with vertex angles of 90°

produced overpressures of 28 to 37 psi near the vertex with wall lengths from 28.3 to 113 meters. These overpressures are 1.98 and 2.66 times the peak reflected overpressure of 13.9 psi due to reflection from a flat wall at normal incidence. This result is important because many buildings are constructed with such corners. The greatest reflected overpressure observed in this study was 8.6 times the incident overpressure, and was observed with the building of case eleven. This building had a vertex angle of 53° and its walls were 89.4 meters long.

Important information about the effects of corners in buildings has been observed, for which more detailed and revealing models can be developed. The general trend shows that the vertex angle has a greater effect than the building wall length on the amplification of the peak overpressure near the vertex or concave corner. The degree to which the vertex angle affects the peak reflected overpressure near the corner relative to the change in length of the wall is evident, but we need a more detailed study to look for an empirical fit which may more accurately predict results without long, tedious, and difficult modeling for each individual case. This leads to recommendations for future modeling.

Future Studies

There are several examples where more detailed study may prove valuable. Further study can be done to establish more detailed trends

over a finer space and time structure (smaller mesh cells, more frequent data recording, etc.). Some specific examples include more detail along the length of the wall with a vertex angle of 127 degrees. The two cases studied produced identical results, and it would be instructive to find whether this trend continues with longer walls, and where it begins to break down as the wall becomes shorter. Further study could also examine finer meshes to provide values closer to the corner, and provide data for other angles. An important question is whether there exist regimes where the length of the wall is or is not important, and at what angle the shock reflection becomes forward biased.

Future modeling could also include larger structures closer to the burst point, where the planar shock front approximation is no longer valid, and higher order geometry is required. The cylindrical, and even spherical expansion of a shock wave and its interaction with a variety of structures could be modeled with more capable computer equipment. Shock development from the initial physical dimensions and thermodynamic properties of a fireball could also be examined. One-dimensional spherical representations of an expanding blast wave could be rezoned to three-dimensional geometry for detailed analysis of interaction with structures of finite dimensions. More detail would also allow for consideration of the effects of realistic structural components, such as windows pressure could be relieved, reducing the amplification.

The most accurate modeling would include studies conducted with a three dimensional geometry that could investigate the effect of focussing into a point instead of a line as with two-dimensional geometry. Given the degree of focussing in two dimensions, focussing into a point in three dimensions should result in even greater overpressure amplification. The effect of varying the angle of incidence with respect to the ground and the building walls and the effect of unequal wall lengths and finite building height could also be included.

There are innumerable other fluid dynamic problems that could be examined with CTH. These may include structures of different shapes, such as storage tanks, or the combined reflections from adjacent buildings such as in cities. The existence of an installed, working code, and in-house knowledge of its operation and application will allow the future development of more meaningful blast phenomena problems and a great variety of fluid dynamics problems in other areas of interest.

Bibliography

1. Bridgman, Charles J. *The Physics of Nuclear Explosives*. Class notes for NENG-605, Physics of Nuclear Explosives, and NENG-631, Prompt Effects of Nuclear Weapons. School of Engineering, Air Force Institute of Technology (AU), Wright-Patterson AFB OH, 28 April 1986.
2. CTH Code Development Group. *CTHPLT User's Guide and Input Instructions* (Version 1.00). Albuquerque, NM: Computational Physics and Mechanics 1, Division 1531, Sandia National Laboratories, 1992.
3. CTH Code Development Team. *CTH User's Manual and Input Instructions* (Version 1.026). Albuquerque, NM: Sandia National Laboratories, 1992.
4. Glasstone, Samuel and Philip J. Dolan. *The Effects of Nuclear Weapons* (Third Edition). Washington: Government Printing Office, 1977.
5. Harlow, Francis H. and Anthony A. Amsden. *Fluid Dynamics - A LASL Monograph*. Report LA-4700. United States Atomic Energy Commission Contract W-7405-ENG.36. Los Alamos, New Mexico: Los Alamos Scientific Laboratory of the University of California, June 1971.
6. Rottler, Stephen J. and Samuel L. Thompson. *HISPLT: A History Graphics Post Processor for Wave Propagation Codes* (Version 3.20). Albuquerque, NM: Computational Physics and Mechanics Division I, Sandia National Laboratories, 1990.
7. Yarrington, L. *CTHREZ User's Guide and Input Instructions* (Version 1.0). Albuquerque, NM: CTH Development Project, Sandia National Laboratories, 1992.

Appendix A

Input Data Files

This appendix presents the input data files that provide the information to the various CTH programs to model the problems described in this effort. These files are presented for continuity. The file that provides the necessary information to both CTHGEN to set-up the shock generation problem, and to CTH to run it is presented first. This file begins on page 55. The information for these two programs (and any others that may be needed to process a problem) may be combined in a single file as is done in this file called "SHOCK.GEN." The lines that begin with *eor* separate the information for the two programs. The individual programs search for this indicator followed the program's identifier. The identifiers are "genin," "cthin," "rezin," "hisin," and "pltin" for CTHGEN, CTH, REZIN, HISPLT, and CTHPLT, respectively.

The rezone file used to insert the building for case cne, and the material insertion sections of the rezone files for each of the other cases are given beginning on page 60. The material insertion section is the only part that changes between the various cases. The input file that provides information required for the CTH program to run the separate

cases after rezoning begins on page 71. Plot input files used to generate the plots in Appendix B are presented beginning on page 73. The following file is the input that generated the final form of the shock front used in this study. The file contains instructions for both the CTHGEN and CTH programs.

```
*****
*
* shock.gen
*
* air @ 2 atm in 10000 cm
*   |
*   |                               190000 cm |
*   V                               V
*   -----
*   |///|
*   |///|
*   |///| air @ 1 atm
*   |///|
*   |///|
*   |///|----->
*   |///|
*   |///|
*   |///|
*   |///|
*   -----
*****
*
* *eor* genin
*
*****
*
* Title record
*
Shock generated by 2 atm in 10000 X 12000 cm (50 X 60 cells)- 2dr
*
*****
```

```

*
* control records
*
control
  mmp
endc
*
*****
*
* edit records
*
edit
  block 1
    expanded
  endb
ende
*
*****
*
* mesh records
*
mesh
  block 1 geom=2dr type=e
    x0 -180000
    x1 n=950 r=1 w=190000
  endx
  y0 0
  y1 n=60 r=1 w=12000
  endy
  xact -180000,-170000
endb
endm
*
*****
*
* material insertion records:
*
insertion
  block 1
*
*
package compressed air

```

```

    material 1
    pressure 2e6
    insert box
      p1 -180000,0
      p2 -170000,12000
    endi
  endp
*
  package ambient air
  material 1
  pressure 1.e6
  insert box
    p1 -180000,0
    p2 10000,12000
  endi
  endp
*
  endb
endi
*
*****
*
* eos records
*
eos
  mat1 sesame eos=5031 feos='aneos'      *air sesame
ende
*
*****
*
*eor* cthin
*
*****
*
* Title record
*
Shock generated by 2 atm in 10000 X 12000 cm (50 X 60 cells)- 2dr
*
*****
* tracer records
*
tracer
  block 1

```

```

add -10,0 to -4010,0 n=3 fixed xy
add -8010,0 fixed xy
add -10,2000 to -4010,2000 n=3 fixed xy
add -8010,2000 fixed xy
add -10,4000 to -4010,4000 n=3 fixed xy
add -8010,4000 fixed xy
add -10,8000 to -4010,8000 n=3 fixed xy
add -8010,8000 fixed xy
add -10,10 to -4010,0 n=3
add -8010,0
add -10,2000 to -4010,2000 n=3
add -8010,2000
add -10,4000 to -4010,4000 n=3
add -8010,4000
add -10,8000 to -4010,8000 n=3
add -8010,8000
endb
endt
*
*****
*
* control records
*
control
  tst 2.5
  rdu 1800.
endc
*
*****
*
* cell thermo records
*
cellthe
  mmp
endc
*
*****
*
* edit records
*
edit
  shortc
  cycle = 0 dc = 1000

```

```

ends
longt
  time = 0. dt = 1e5
endl
plott
  time = 0. dt = 5e-1
endp
ende
*
*****
*
* boundary condition records
*
*****
*
boundary
  bhydro
    block 1
      bxb = 0 bxt = 1
      byb = 0 byt = 0
    endb
  endh
endb
*
*****

```

The next set of files provide instructions to CTHREZ for the rezoning step used to insert the shock front and the buildings together in separate problems. These files select the portion of the wave that represents the positive phase, insert the buildings, and set up the initiation point for each case. They do not run the calculations. The rezone input file for case one is "rez.0.2.2." It and only the header and material insertion sections of the files for the remaining cases follow. The material insertion data are the only differences between the files. The files are similarly named; the first and second numerals indicate the magnitudes of the coordinates of the building end corner (in tens of meters). The last numeral in the name is two for all cases, and indicates that these were version two of the files.

```
*****
*
* rez0.2.2
*
* Inserts wall with end corner at 0m left and 20m up from vertex.
*
*****
*
*eor*rezn
*
*****
*
* Title record
*
rezone to include wall and new tracers
*
*****
*
prerezone
```

```

ofile='wave'  *shock wave in air
file='rsctw'
time=2.5
numsub=50
xmin=-60000
xmax=-10000
*
geometry
mapping=2dto2d
  cel=0.0
  ce2=0.250000 *no rotation
endgeometry
*
mrt
  save=all
endm
*
endprerezone
*****
* control records
control
  time=0
  mmp
endc
*
*****
*
* edit records
*
*edit
* block 1
*   expanded
* endb
*ende
*
*****
*
* mesh records
*
mesh
  block 1 geom=2dr type=e
    :.0 -60000.
      x1 n=350 r=1 w=70000

```



```

endx
y0 0.
  y1 n=60 r=1 w=12000
endy
xact=-60000,-10000
endb
endm
*
*****
*
* tracer records
*
tracer
  block 1
    add -300,0 to -1100,0 n=5 fixed xy
  endb
endt
*
*****
*
rezone
  file='wave'
endrezone
*
*****
*
* material insertion records
*
insertion
  block 1
    package steel
    material 2
    numsub 50
    pressure 1.e6
    insert box
      p1 0,0
      p2 1000,2000
    ppoint 0,0
    angle=0      *angle is rotation angle from y axis
    * 0, 14.03624347, 26.56505118, 45, 63.43494882, or 75.96375654
  endi
endp
*

```

```

package ambient air
material 1
pressure 1.e6
insert box
  p1 -10000,0
  p2 10000,12000
endi
endp
*
endb
endi
*
*****
rezone
  file='wave'
endrezone
*
*****
* eos records
*
eos
  mat1 sesame eos=5031 feos='aneos' *air sesame
  mat2 sesame eos=4271 feos='aneos' *steel sesame
ende
*
*****

*****
*
* rez0.4.2
*
* Inserts wall with end corner at 0m left and 40m up from vertex.
*
*****
*
* material insertion records
*
insertion
  block 1
    package steel
    material 2
    numsub 50

```

```

    pressure 1.e6
    insert box
      p1 0,0
      p2 1000,4000
      ppoint 0,0
      angle=0      *angle is rotation angle from y axis
    * 0, 14.03624347, 26.56505118, 45, 63.43494882, or 75.96375654
    endi
  endp

```

```

*****
*
* rez0.8.2
*
* Inserts wall with end corner at 0m left and 80m up from vertex.
*

```

```

*****
*
* material insertion records
*
insertion
  block 1
    package steel
    material 2
    numsub 50
    pressure 1.e6
    insert box
      p1 0,-4000
      p2 1000,8000
      ppoint 0,0
      angle=0      *angle is rotation angle from y axis
    * 0, 14.03624347, 26.56505118, 45, 63.43494882, or 75.96375654
    endi
  endp

```

```

*****
*
* rez2.2.2
*
* Inserts wall with end corner at 20m up and 20m left from vertex.
*

```

* material insertion records

*

insertion

block 1

package steel

material 2

numsub 50

pressure 1.e6

insert box

p1 0,-4000

p2 1000,2828.427125

ppoint 0,0

angle=45

*angle is rotation angle from y axis

* 0, 14.03624347, 26.56505118, 45, 63.43494882, or 75.96375654

endi

endp

*

* rez2.4.2

*

* Inserts wall with end corner at 20m left and 40m up from vertex.

*

*

* material insertion records

*

insertion

block 1

package steel

material 2

numsub 50

pressure 1.e6

insert box

p1 0,-4000

p2 1000,4472.135955

ppoint 0,0

angle=26.56505118

*angle is rotation angle from y axis

* 0, 14.03624347, 26.56505118, 45, 63.43494882, or 75.96375654

endi

endp

*

* rez2.8.2

*

* Inserts wall with end corner at 20m left and 80m up from vertex.

*

*

* material insertion records

*

insertion

block 1

package steel

material 2

numsub 50

pressure 1.e6

insert box

p1 0,-4000

p2 1000,8246.211251

ppcint 0,0

angle=14.03624347 *angle is rotation angle from y axis

* 0, 14.03624347, 26.56505118, 45, 63.43494882, or 75.96375654

endi

endp

*

* rez4.2.2

*

* Inserts wall with end corner at 40m left and 20m up from vertex.

*

*

* material insertion records

*

insertion

block 1

package steel

material 2

numsub 50

pressure 1.e6

insert box

p1 0,-4000

```

      p2 1000,4472.135955
      ppoint 0,0
      angle=63.43494882      *angle is rotation angle from y axis
* 0, 14.03624347, 26.56505118, 45, 63.43494882, or 75.96375654
      endi
    endp

```

```

*****
*
* rez4.4.2
*
* Inserts wall with end corner at 40m up and 40m left from vertex.
*

```

```

*****
*
* material insertion records
*
insertion
  block 1
    package steel
    material 2
    numsub 50
    pressure 1.e6
    insert box
      p1 0,-4000
      p2 1000,5656.854249
      ppoint 0,0
      angle=45      *angle is rotation angle from y axis
* 0, 14.03624347, 26.56505118, 45, 63.43494882, or 75.96375654
      endi
    endp

```

```

*****
*
* rez4.8.2
*
* Inserts wall with end corner at 40m left and 80m up from vertex.
*
*****
*
* material insertion records
*
insertion

```

```

block 1
  package steel
  material 2
  numsub 50
  pressure 1.e6
  insert box
    p1 0,-4000
    p2 1000,8944.271910
  ppoint 0,0
  angle=26.56505118      *angle is rotation angle from y axis
* 0, 14.03624347, 26.56505118, 45, 63.43494882, or 75.96375654
  endi
endp

```

```

*****
*
* rez8.2.2
*
* Inserts wall with end corner at 80m left and 20m up from vertex.
*

```

```

*****

```

```

*
* material insertion records
*

```

```

insertion
  block 1
    package steel
    material 2
    numsub 50
    pressure 1.e6
    insert box
      p1 0,-4000
      p2 1000,8246.211251
    ppoint 0,0
    angle=75.96375654      *angle is rotation angle from y axis
* 0, 14.03624347, 26.56505118, 45, 63.43494882, or 75.96375654
  endi
endp

```

```

*****
*
* rez8.4.2
*
* Inserts wall with end corner at 80m left and 40m up from vertex.
*
*****
*
* material insertion records
*
insertion
  block 1
    package steel
    material 2
    numsub 50
    pressure 1.e6
    insert box
      p1 0,-4000
      p2 1000,8944.271910
    ppoint 0,0
    angle=63.43494882      *angle is rotation angle from y axis
  * 0, 14.03624347, 26.56505118, 45, 63.43494882, or 75.96375654
  endi
  endp

```

```

*****
*
* rez8.8.2
*
* Inserts wall with end corner at 80m left and 80m up from vertex.
*
*****
*
* material insertion records
*
insertion
  block 1
    package steel
    material 2
    numsub 50
    pressure 1.e6
    insert box
      p1 0,-4000

```


p2 1000,11313.7085
ppoint 0,0
angle=45 *angle is rotation angle from y axis
• 0, 14.03624347, 26.56505118, 45, 63.43494882, or 75.96375654
endi
endp

The CTH program uses the following file to run the previously rezoned problems from their start point to completion.

```
*****
*
* rezrun   runs shock into structures.
*
*****
*
*eor* cthin
*
*****
*
* Title record
*
Air Shock into structure
*
*****
* control records
*
control
  tst .5
  rdu 1800.
endc
*
*****
*
* cell thermo records
*
cellthe
  mmp
endc
*
*****
*
* edit records
*
edit
  shortc
  cycle = 0  dc = 1000
ends
longt
```

```

    time = 0. dt = 1e5
endl
  plott
    time = 0. dt = 5e-2
  endp
  histt
    time = 0. dt = 5e-4
    htr all
  endh
ende
.
.....
. tracers
.
.
.....
.
. boundary condition records
.
.....
.
boundary
  bhydro
    block 1
      bxb = 0 bxt = 1
      byb = 0 byt = 0
    endb
  endh
endb
.
.....

```

The next set of files are the input files used by HISPLT and CTHPLT to create the plots in Appendix B. First, is the file 'shockplt' used by CTHPLT to create the spacial plots of the shock wave generation step. The plots will show the spatial distribution of the shock wave as the calculation proceeded to completion at 2.5 seconds. The plots are generated for each data dump that was made according to the time information entered into the file 'shock.gen' shown before.

```

.....
*
* shockplt:  Generates 1d plots of temp, pressure, and density for
*             developing shock front
*
.....
*
*cor* pltin
*
.....
*
units cgsev
dump=1 ddump=1
*
1dfix y=0 z=0
plot position pressure v2=temperature v3=density
*
.....

```

The next file, 'hisgrid.flx' is read by HISPLT to generate the time history plots for the grid points as the shock propagates past without a building in place (free-field). These plots will include four additional grid points along the "x" axis, which are not used for building placement.

```

.....
*
* hisgrid.flx:  Generates time history plots of  pressure at each of the
*               fixed tracers at the grid points.
*
.....
*
*cor* hisin
*
units cgsev
bottom=off
*
title='Free-Field Overpressure at Grid Point (0, 0)
plot time pressure.1
*
title='Free-Field Overpressure at Grid Point (-20, 0)
plot time pressure.2
*
title='Free-Field Overpressure at Grid Point (-40, 0)
plot time pressure.3
*
title='Free-Field Overpressure at Grid Point (-80, 0)
plot time pressure.4
*
title='Free-Field Overpressure at Grid Point (0, 20)
plot time pressure.5
*
title='Free-Field Overpressure at Grid Point (-20, 20)
plot time pressure.6
*
title='Free-Field Overpressure at Grid Point (-40, 20)
plot time pressure.7
*
title='Free-Field Overpressure at Grid Point (-80, 20)

```

plot time pressure.8

•

title='Free-Field Overpressure at Grid Point (0, 40)

plot time pressure.9

•

title='Free-Field Overpressure at Grid Point (-20, 40)

plot time pressure.10

•

title='Free-Field Overpressure at Grid Point (-40, 40)

plot time pressure.11

•

title='Free-Field Overpressure at Grid Point (-80, 40)

plot time pressure.12

•

title='Free-Field Overpressure at Grid Point (0, 80)

plot time pressure.13

•

title='Free-Field Overpressure at Grid Point (-20, 80)

plot time pressure.14

•

title='Free-Field Overpressure at Grid Point (-40, 80)

plot time pressure.15

•

title='Free-Field Overpressure at Grid Point (-80, 80)

plot time pressure.16

.....

The next file, 'histrace,' is also used by HISPLT, and generates the plots of overpressure at the five tracers near the vertex for each of the twelve building cases. This file demonstrates the use of multiple file designation. Files may be named in the input file or in the command line to run the problem.

```

*****
*
* histrace:  Generates time history plots of  pressure at each of the
*             five tracers near the vertex of each of the 12 buildings.
*
*****
*
*eor* hisin
*
*****
units cgsev
bottom=off
file1='hctk'
file2='hctl'
file3='hctm'
file4='hctn'
file5='hcto'
file6='hctp'
file7='hctq'
file8='hctr'
file9='hcts'
file10='hctt'
file11='hctu'
file12='hctv'
*
title='Overpressure at Tracer (-3, 0), Case 1
plot time pressure.33 file=1
*
title='Overpressure at Tracer (-5, 0), Case 1
plot time pressure.34 file=1
*
title='Overpressure at Tracer (-7, 0), Case 1
plot time pressure.35 file=1

```

•
title='Overpressure at Tracer (-9, 0), Case 1
plot time pressure.36 file=1
•

title='Overpressure at Tracer (-11, 0), Case 1
plot time pressure.37 file=1
•

.....
title='Overpressure at Tracer (-3, 0), Case 2
plot time pressure.33 file=2
•

title='Overpressure at Tracer (-5, 0), Case 2
plot time pressure.34 file=2
•

title='Overpressure at Tracer (-7, 0), Case 2
plot time pressure.35 file=2
•

title='Overpressure at Tracer (-9, 0), Case 2
plot time pressure.36 file=2
•

title='Overpressure at Tracer (-11, 0), Case 2
plot time pressure.37 file=2
•

.....
title='Overpressure at Tracer (-3, 0), Case 3
plot time pressure.33 file=3
•

title='Overpressure at Tracer (-5, 0), Case 3
plot time pressure.34 file=3
•

title='Overpressure at Tracer (-7, 0), Case 3
plot time pressure.35 file=3
•

title='Overpressure at Tracer (-9, 0), Case 3
plot time pressure.36 file=3
•

title='Overpressure at Tracer (-11, 0), Case 3
plot time pressure.37 file=3
•

.....
title='Overpressure at Tracer (-3, 0), Case 4
plot time pressure.33 file=4
•

title='Overpressure at Tracer (-5, 0), Case 4
plot time pressure.34 file=4
•

title='Overpressure at Tracer (-7, 0), Case 4
plot time pressure.35 file=4
•

title='Overpressure at Tracer (-9, 0), Case 4
plot time pressure.36 file=4
•

title='Overpressure at Tracer (-11, 0), Case 4
plot time pressure.37 file=4
•

.....
title='Overpressure at Tracer (-3, 0), Case 5
plot time pressure.33 file=5
•

title='Overpressure at Tracer (-5, 0), Case 5
plot time pressure.34 file=5
•

title='Overpressure at Tracer (-7, 0), Case 5
plot time pressure.35 file=5
•

title='Overpressure at Tracer (-9, 0), Case 5
plot time pressure.36 file=5
•

title='Overpressure at Tracer (-11, 0), Case 5
plot time pressure.37 file=5
•

.....
title='Overpressure at Tracer (-3, 0), Case 6
plot time pressure.33 file=6
•

title='Overpressure at Tracer (-5, 0), Case 6
plot time pressure.34 file=6
•

title='Overpressure at Tracer (-7, 0), Case 6
plot time pressure.35 file=6
•

title='Overpressure at Tracer (-9, 0), Case 6
plot time pressure.36 file=6
•

title='Overpressure at Tracer (-11, 0), Case 6
plot time pressure.37 file=6
•

.....
title='Overpressure at Tracer (-3, 0), Case 7
plot time pressure.33 file=7
•

title='Overpressure at Tracer (-5, 0), Case 7

plot time pressure.34 file=7

•

title='Overpressure at Tracer (-7, 0), Case 7

plot time pressure.35 file=7

•

title='Overpressure at Tracer (-9, 0), Case 7

plot time pressure.36 file=7

•

title='Overpressure at Tracer (-11, 0), Case 7

plot time pressure.37 file=7

title='Overpressure at Tracer (-3, 0), Case 8

plot time pressure.33 file=8

•

title='Overpressure at Tracer (-5, 0), Case 8

plot time pressure.34 file=8

•

title='Overpressure at Tracer (-7, 0), Case 8

plot time pressure.35 file=8

•

title='Overpressure at Tracer (-9, 0), Case 8

plot time pressure.36 file=8

•

title='Overpressure at Tracer (-11, 0), Case 8

plot time pressure.37 file=8

title='Overpressure at Tracer (-3, 0), Case 9

plot time pressure.33 file=9

•

title='Overpressure at Tracer (-5, 0), Case 9

plot time pressure.34 file=9

•

title='Overpressure at Tracer (-7, 0), Case 9

plot time pressure.35 file=9

•

title='Overpressure at Tracer (-9, 0), Case 9

plot time pressure.36 file=9

•

title='Overpressure at Tracer (-11, 0), Case 9

plot time pressure.37 file=9

title='Overpressure at Tracer (-3, 0), Case 10

plot time pressure.33 file=10

•
title='Overpressure at Tracer (-5, 0), Case 10
plot time pressure.34 file=10
•

title='Overpressure at Tracer (-7, 0), Case 10
plot time pressure.35 file=10
•

title='Overpressure at Tracer (-9, 0), Case 10
plot time pressure.36 file=10
•

title='Overpressure at Tracer (-11, 0), Case 10
plot time pressure.37 file=10
•

title='Overpressure at Tracer (-3, 0), Case 11
plot time pressure.33 file=11
•

title='Overpressure at Tracer (-5, 0), Case 11
plot time pressure.34 file=11
•

title='Overpressure at Tracer (-7, 0), Case 11
plot time pressure.35 file=11
•

title='Overpressure at Tracer (-9, 0), Case 11
plot time pressure.36 file=11
•

title='Overpressure at Tracer (-11, 0), Case 11
plot time pressure.37 file=11
•

*title='Overpressure at Tracer (-3, 0), Case 12
*plot time pressure.33 file=12
•

*title='Overpressure at Tracer (-5, 0), Case 12
*plot time pressure.34 file=12
•

*title='Overpressure at Tracer (-7, 0), Case 12
*plot time pressure.35 file=12
•

*title='Overpressure at Tracer (-9, 0), Case 12
*plot time pressure.36 file=12
•

*title='Overpressure at Tracer (-11, 0), Case 12
*plot time pressure.37 file=12

The last file is 'contour', and is used by CTHPLT to make the two-dimensional mirror-image plots of the shock interacting with the building of case twelve. This file is used with the selected data dump or "rsct" file, with the title line changed, as appropriate.

```
*****
*
*contour:Generates 2D contour plots mirrored about the x axis
*
*****
*
*eor* pltin
*
*****
*
units cgsev
dump=1 ddump=1
limits x=-15000,10000
noid
title='Shock Front Approaching Building (Case 12)'
CONTOURS=1.001e6, 1.42e6, 1.5e6, 1.6e6, 1.7e6, 1.8e6, 1.9e6, 2e6,
2.1e6, 2.2e6
MCONTOURS=2.3e6, 2.4e6, 2.5e6, 2.6e6, 2.7e6, 2.8e6, 2.9e6, 3e6,
3.1e6, 3.2e6
MCONTOURS=3.3e6, 3.4e6, 3.5e6, 3.6e6, 3.7e6, 3.8e6, 3.9e6, 4e6
up=if tracers co
down=if co
2DPLOT mirror=v IF tracers CONTOURS=pressure
*
*****
```

Appendix B

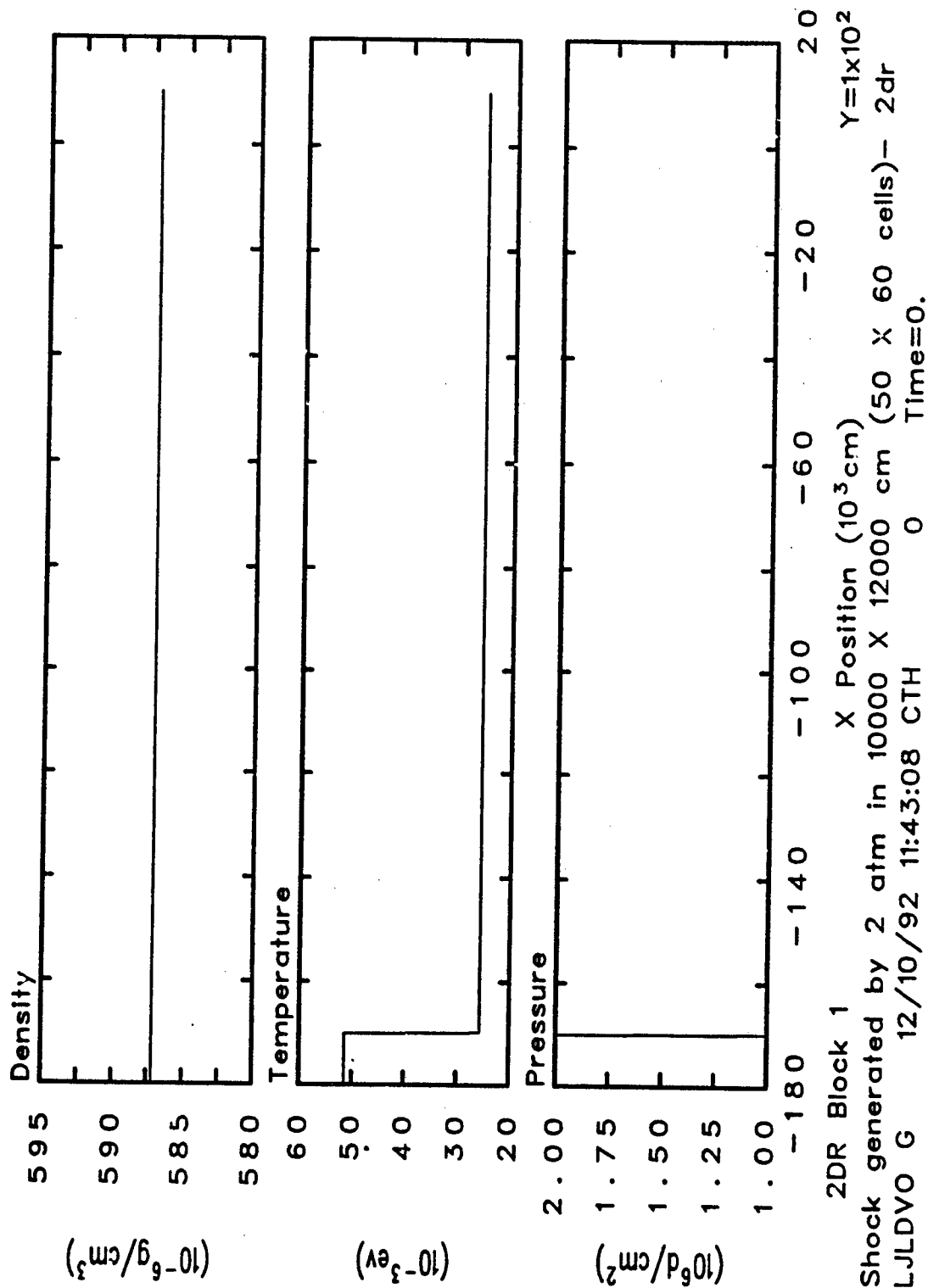
Output Data Plots

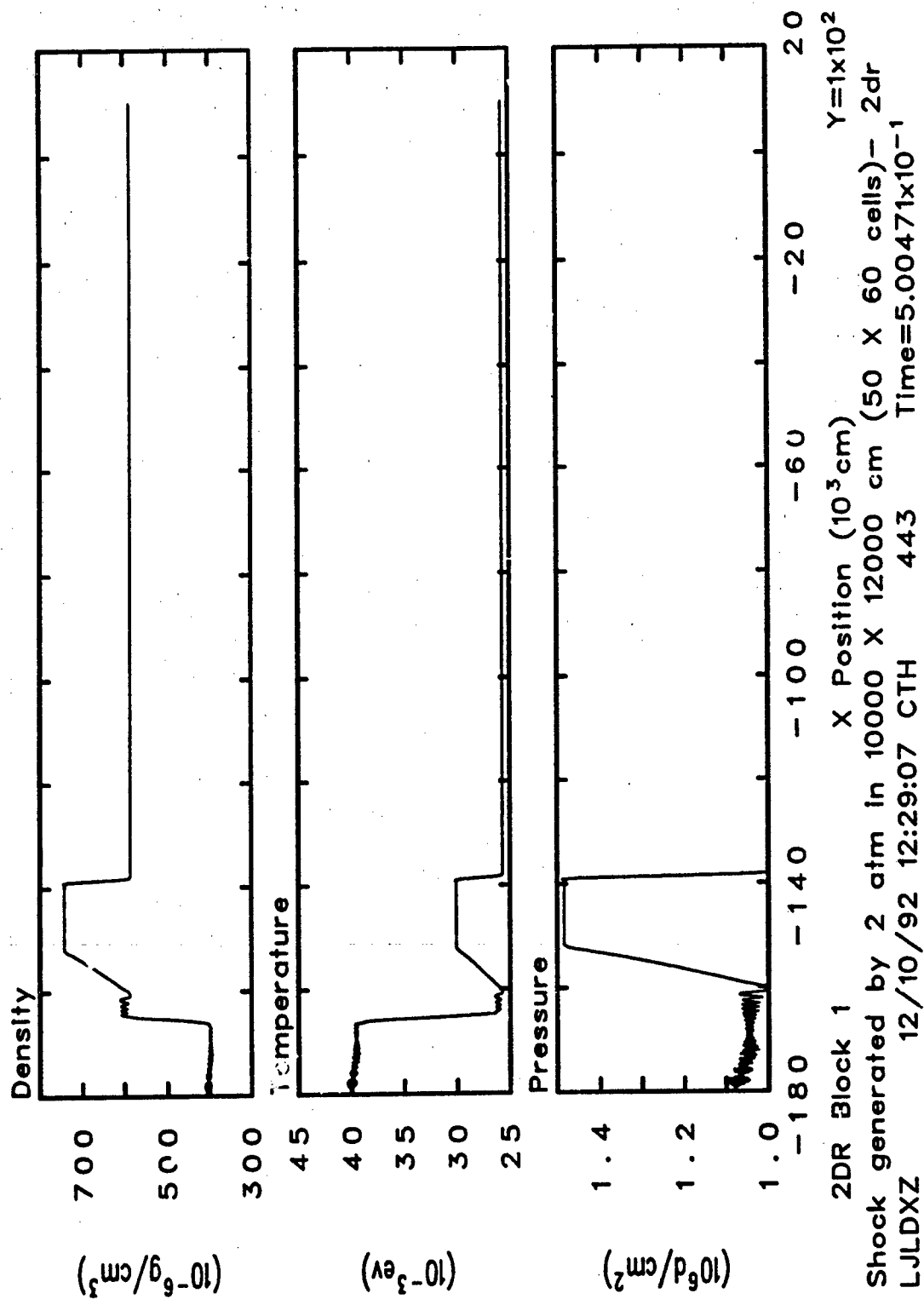
The plots in this appendix follow the order of the plot generation files given in Appendix A. The first set of plots show the shock front during the generation phase. The input file used to create these plots is found in Appendix A on page 73.

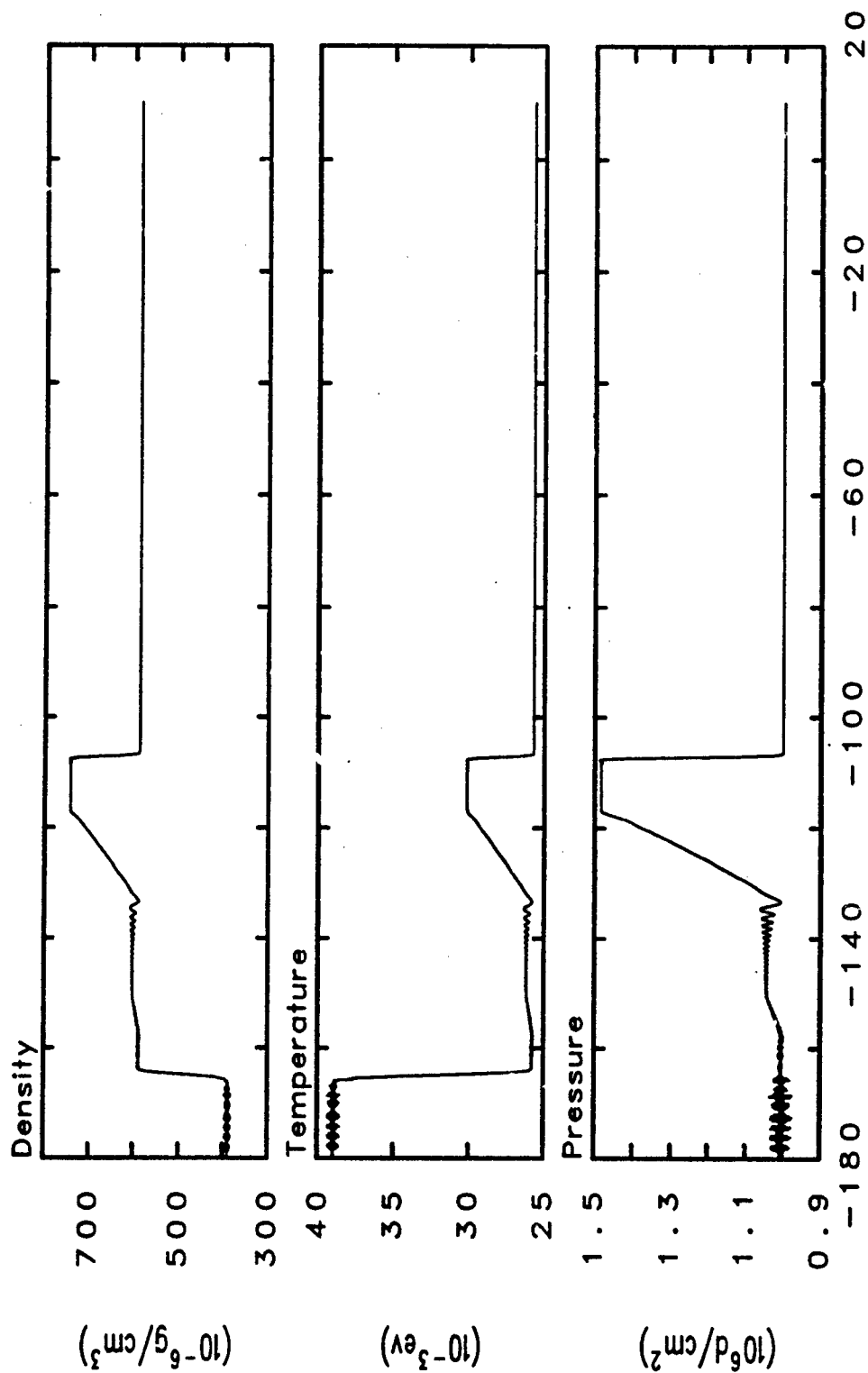
The plots beginning on page 89 show the pressure history as the shock front passes the 16 grid points. These represent the free-field condition for the shock wave passage. The input file "hisgrid.fix" generates these plots, and is presented in Appendix A, on page 74.

Time history plots of the overpressure at each of the five tracers near the vertex of each of the twelve buildings are presented beginning on page 105. The input file for generating these, "histrace," is given in Appendix A, on page 76.

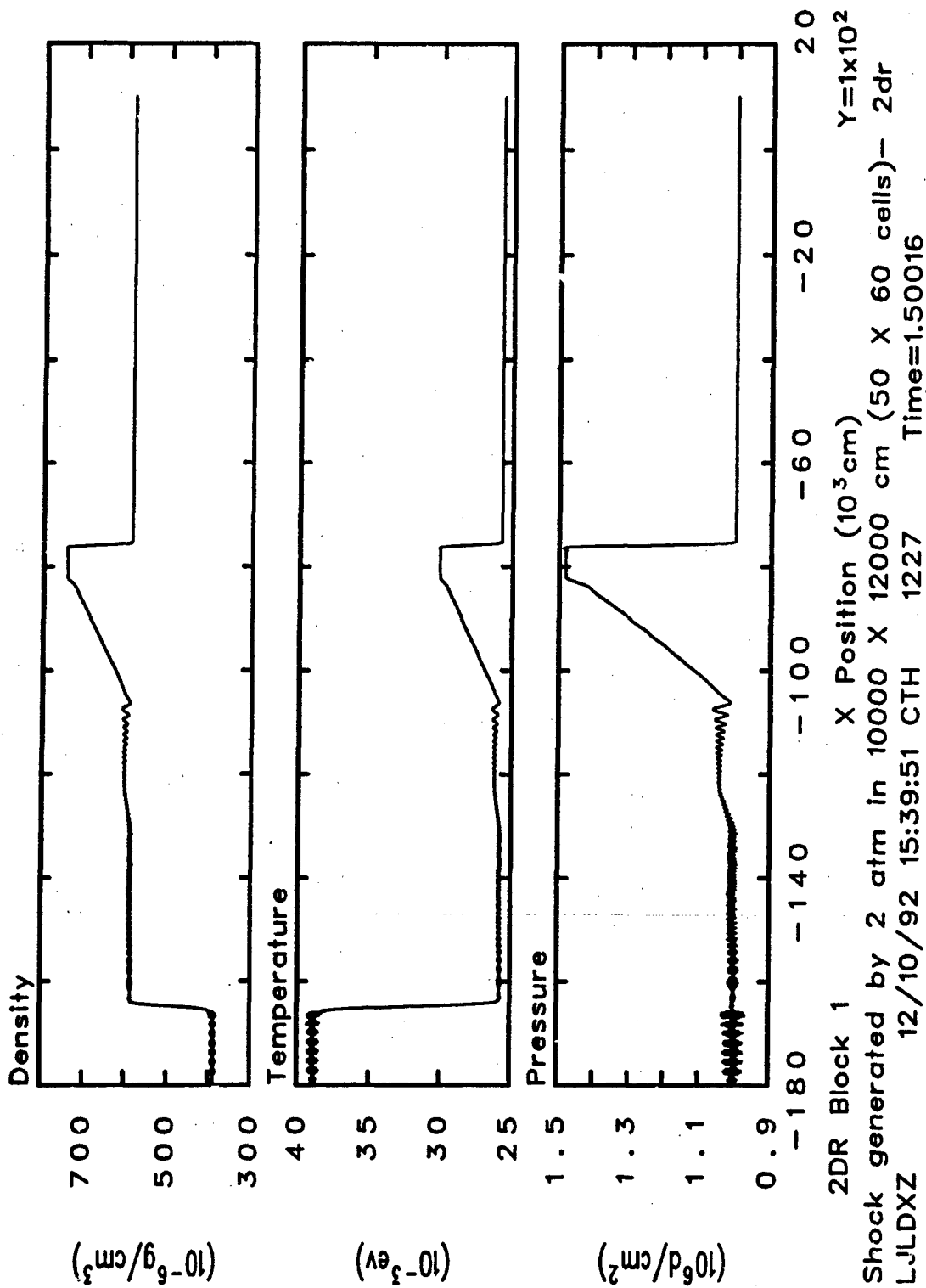
Finally, selected two-dimensional contour plots showing the interaction of the shock wave into the buildings of cases twelve, six, and ten begin on page 165. These contour plots are preceded by a contour pressure legend that applies to all the contour plots. The input data file "contour," presented on page 81 of Appendix A, generates these plots.

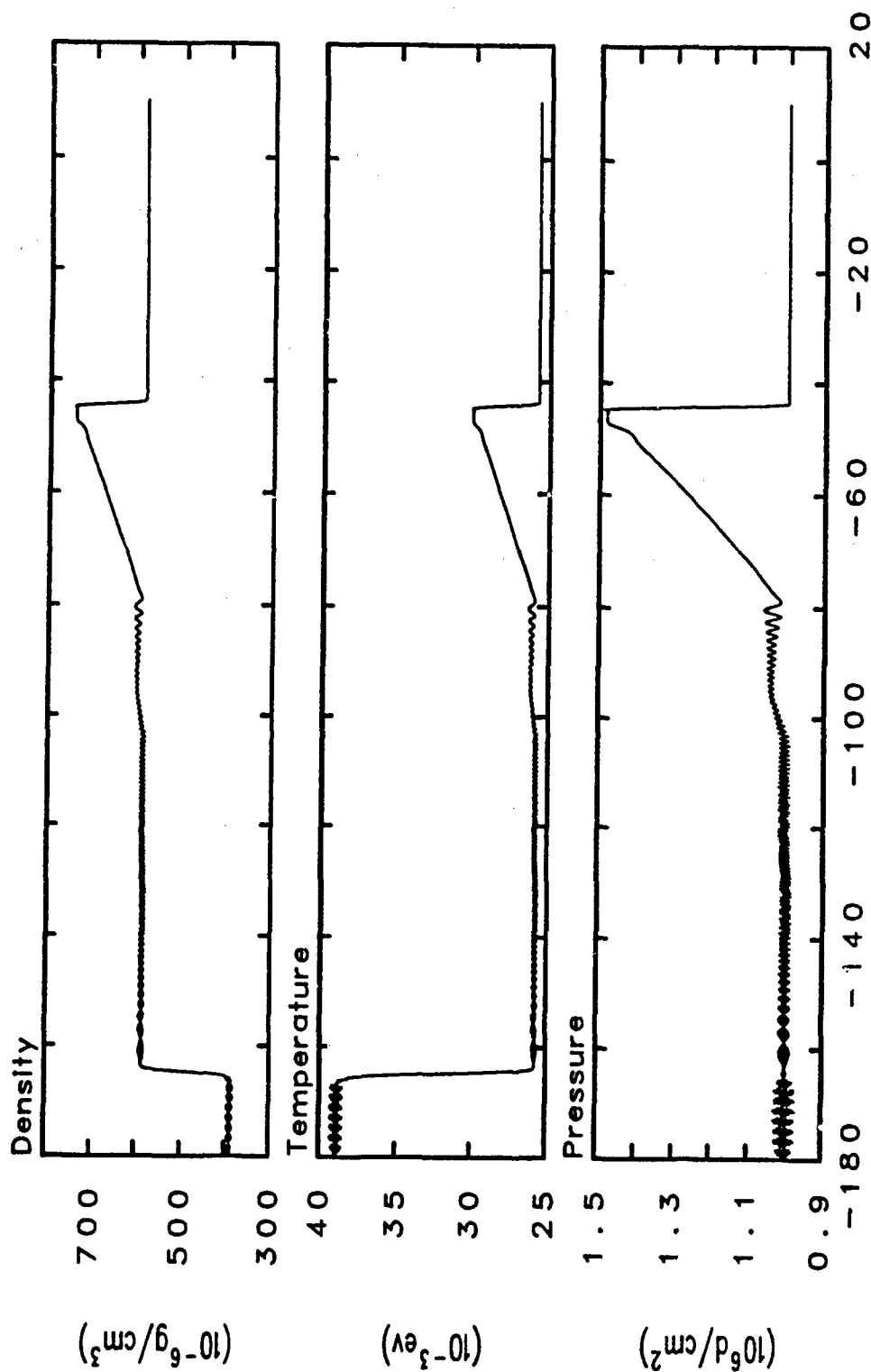




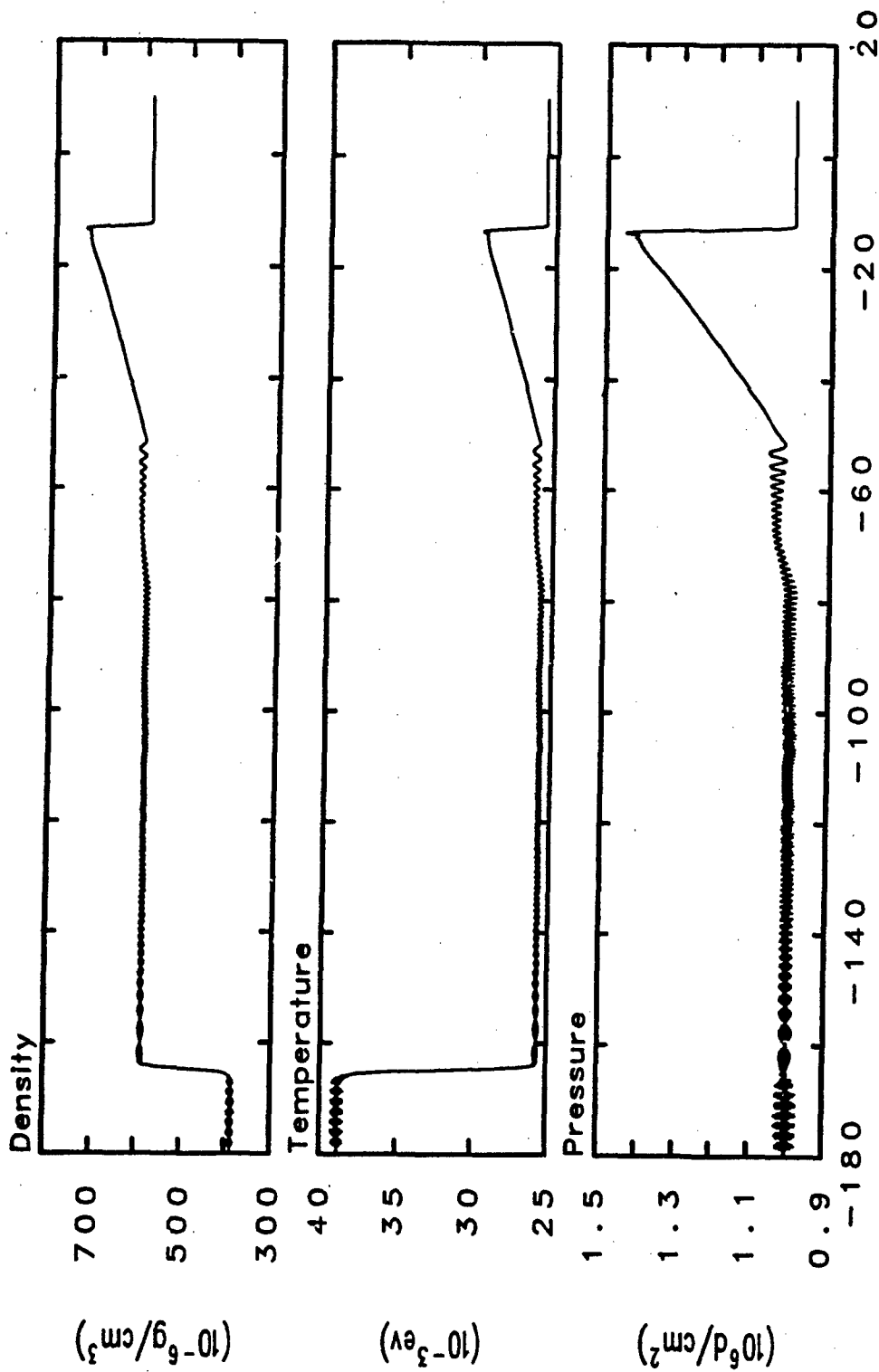


2DR Block 1 X Position (10^3 cm) $Y=1 \times 10^2$
 Shock generated by 2 atm in 10000 X 12000 cm (50 X 60 cells) - 2dr
 LJ'DXZ 12/10/92 13:43:05 CTH 835 Time=1.00031

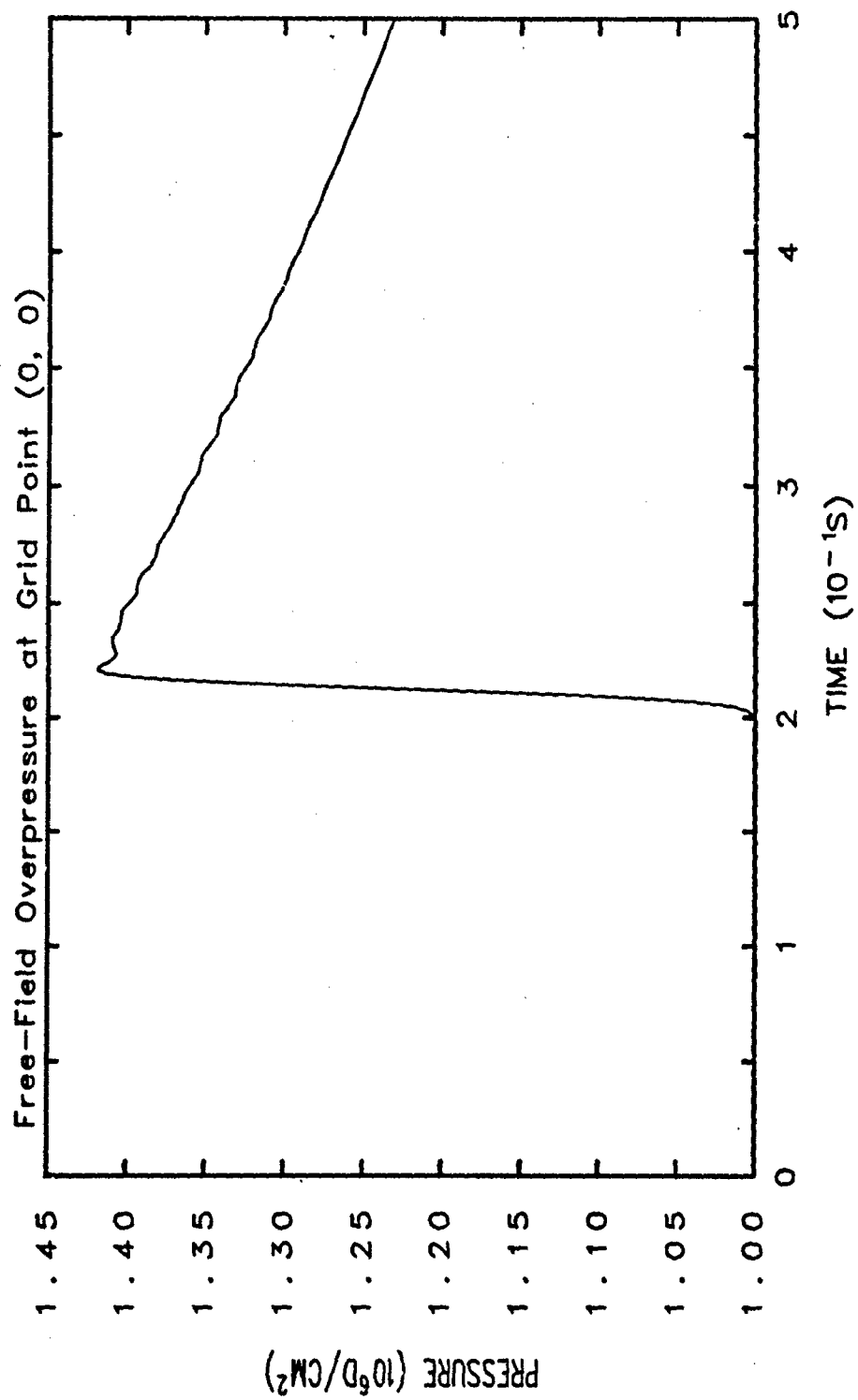


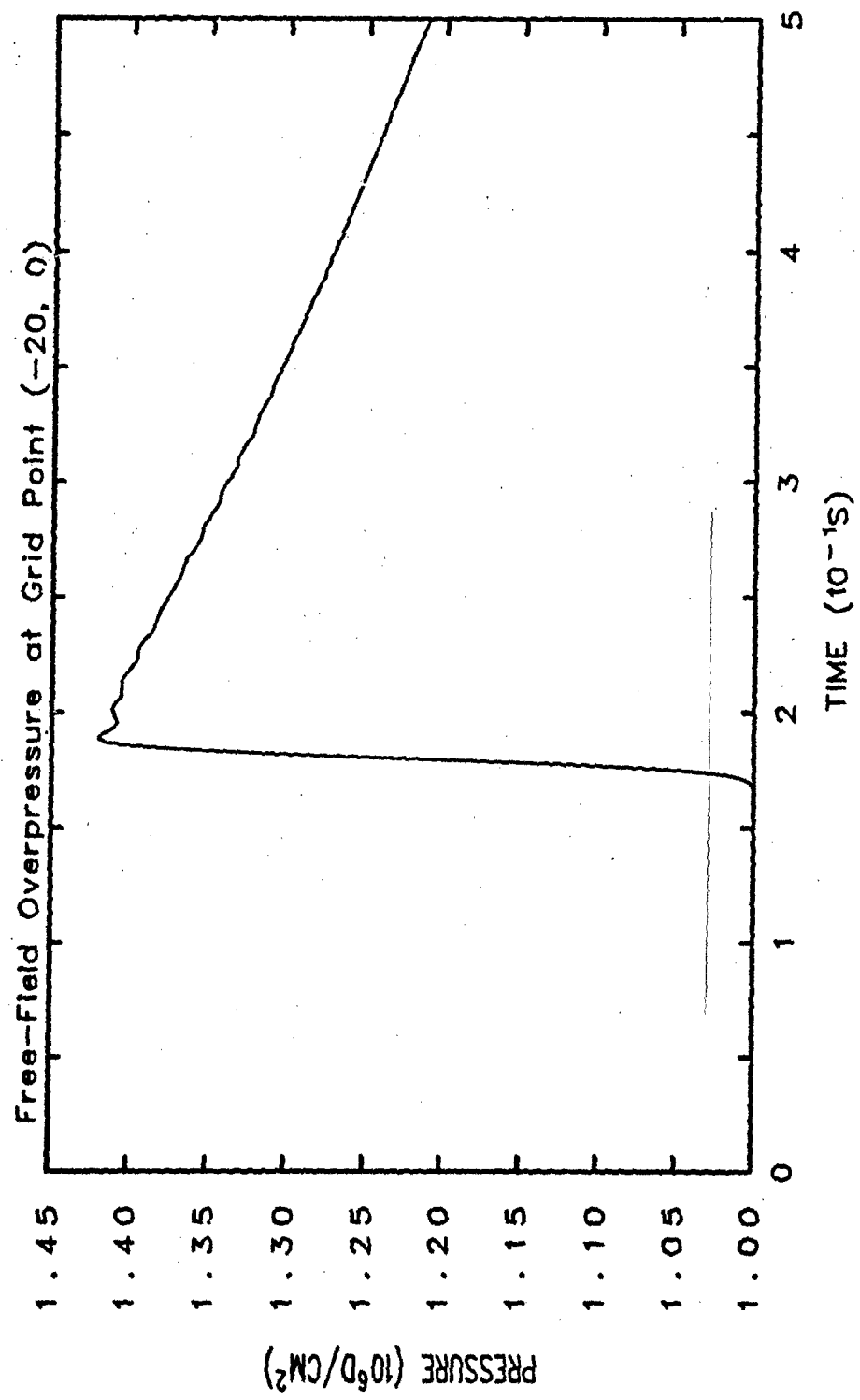


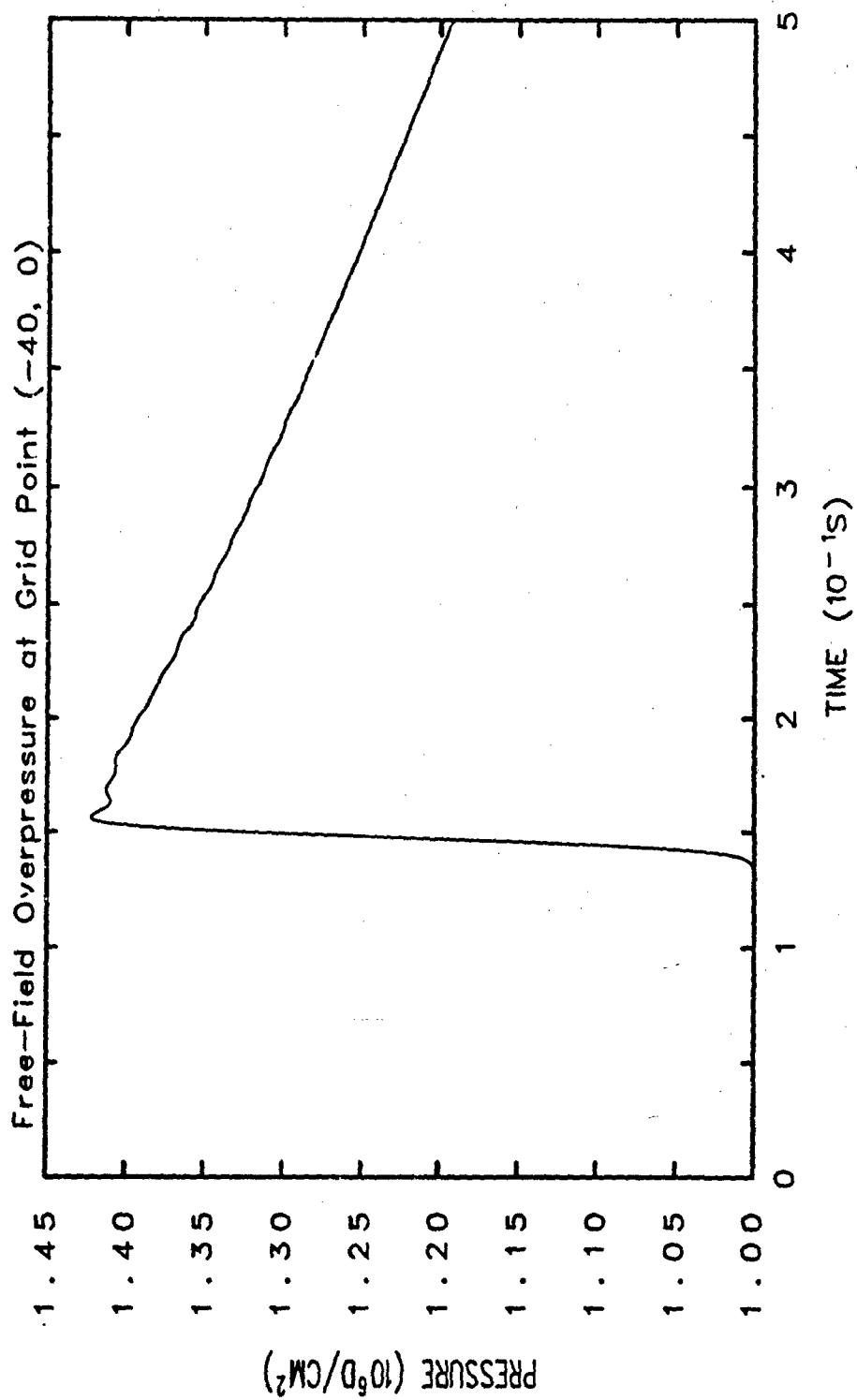
2DR Block 1 X Position (10^3 cm) $\gamma=1 \times 10^2$
 Shock generated by 2 atm in 10000 X 12000 cm (50 X 60 cells)- 2dr
 LJLDXZ 12/10/92 18:24:49 CTH 1619 Time=2.00002

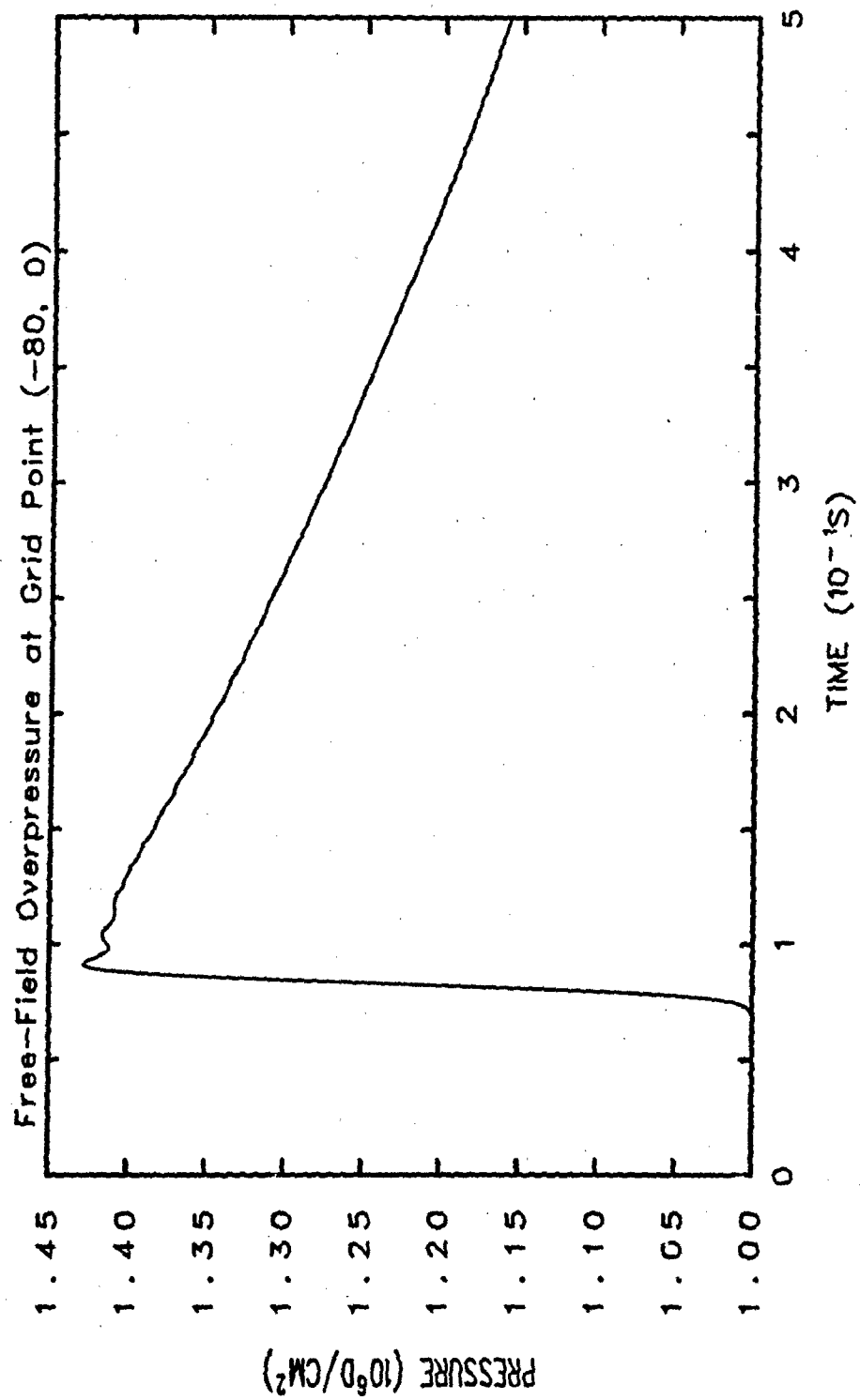


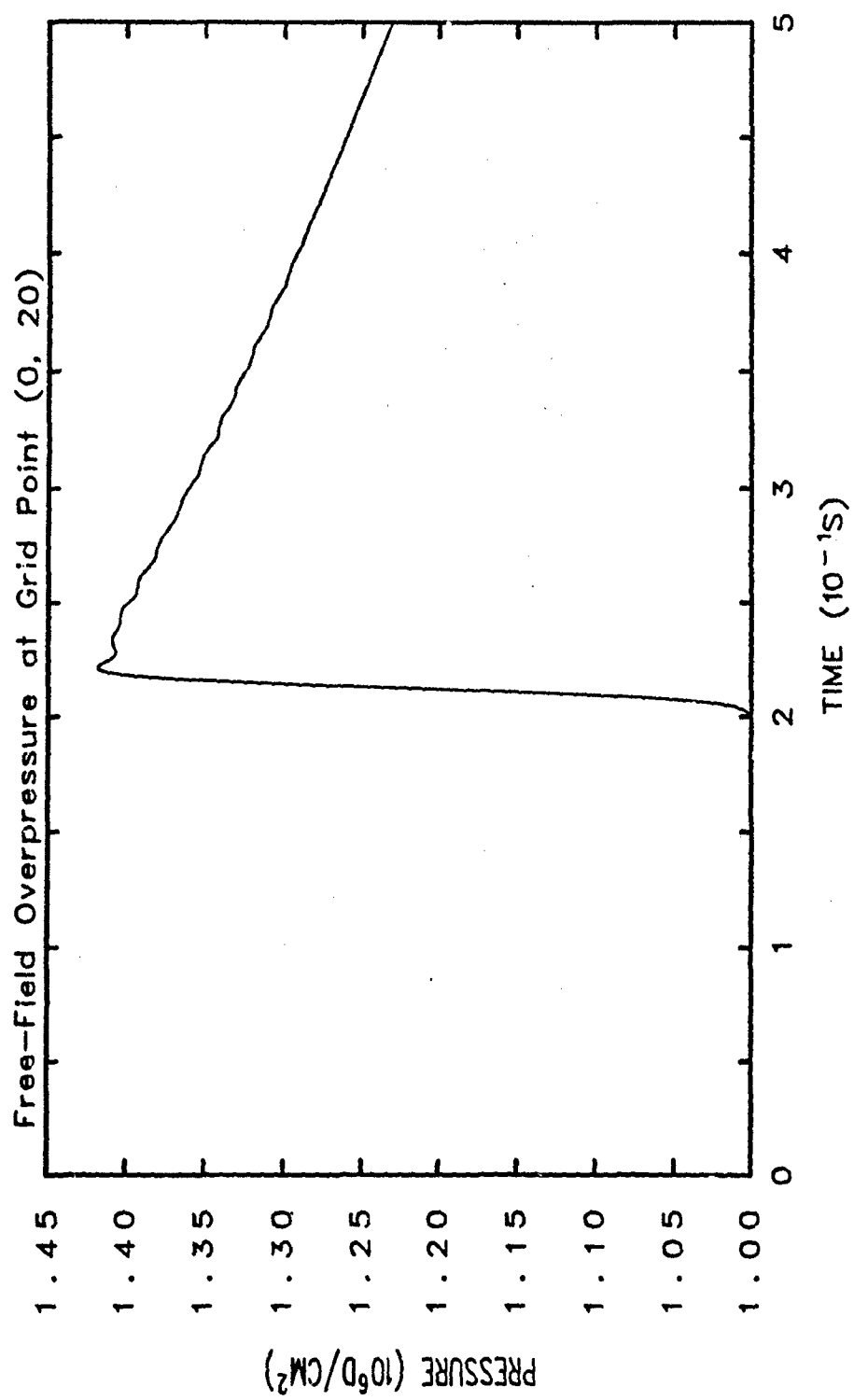
2DR Block 1
 Shock generated by 2 atm in 10000 X 12000 cm (50 X 60 cells)- 2dr
 LJLDXZ 12/10/92 21:51:07 CTH 2010 Time=2.5002
 $Y=1 \times 10^2$

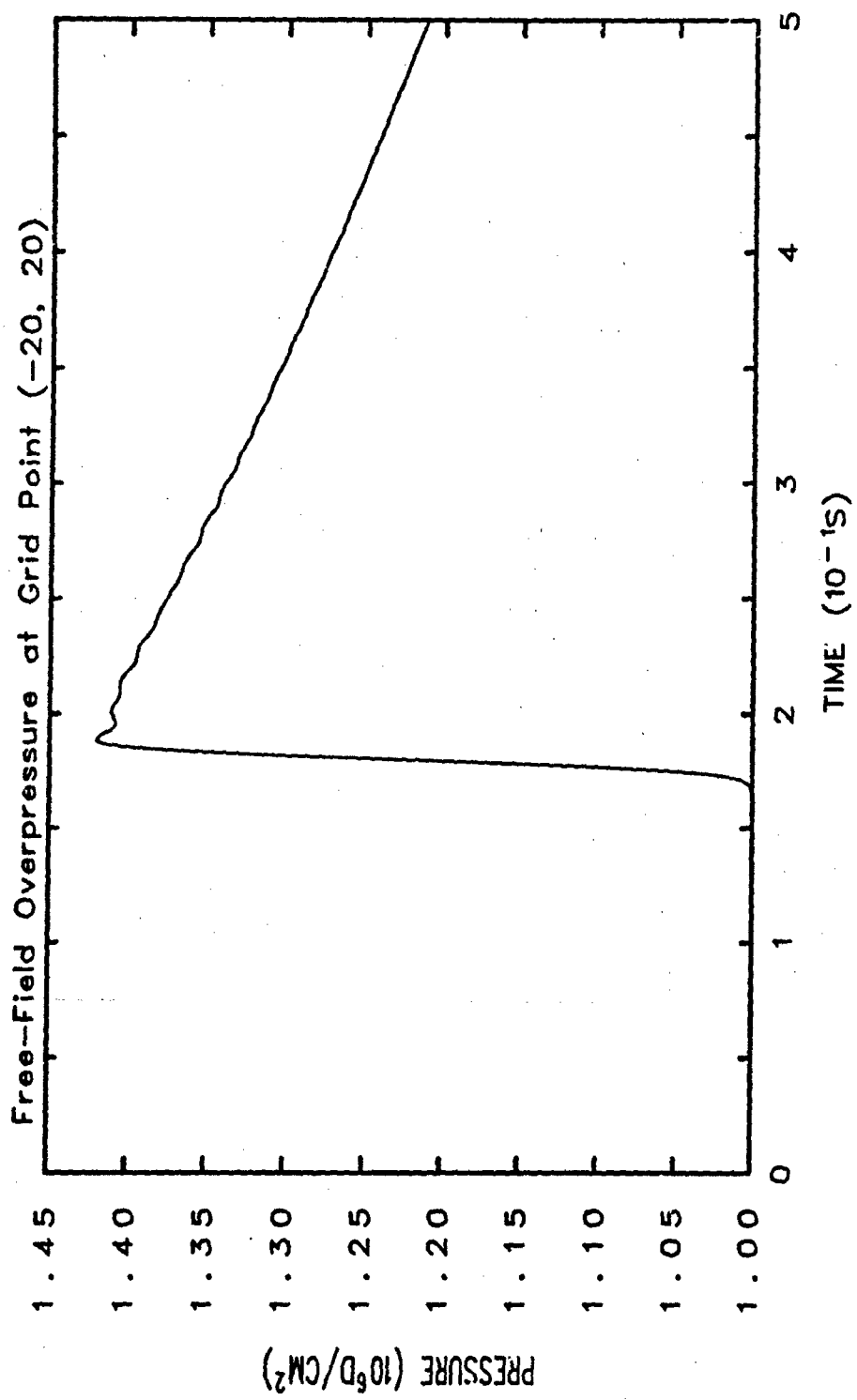


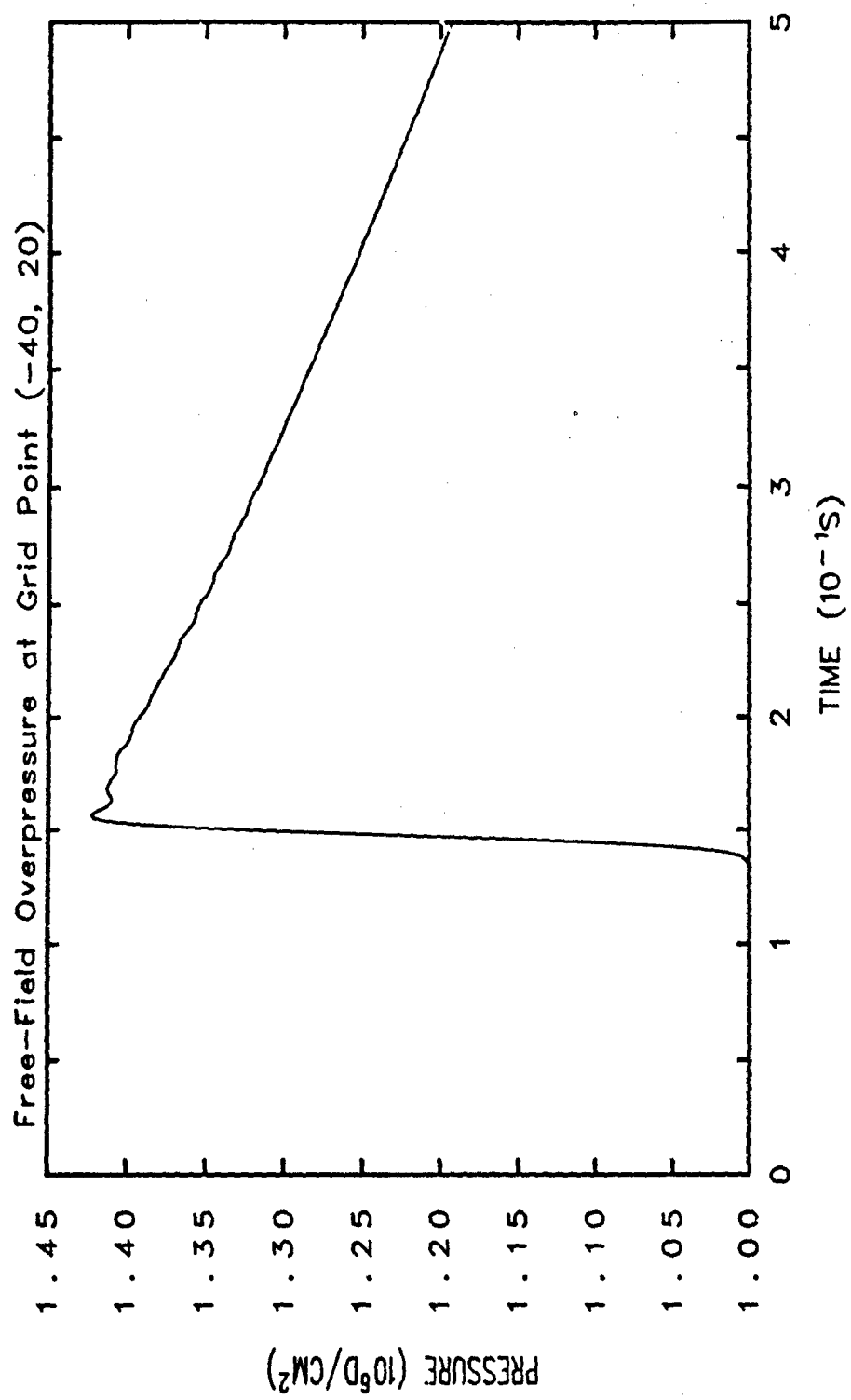


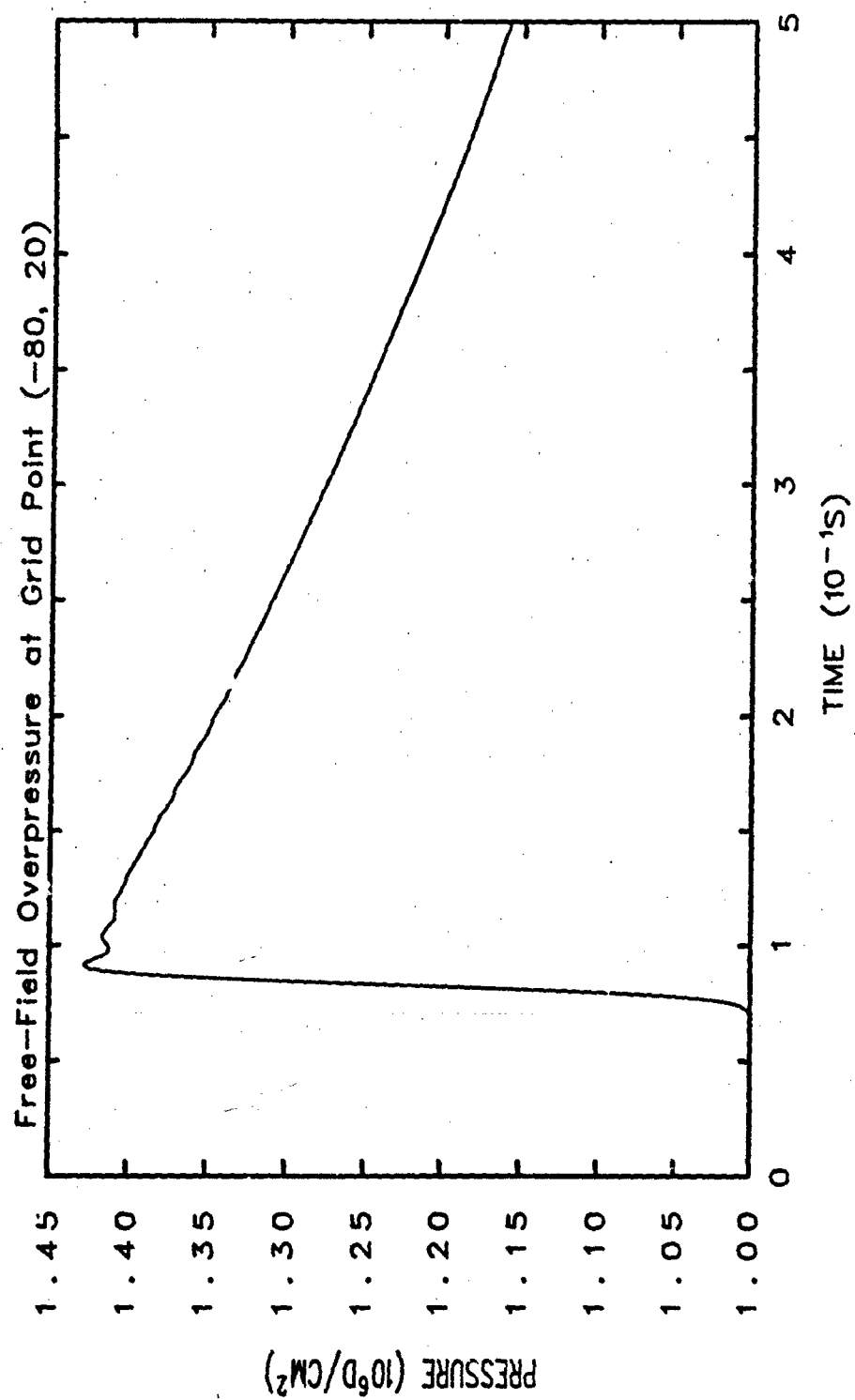


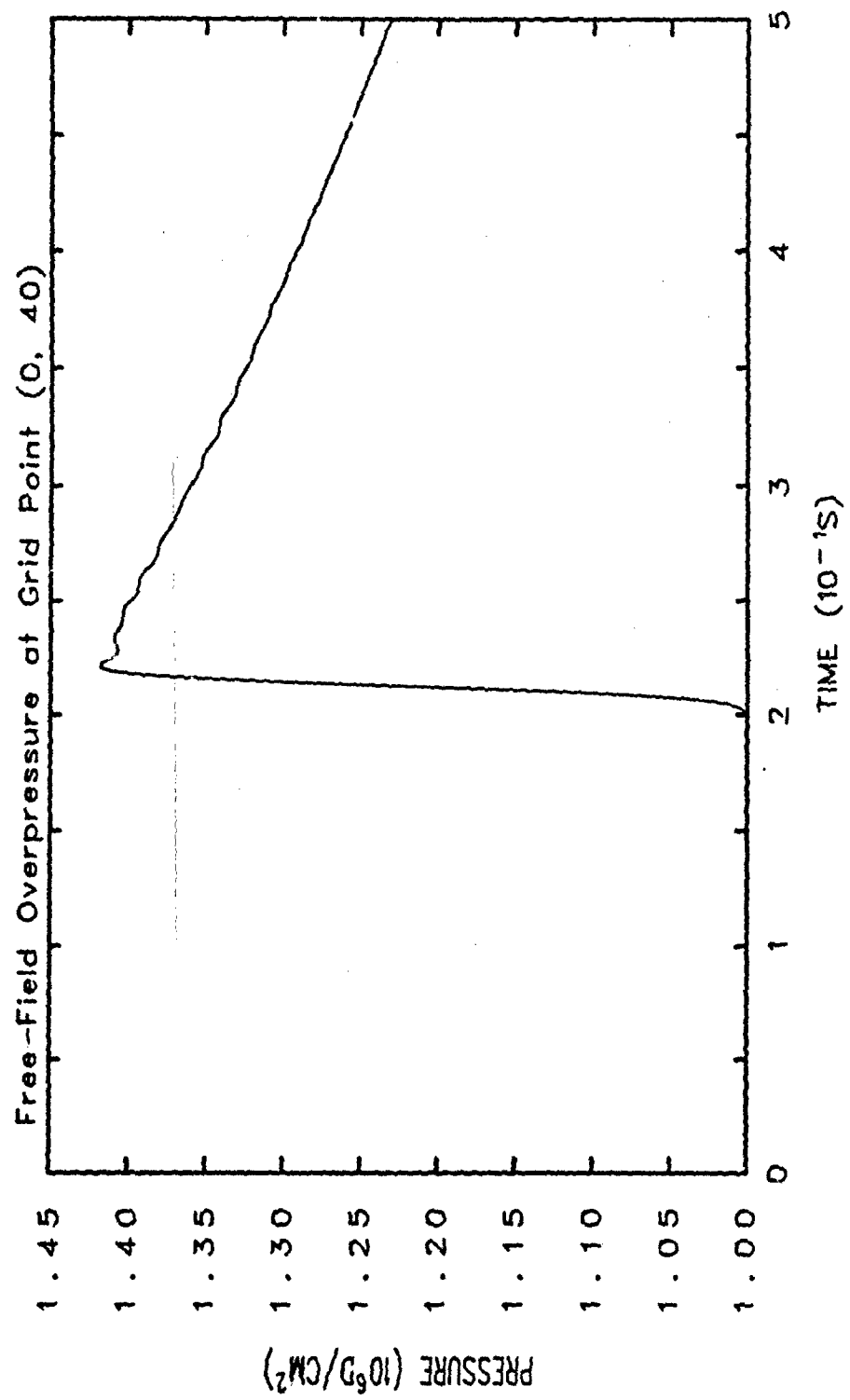


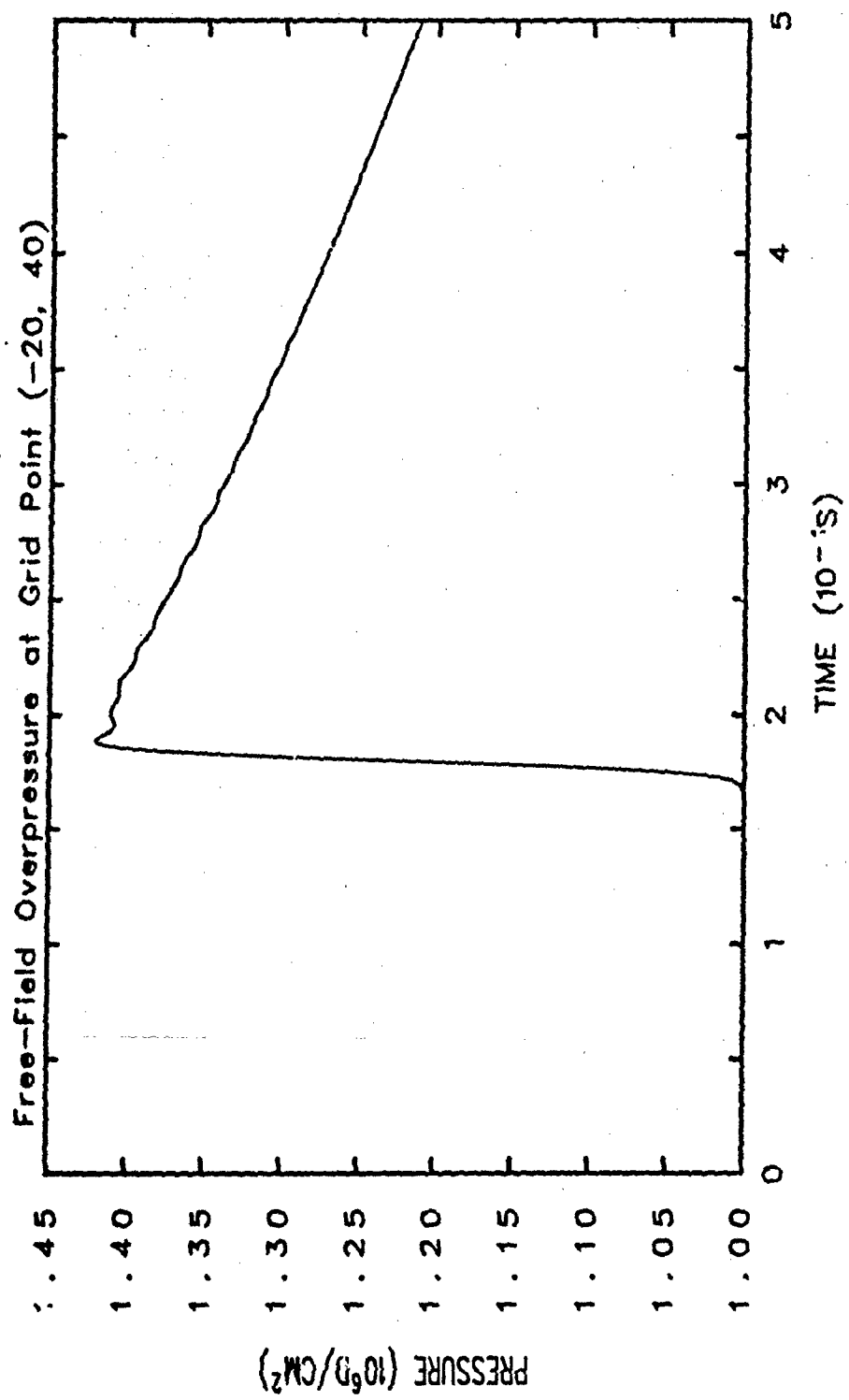


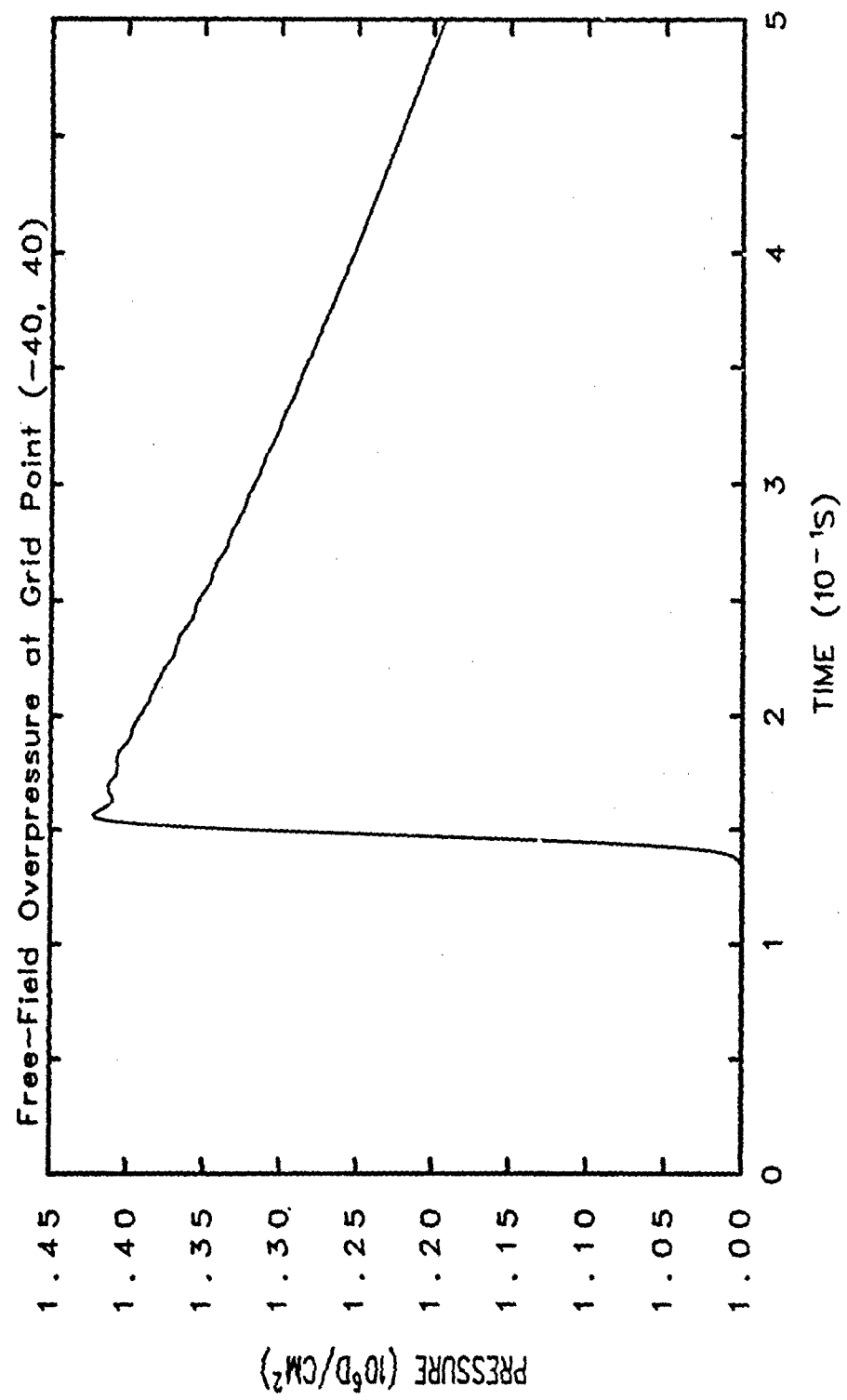


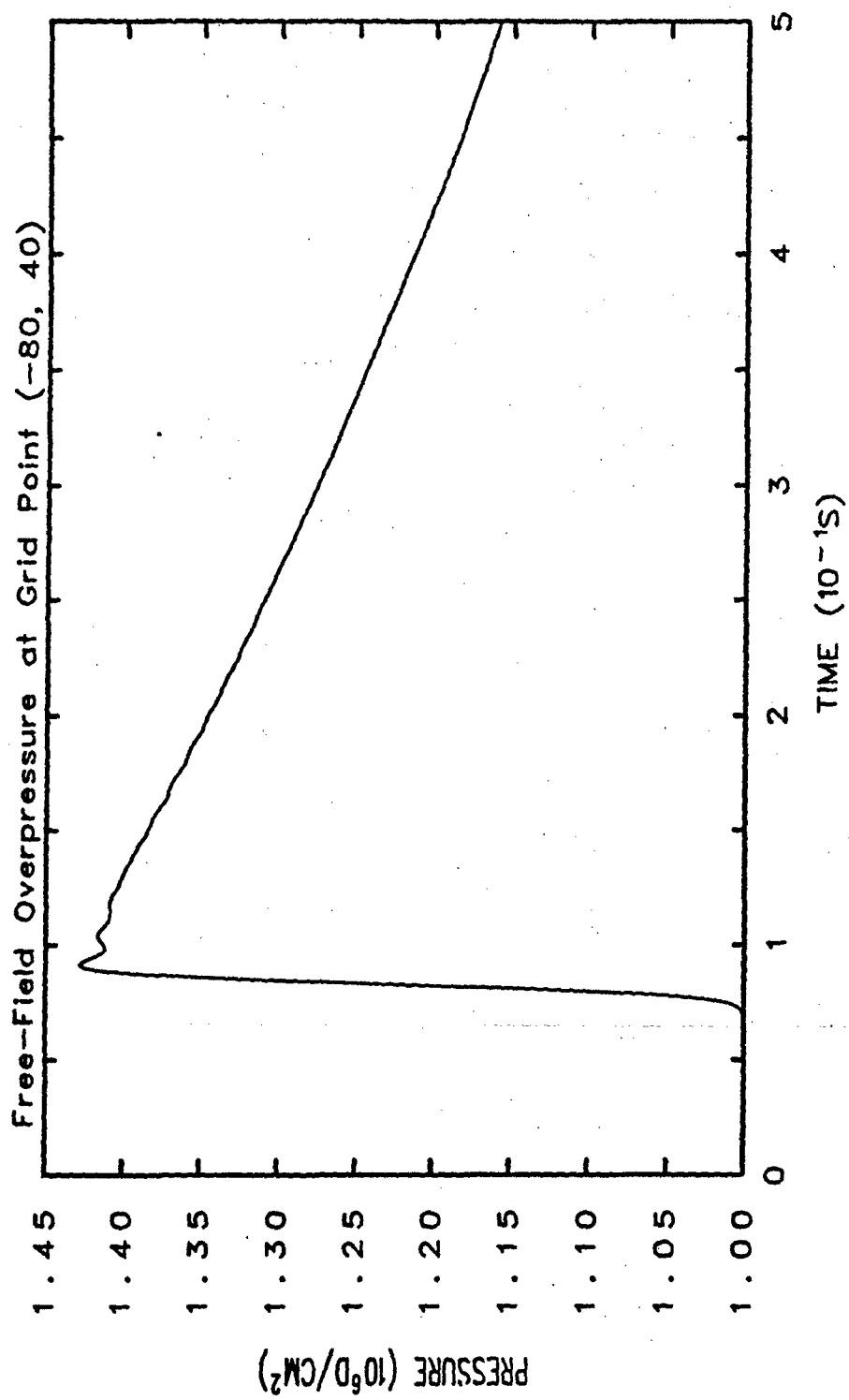


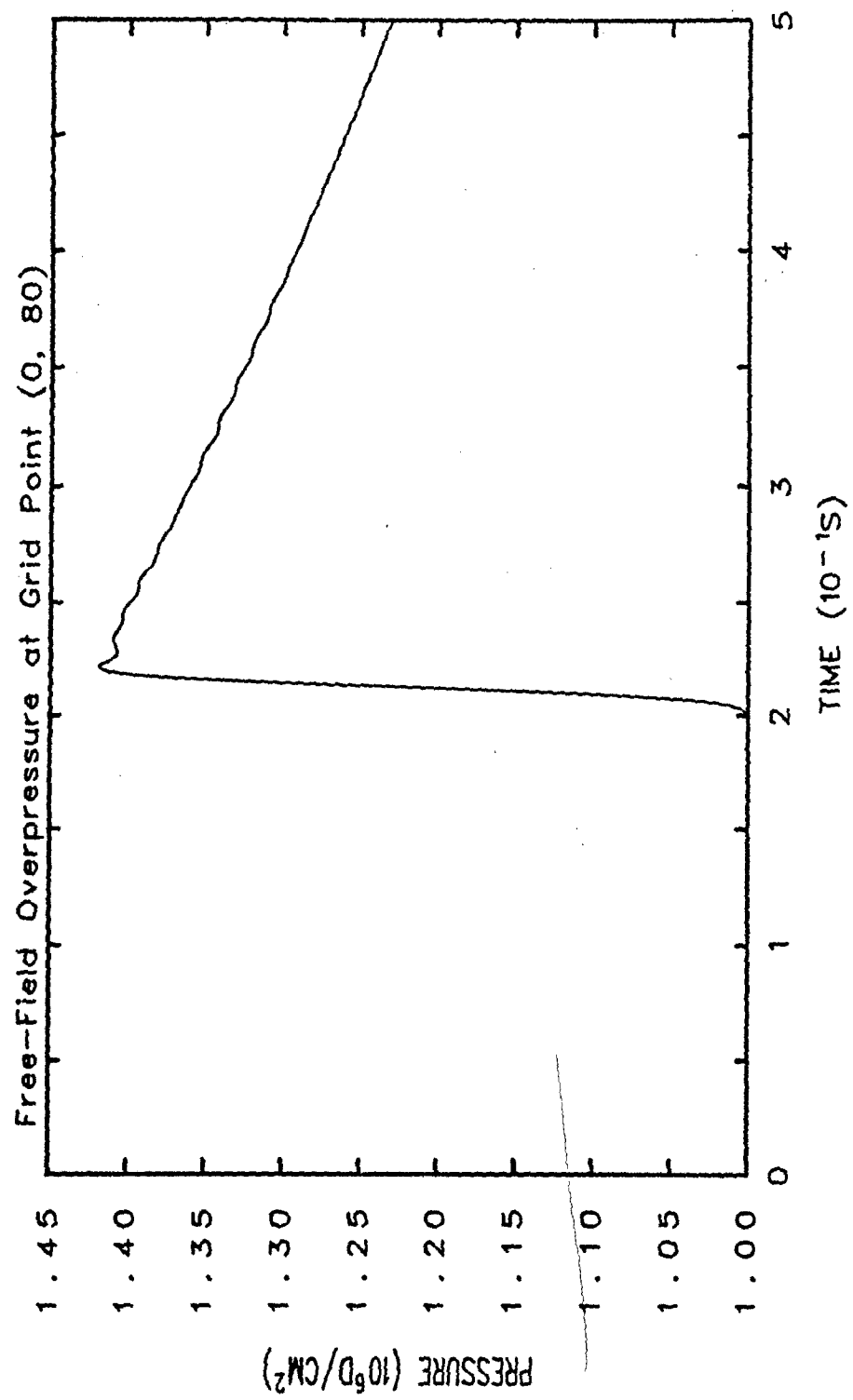


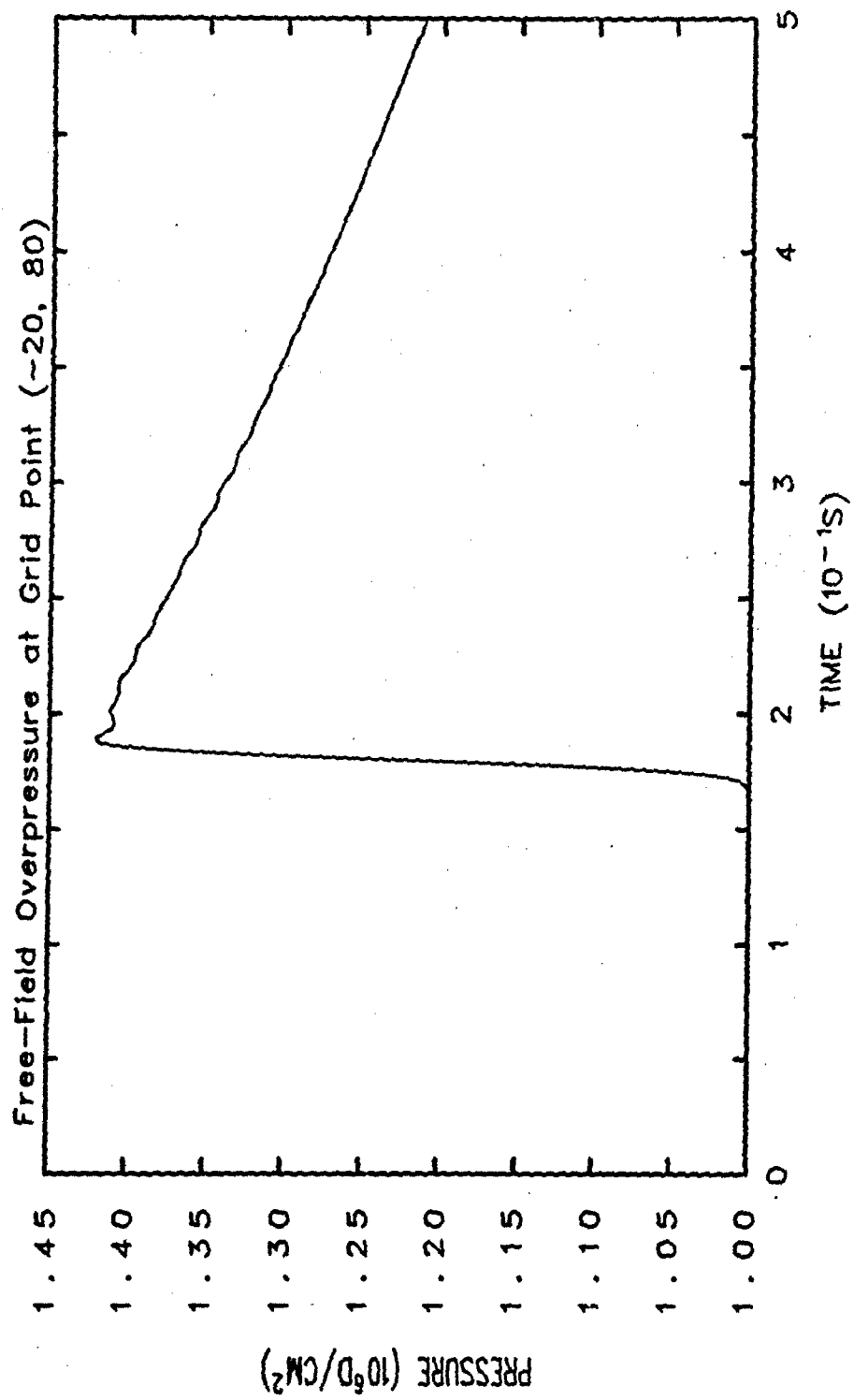


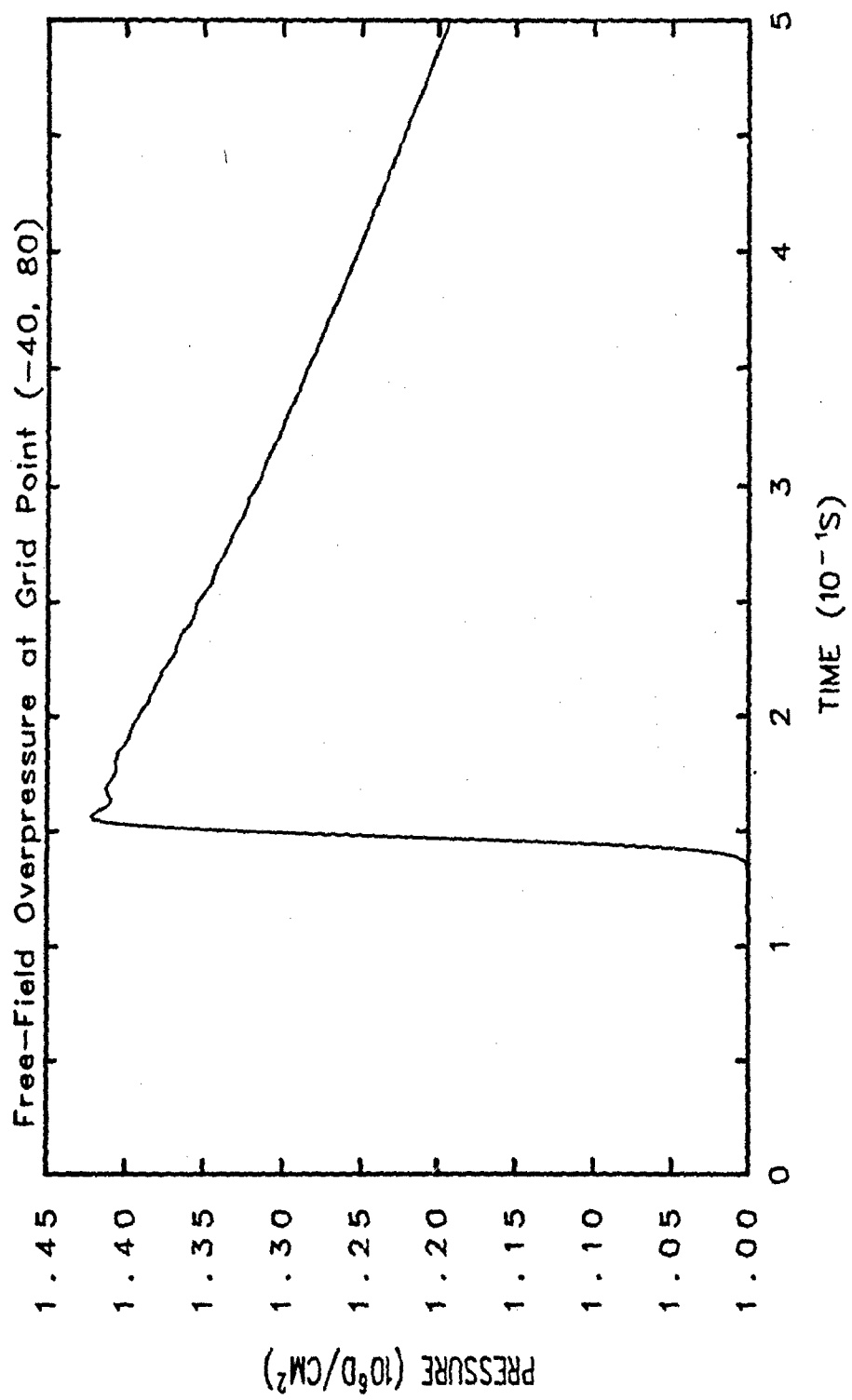


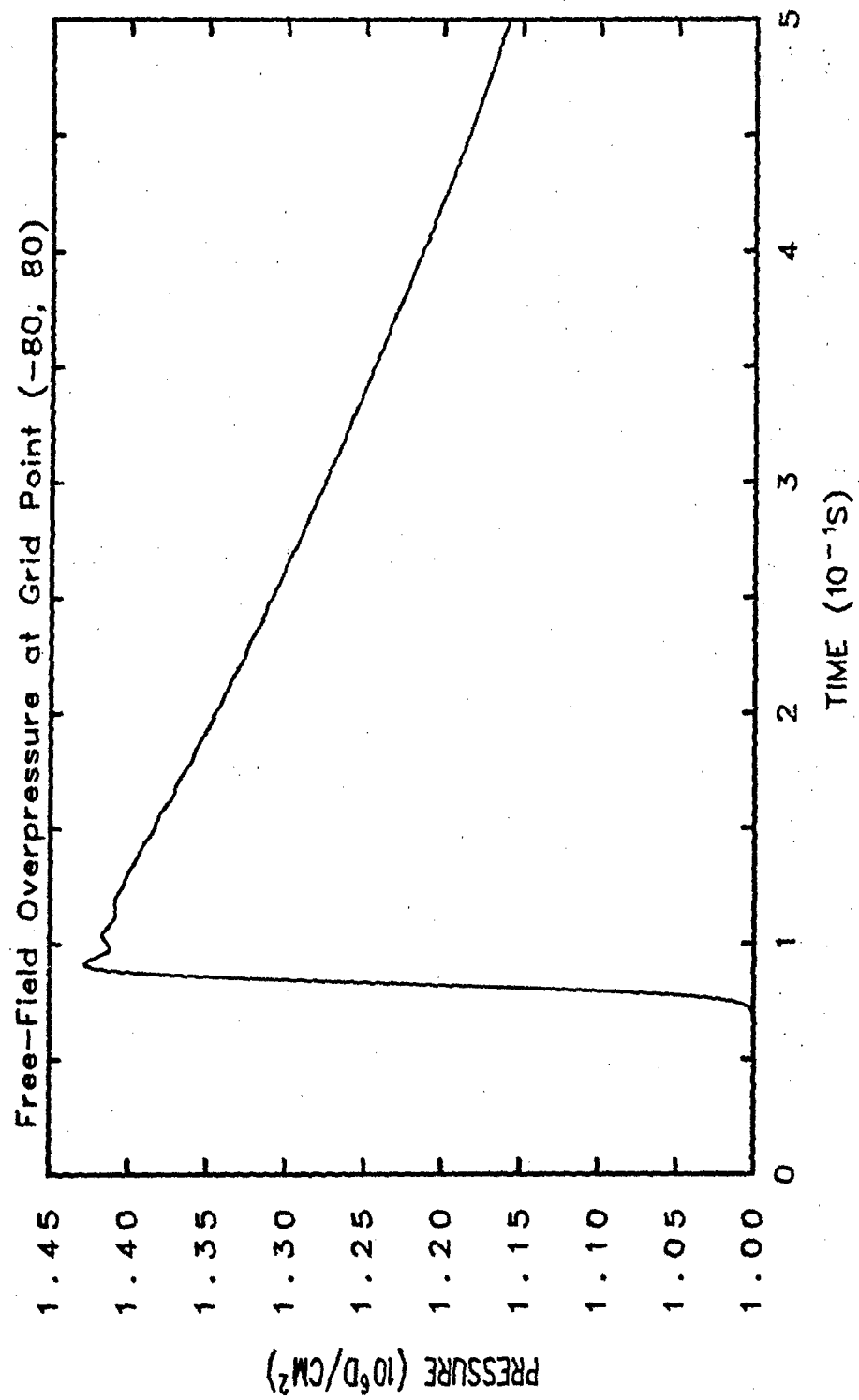


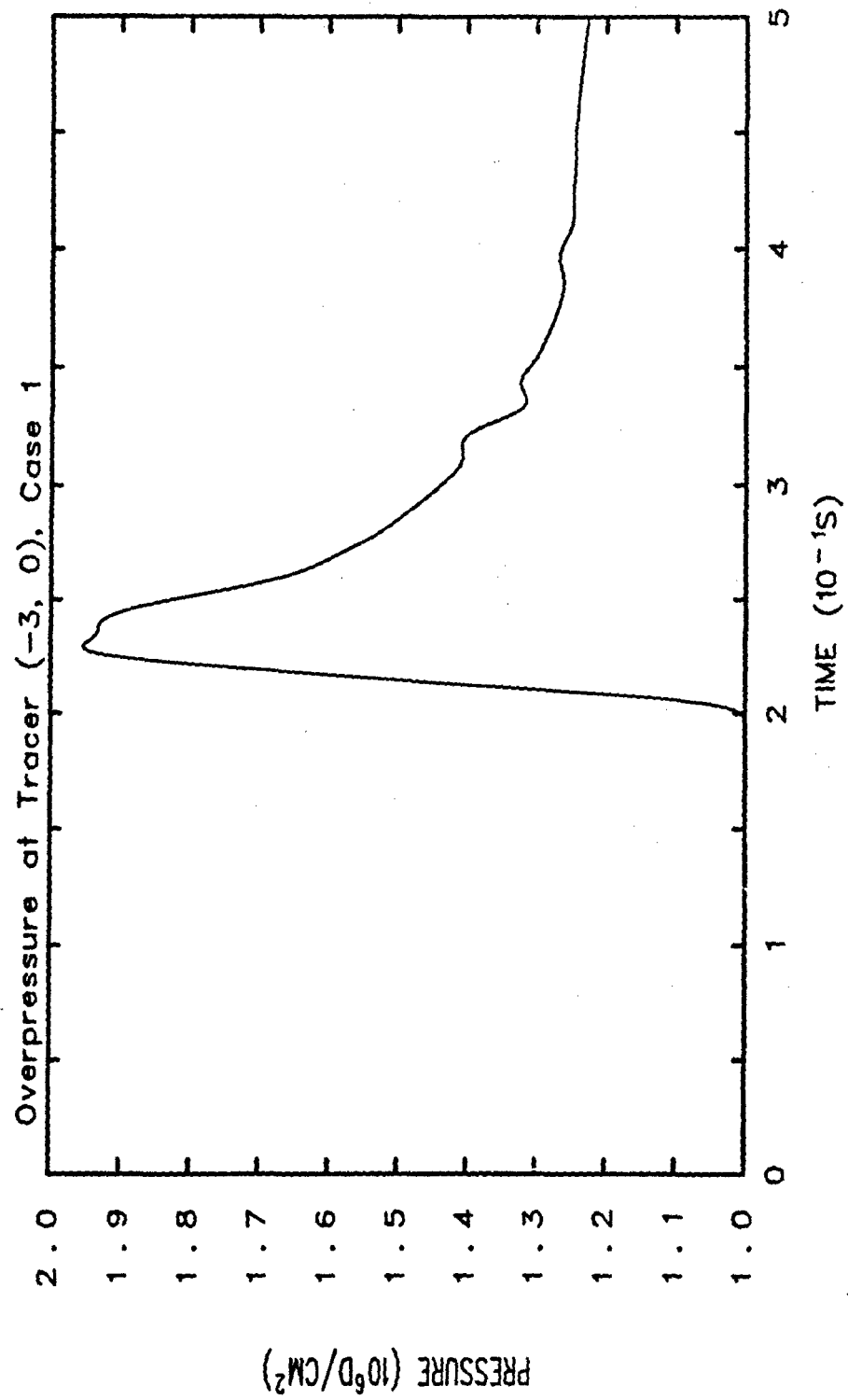


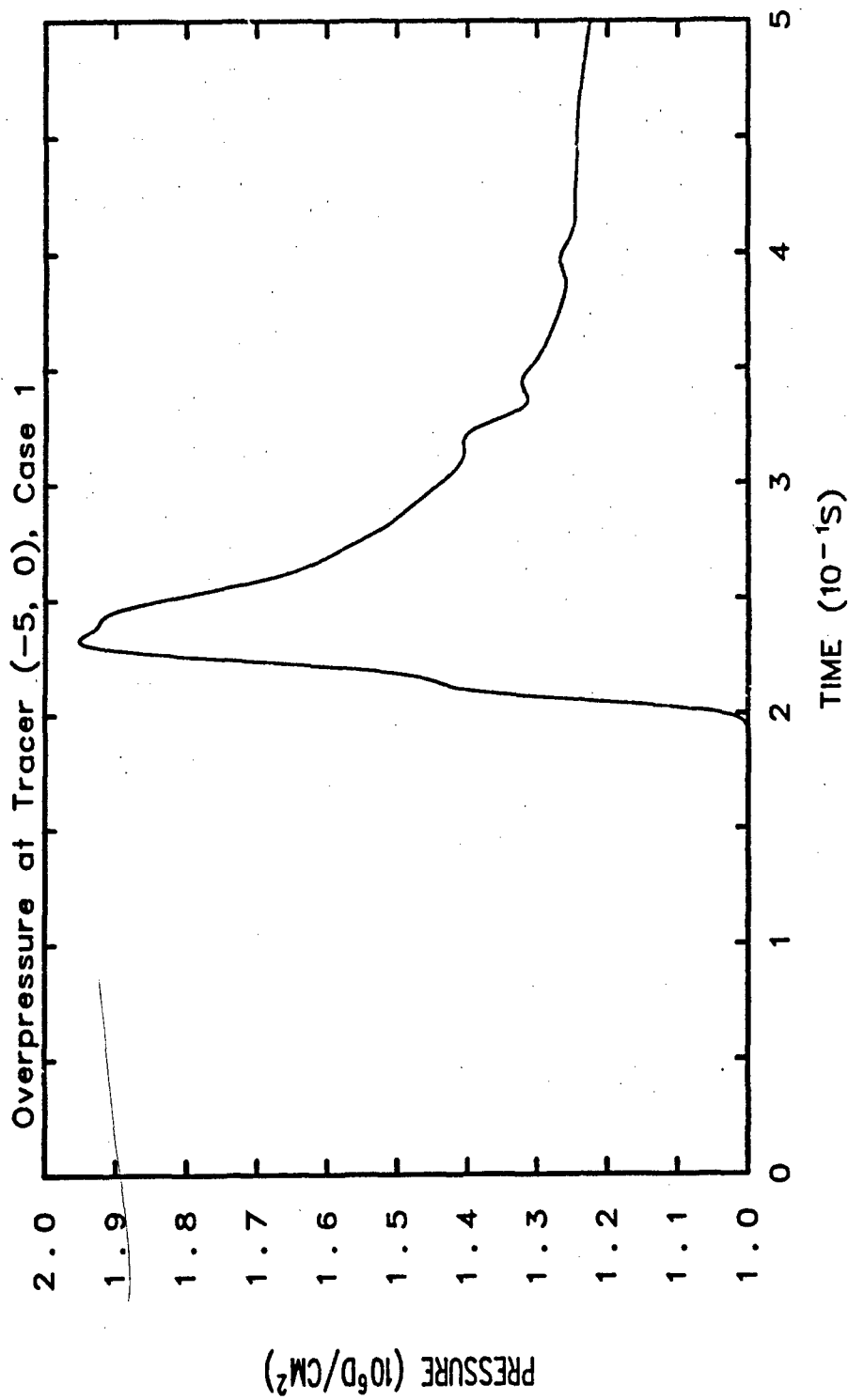


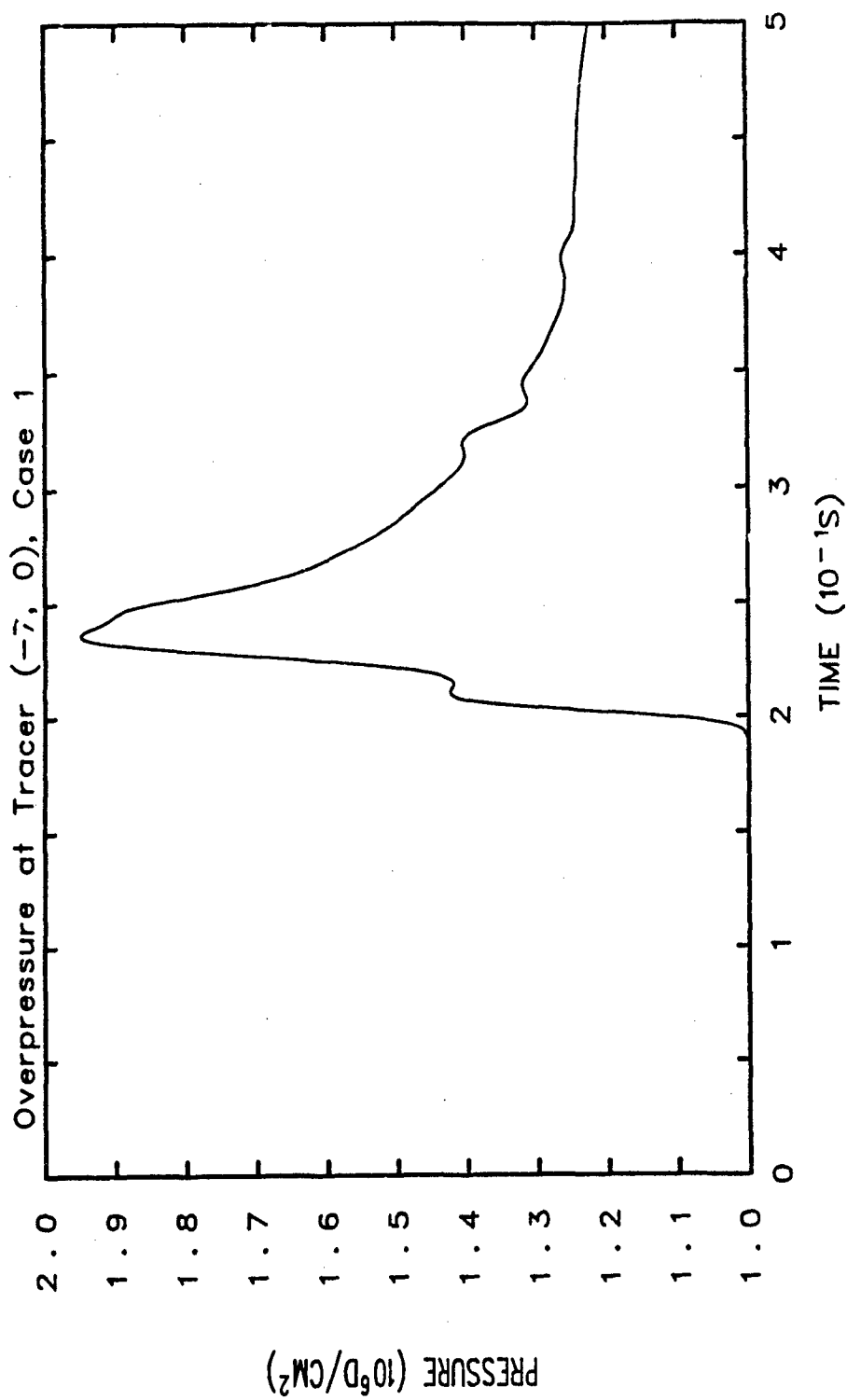


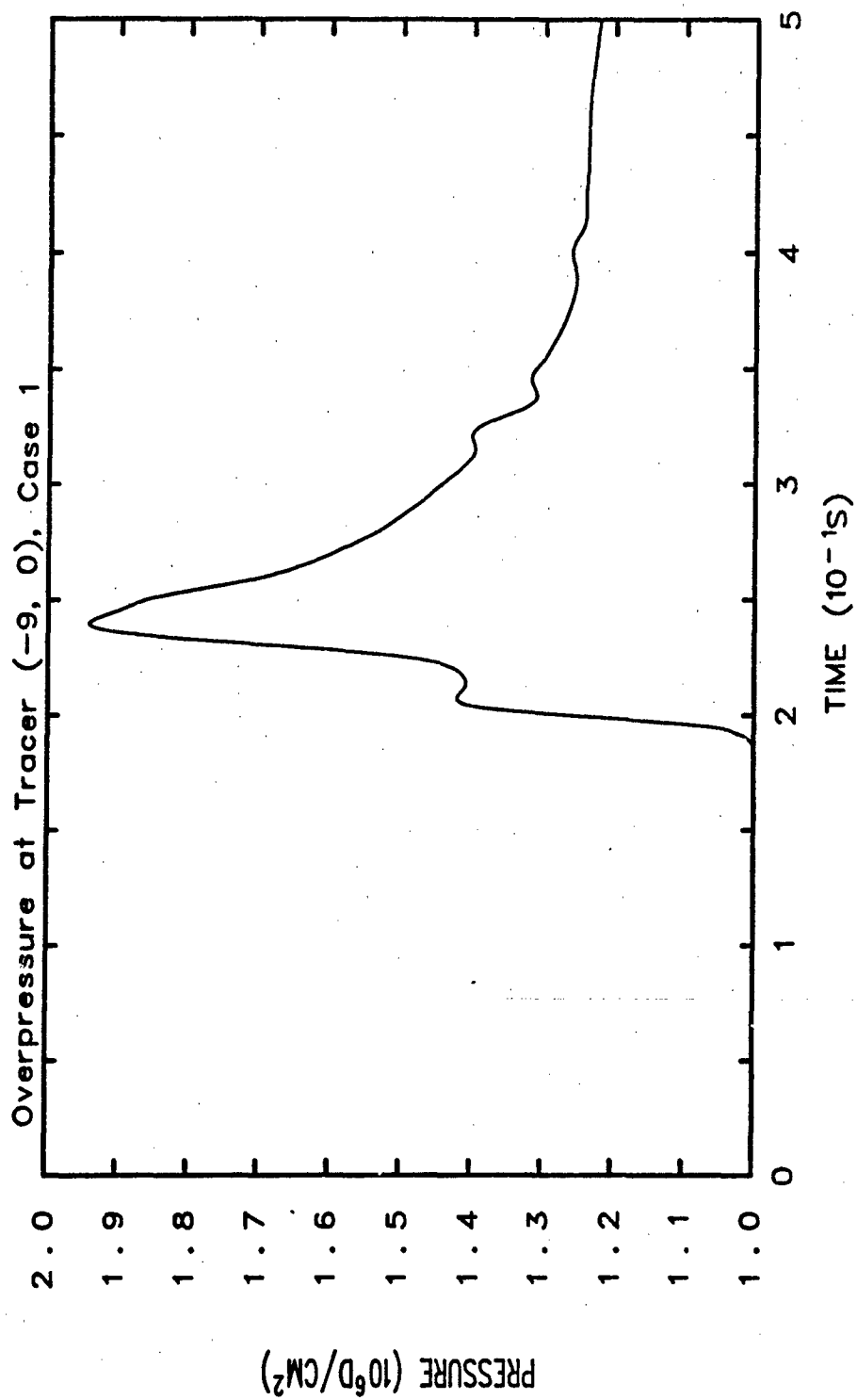


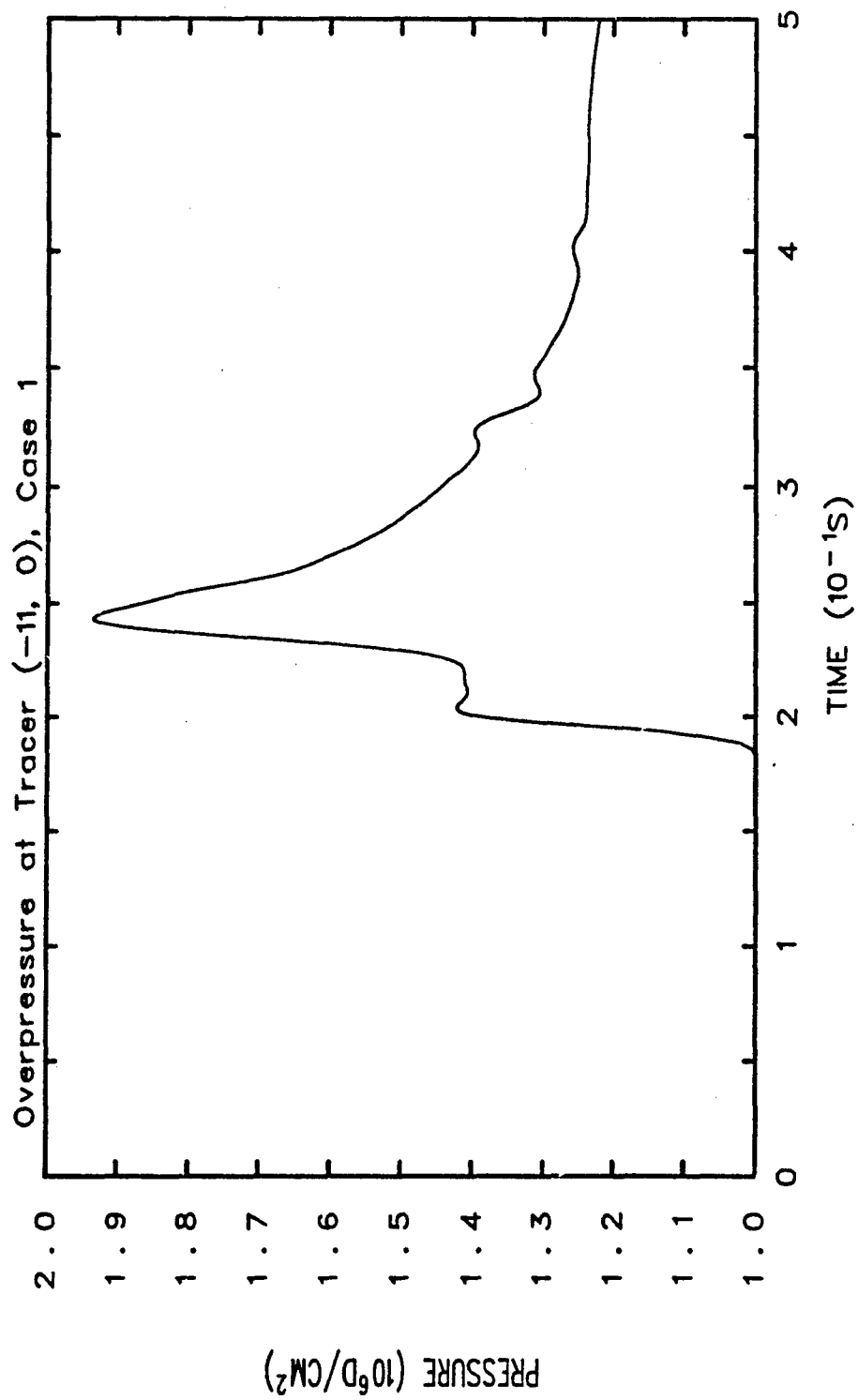


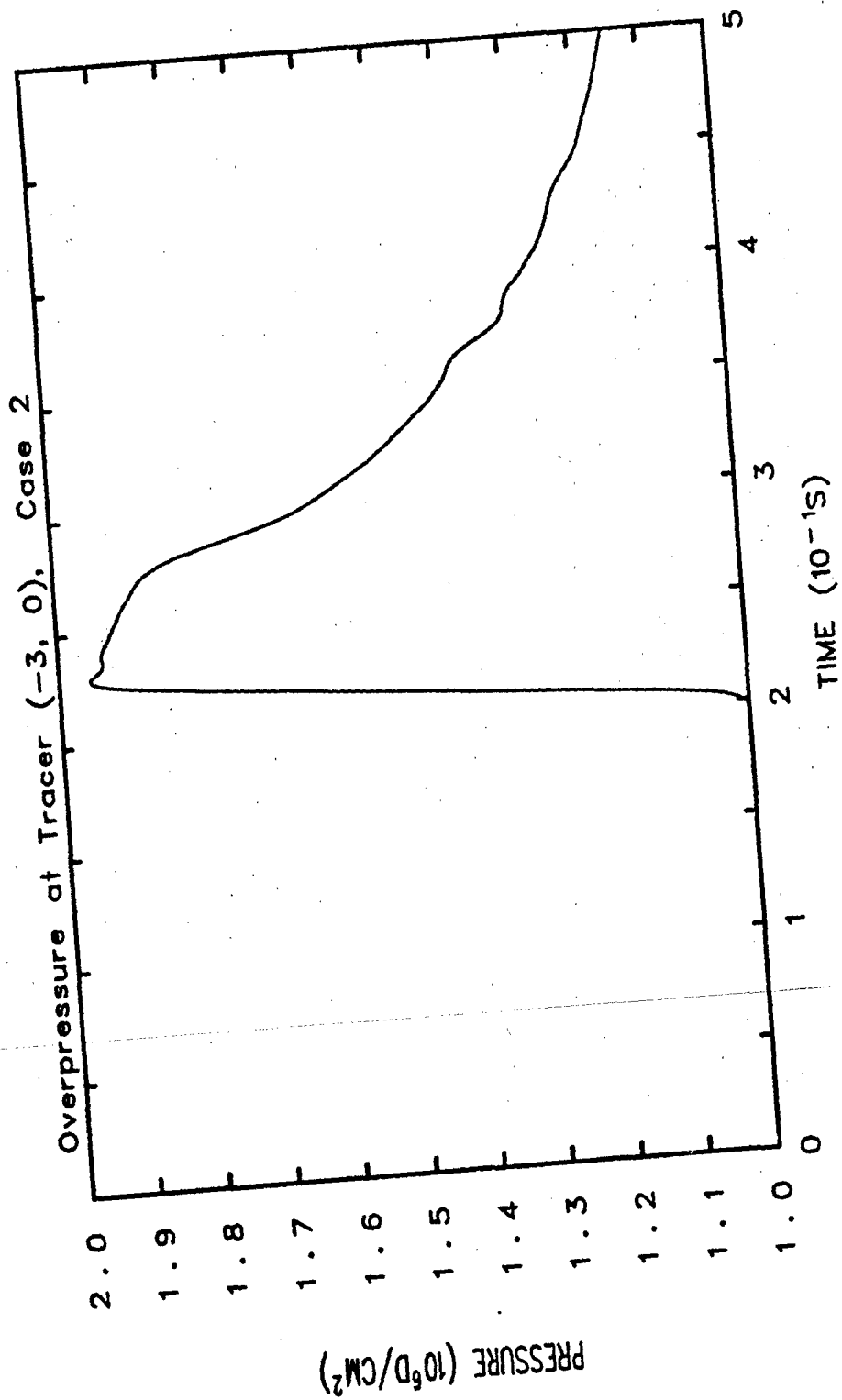


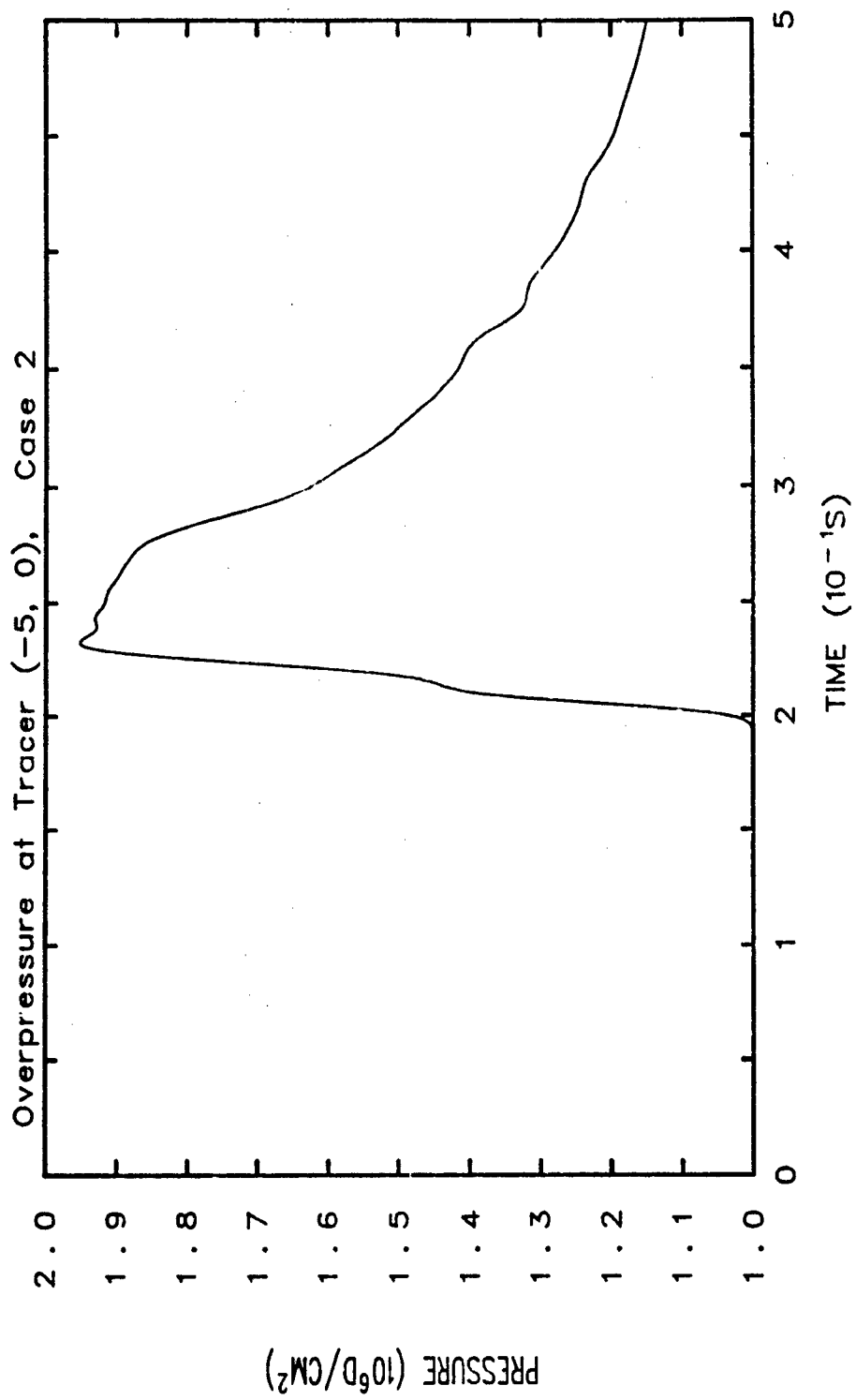


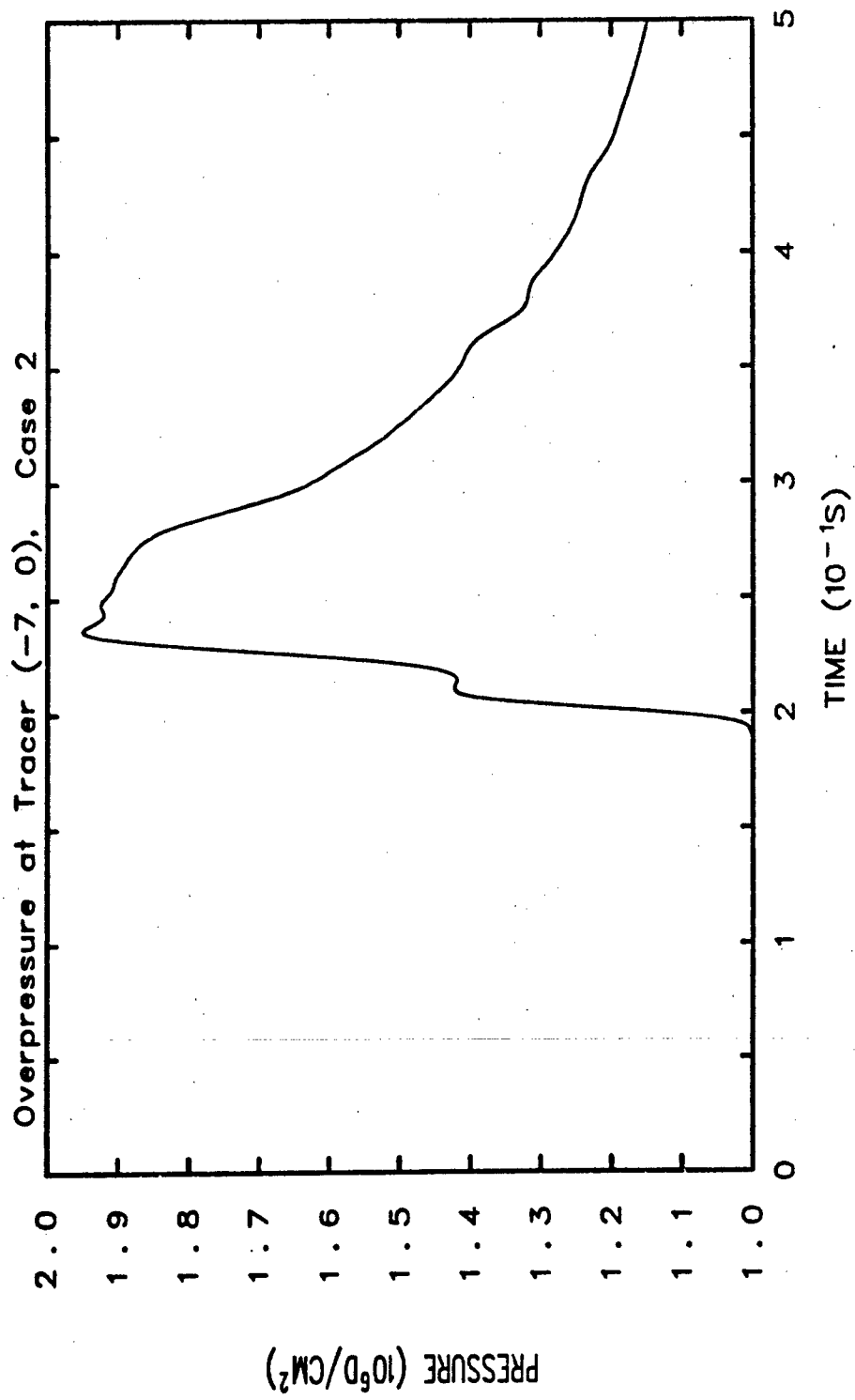


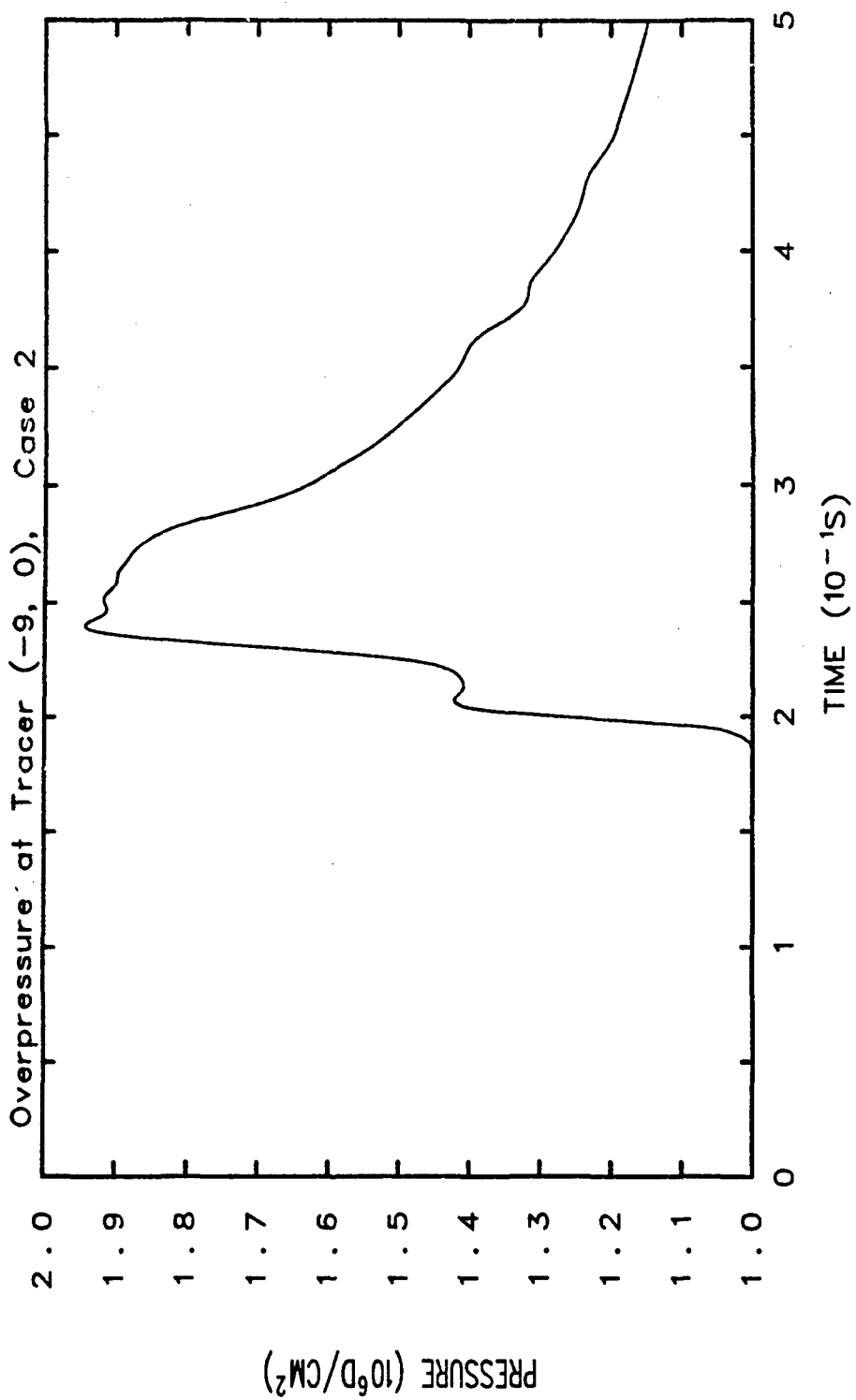


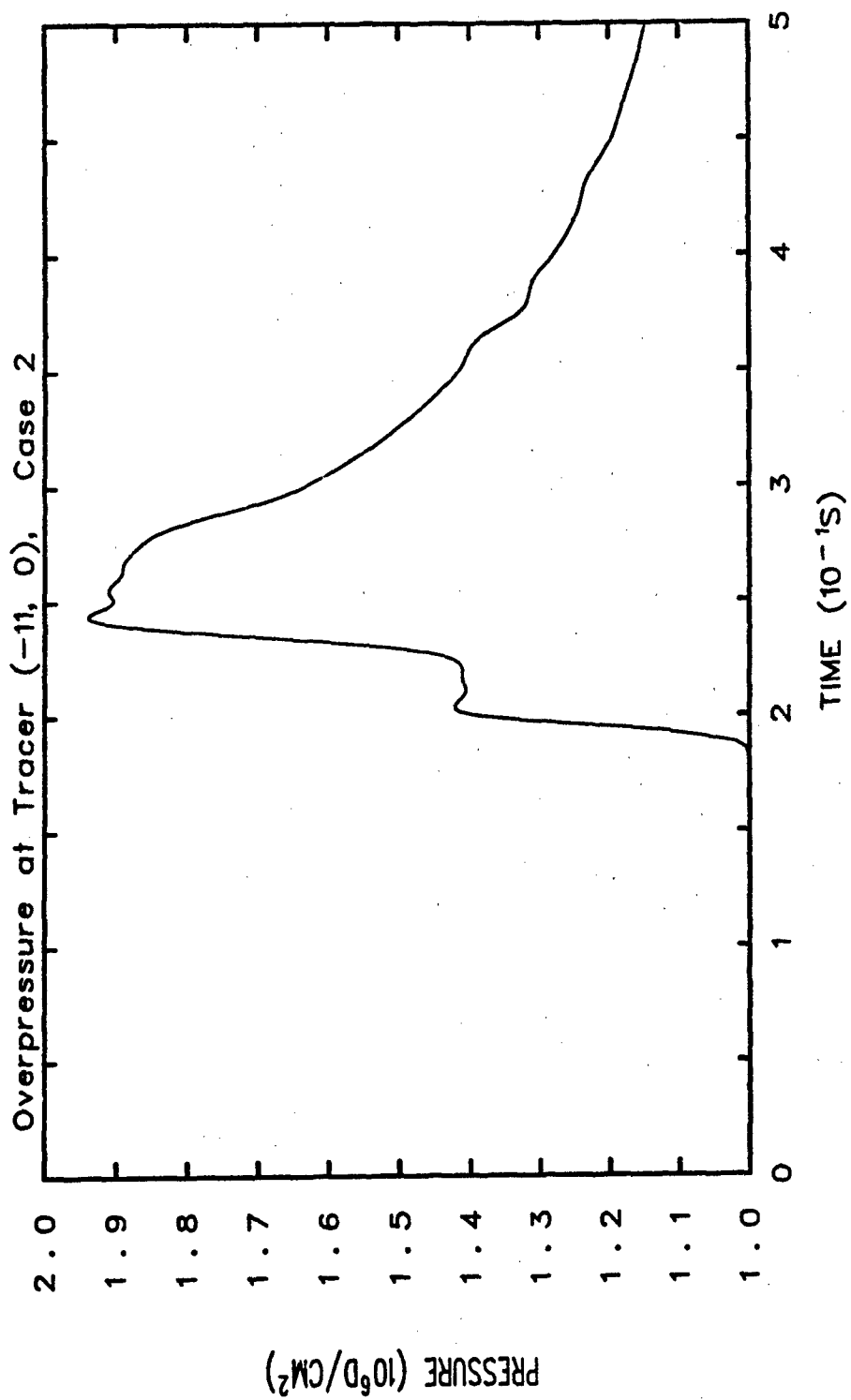


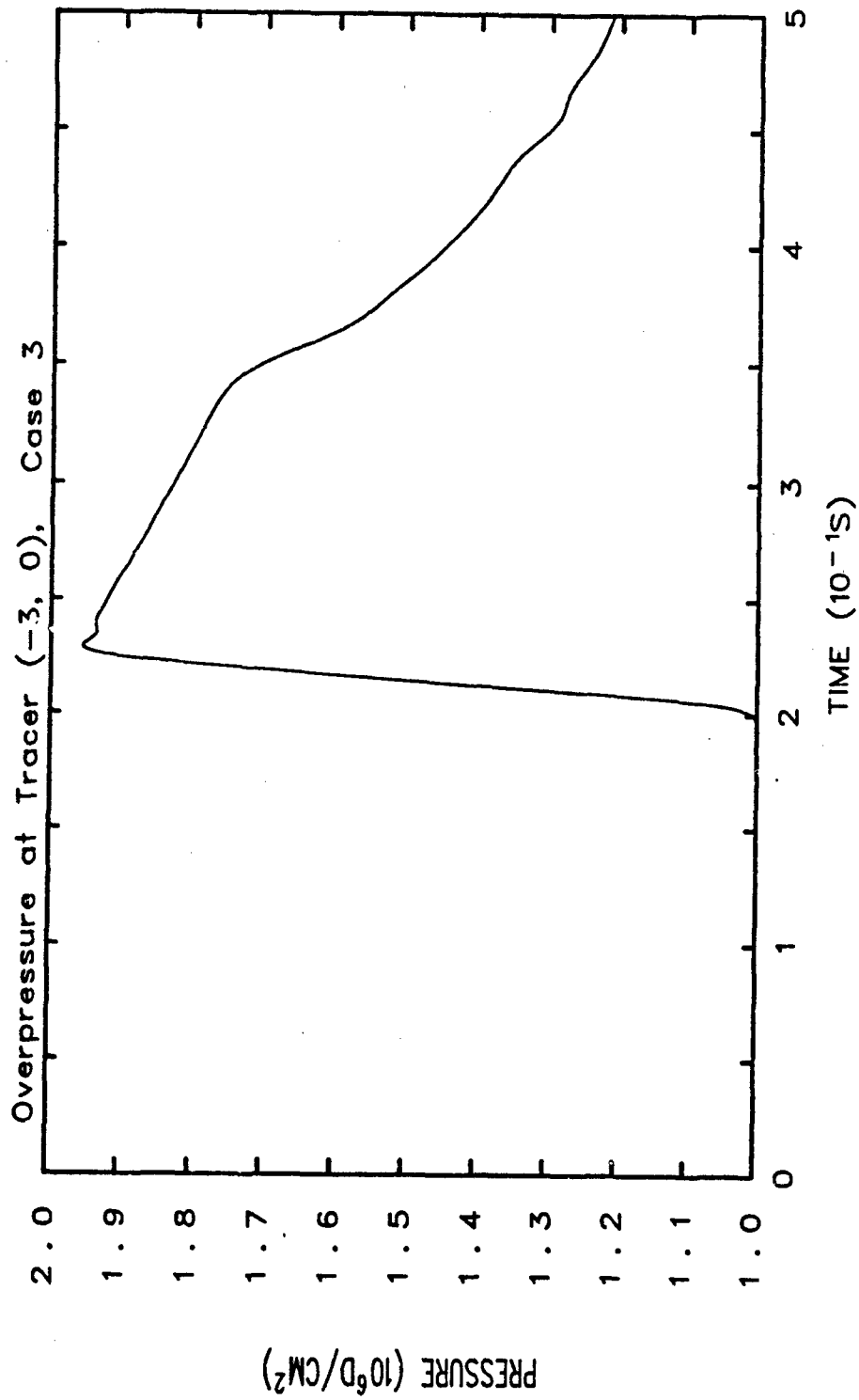


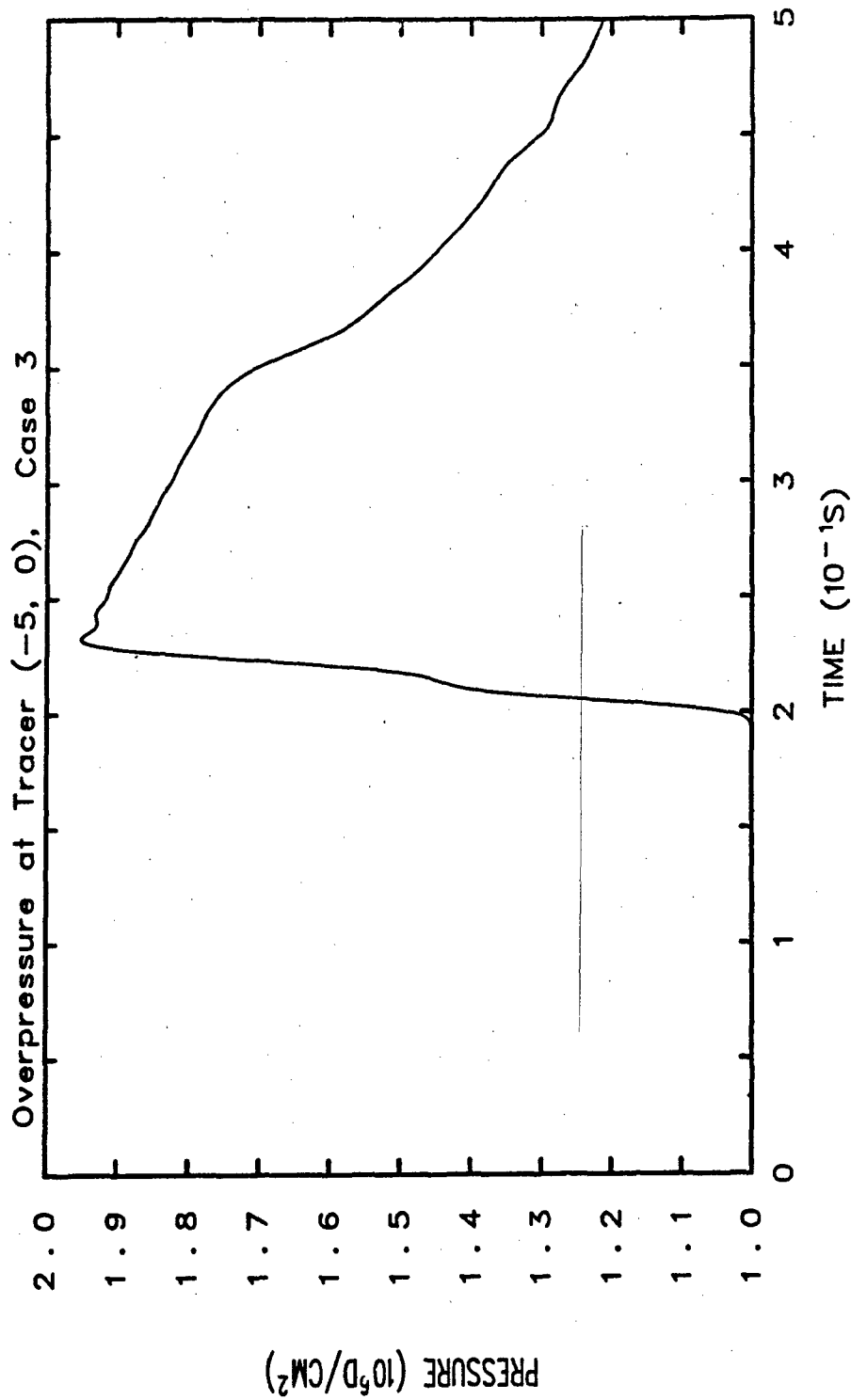


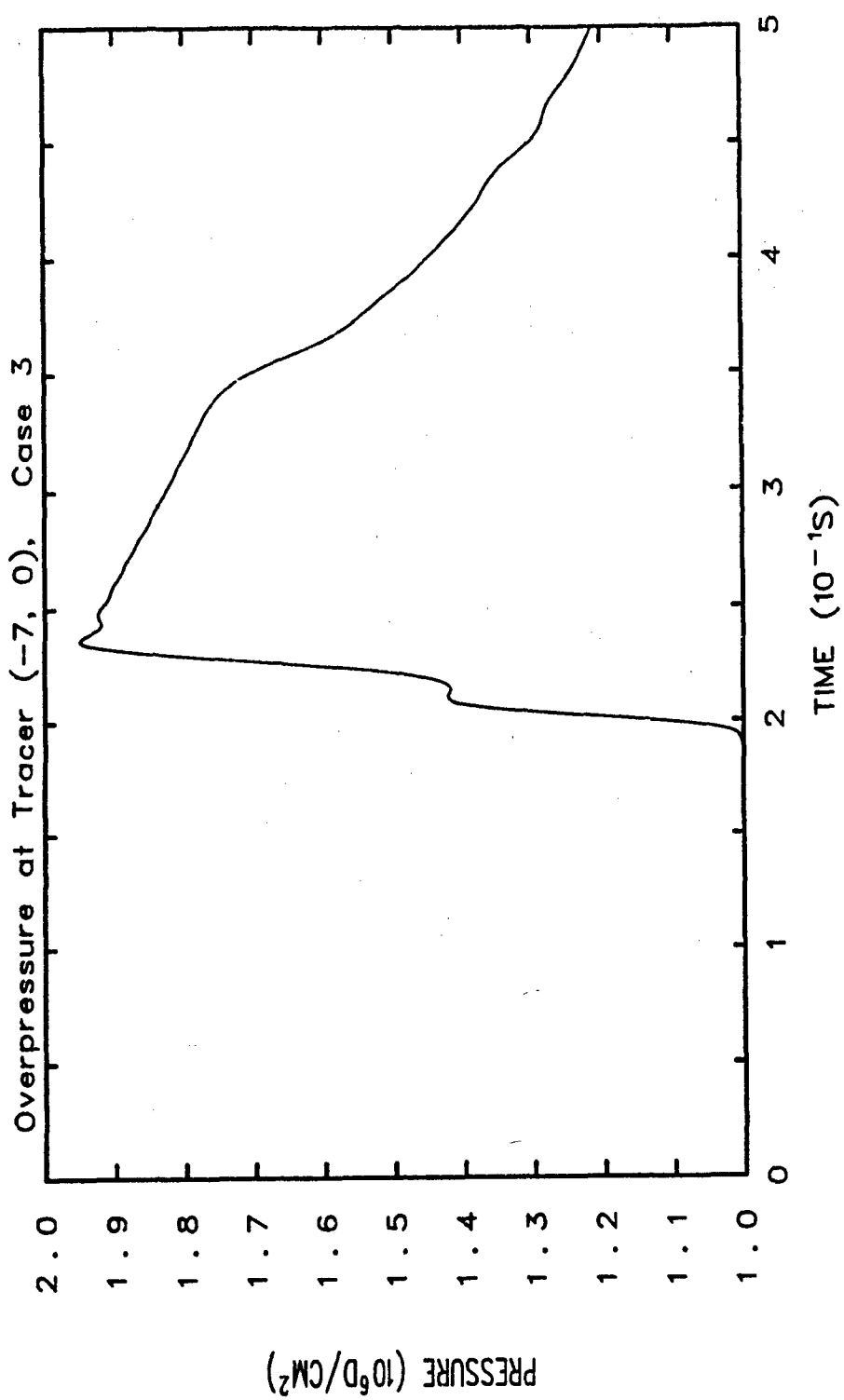


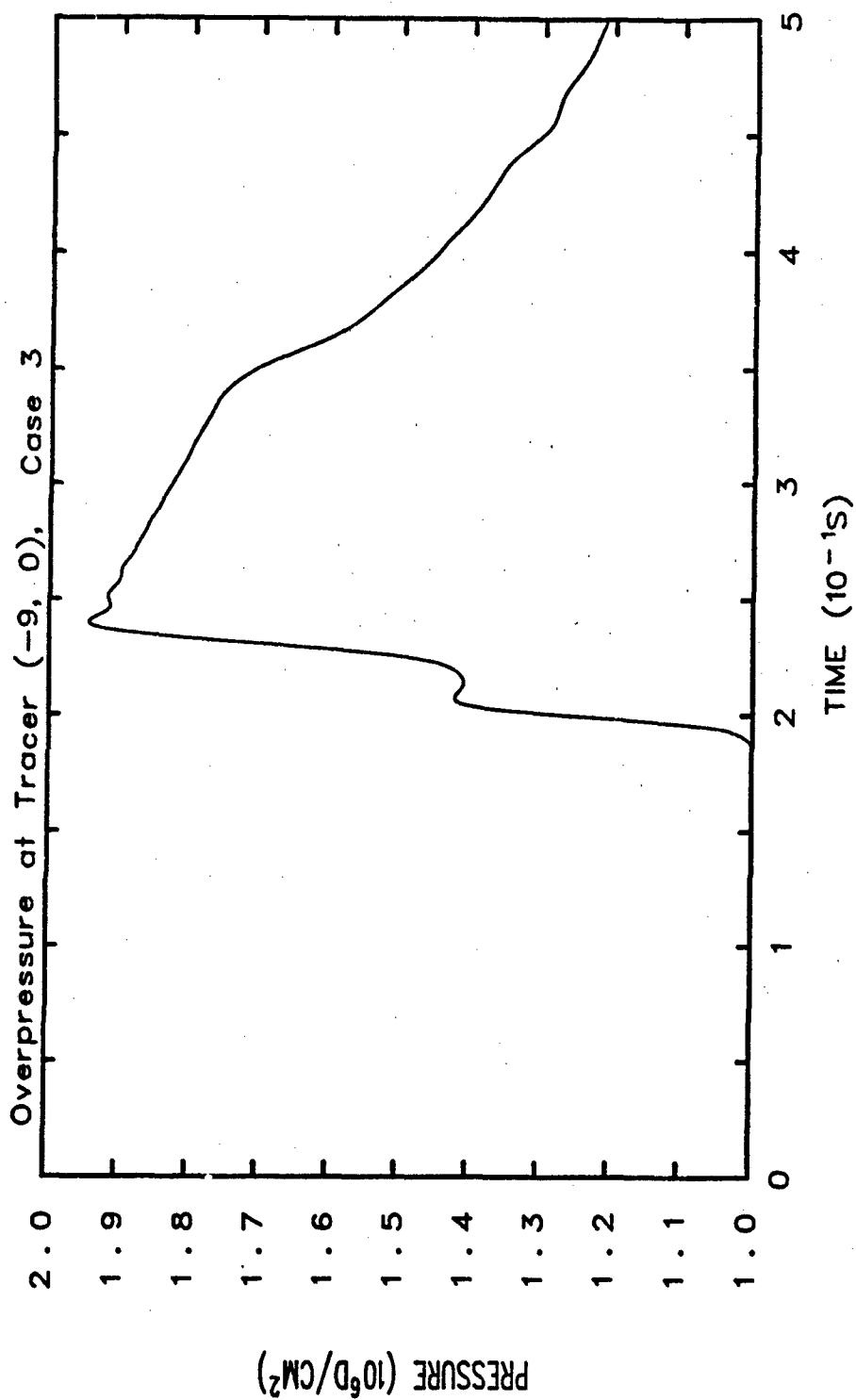


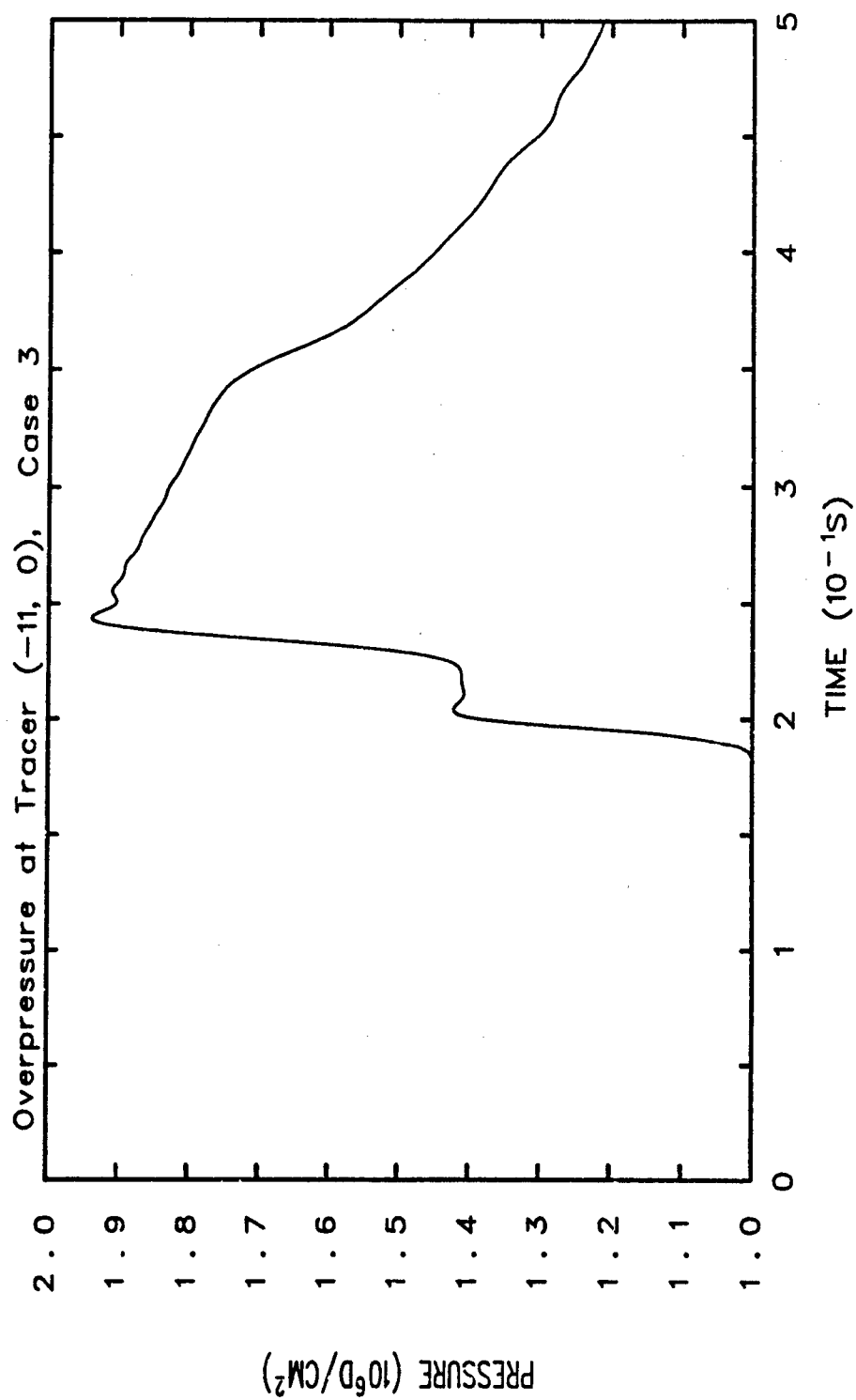


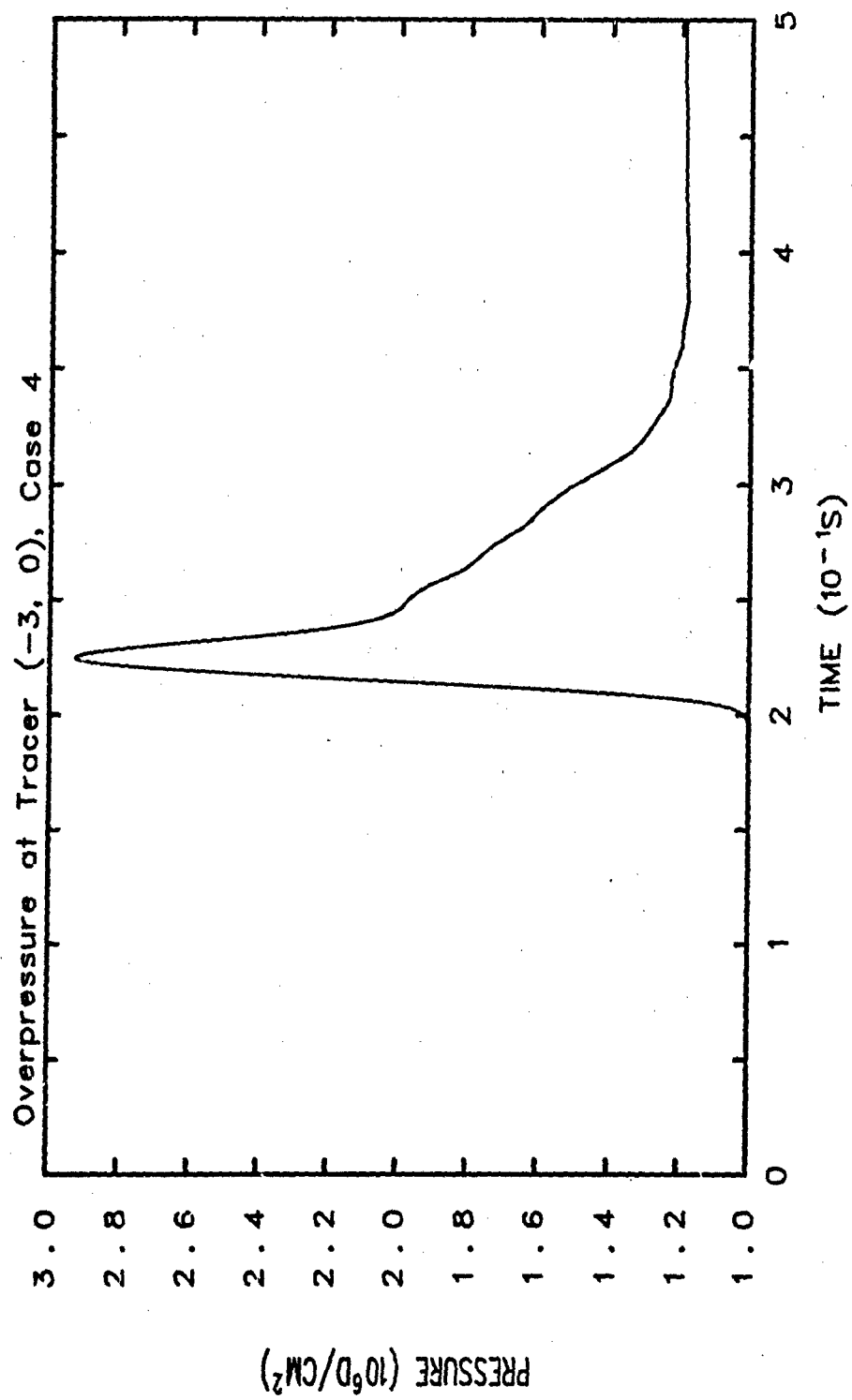


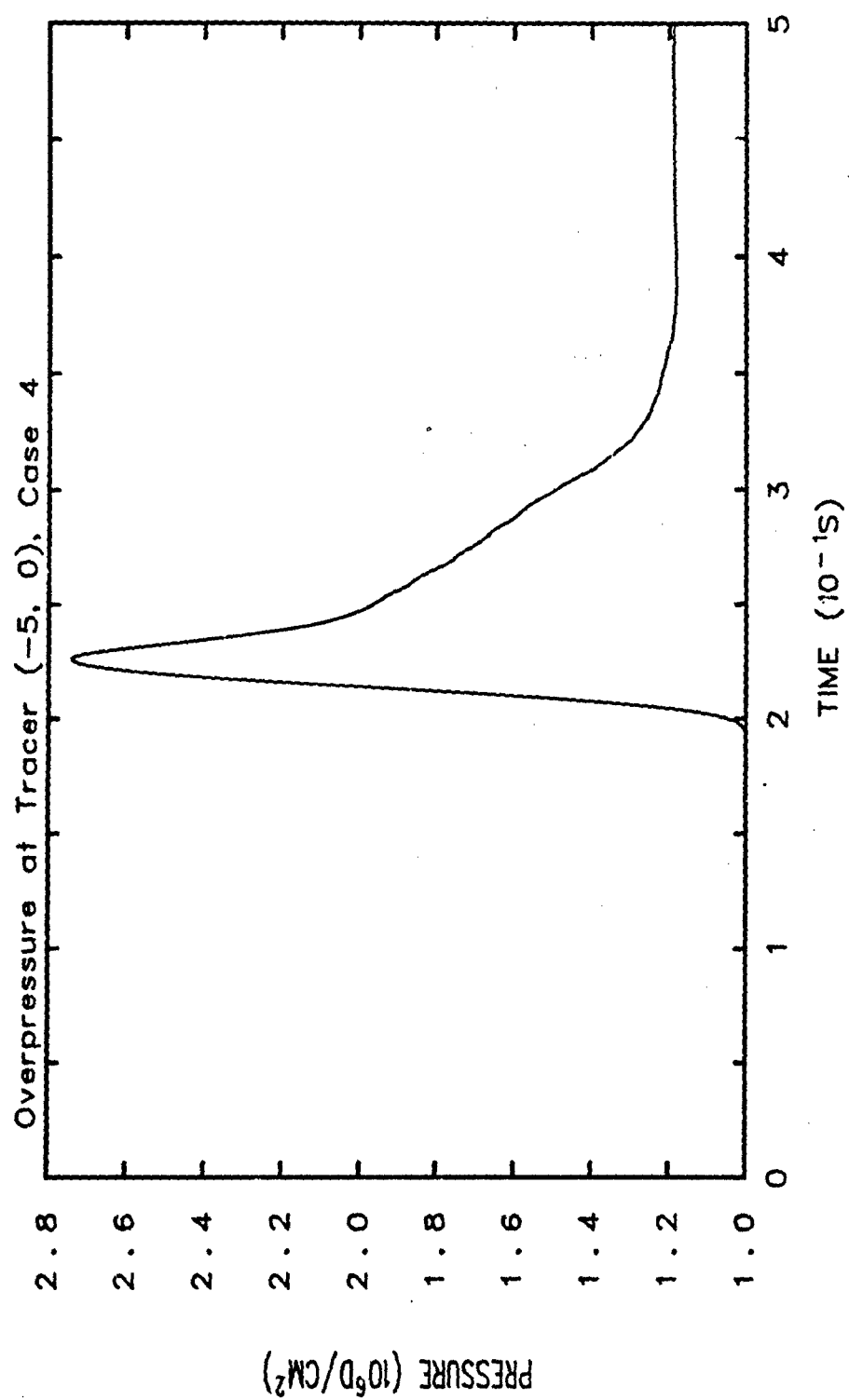


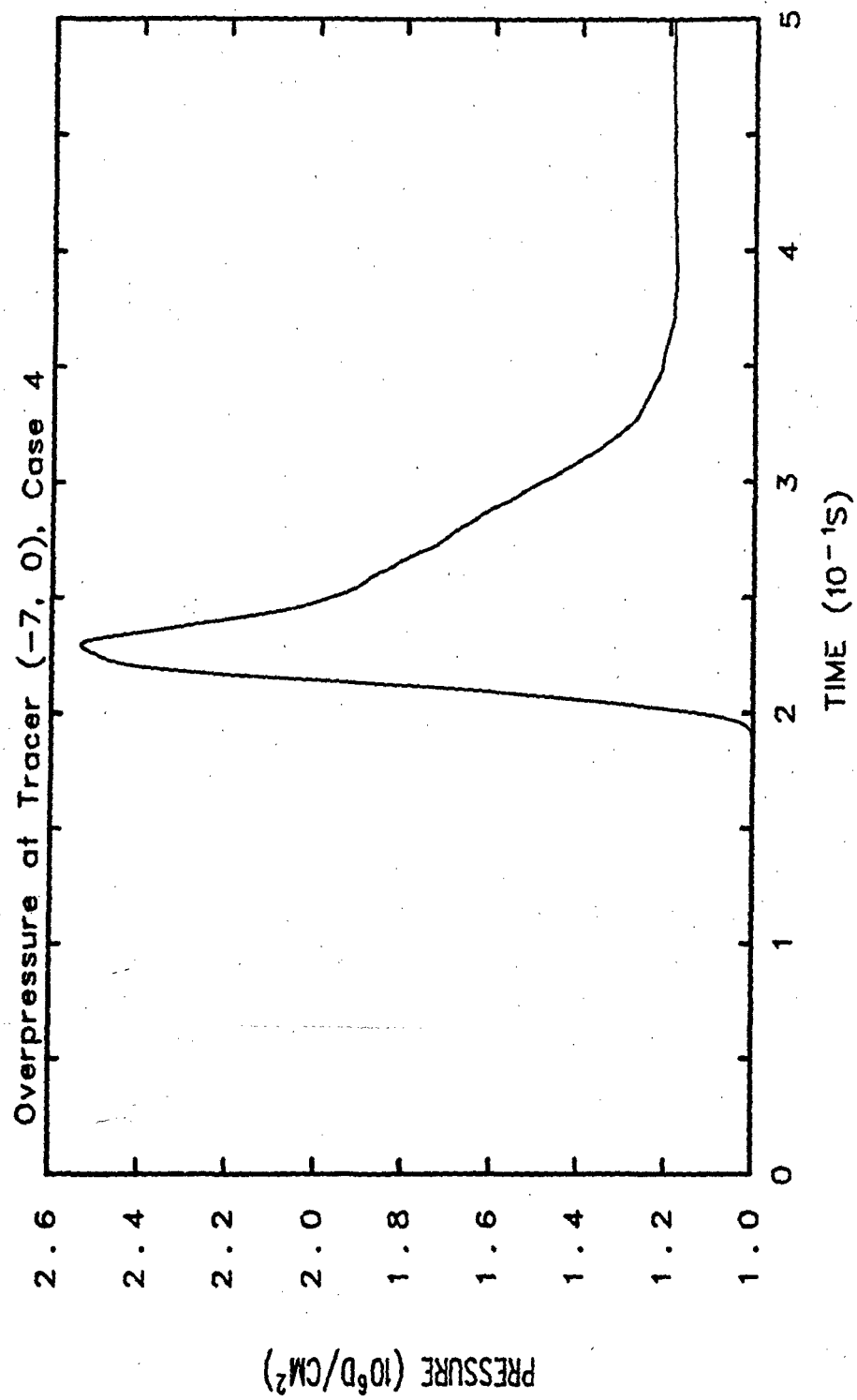


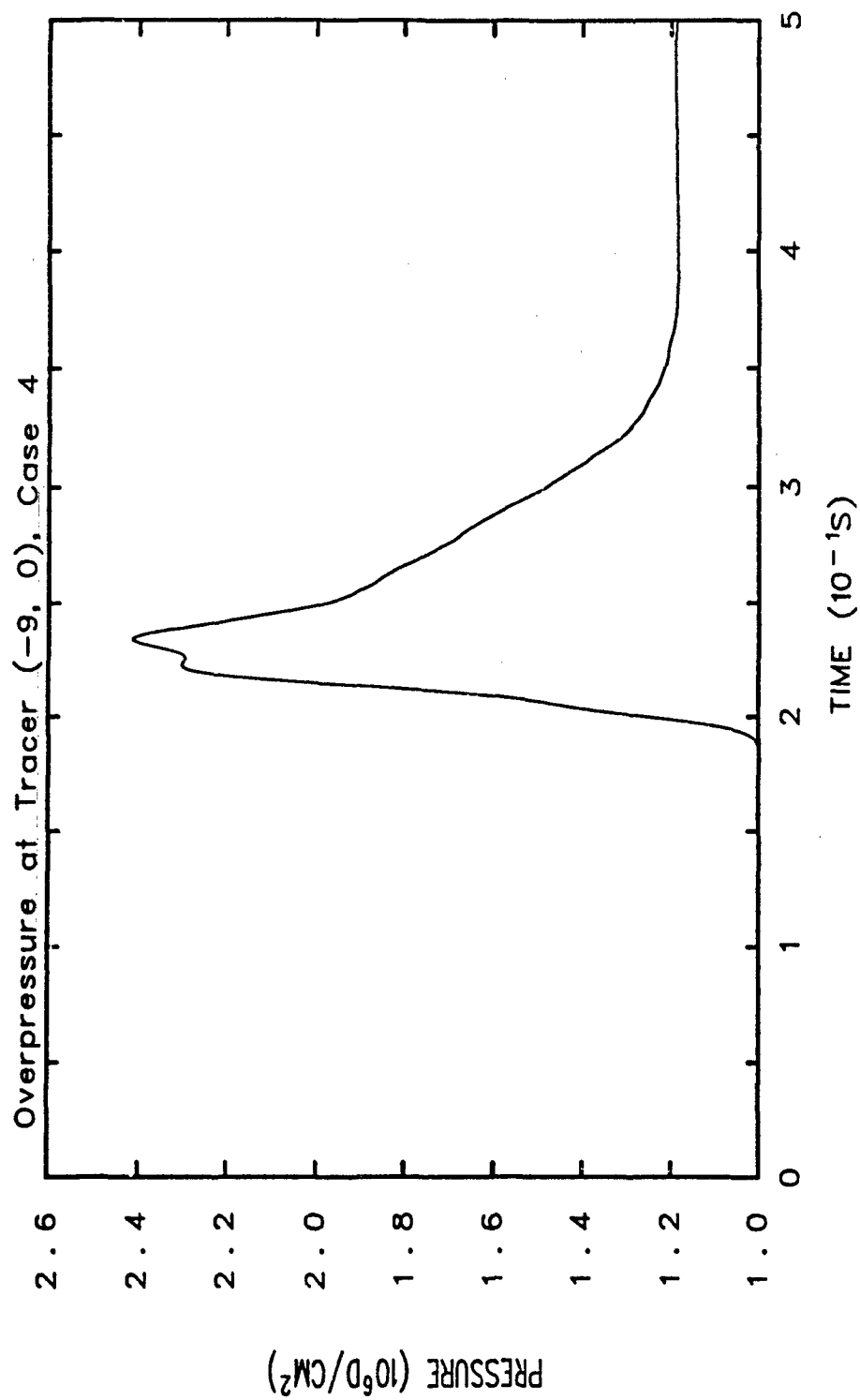


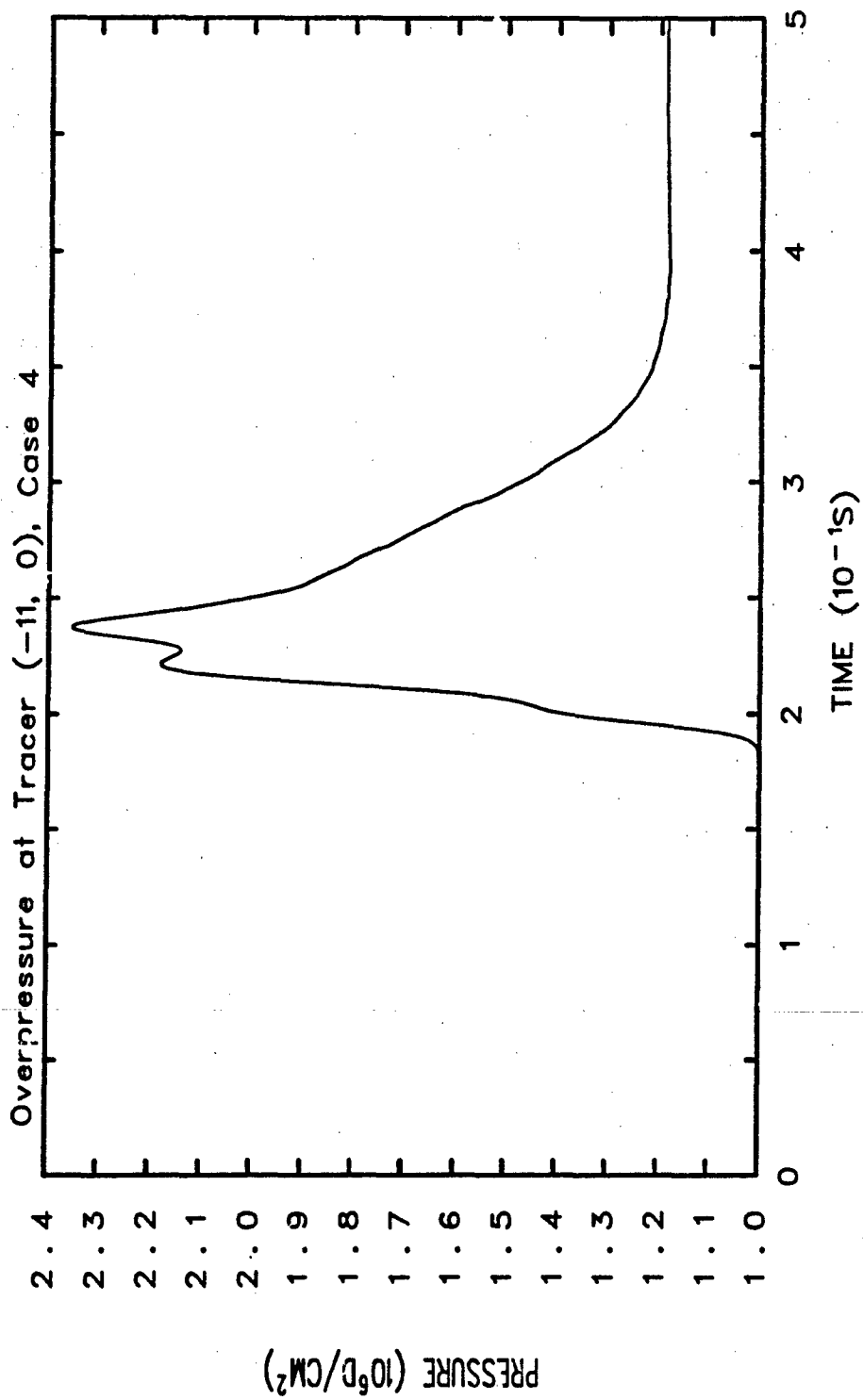


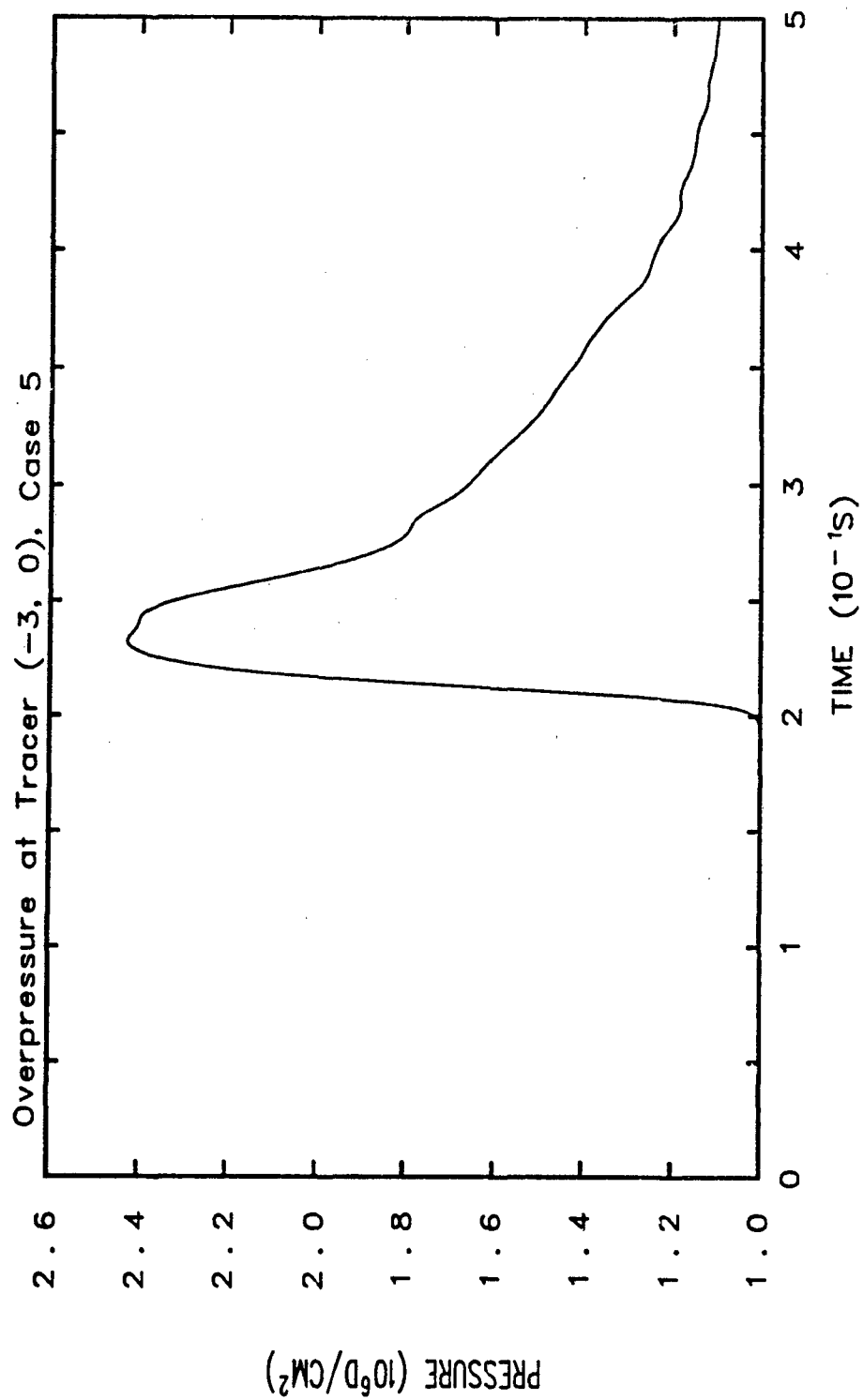


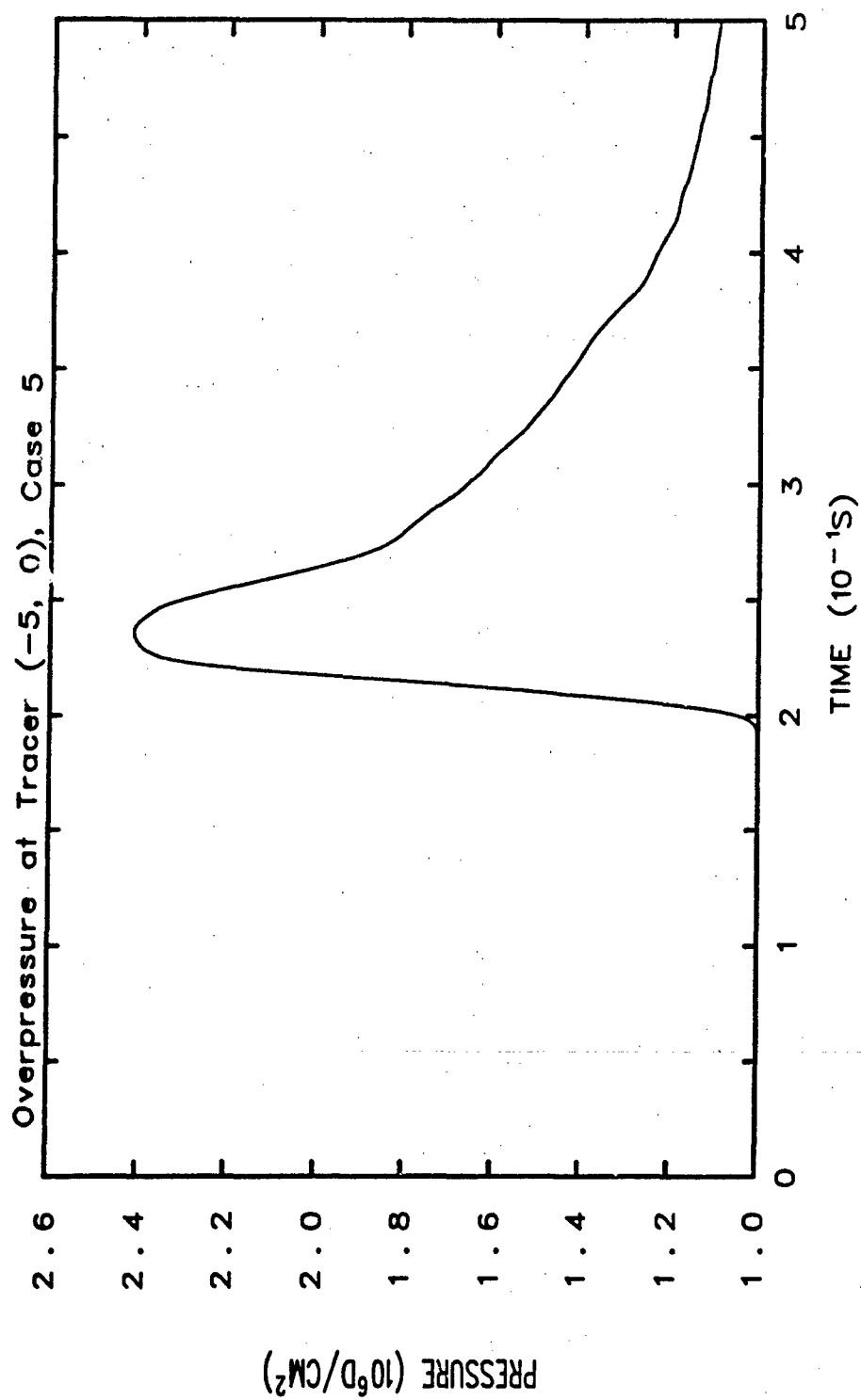


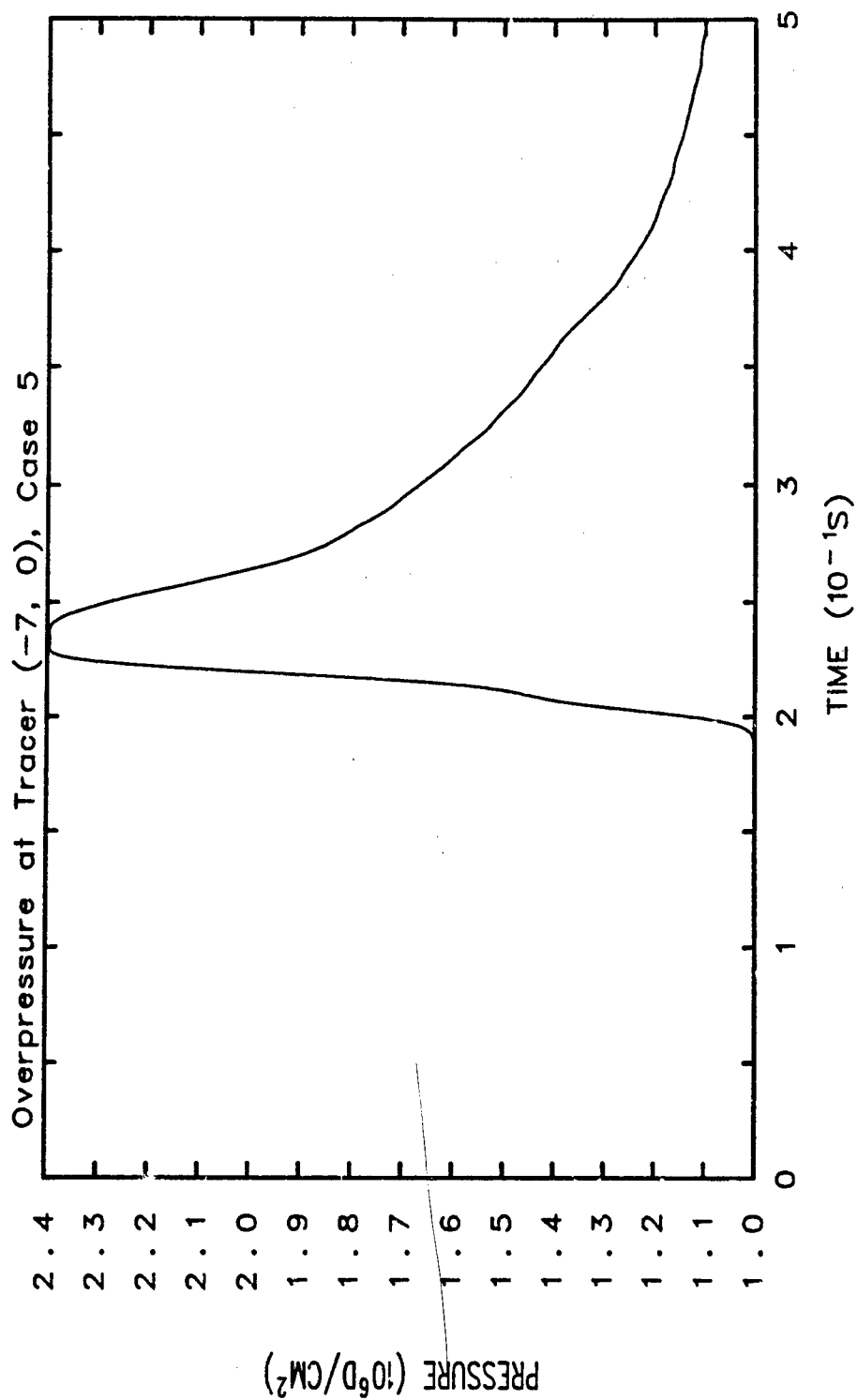


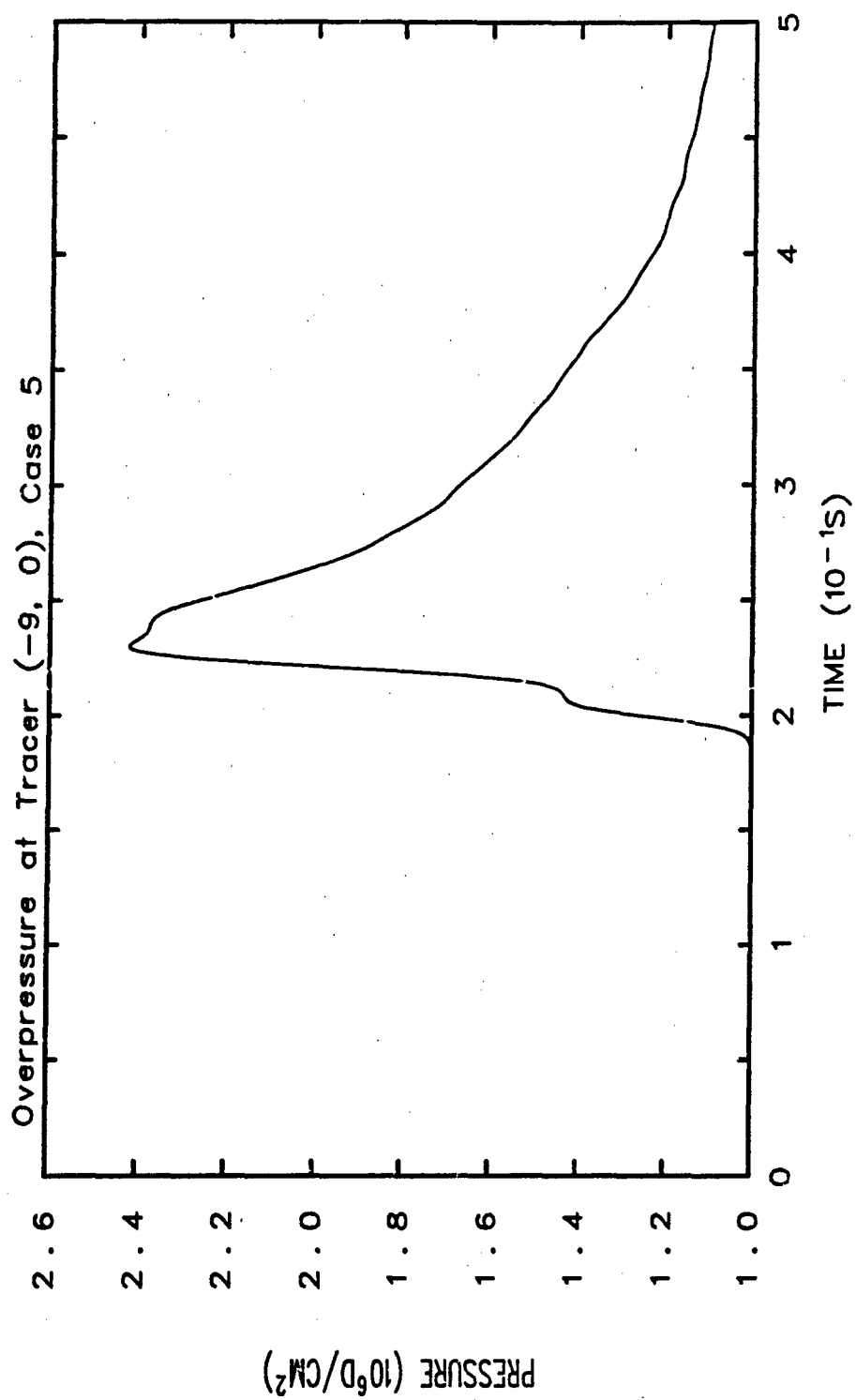


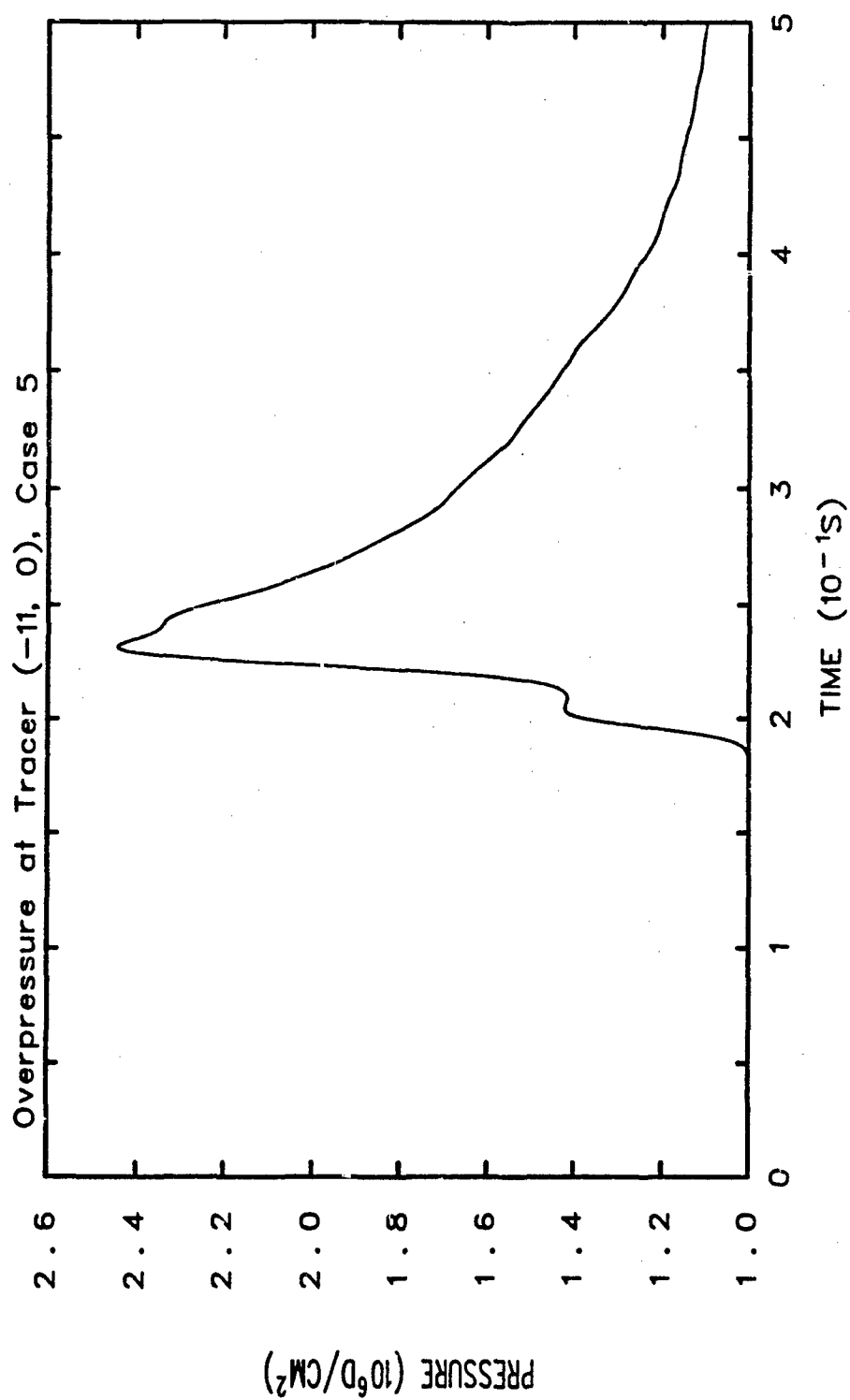


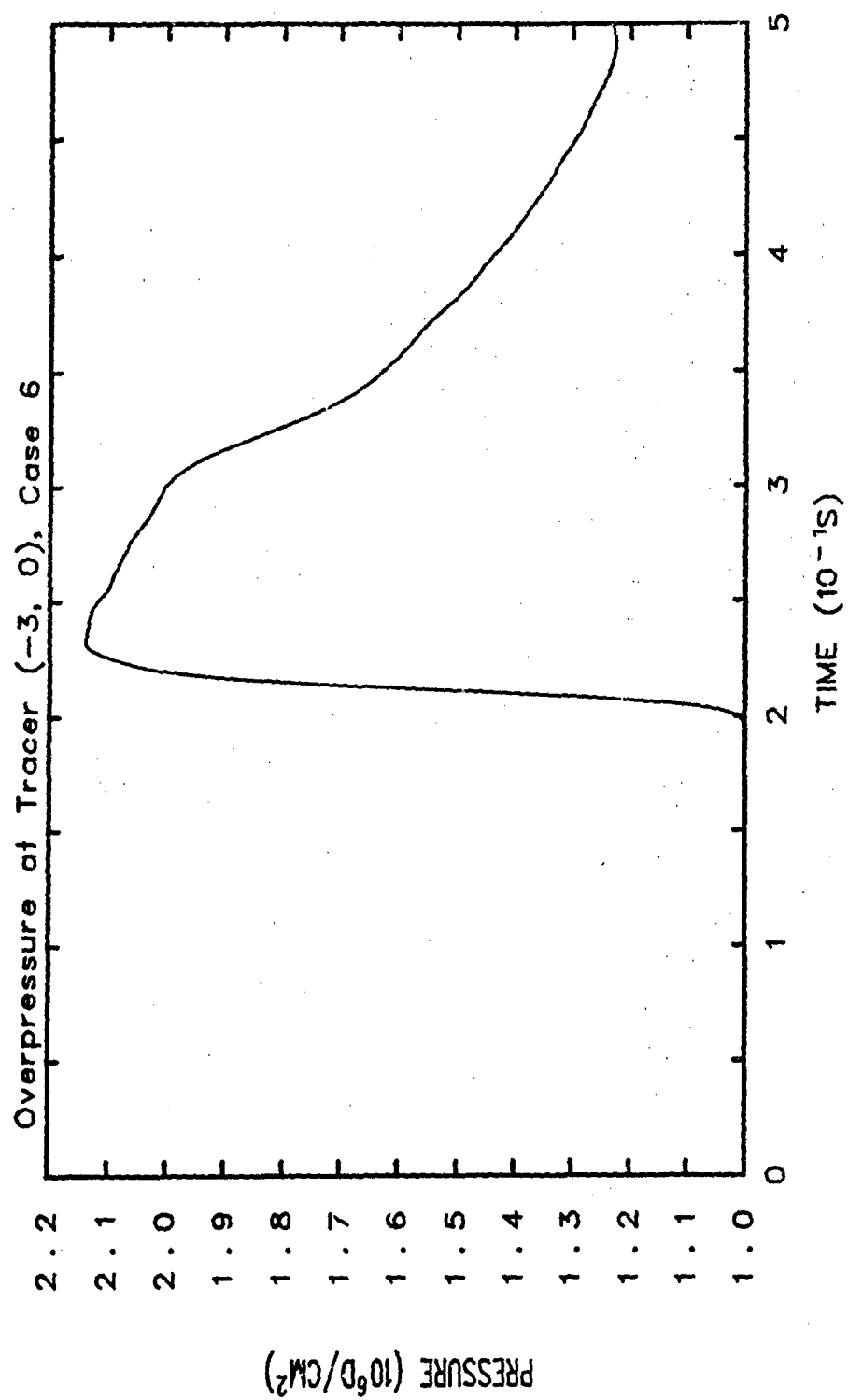


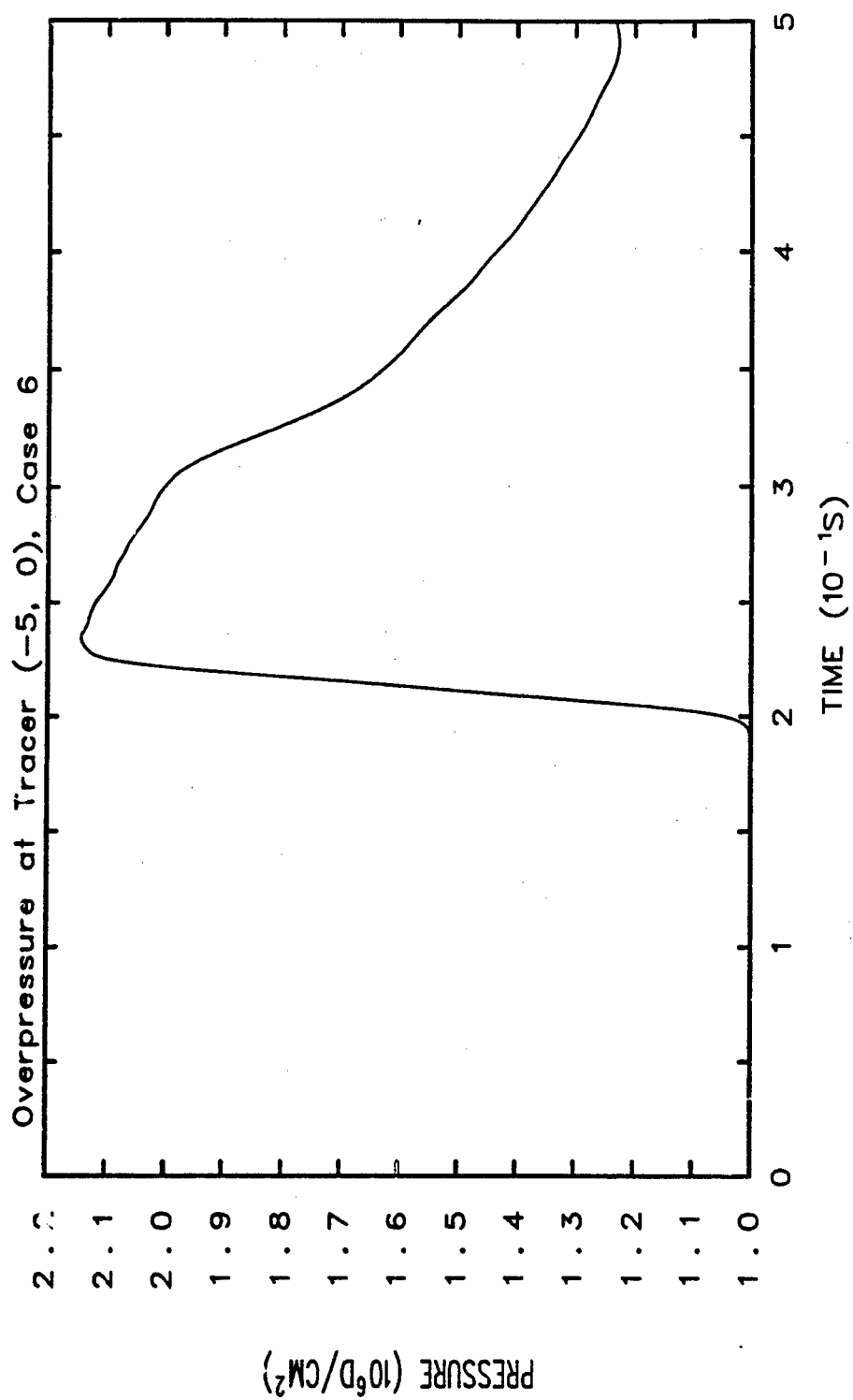


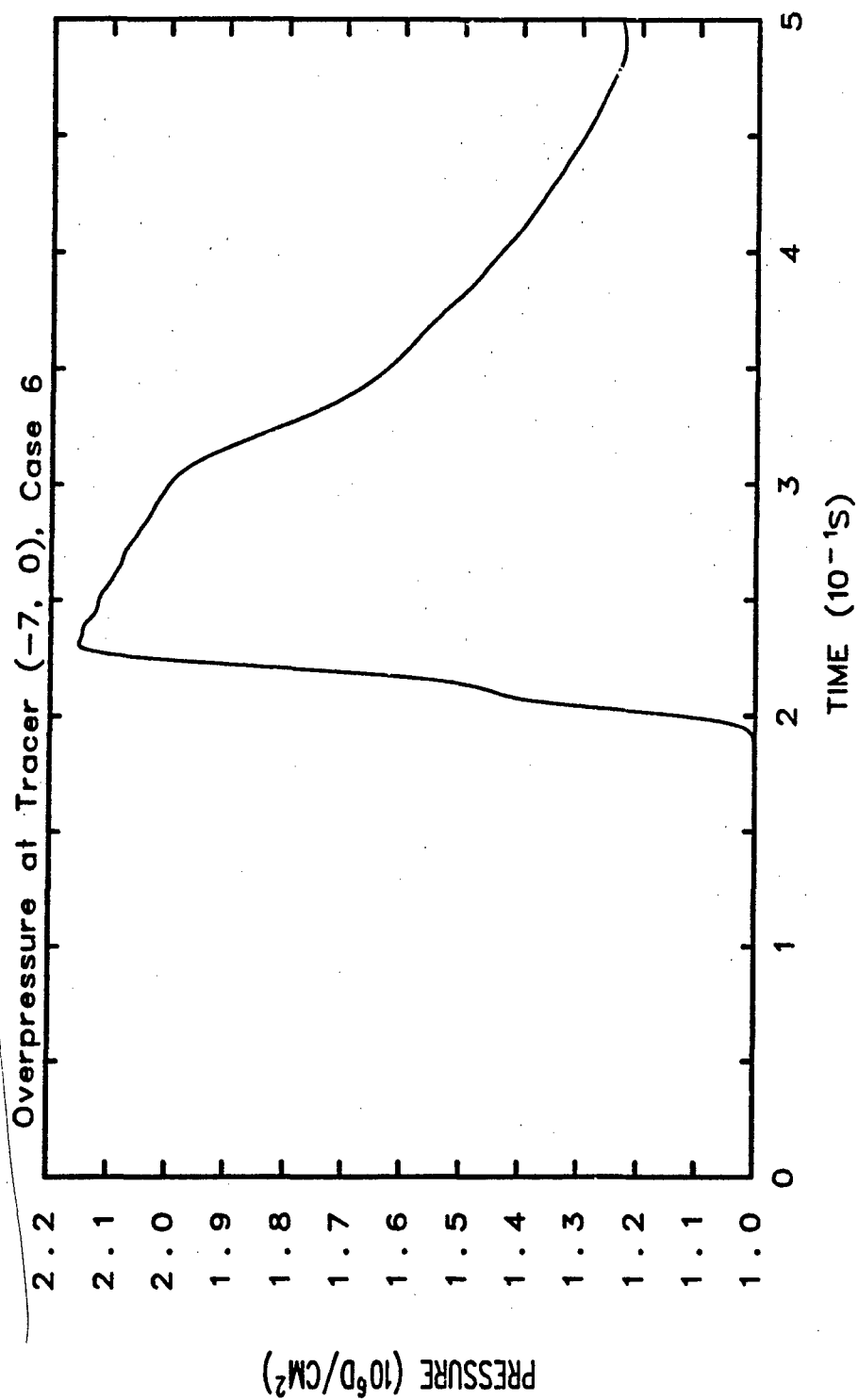


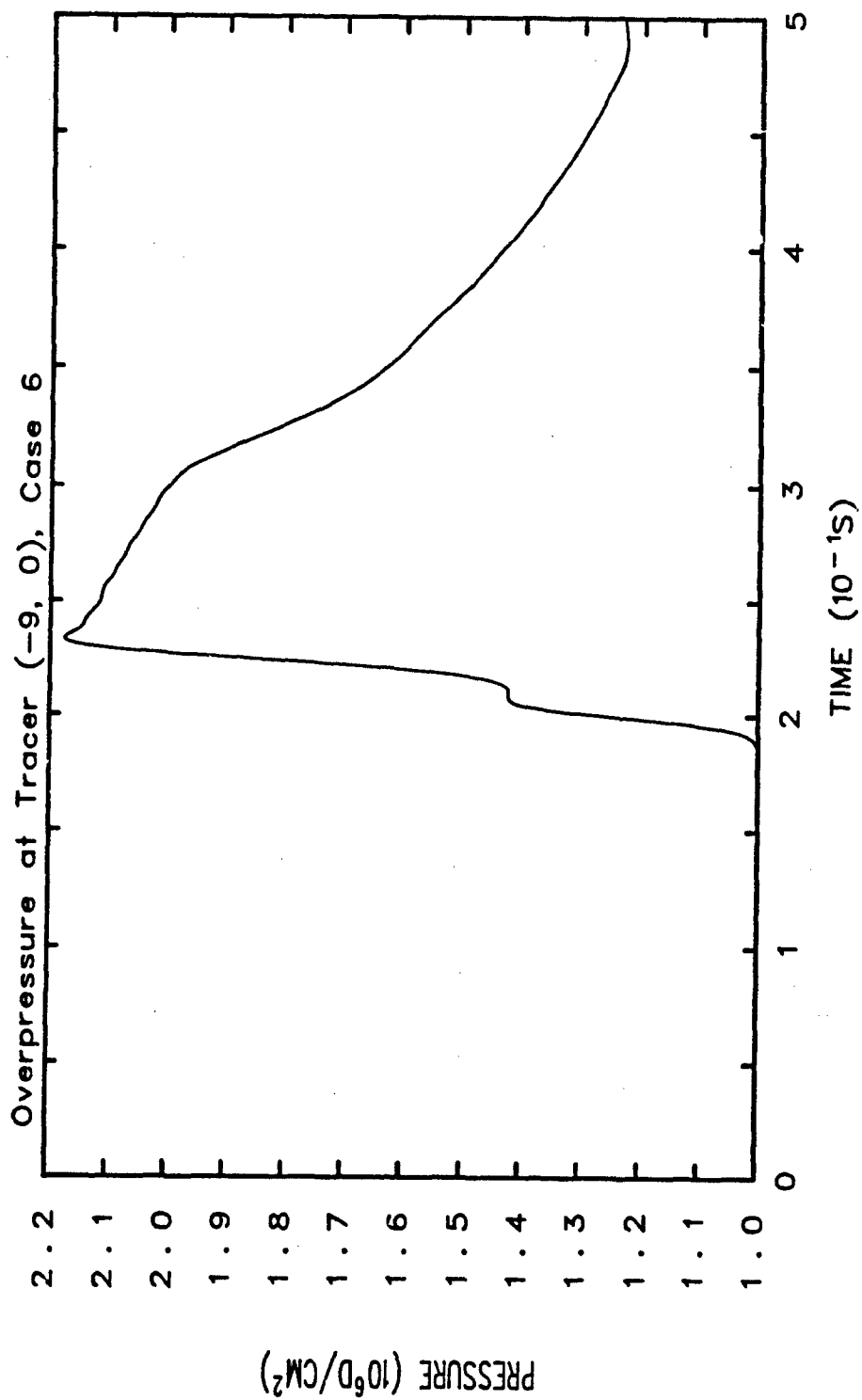


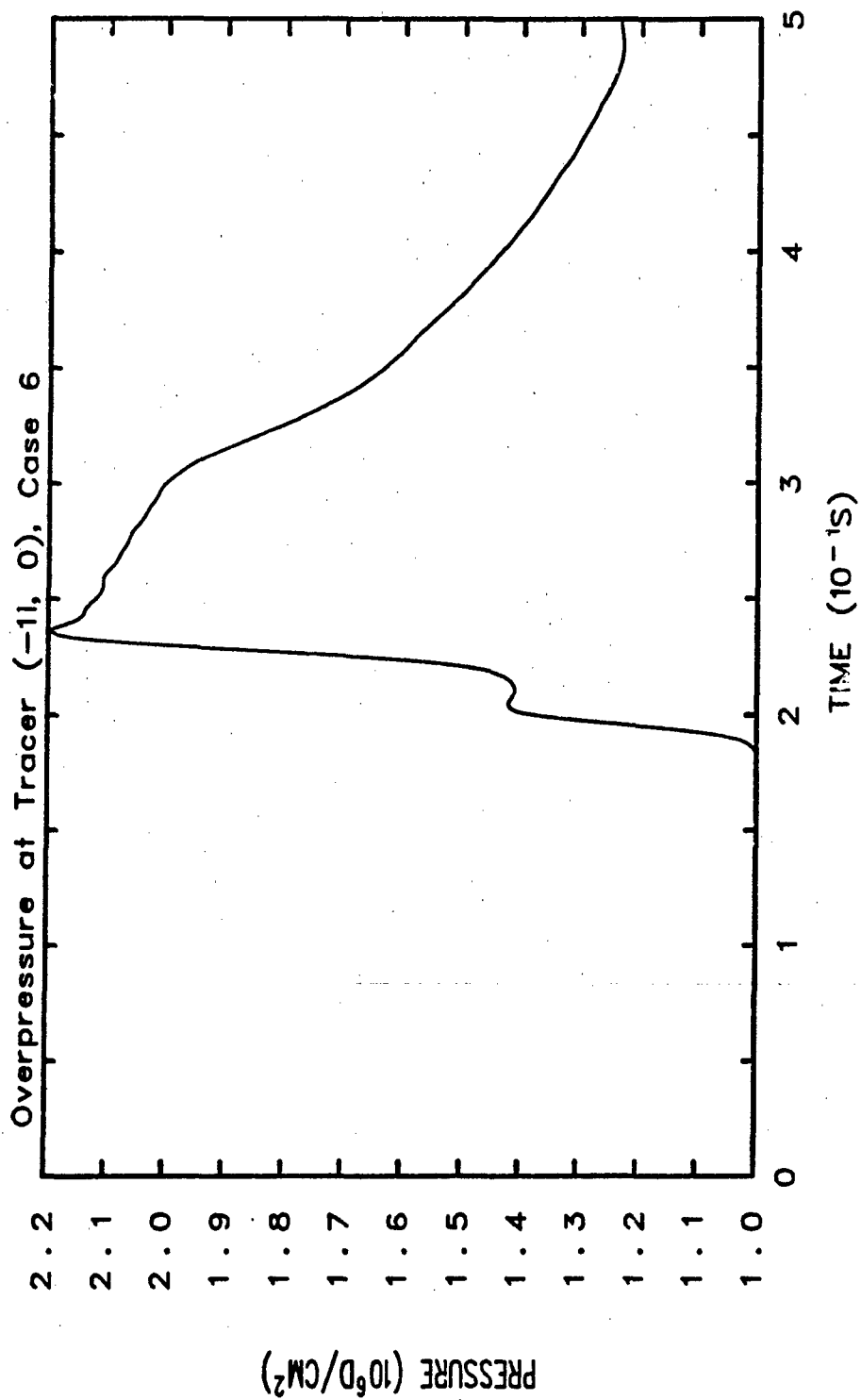


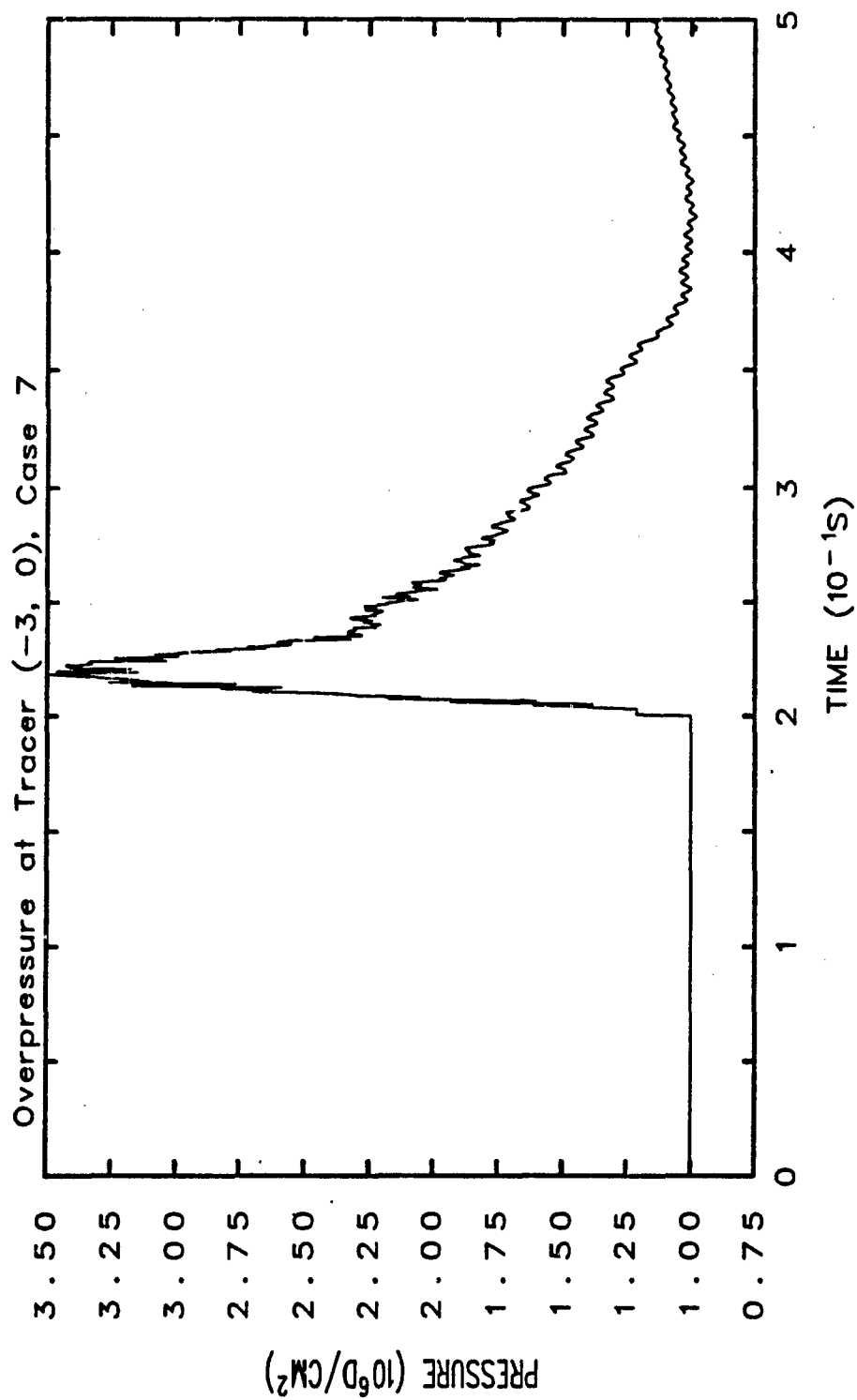


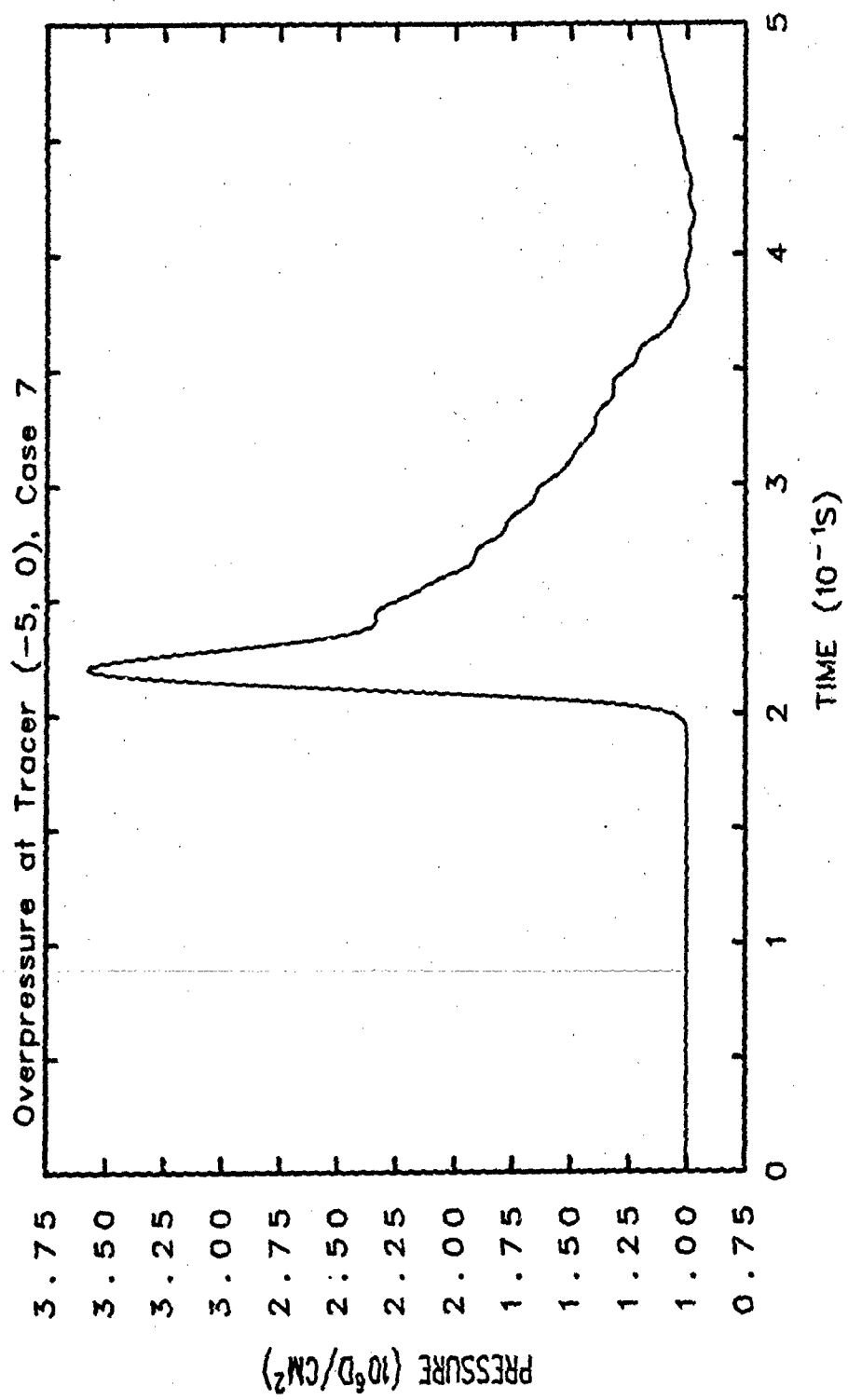


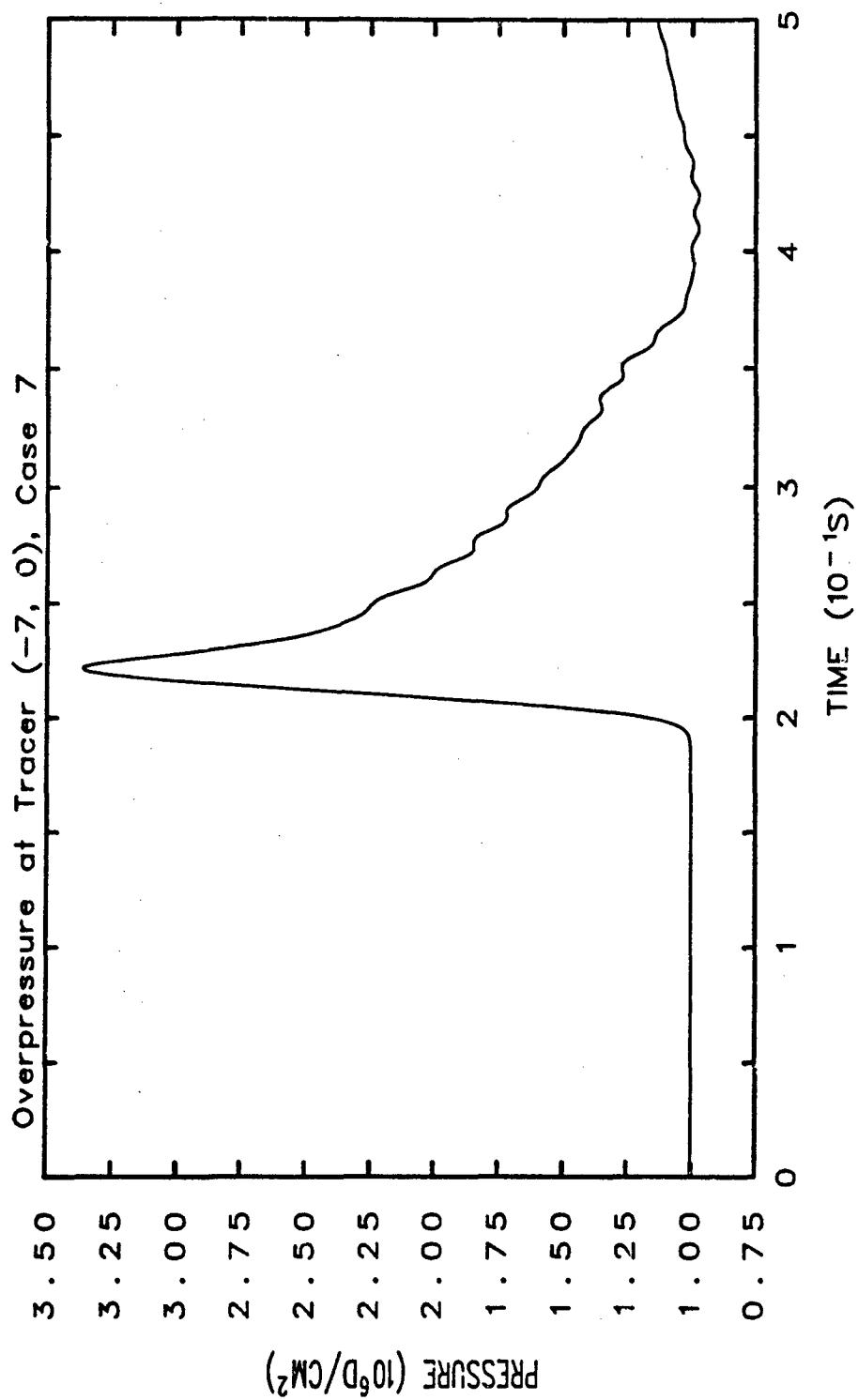


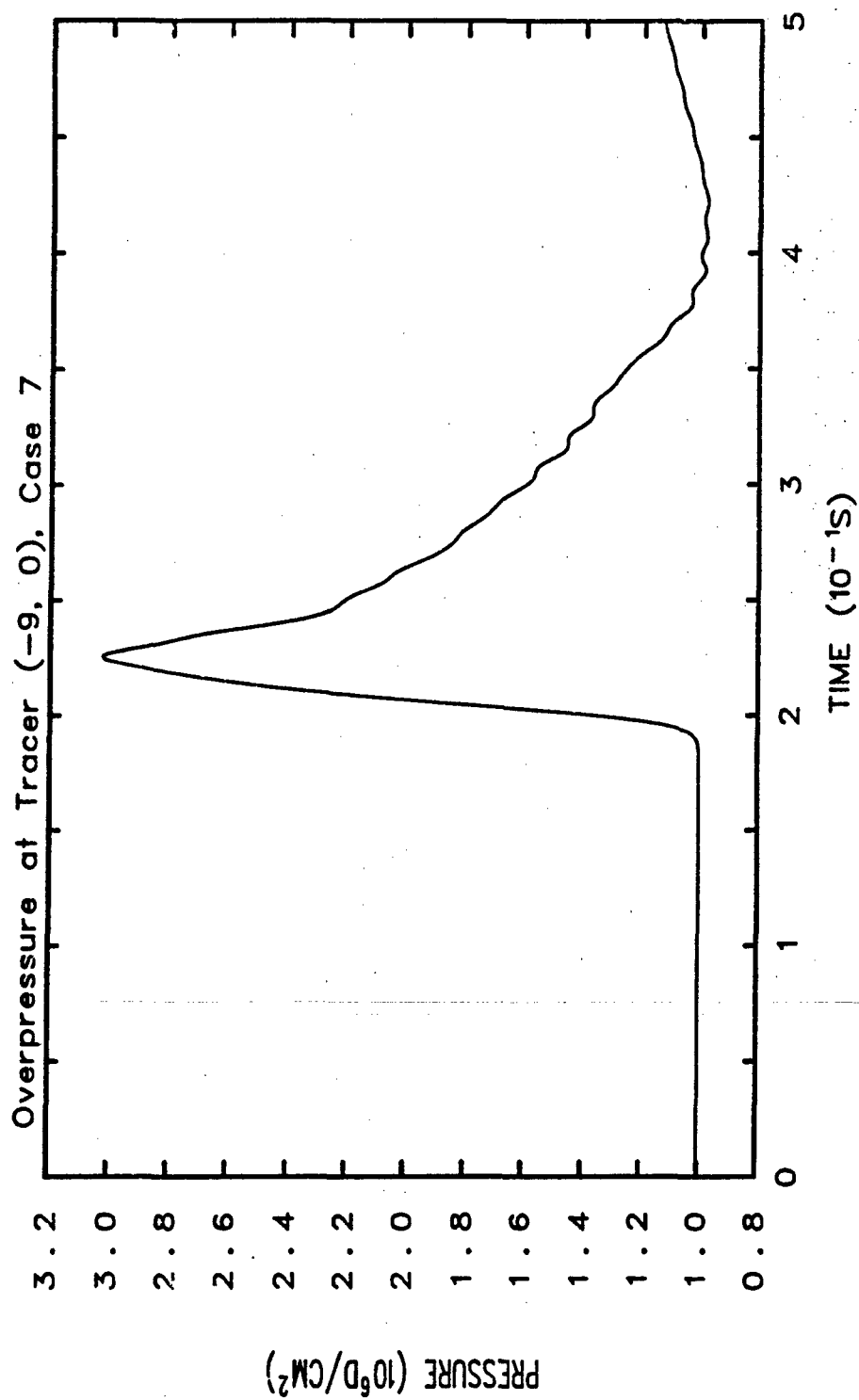


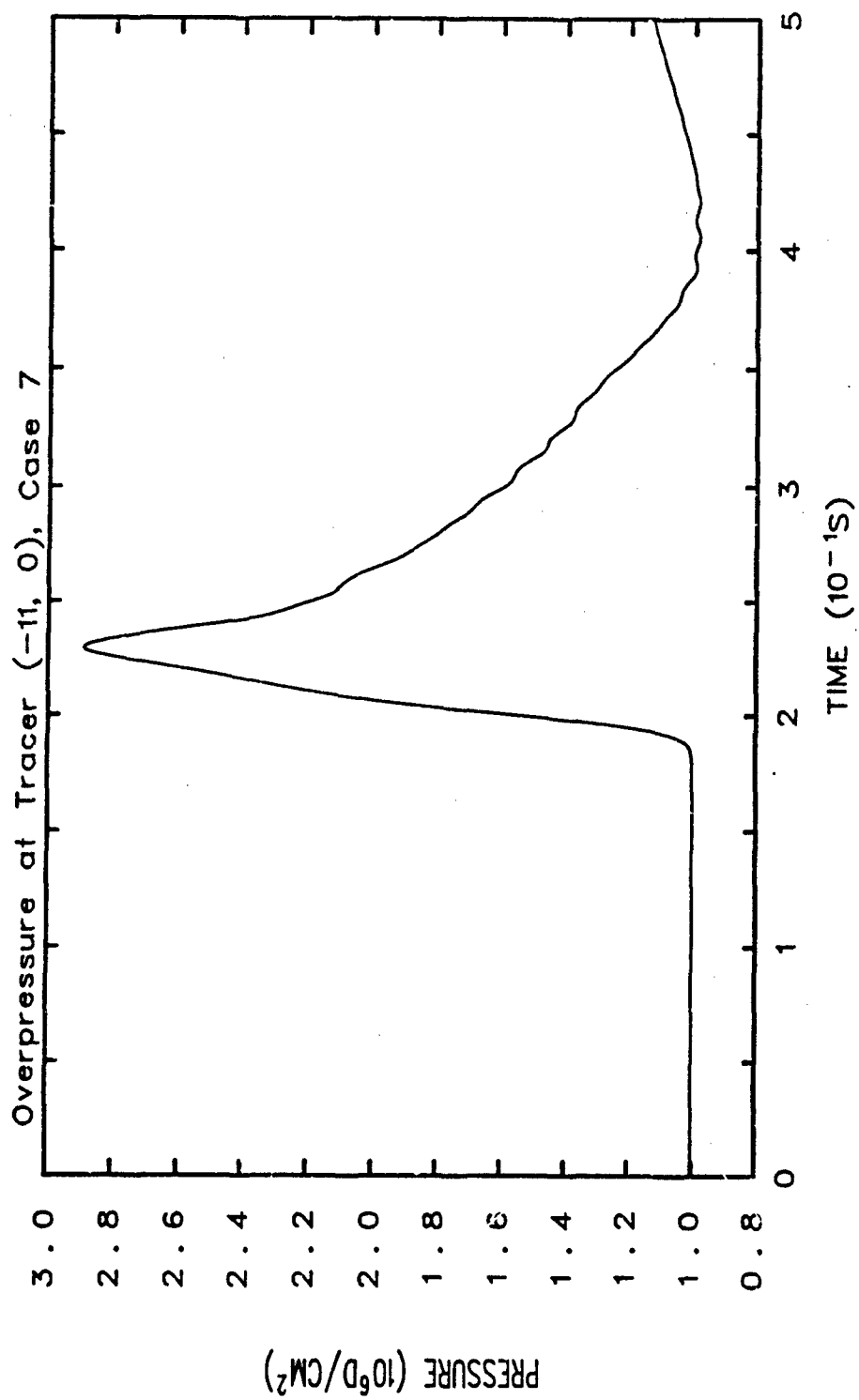


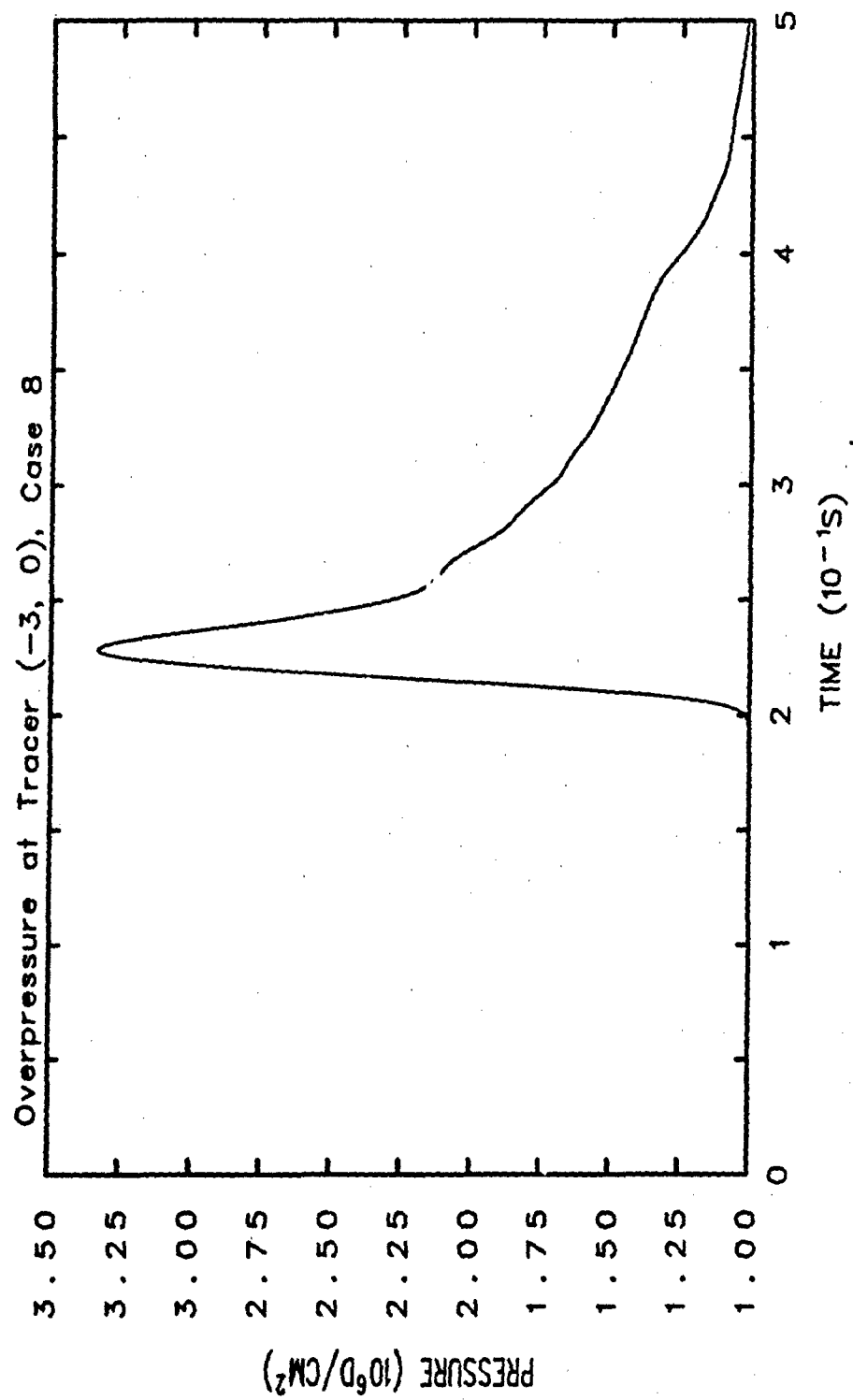


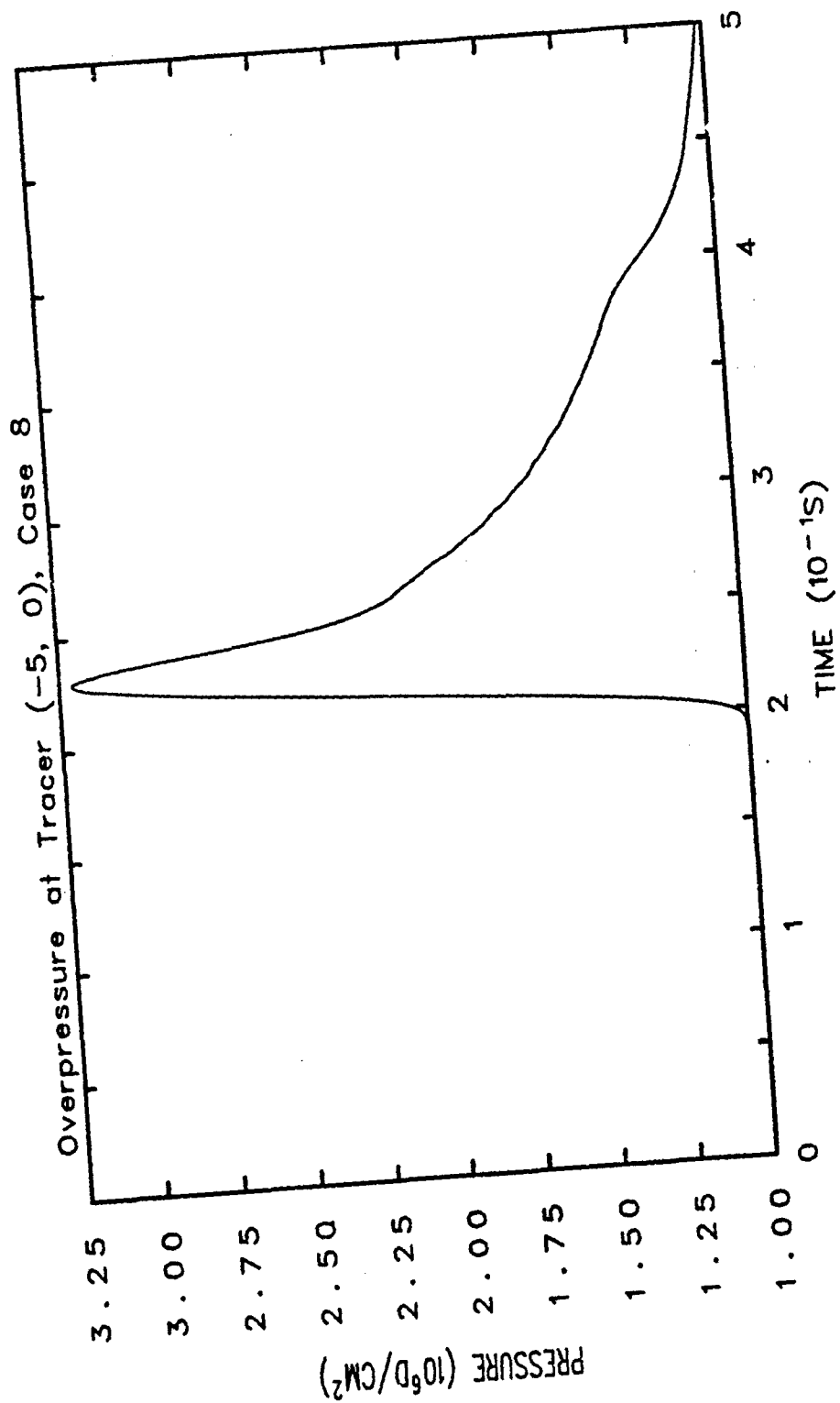


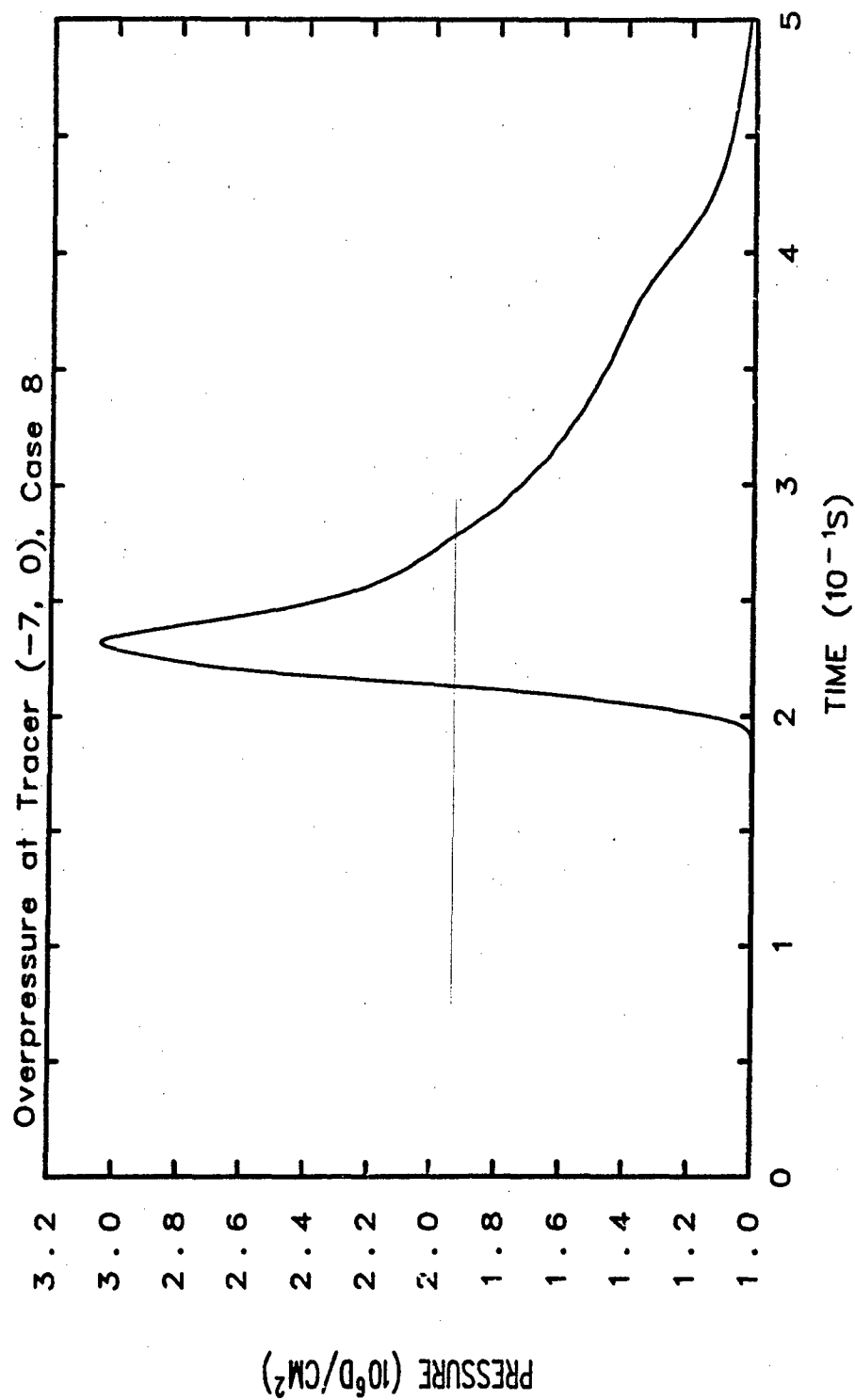


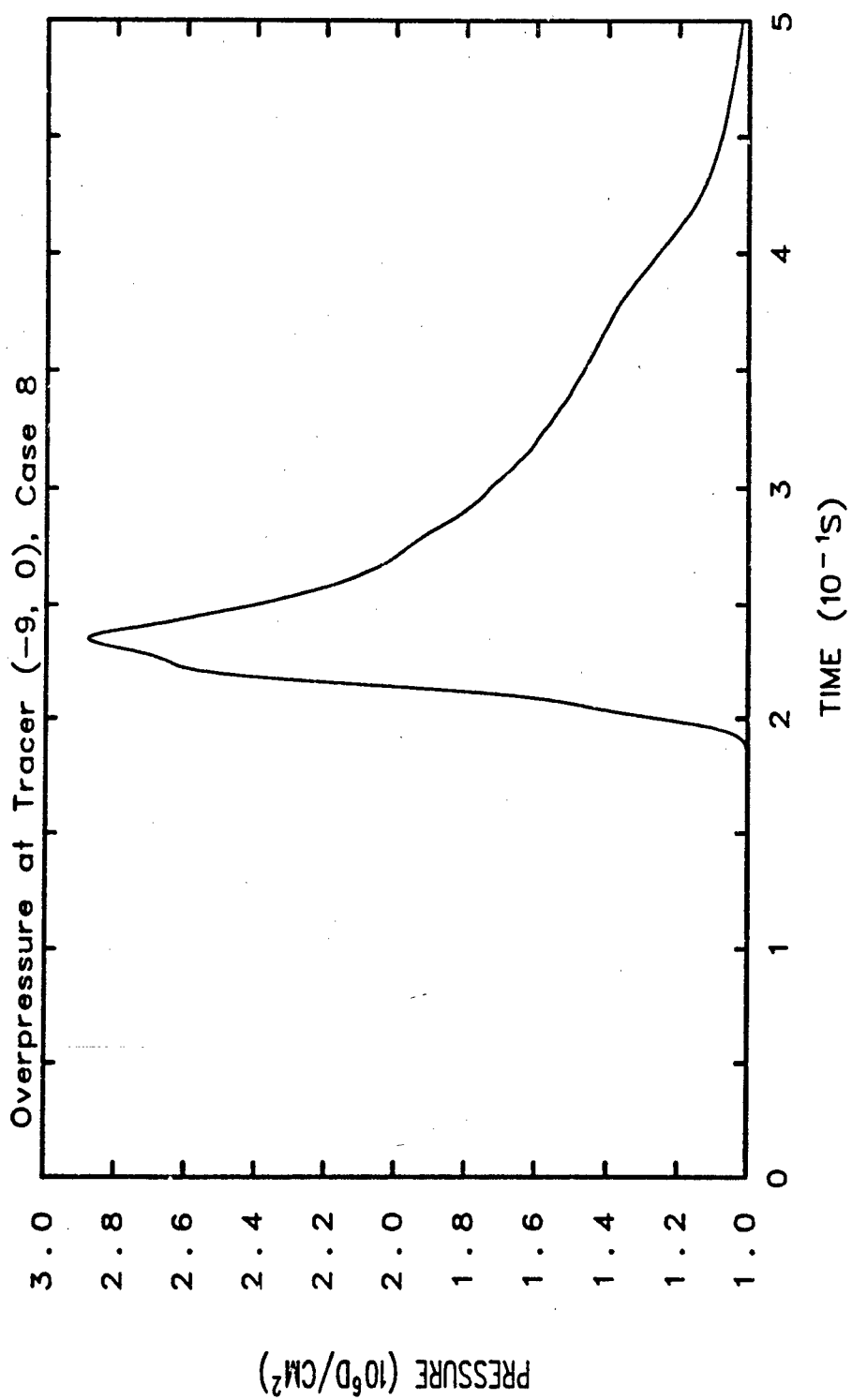


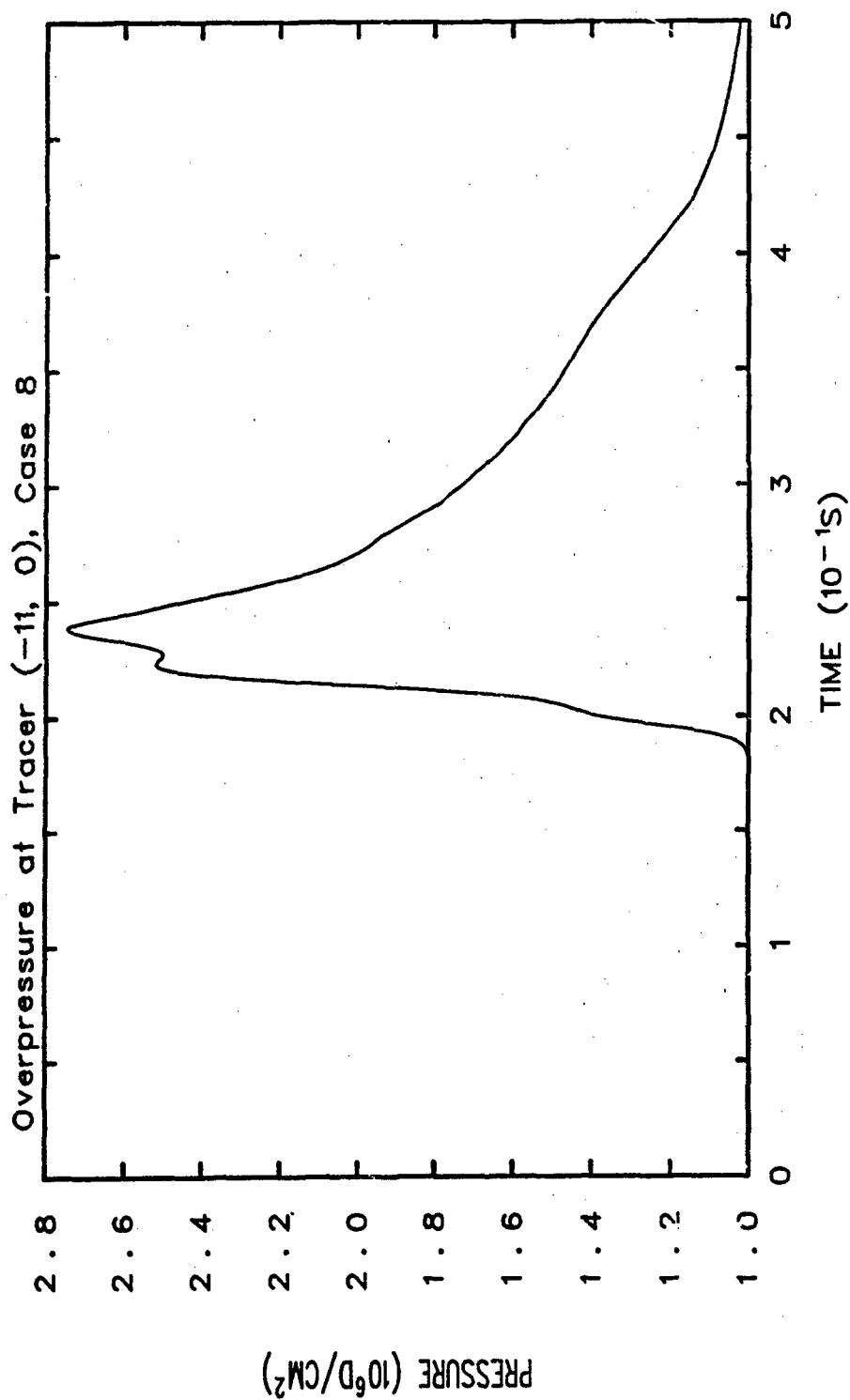


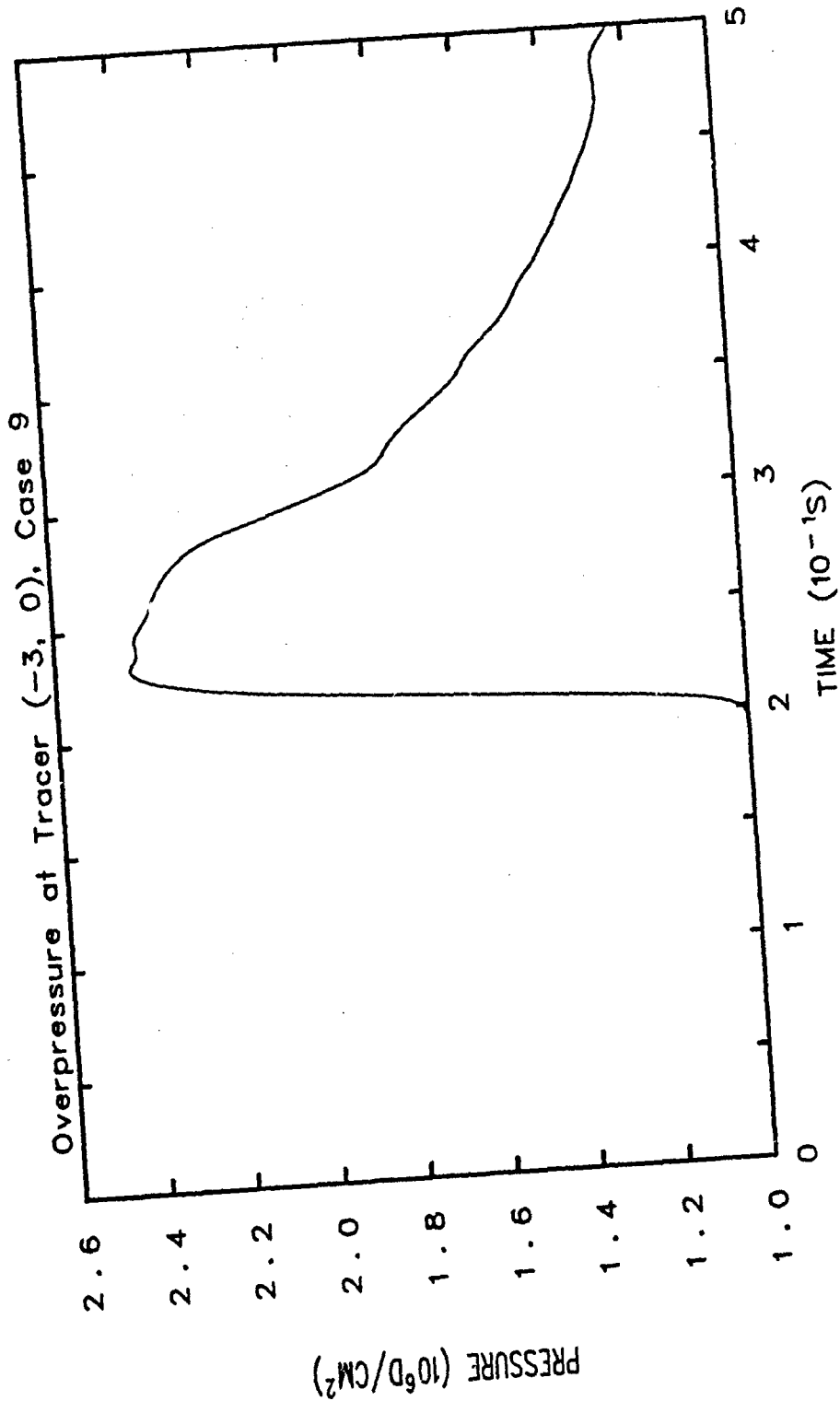


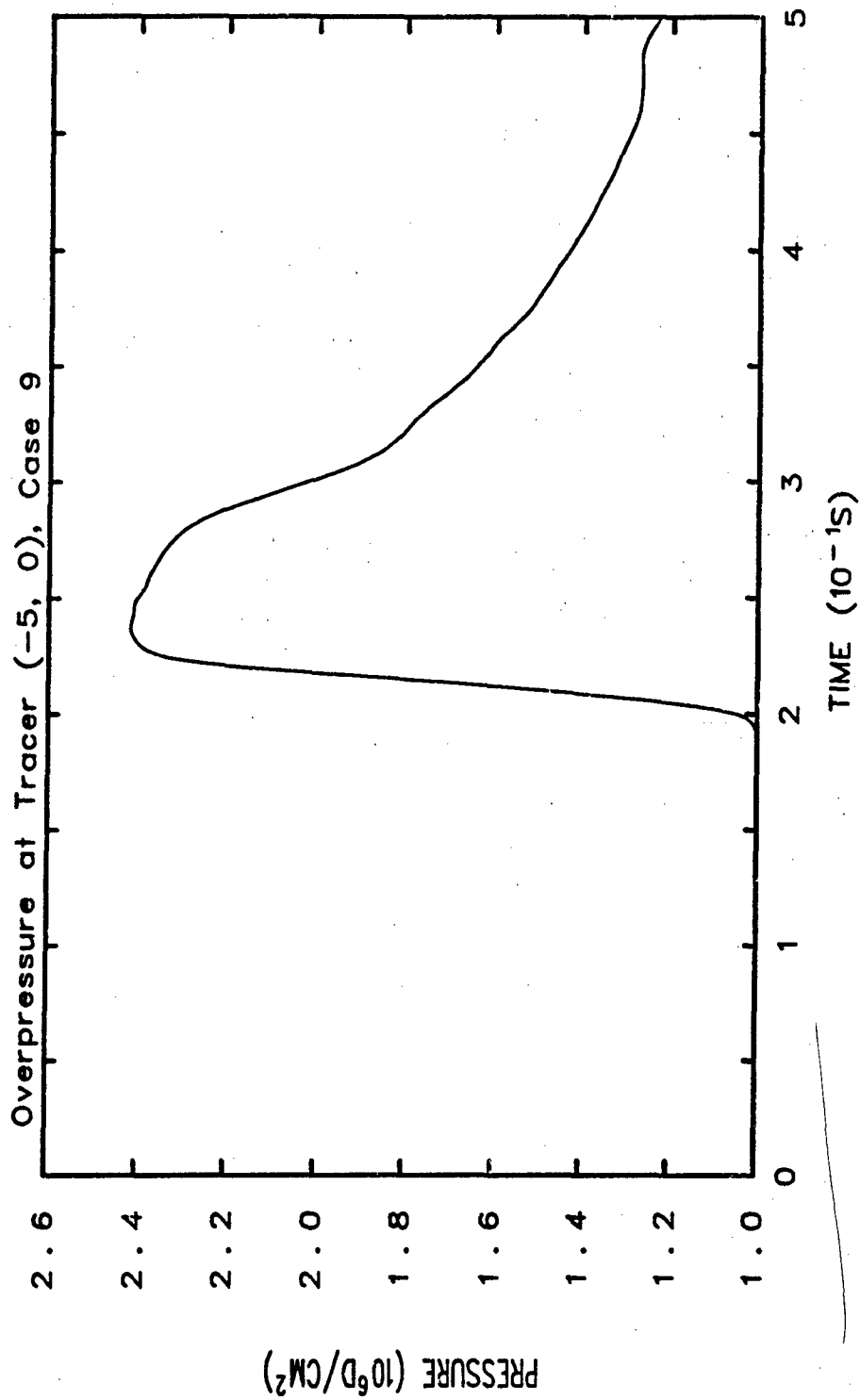


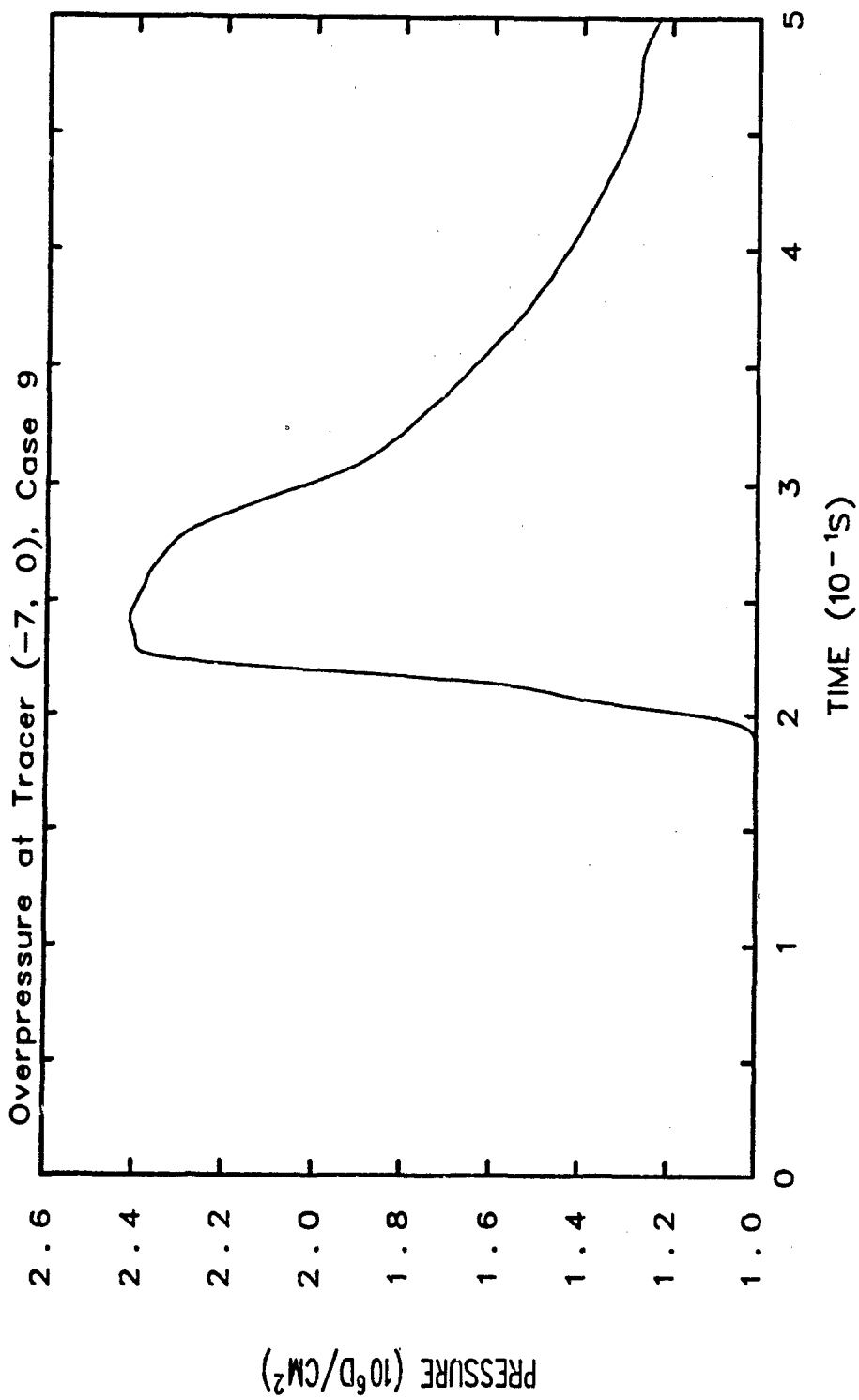


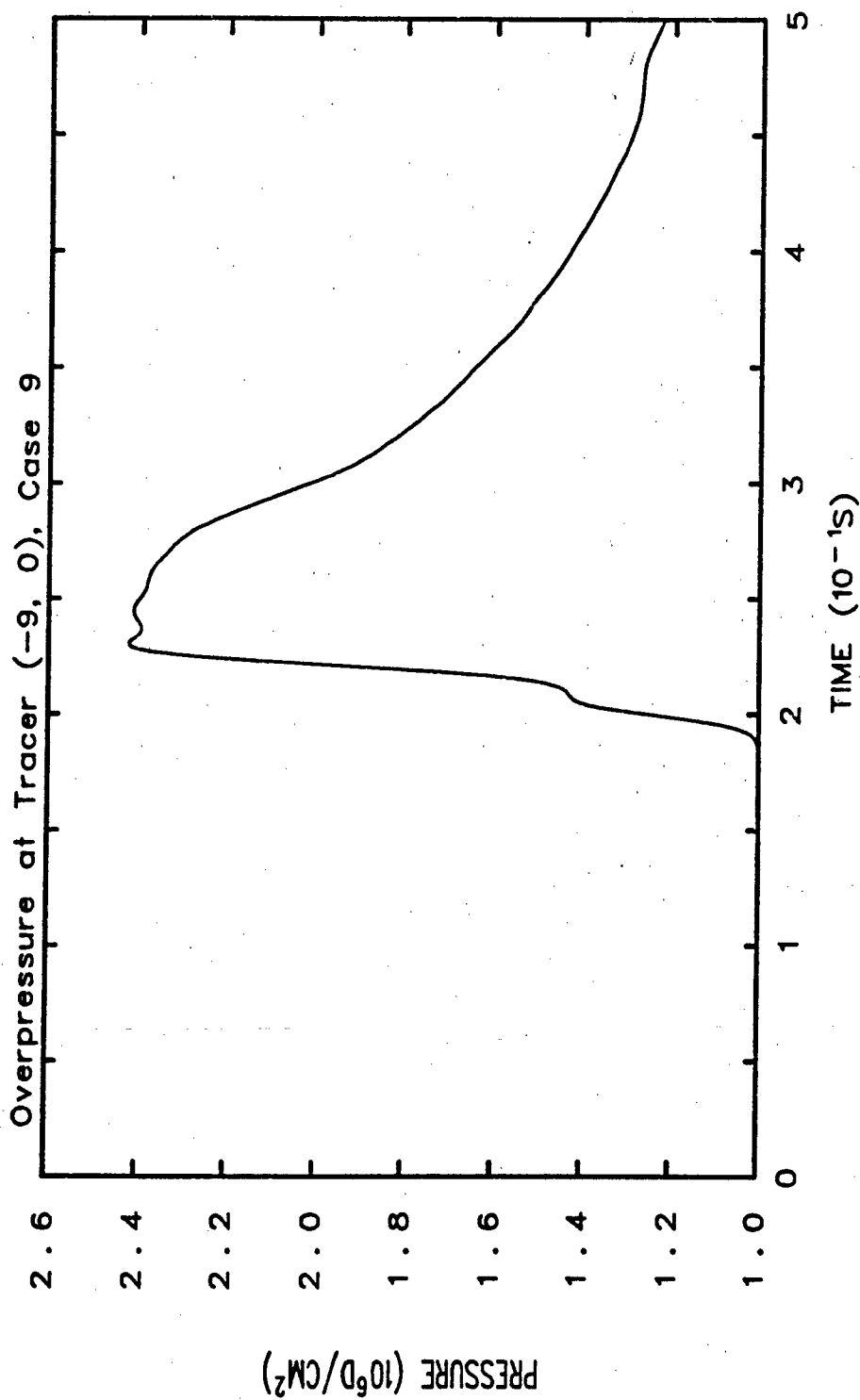


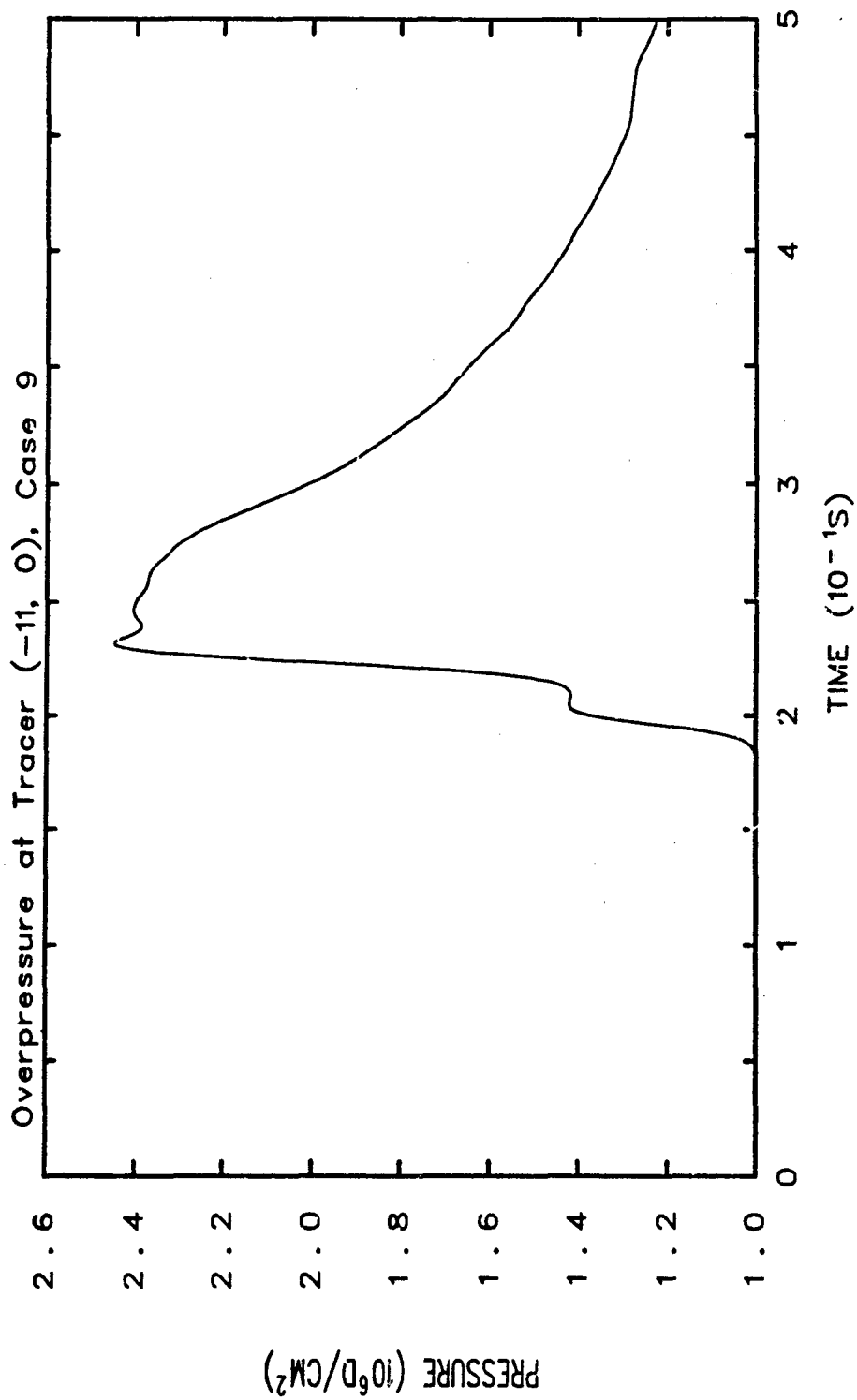


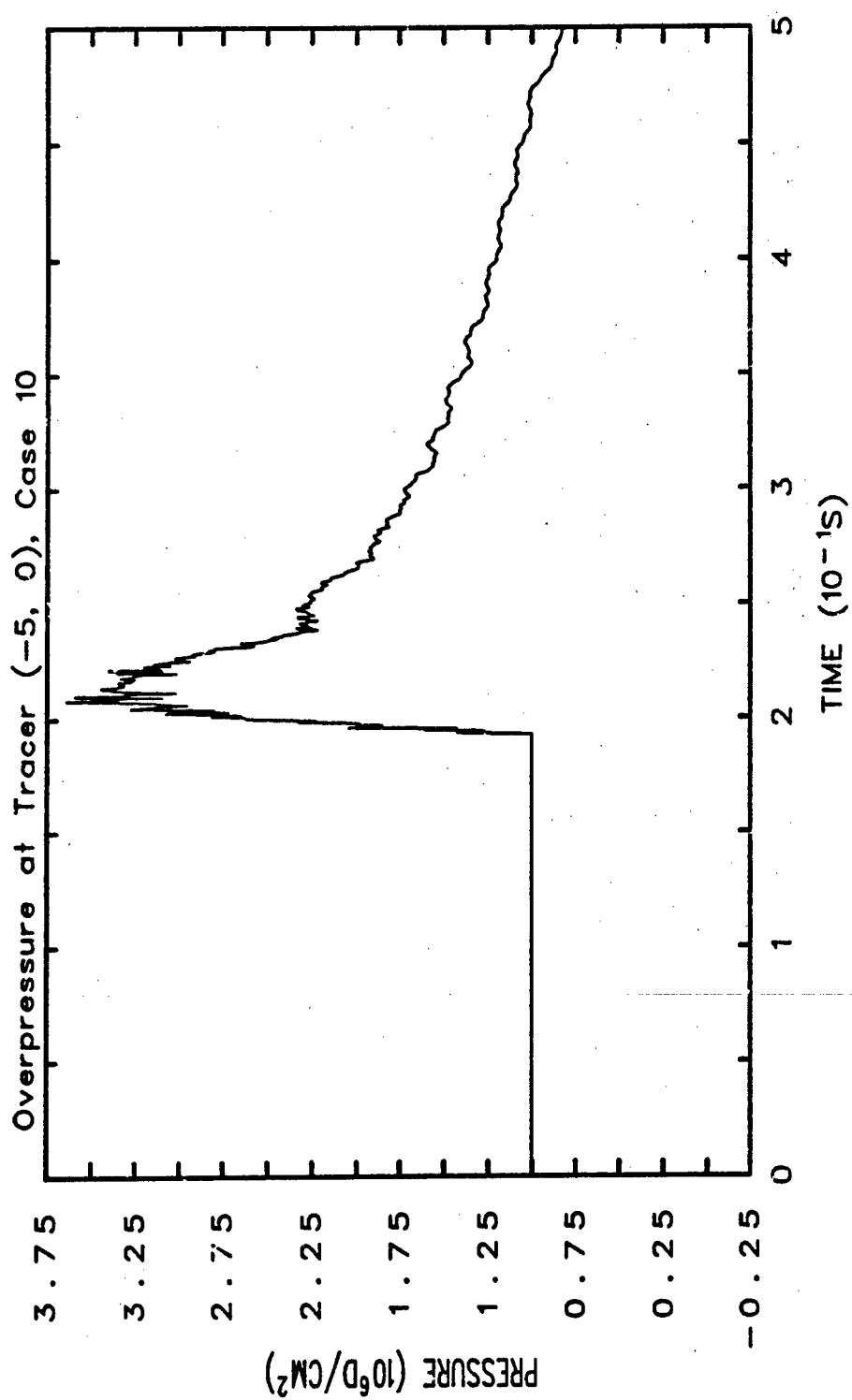


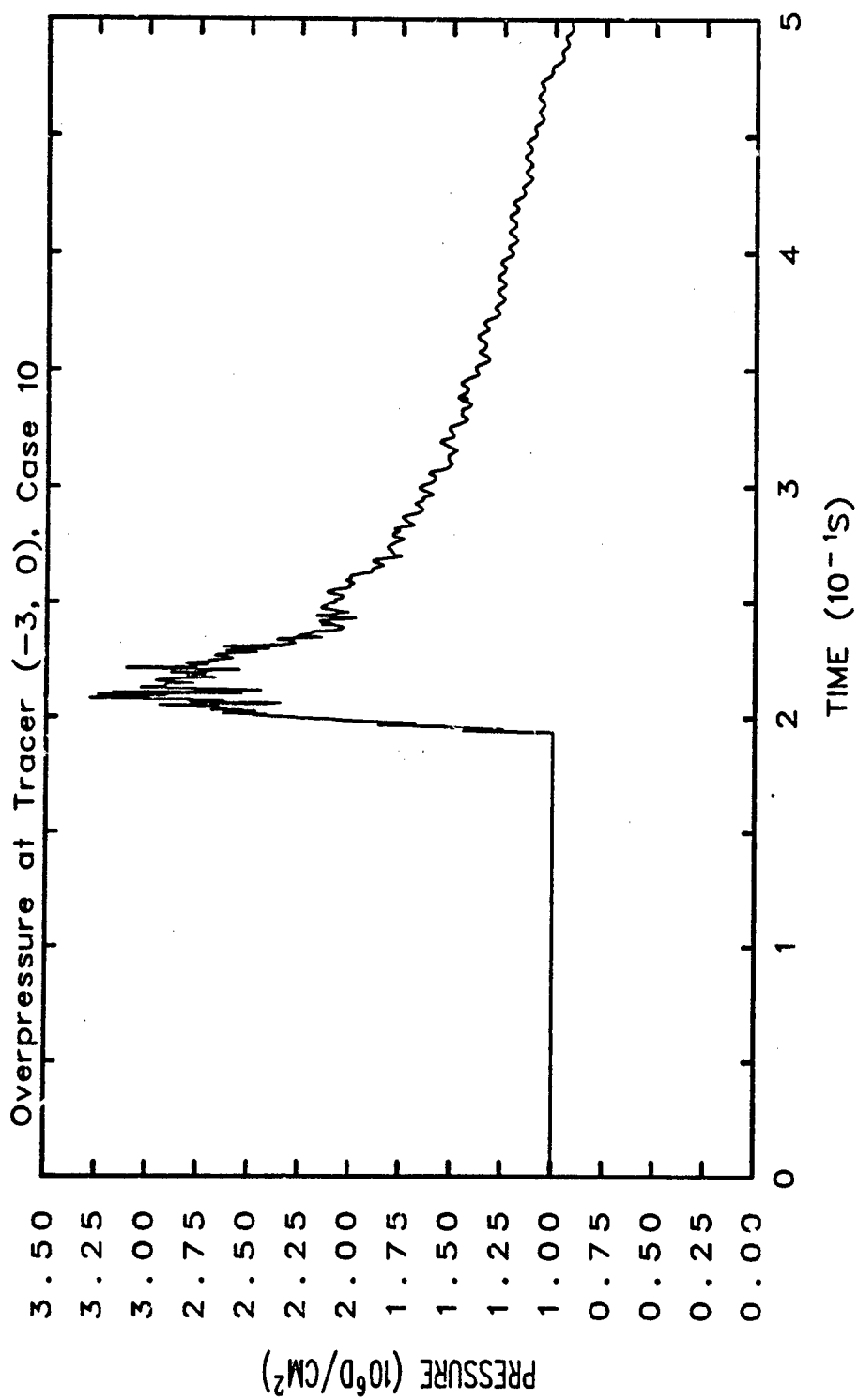


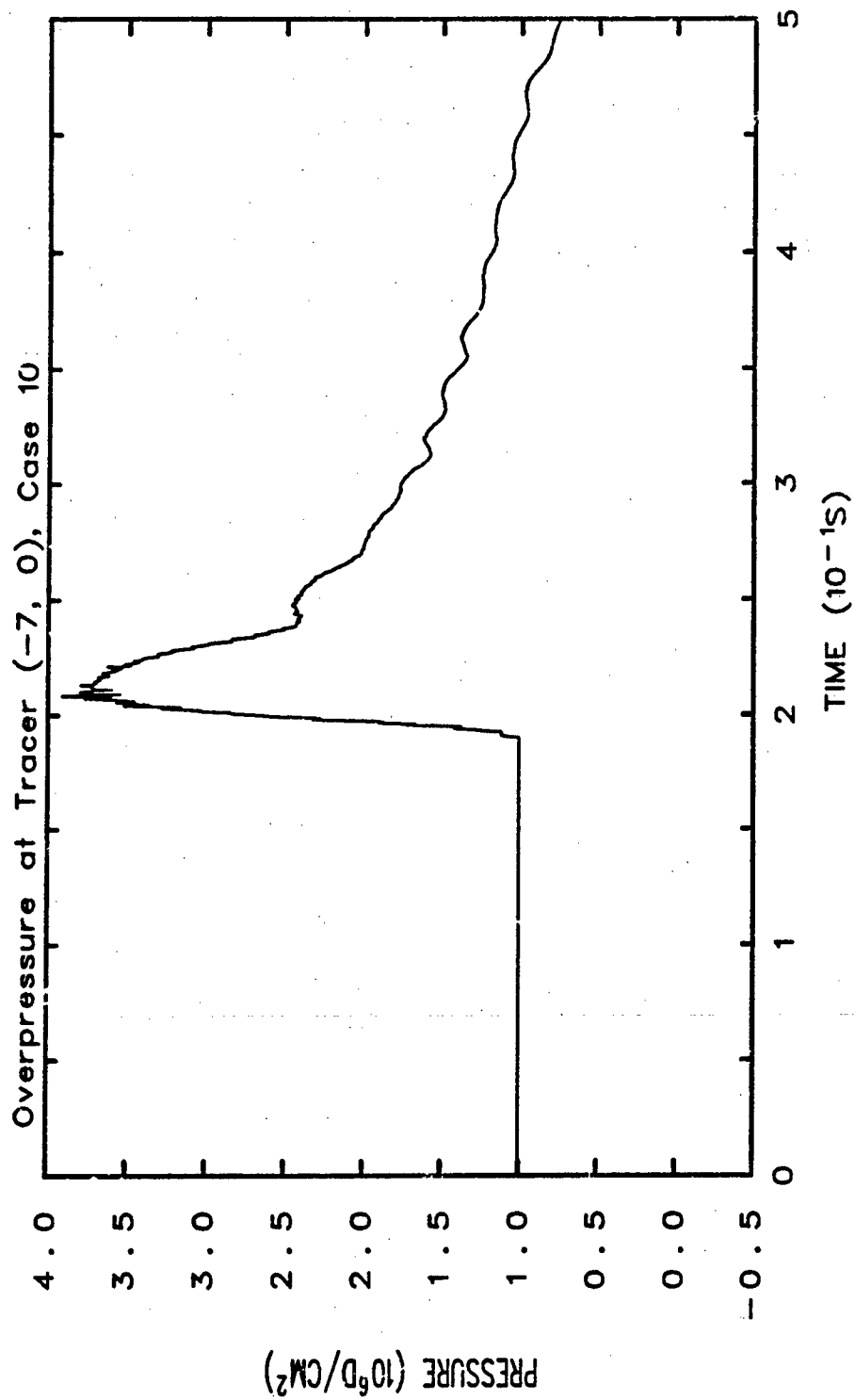


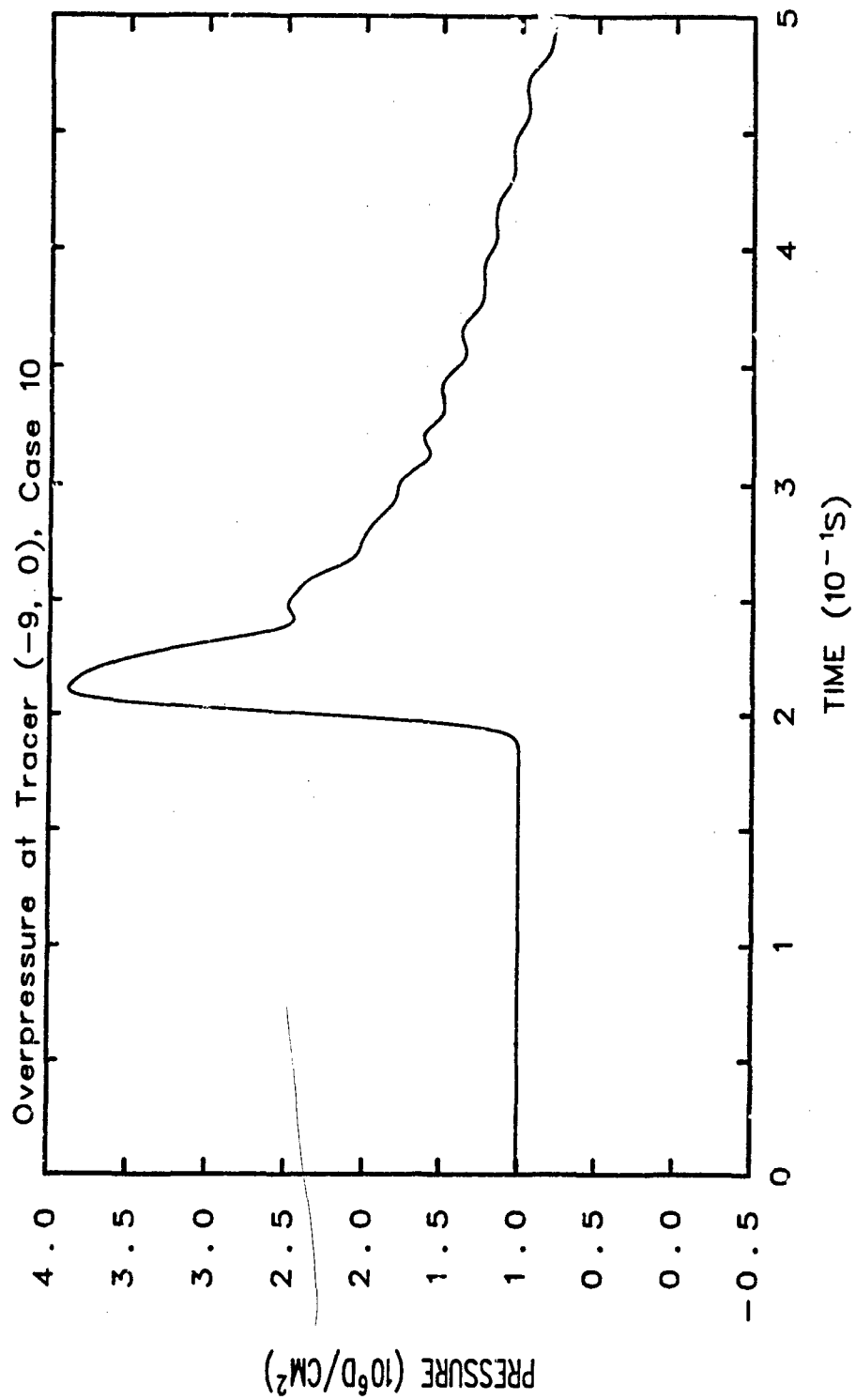


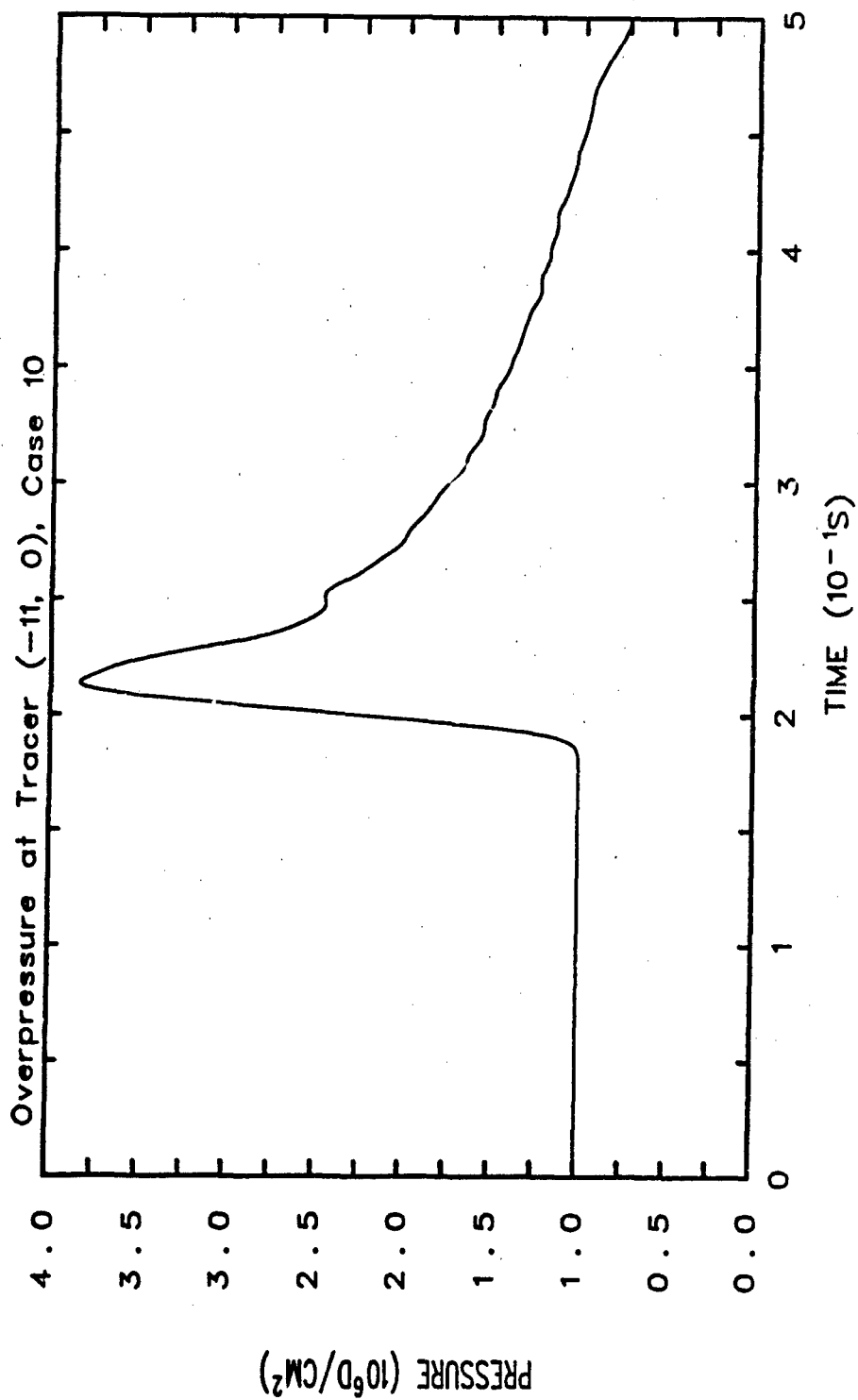


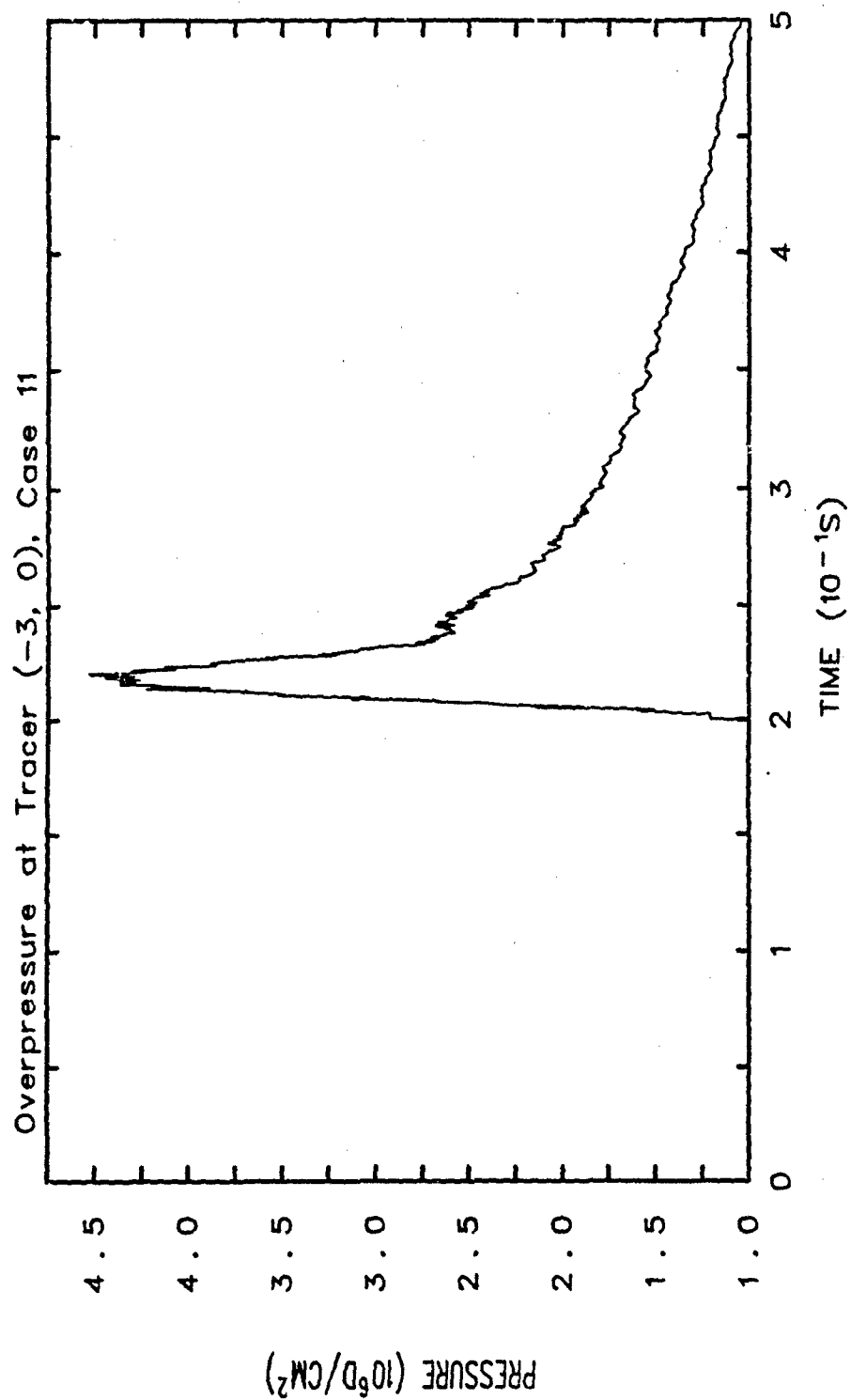


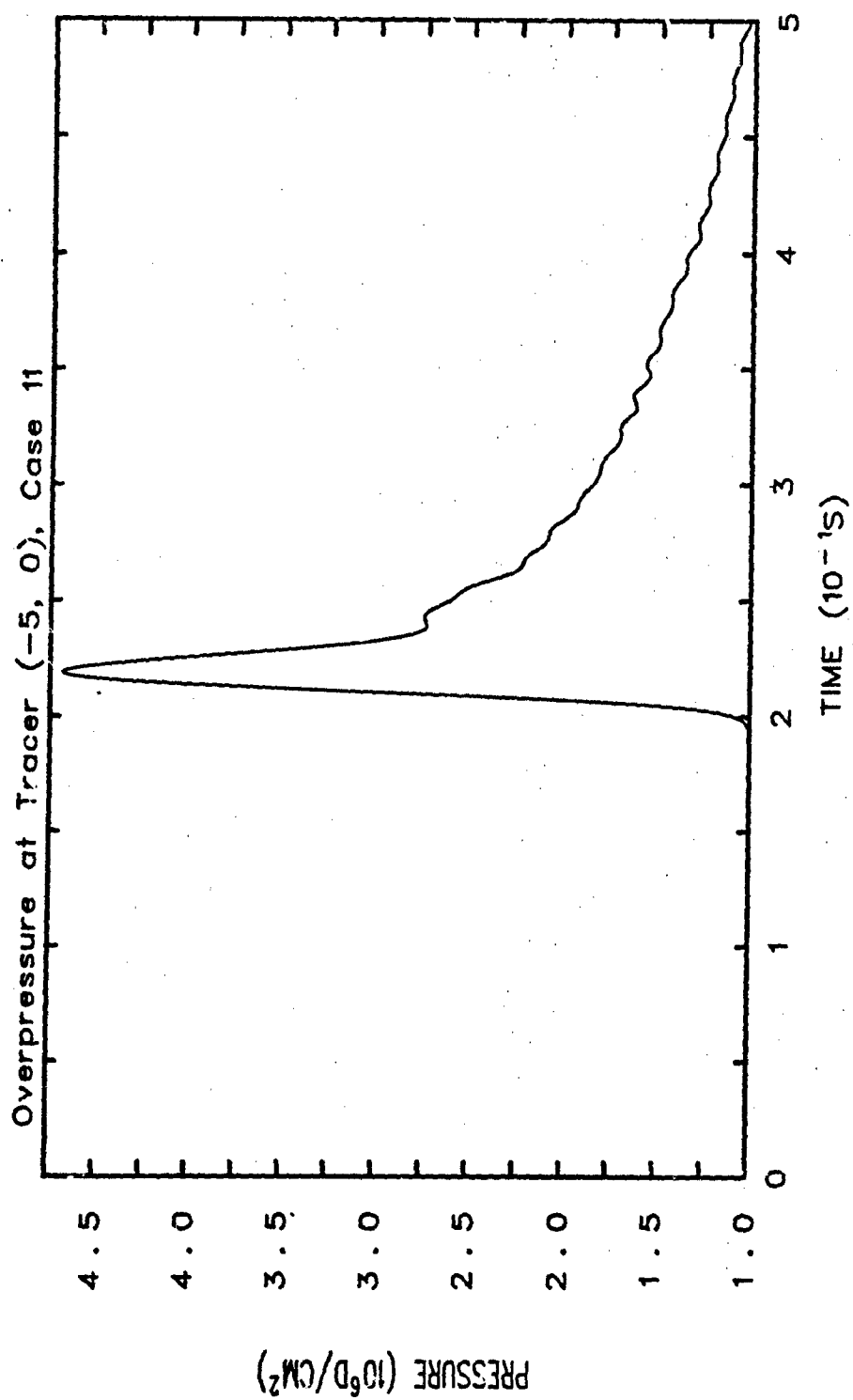


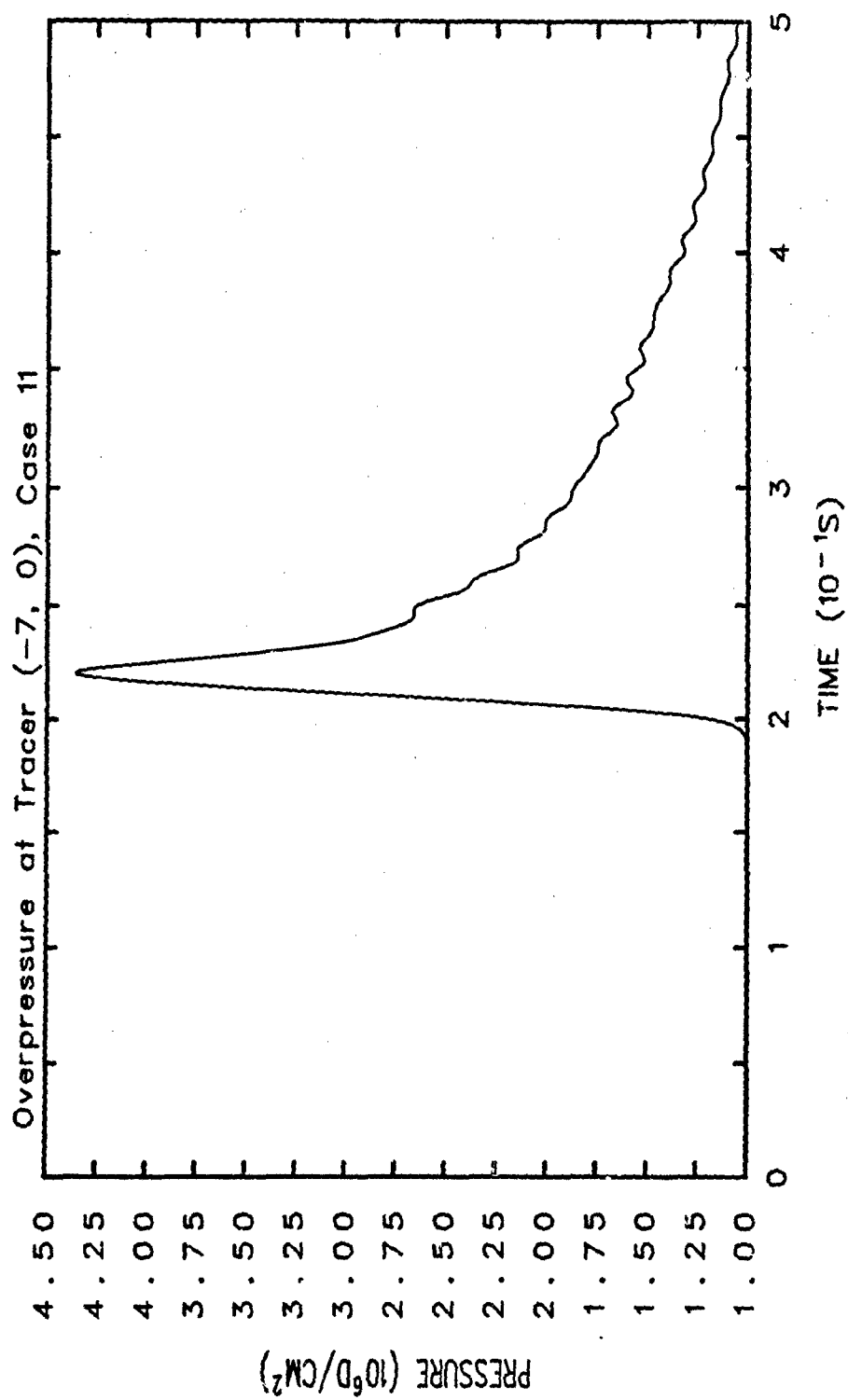


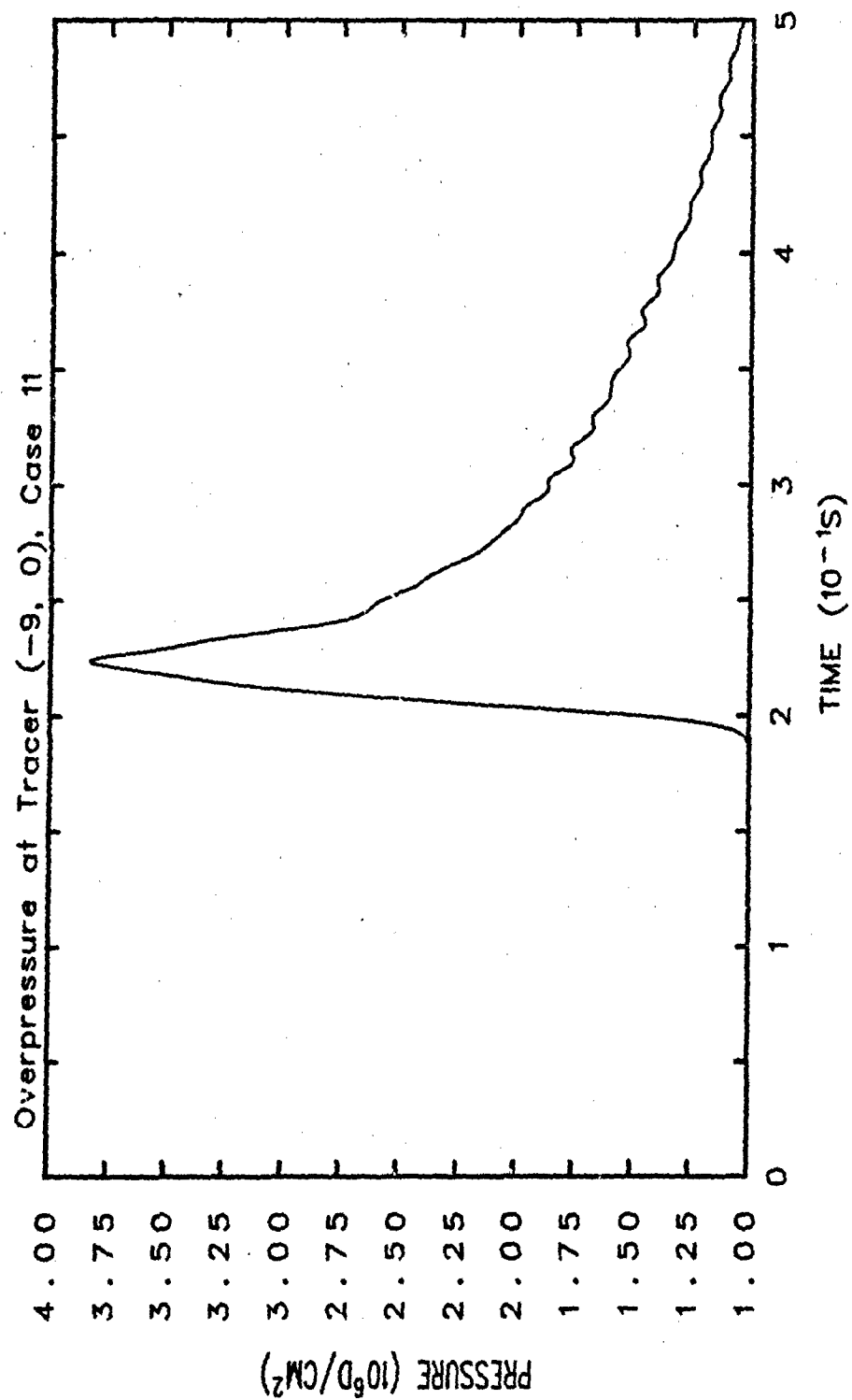


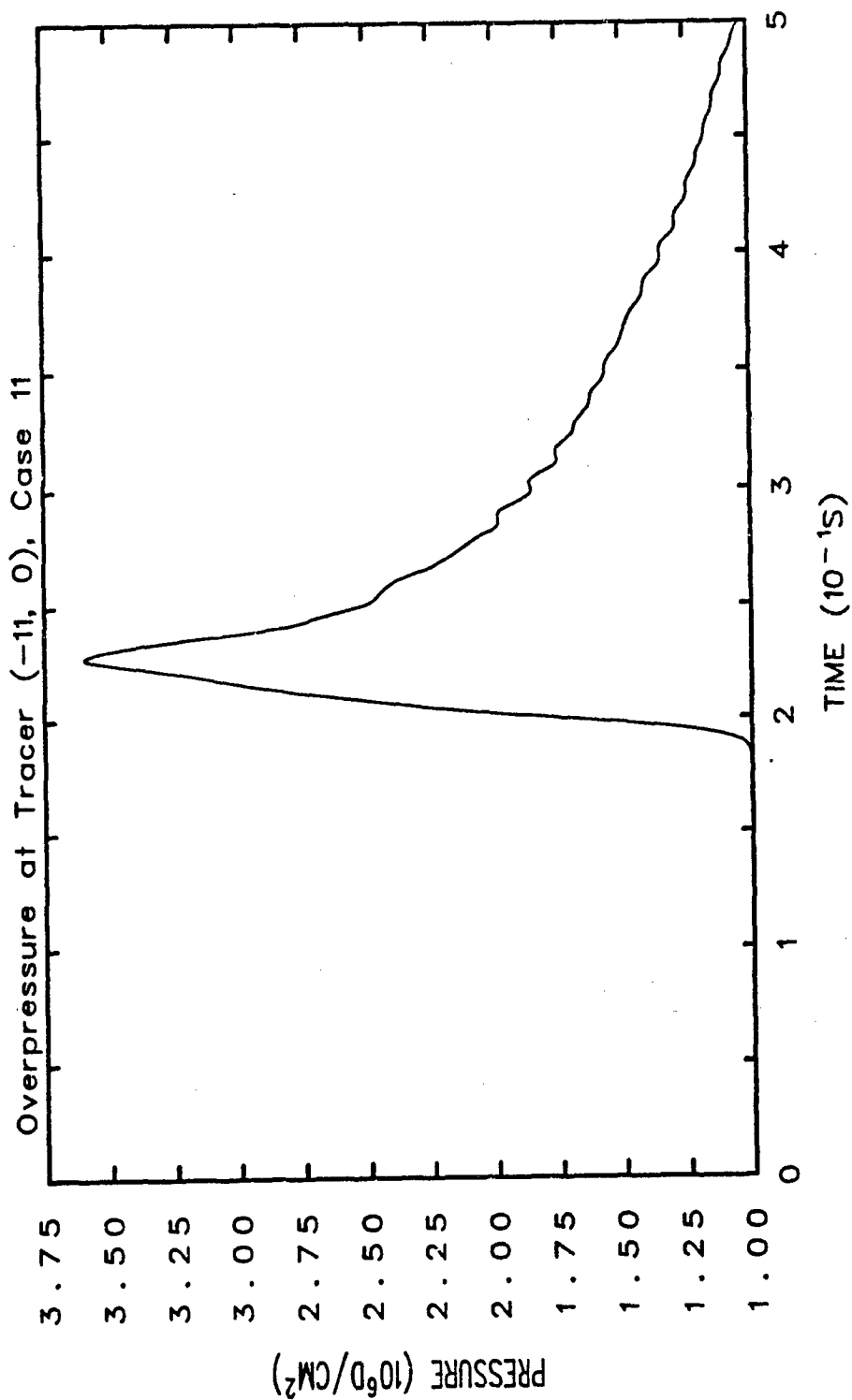


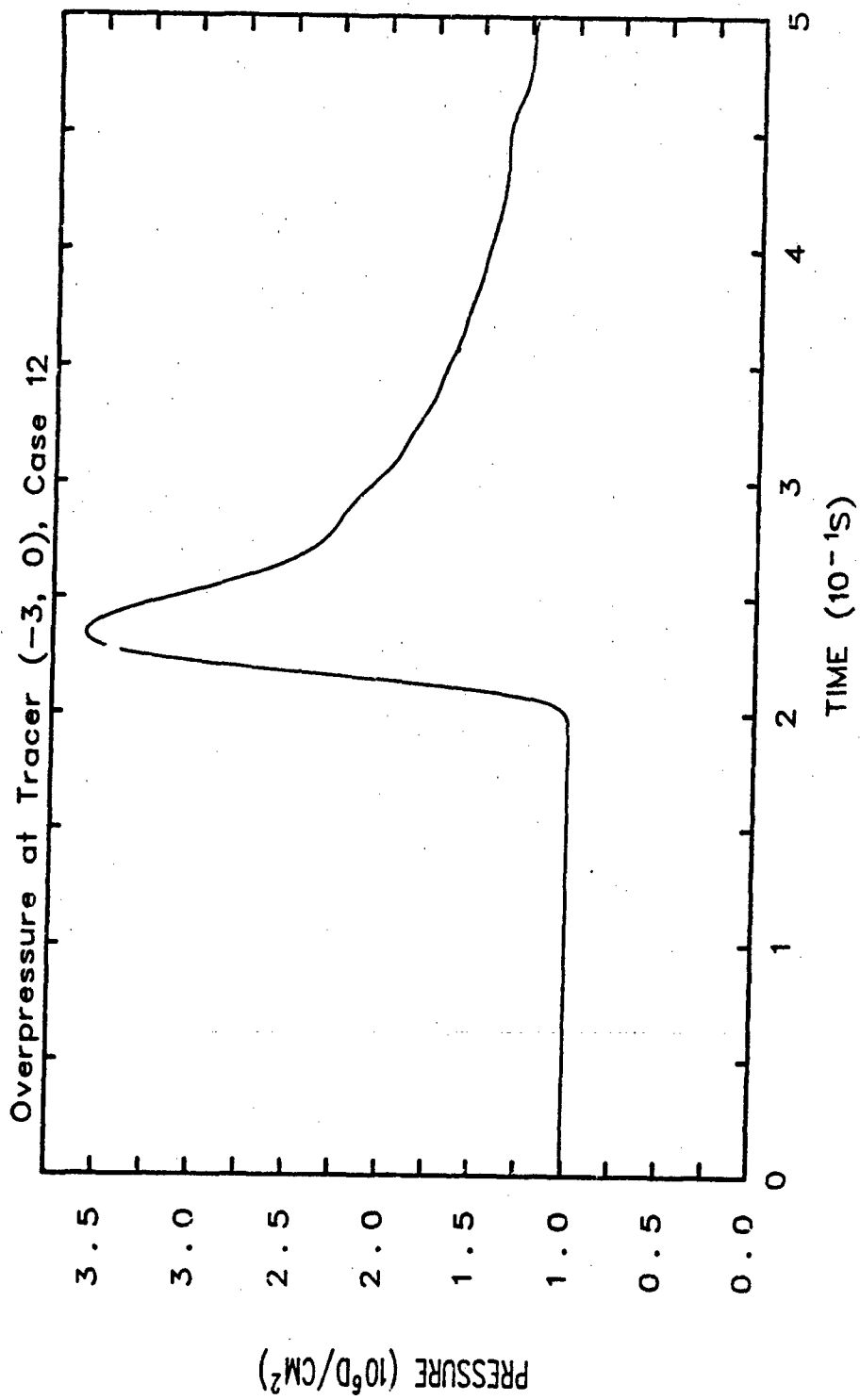


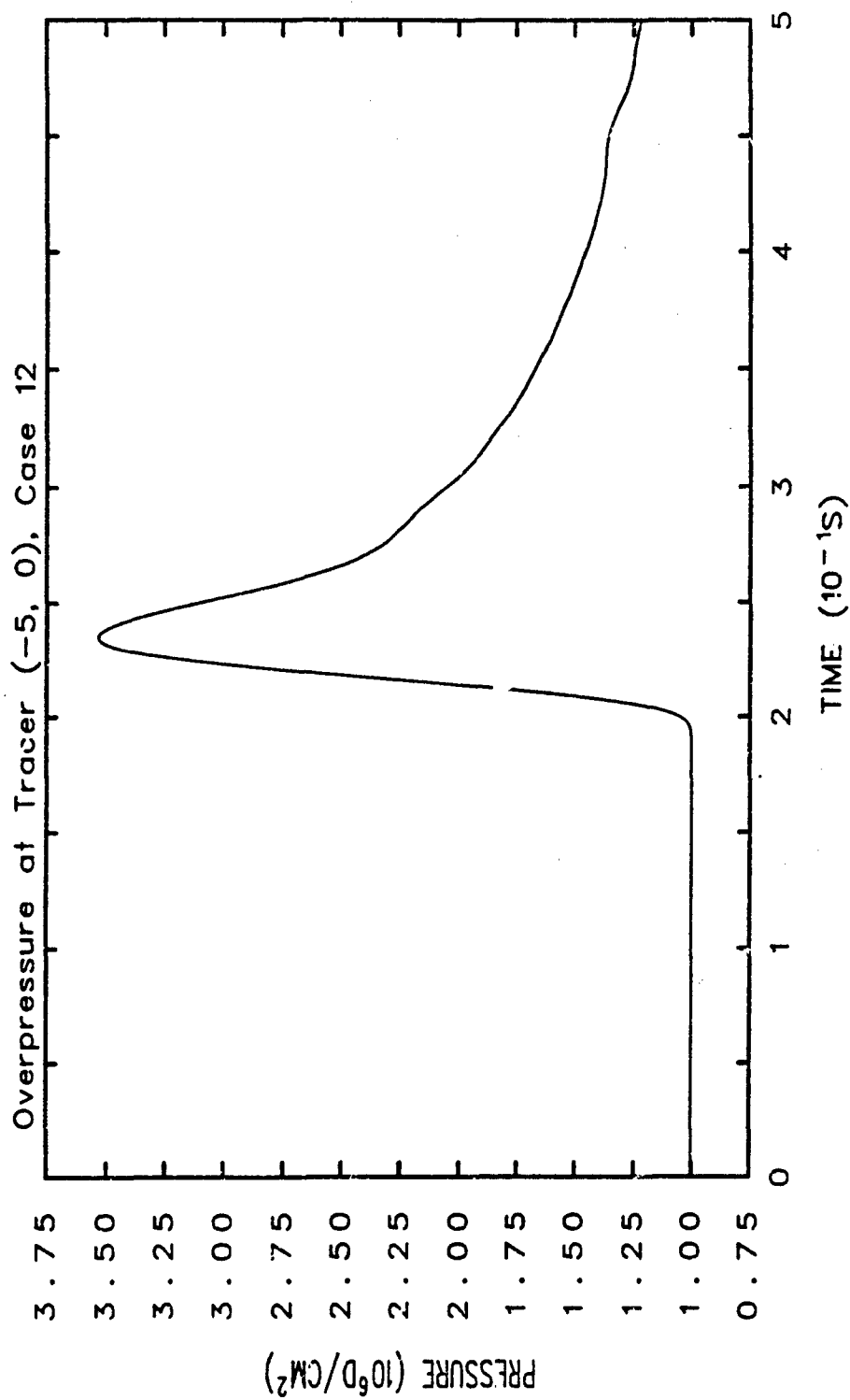


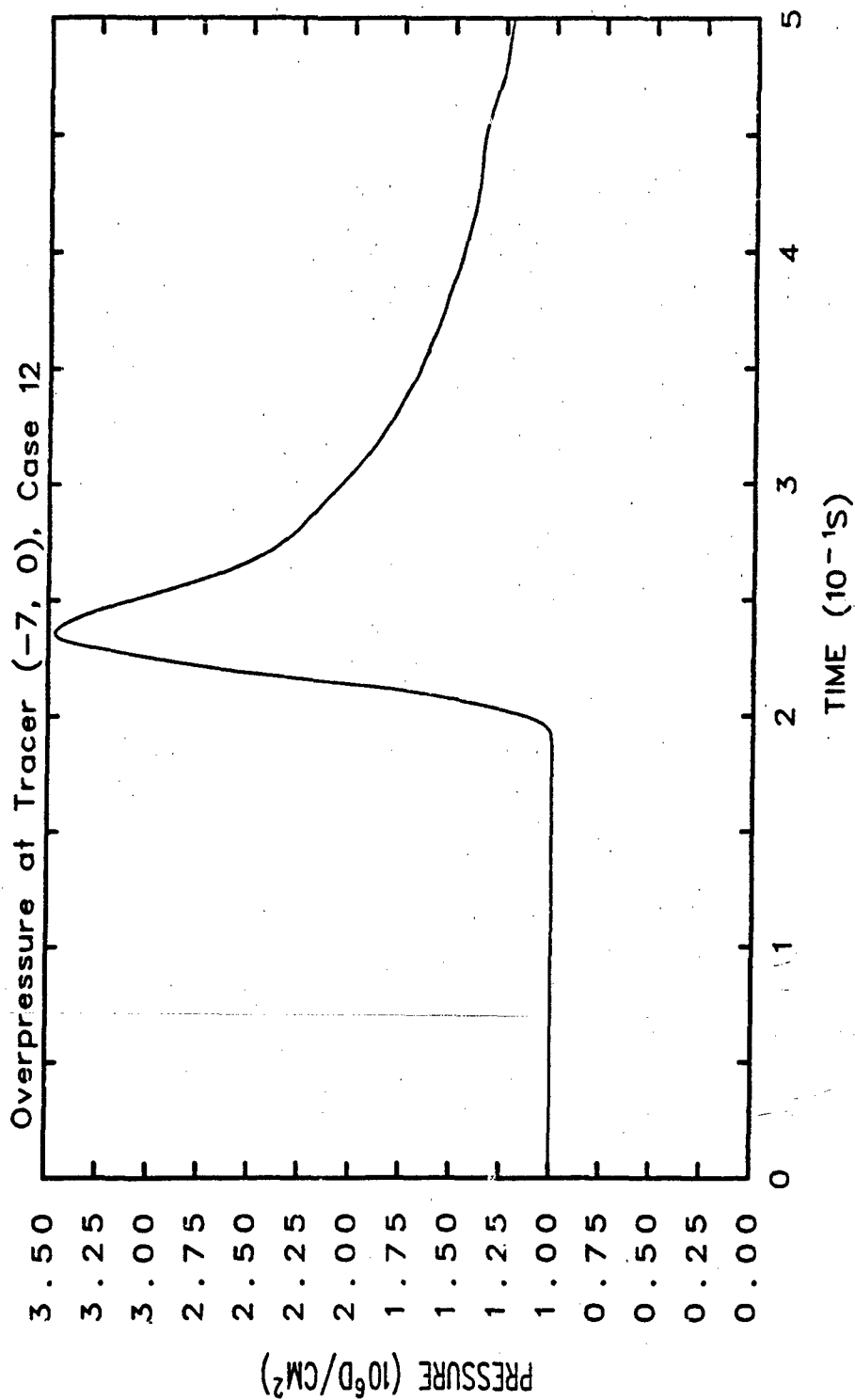


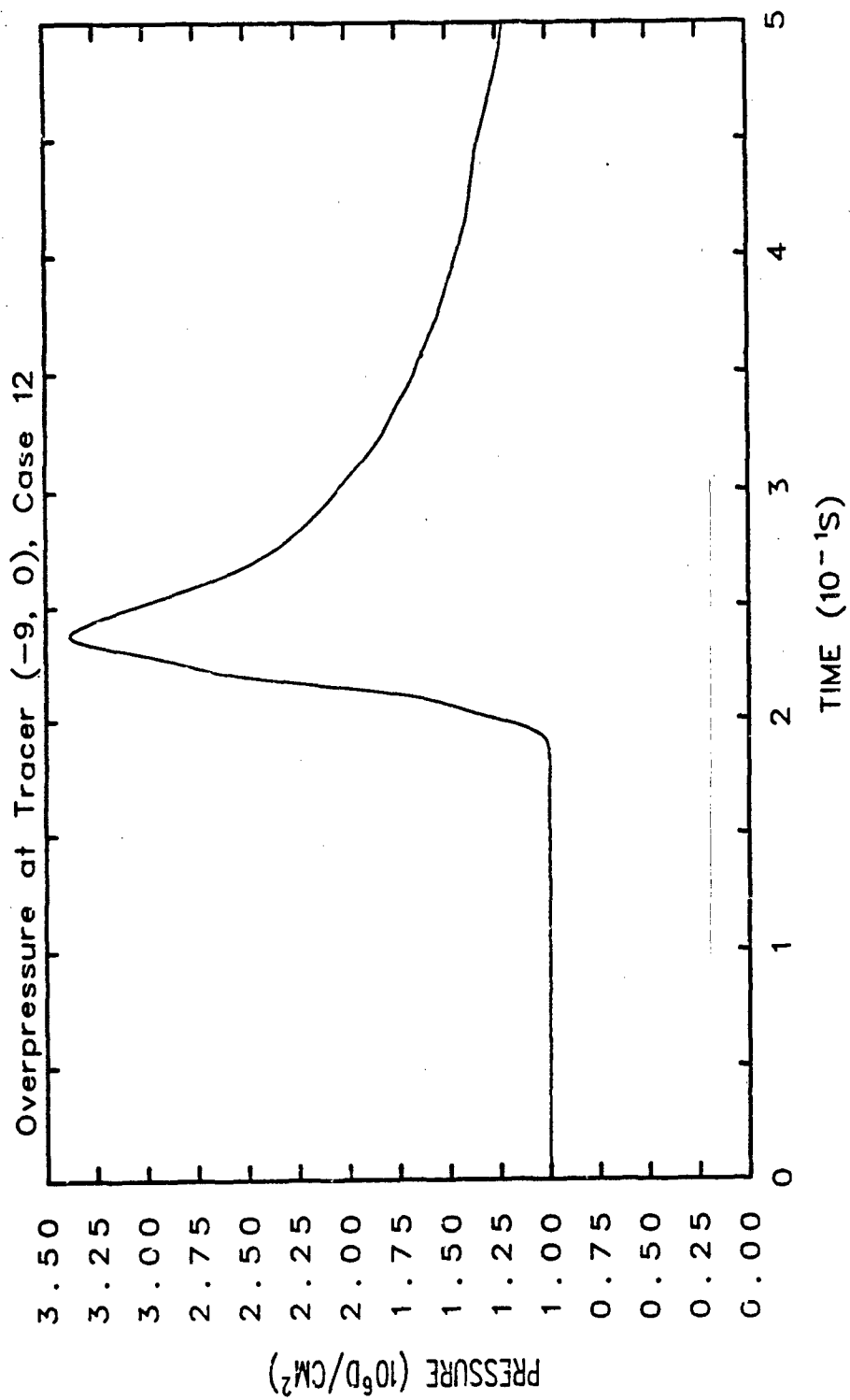


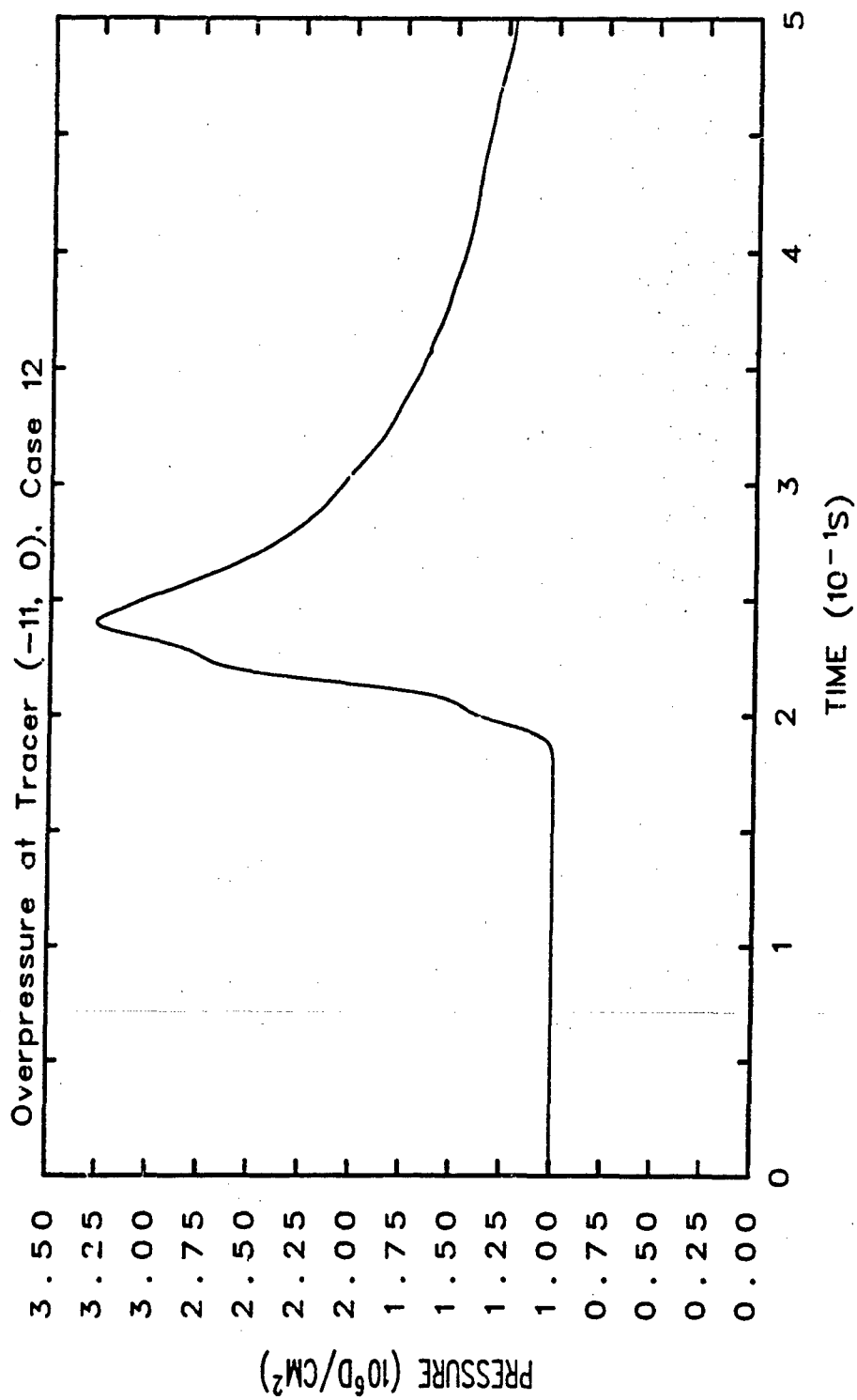








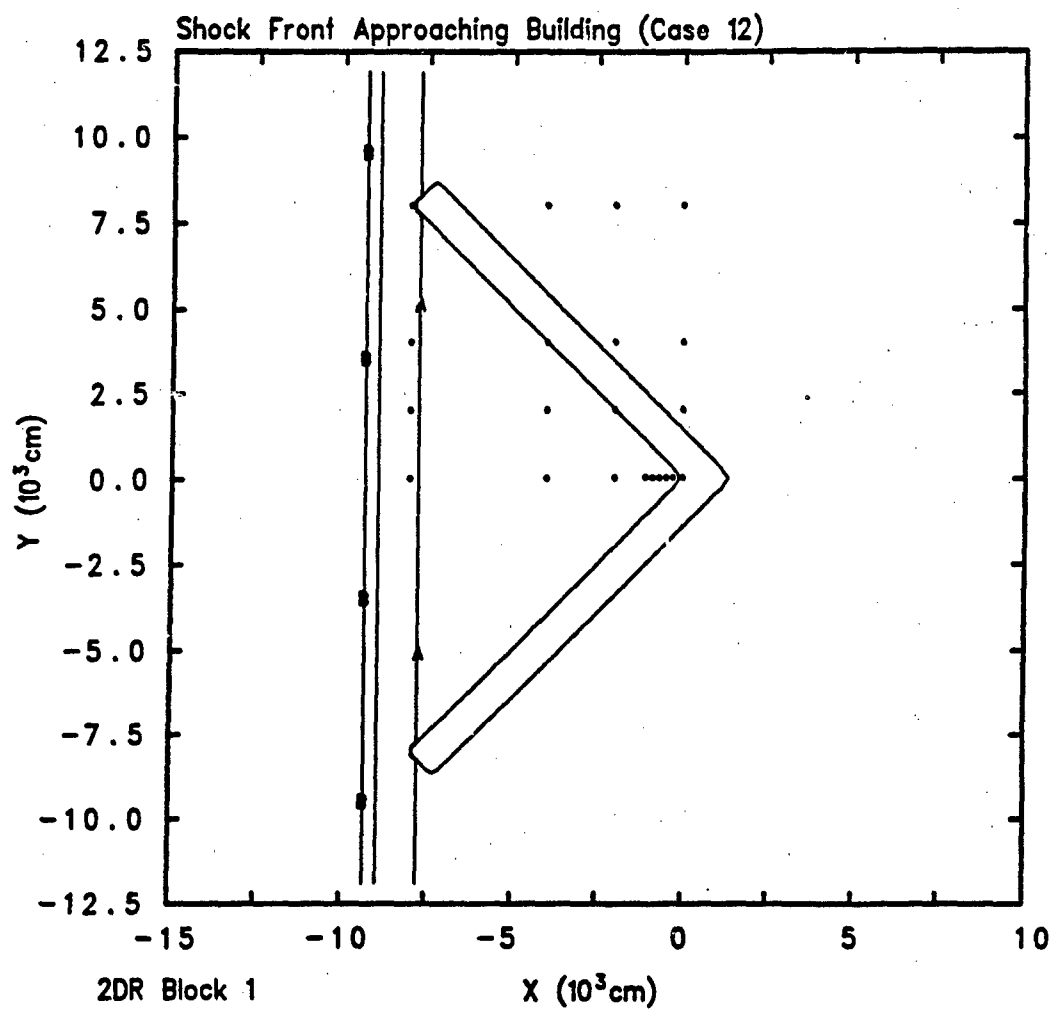




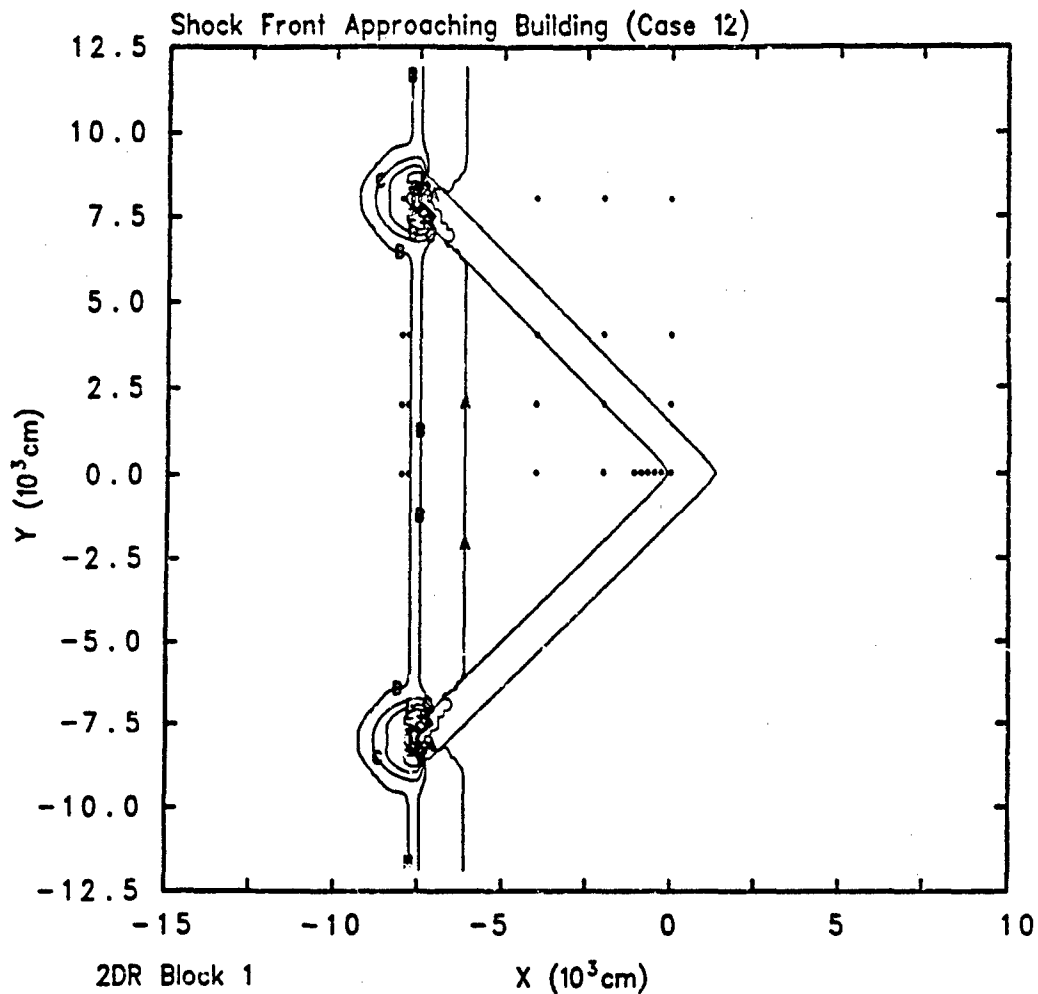
Legend

Pressure Contours (d/cm²)

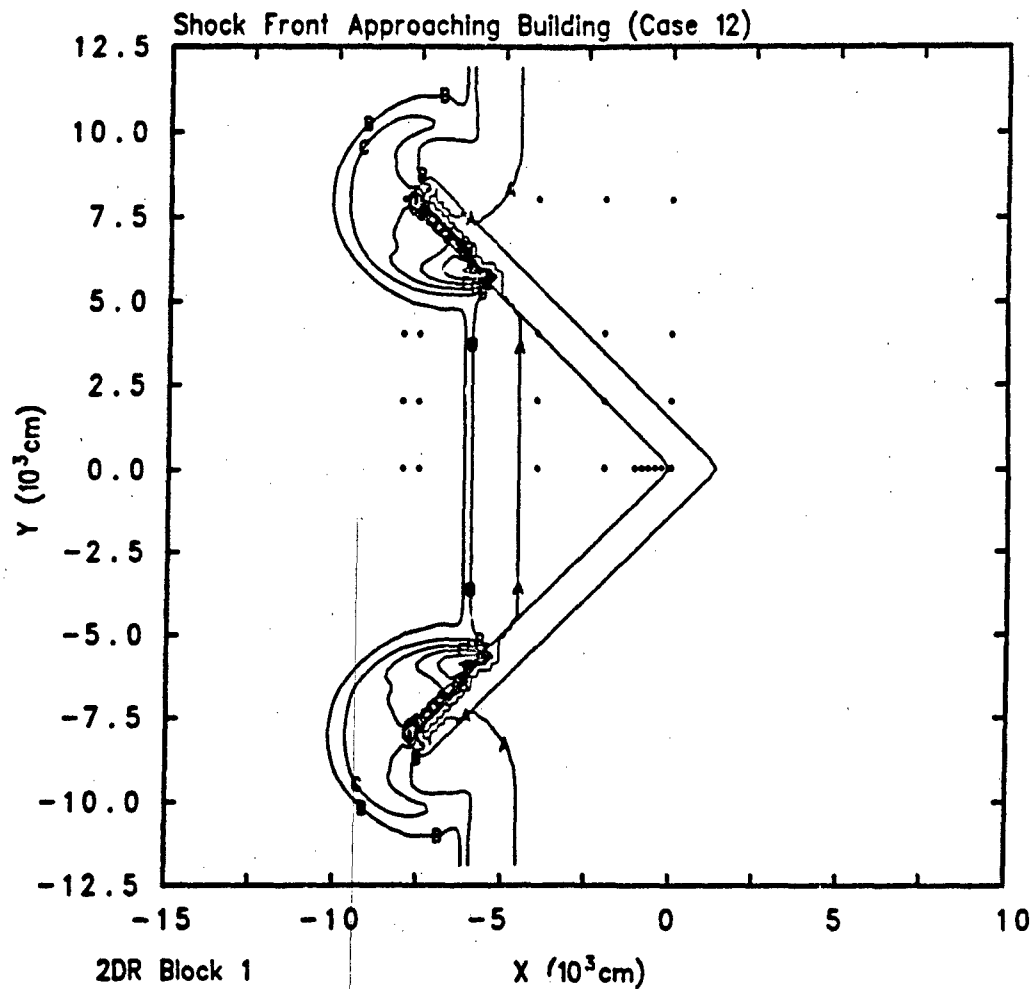
—t—	4.0000E+06	—l—	2.4000E+06
—o—	3.9000E+06	—k—	2.3000E+06
—z—	3.8000E+06	—j—	2.2000E+06
—y—	3.7000E+06	—i—	2.1000E+06
—x—	3.6000E+06	—h—	2.0000E+06
—w—	3.5000E+06	—g—	1.9000E+06
—v—	3.4000E+06	—f—	1.8000E+06
—u—	3.3000E+06	—e—	1.7000E+06
—r—	3.2000E+06	—d—	1.6000E+06
—s—	3.1000E+06	—c—	1.5000E+06
—r—	3.0000E+06	—b—	1.4200E+06
—q—	2.9000E+06	—a—	1.0010E+06
—p—	2.8000E+06		
—o—	2.7000E+06		
—n—	2.6000E+06		
—m—	2.5000E+06		



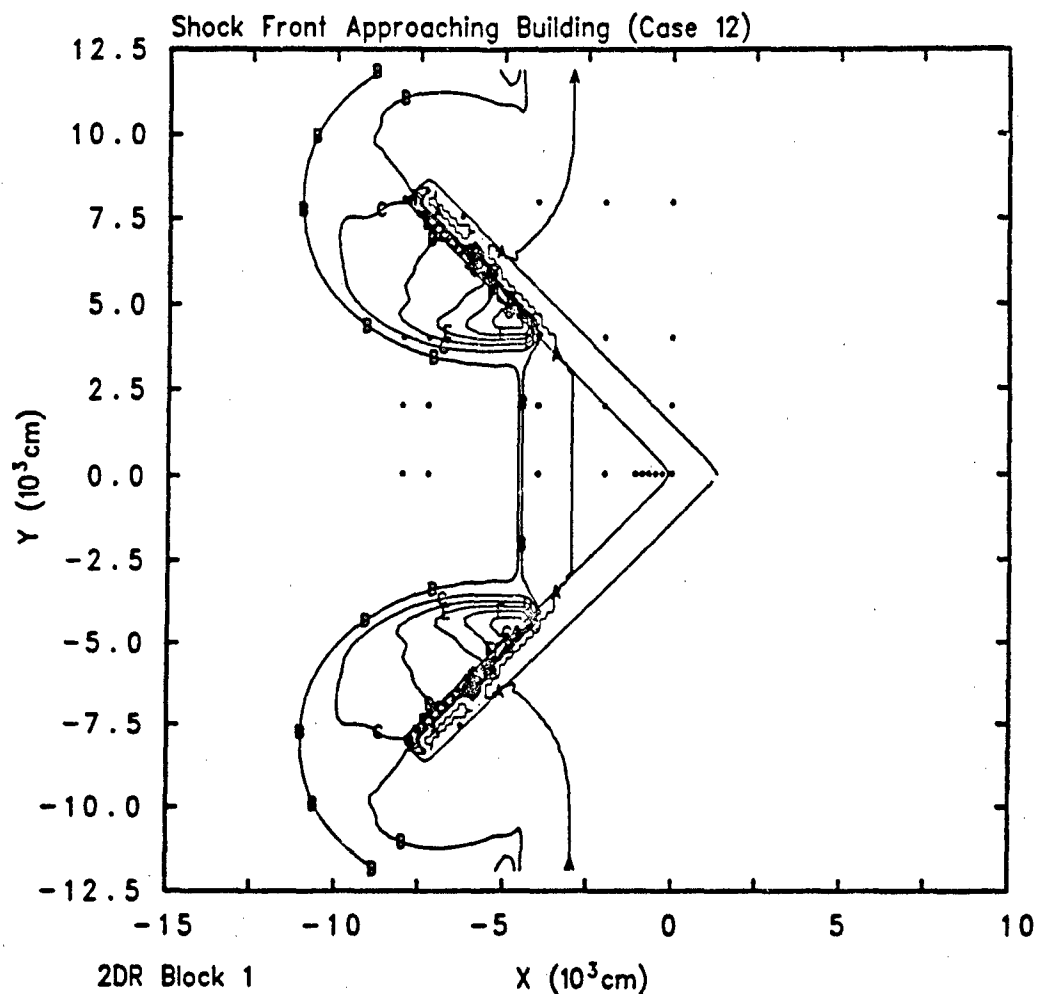
Shock generated by 2 atm in 10000 X 12000 cm (50 X 60 cells)- 2dr
 AGAEQY 1/07/93 01:18:20 CTH 142 Time= 7.50155×10^{-2}



2DR Block 1
 Shock generated by 2 atm in 10000 X 12000 cm (50 X 60 cells)- 2dr
 AGAEQY 1/07/93 01:38:49 CTH 249 Time=1.00171x10⁻¹

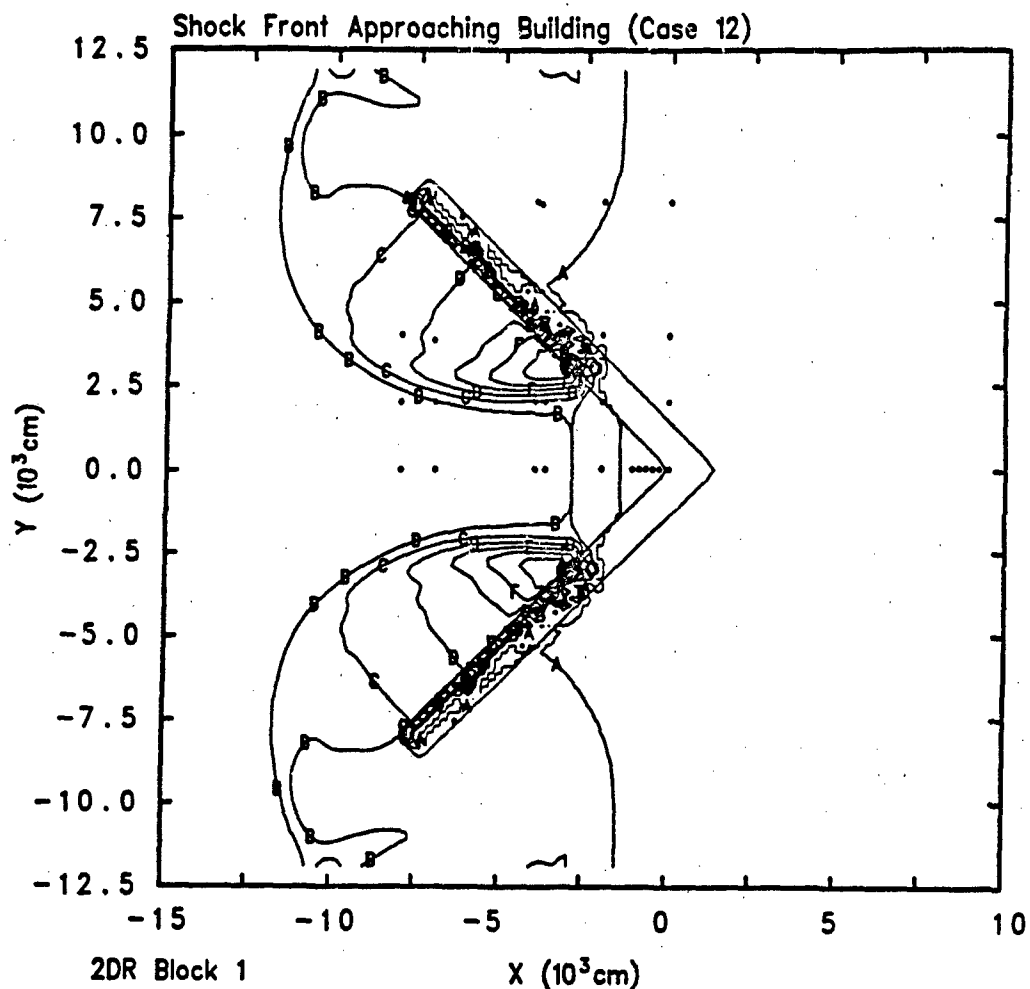


Shock generated by 2 atm in 10000 X 12000 cm (50 X 60 cells)- 2dr
 AGAEQY 1/07/93 02:00:58 CTH 361 Time=1.25101x10⁻¹

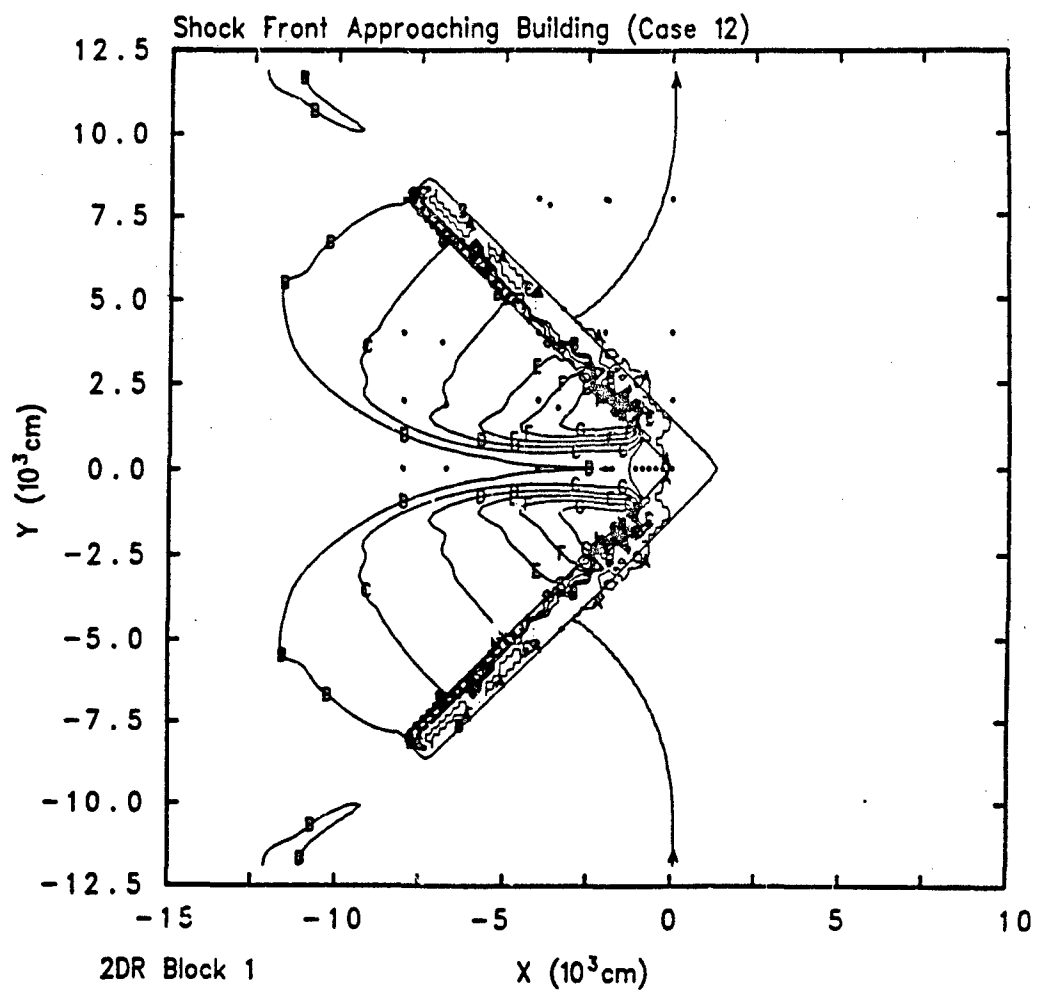


Shock generated by 2 atm in 10000 X 12000 cm (50 X 60 cells)- 2dr

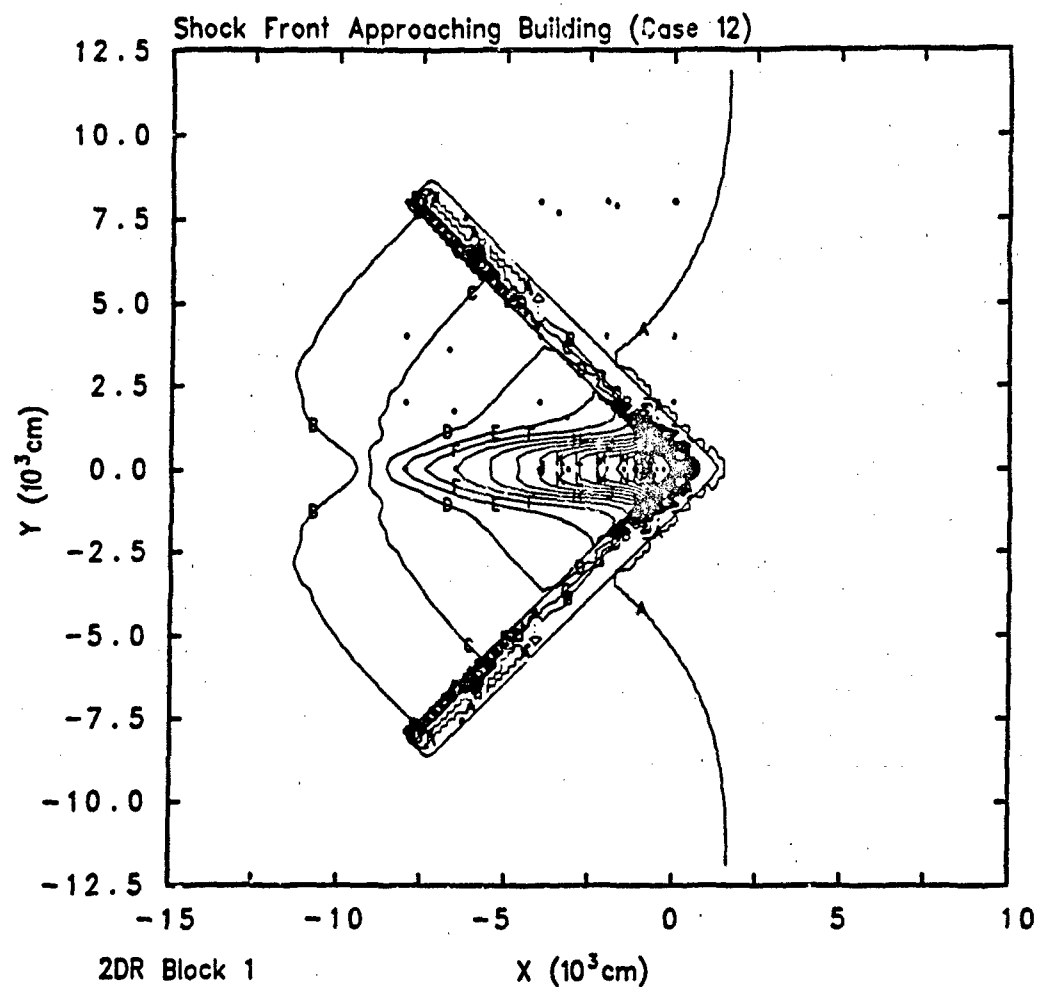
AGAEQY 1/07/93 02:24:05 CTH 474 Time= 1.50214×10^{-1}



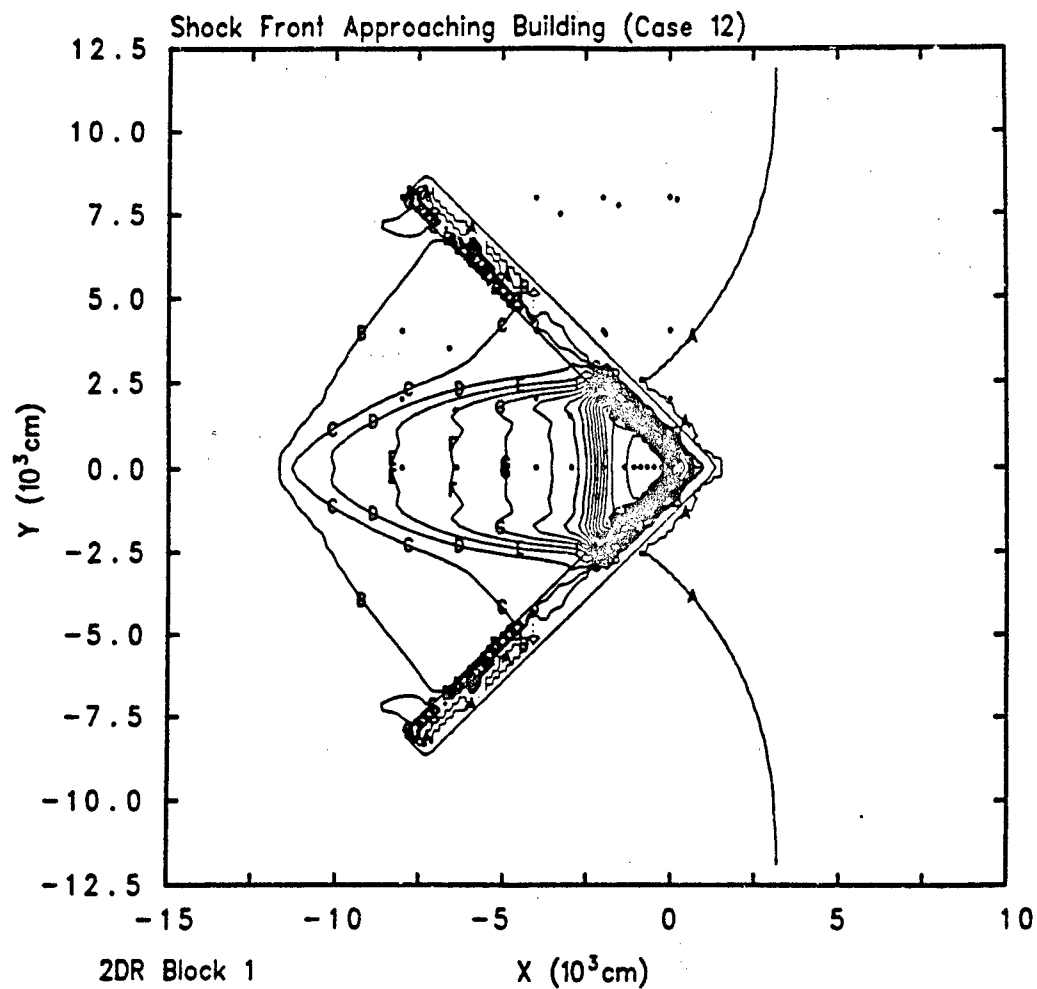
Shock generated by 2 atm in 10000 X 12000 cm (50 X 60 cells)- 2dr
 AGAEQY 1/07/93 02:48:15 CTH 588 Time=1.75159x10⁻¹



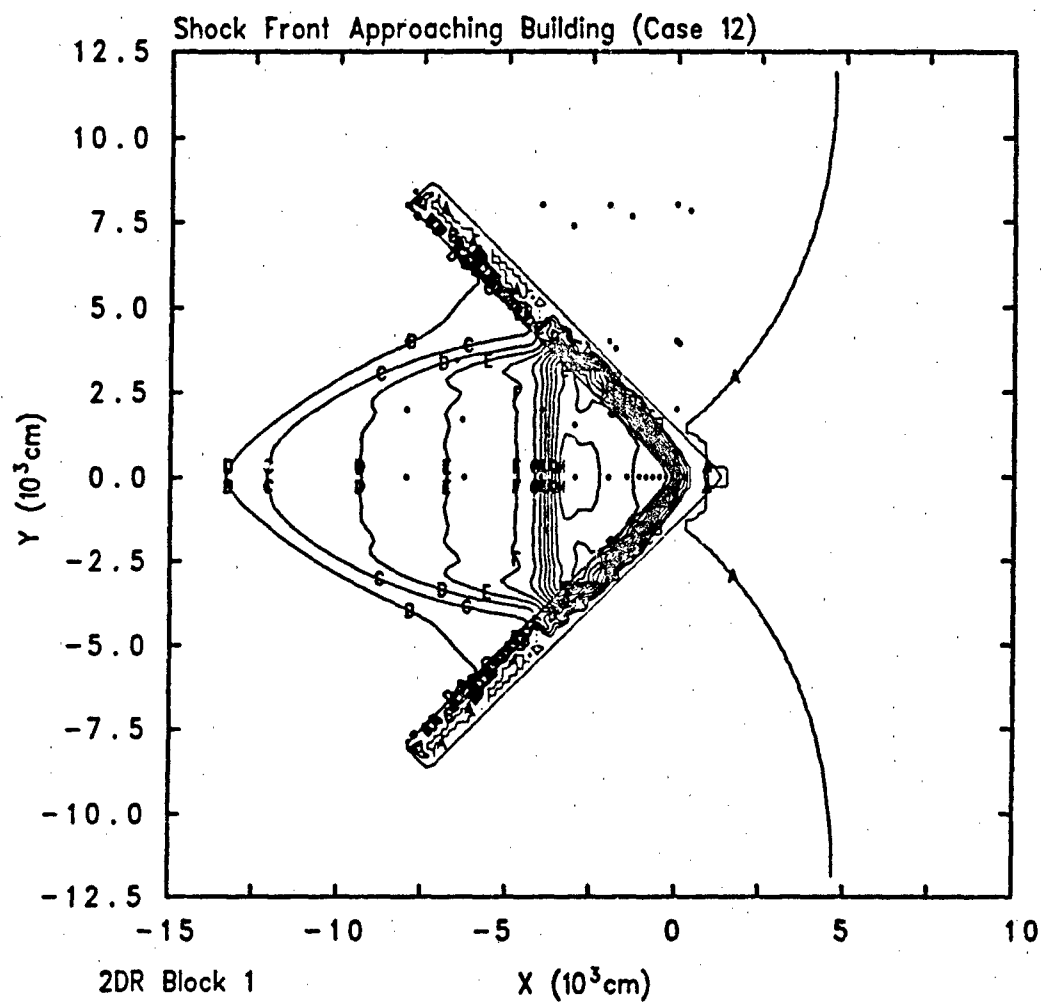
Shock generated by 2 atm in 10000 X 12000 cm (50 X 60 cells)- 2dr
 AGAEQY 1/07/93 03:13:20 CTH 702 Time= 2.00019×10^{-1}



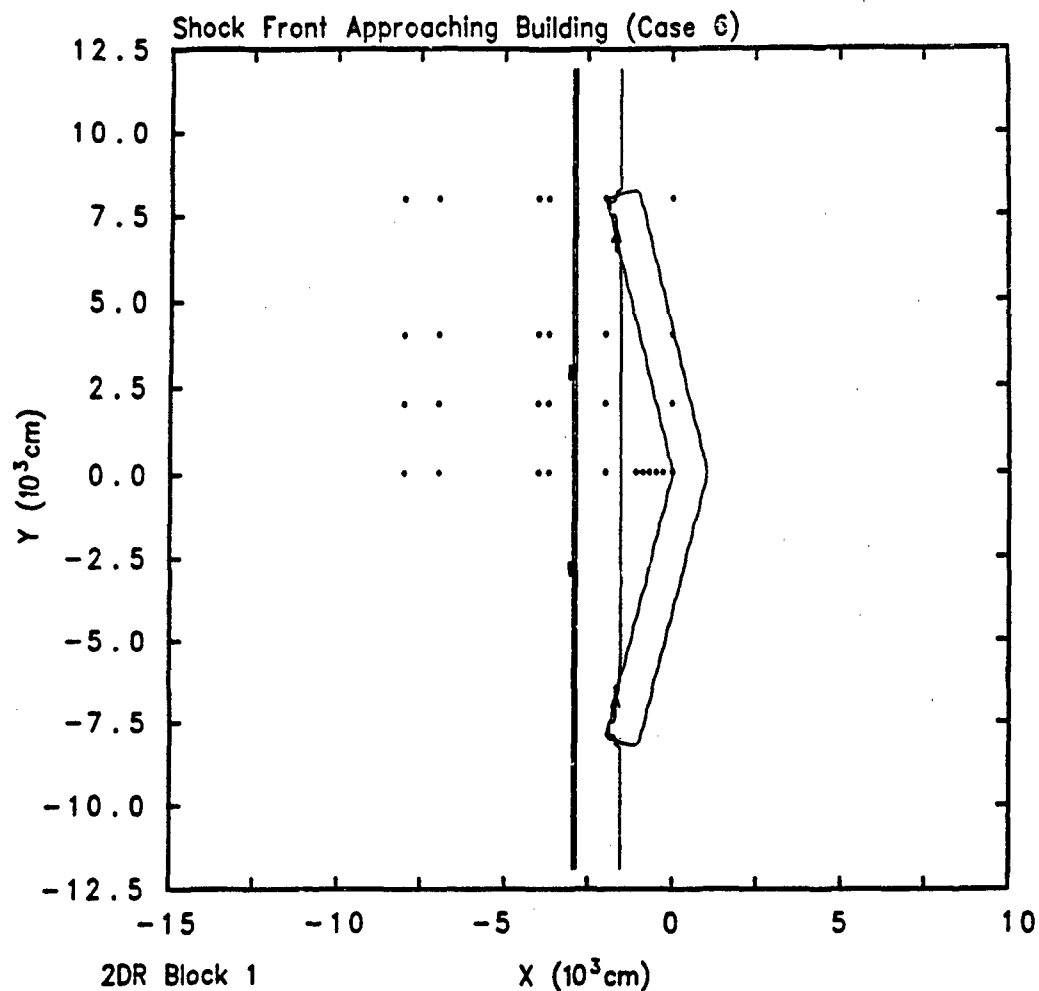
Shock generated by 2 atm in 10000 X 12000 cm (50 X 60 cells)- 2dr
 AGAEQY 1/07/93 03:40:14 CTH 817 Time= 2.25096×10^{-1}



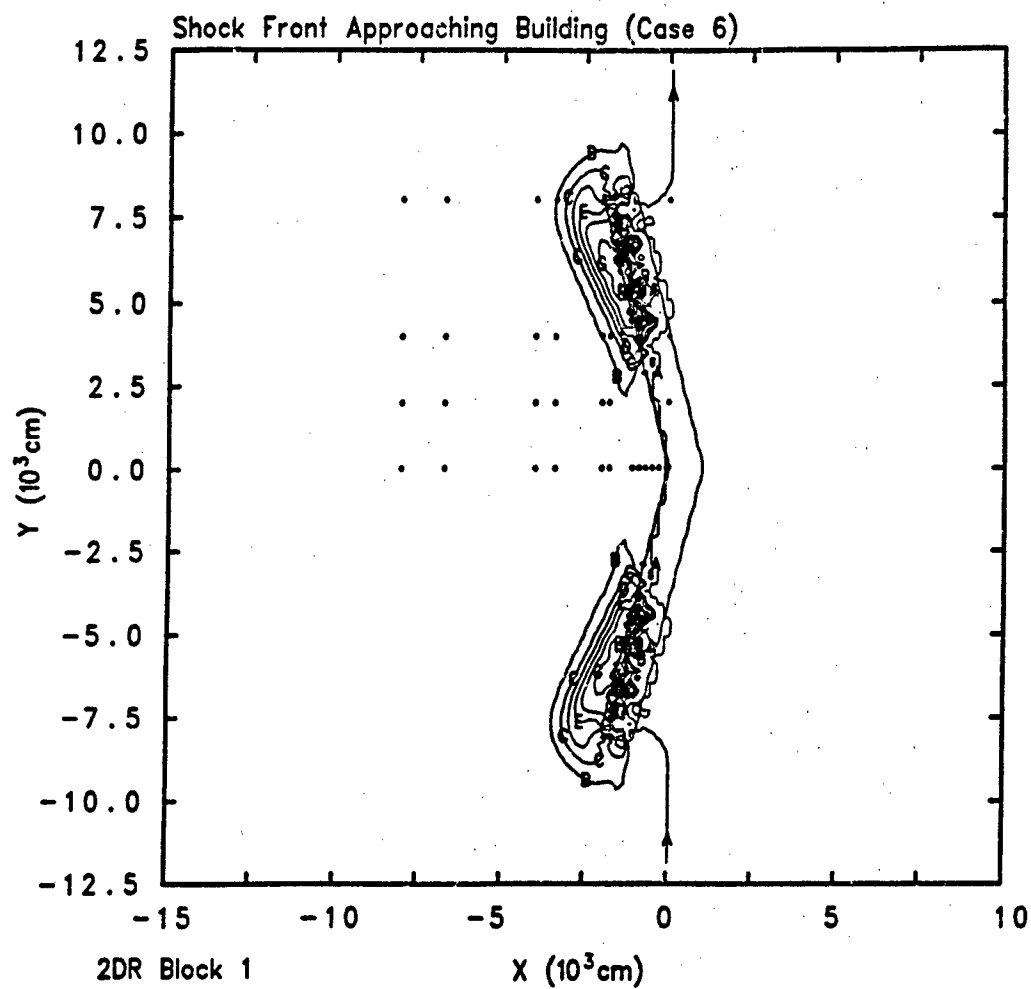
Shock generated by 2 atm in 10000 X 12000 cm (50 X 60 cells)- 2dr
 AGAEQY 1/07/93 04:07:20 CTH 932 Time= 2.50174×10^{-1}



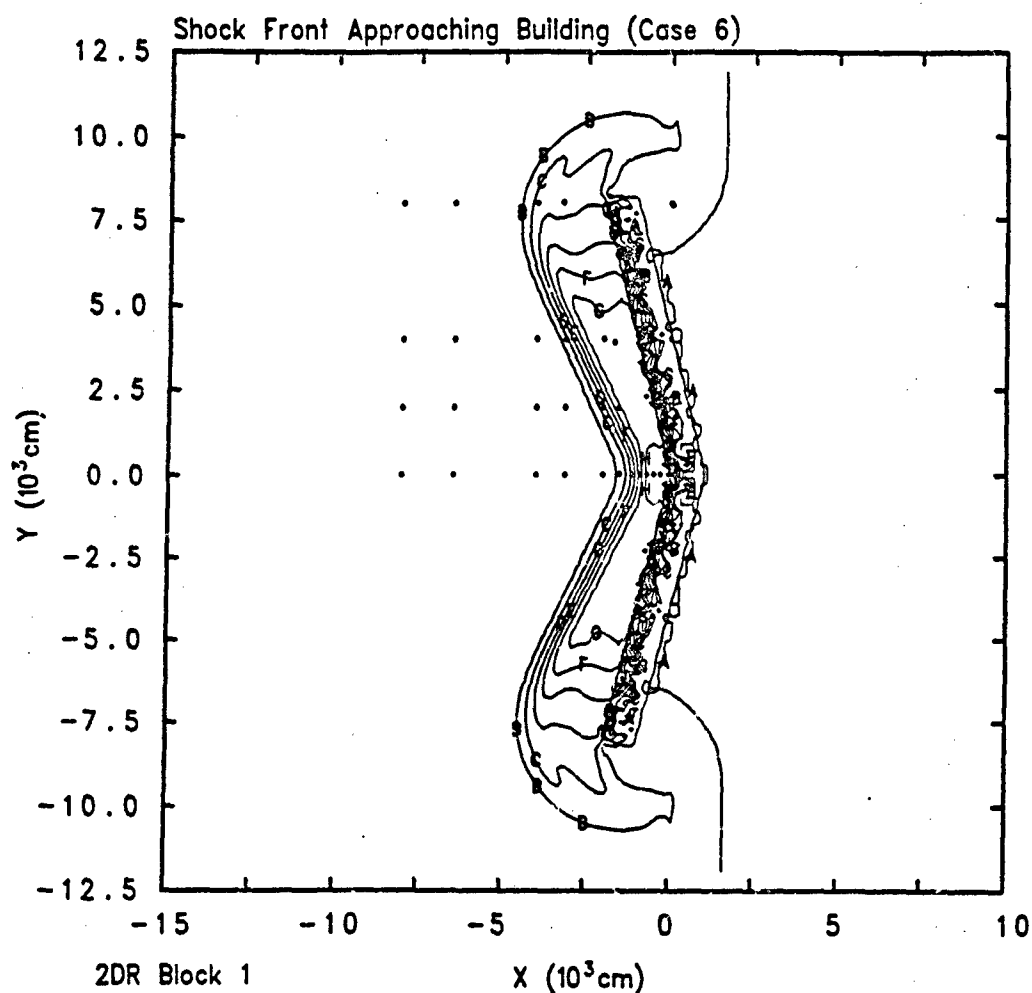
2DR Block 1 X (10^3 cm)
 Shock generated by 2 atm in 10000 X 12000 cm (50 X 60 cells)- 2dr
 AGAEQY 1/07/93 04:34:57 CTH 1046 Time= 2.75033×10^{-1}



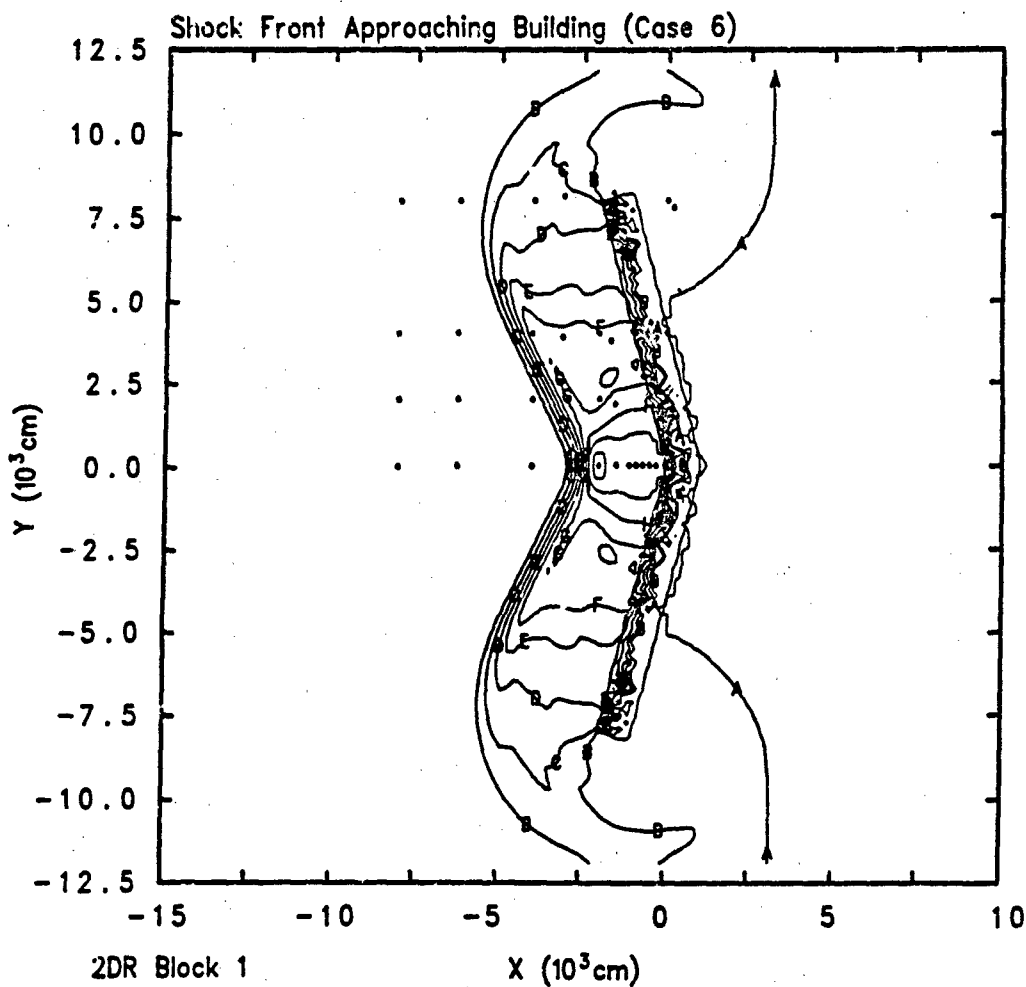
2DR Block 1 X (10^3 cm)
 Shock generated by 2 atm in 10000 X 12000 cm (50 X 60 cells)- 2dr
 LOMBPW 12/15/92 13:03:58 CTH 231 Time= 1.75206×10^{-1}



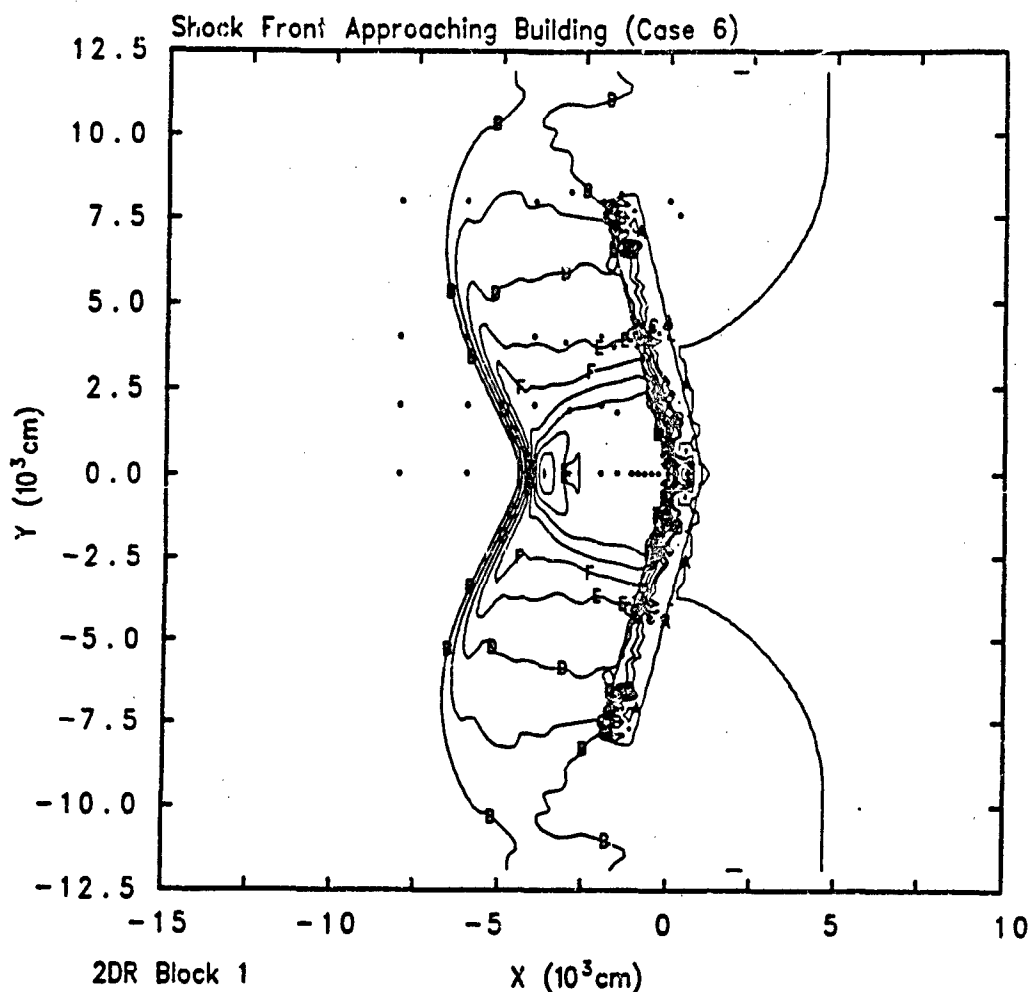
2DR Block 1
 Shock generated by 2 atm in 10000 X 12000 cm (50 X 60 cells)- 2dr
 LOMBPW 12/15/92 13:27:48 CTH 342 Time= 2.0007×10^{-1}



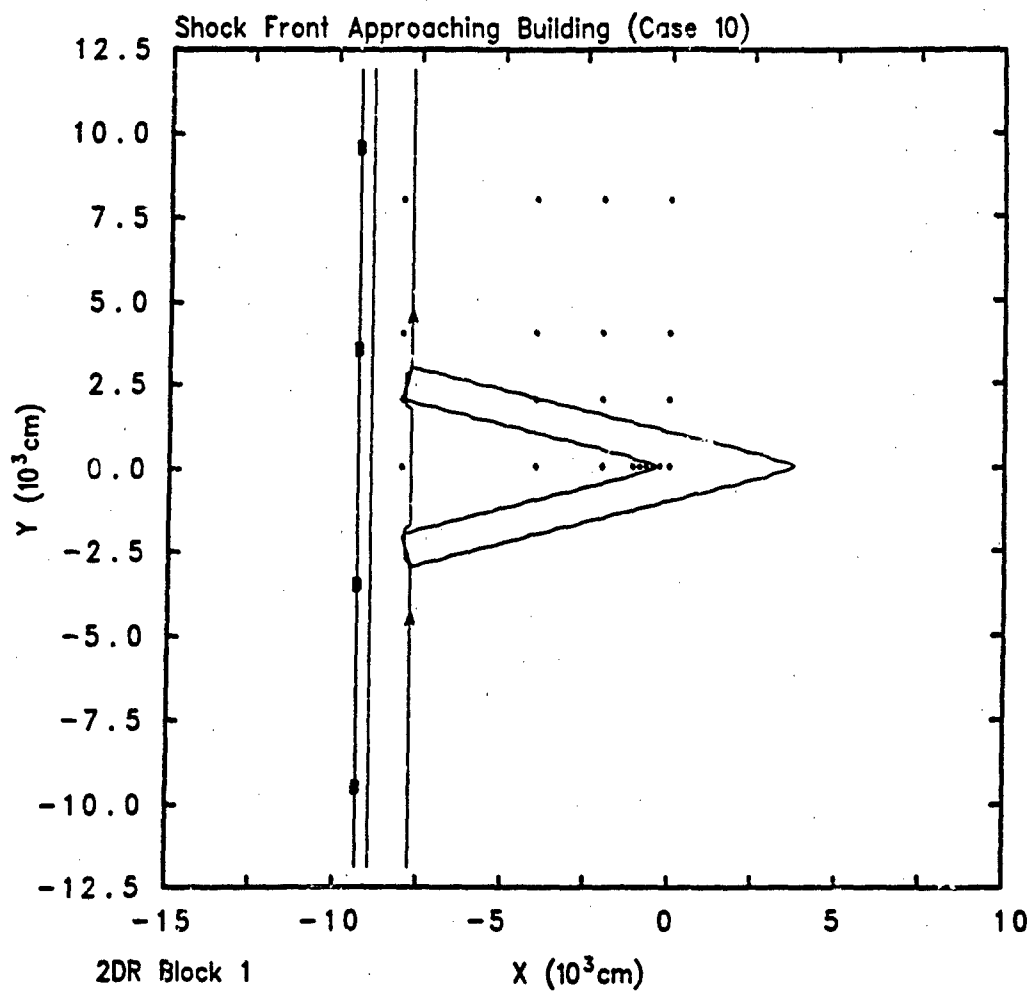
2DR Block 1
 Shock generated by 2 atm in 10000 X 12000 cm (50 X 60 cells)- 2dr
 LOMBPW 12/15/92 13:53:18 CTH 457 Time=2.25148x10⁻¹



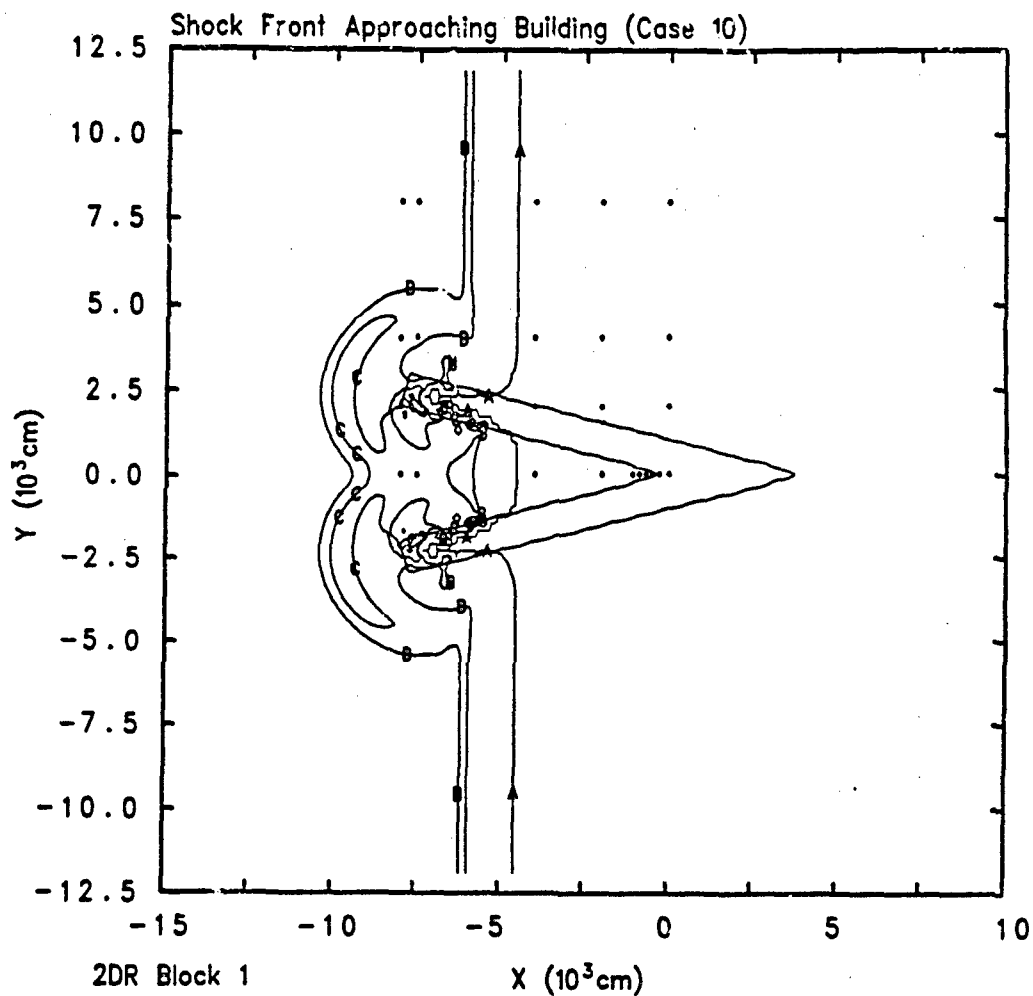
2DR Block 1
 Shock generated by 2 atm in 10000 X 12000 cm (50 X 60 cells)- 2dr
 LOMBPW 12/15/92 14:19:23 CTH 571 Time=2.50008x10⁻¹



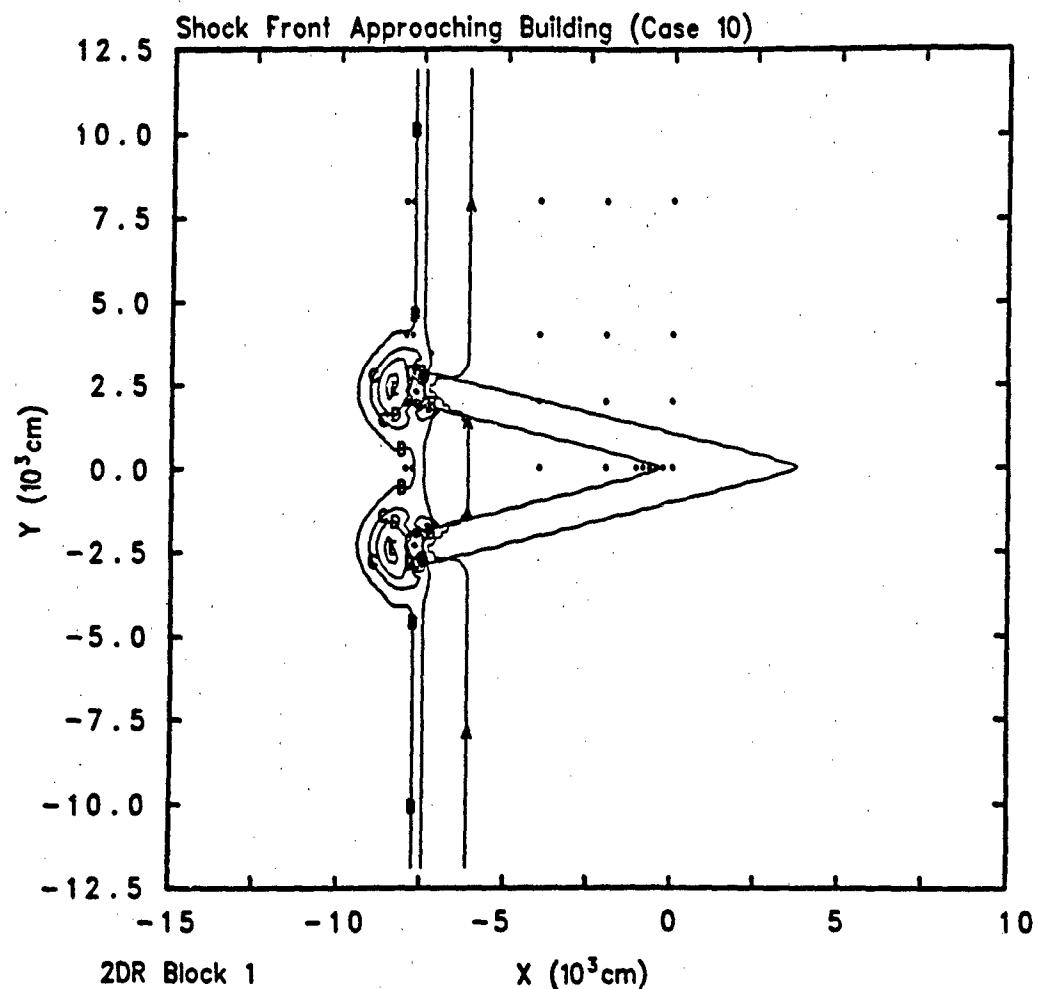
Shock generated by 2 atm in 10000 X 12000 cm (50 X 60 cells)- 2dr
 LOMBPW 12/15/92 14:46:26 CTH 686 Time=2.75086x10⁻¹



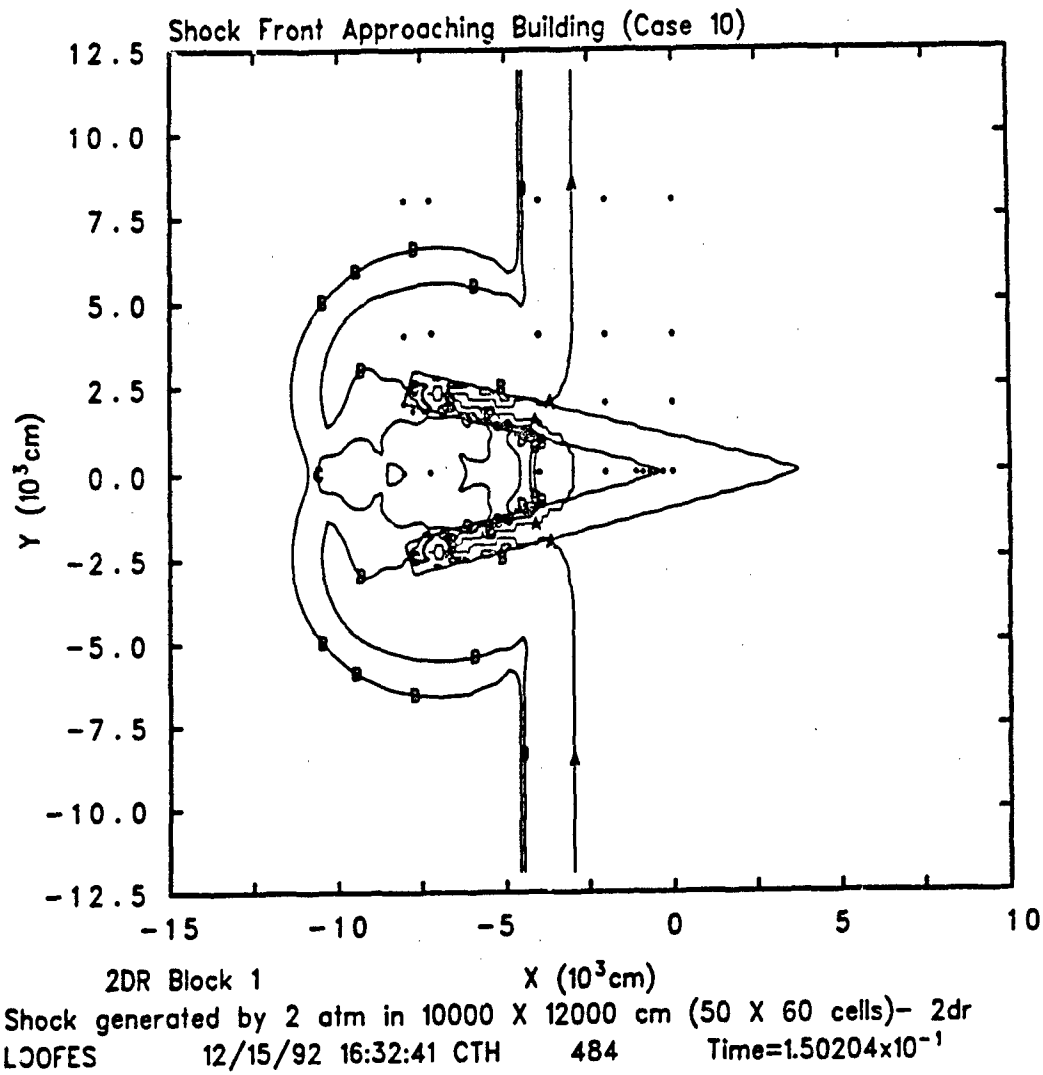
2DR Block 1
 Shock generated by 2 atm in 10000 X 12000 cm (50 X 60 cells)- 2dr
 LOOFES 12/15/92 15:25:03 CTH 145 Time=7.5039x10⁻²

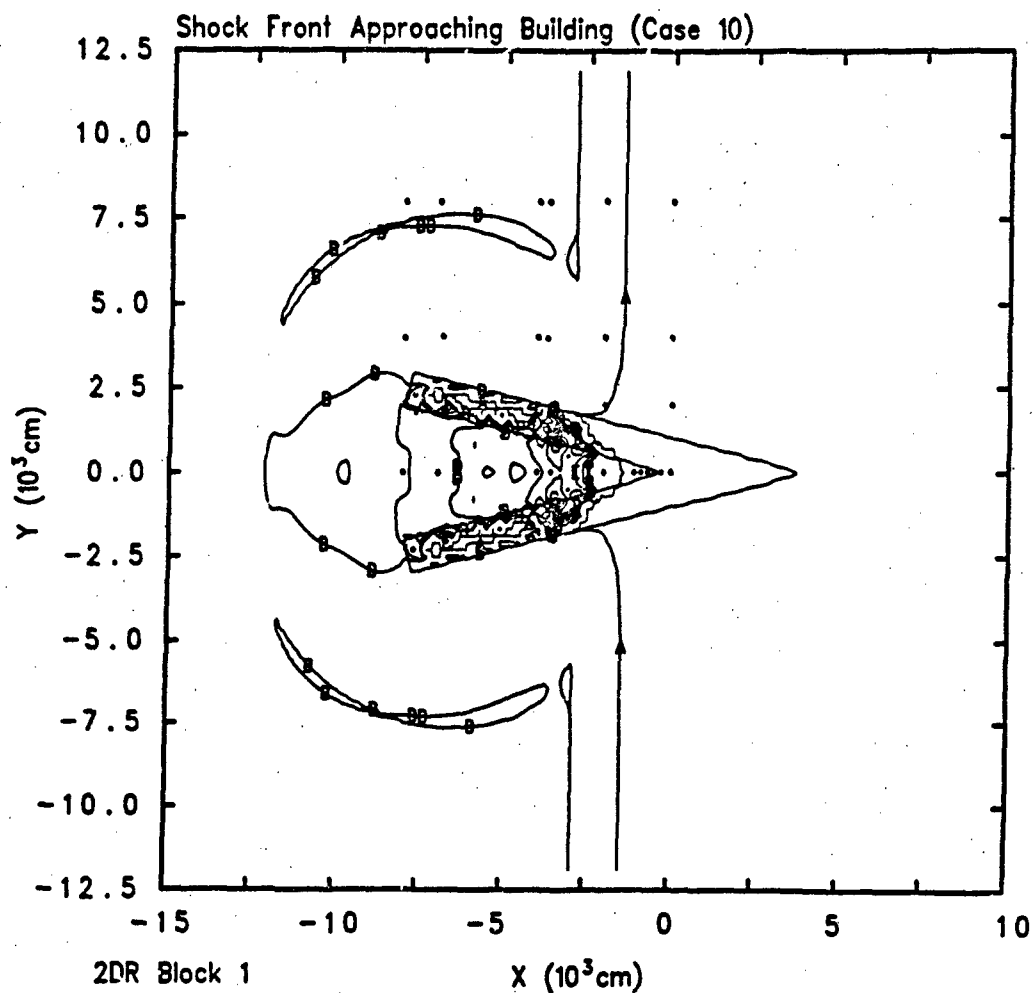


2DR Block 1
 Shock generated by 2 atm in 10000 X 12000 cm (50 X 60 cells)- 2dr
 LOOFES 12/15/92 16:09:04 CTH 370 Time=1.25122x10⁻¹

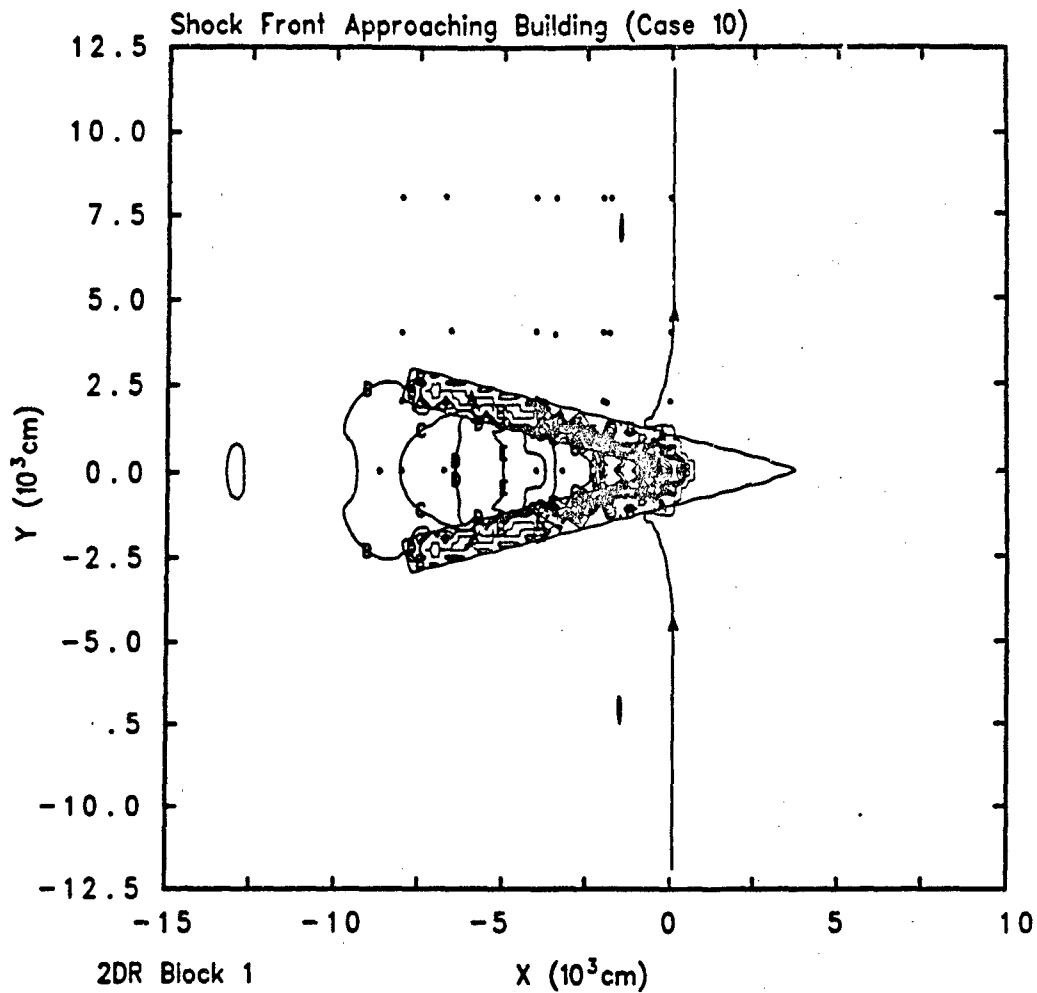


Shock generated by 2 atm in 10000 X 12000 cm (50 X 60 cells)- 2dr
 LOOFES 12/15/92 15:46:24 CTH 256 Time=1.0021x10⁻¹

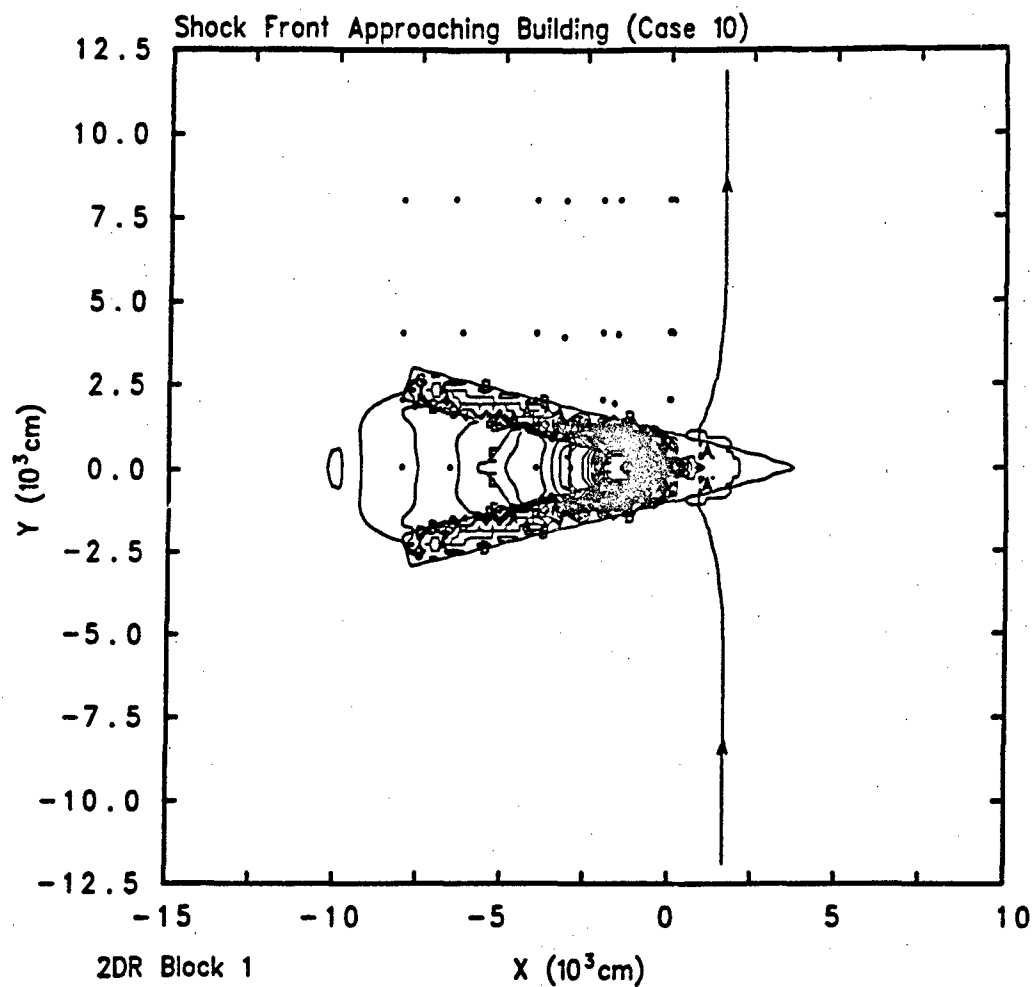




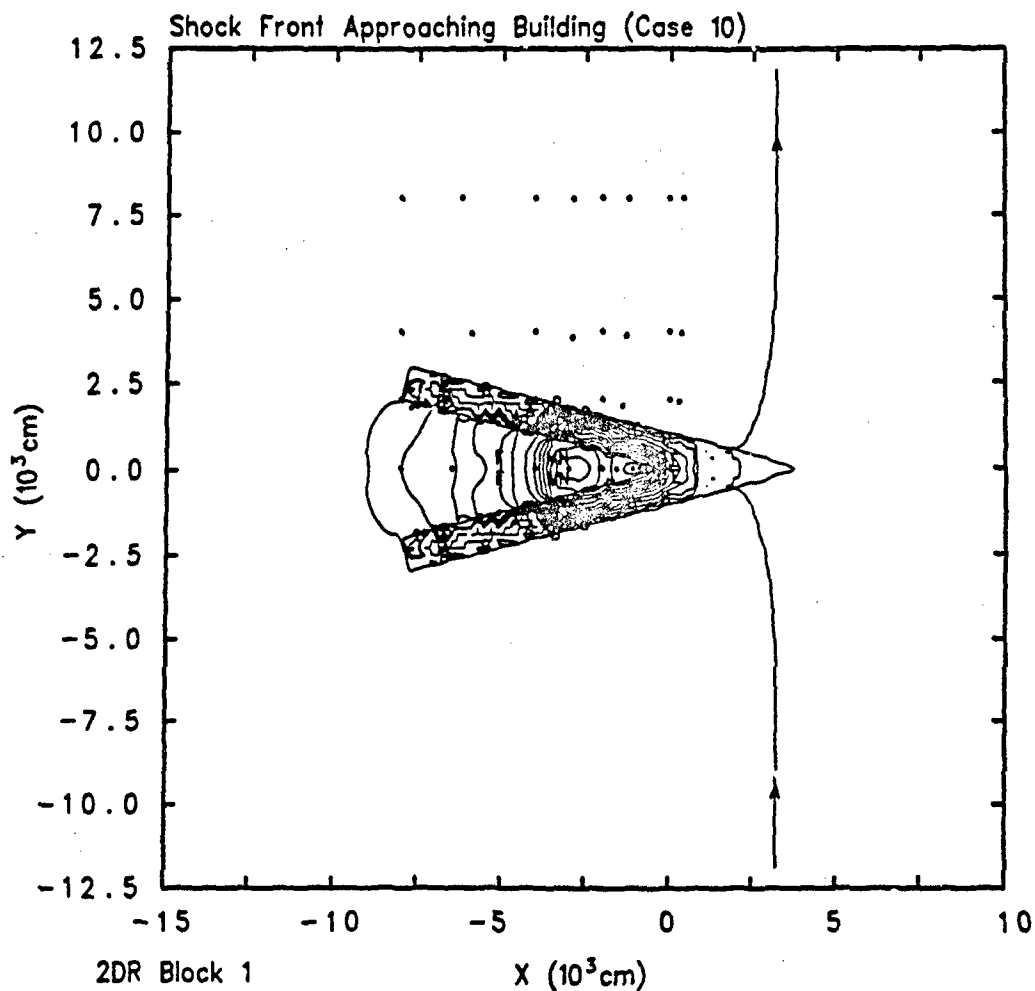
Shock generated by 2 atm in 10000 X 12000 cm (50 X 60 cells)- 2dr
 LOOFES 12/15/92 16:57:07 CTH 598 Time= 1.75188×10^{-1}



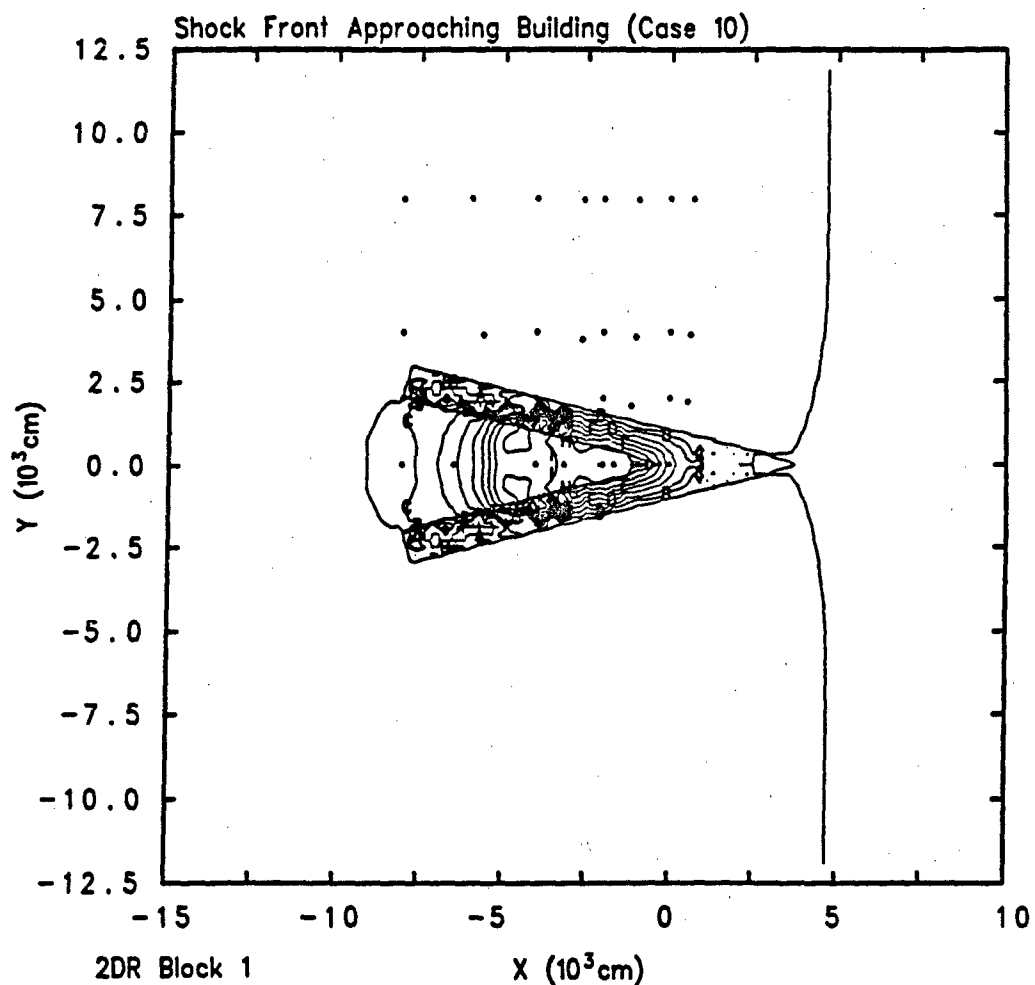
Shock generated by 2 atm in 10000 X 12000 cm (50 X 60 cells)- 2dr
 LOOFES 12/15/92 17:22:26 CTH 712 Time=2.00048x10⁻¹



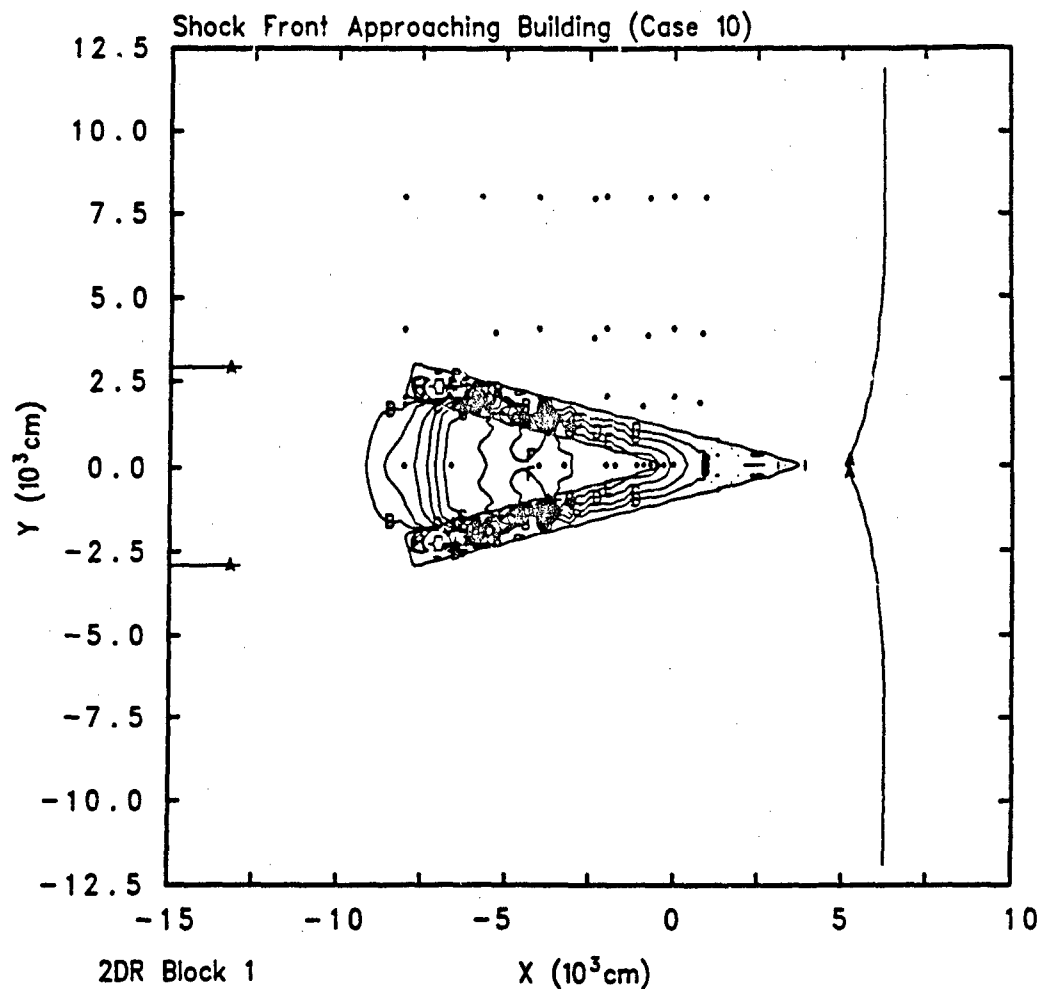
Shock generated by 2 atm in 10000 X 12000 cm (50 X 60 cells)- 2dr
 LOOFES 12/15/92 17:48:49 CTH 827 Time=2.25126x10⁻¹



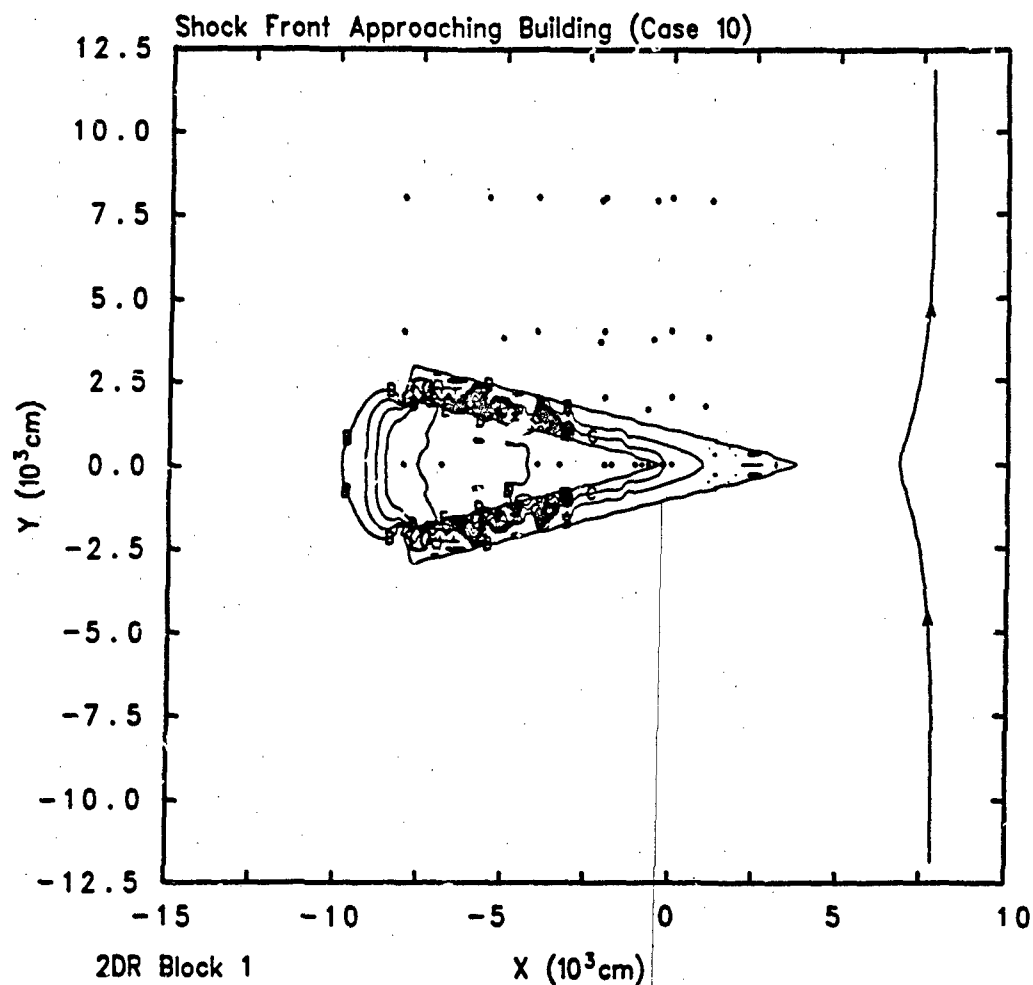
Shock generated by 2 atm in 10000 X 12000 cm (50 X 60 cells)- 2dr
 LOOFES 12/15/92 18:15:59 CTH 942 Time=2.50203x10⁻¹



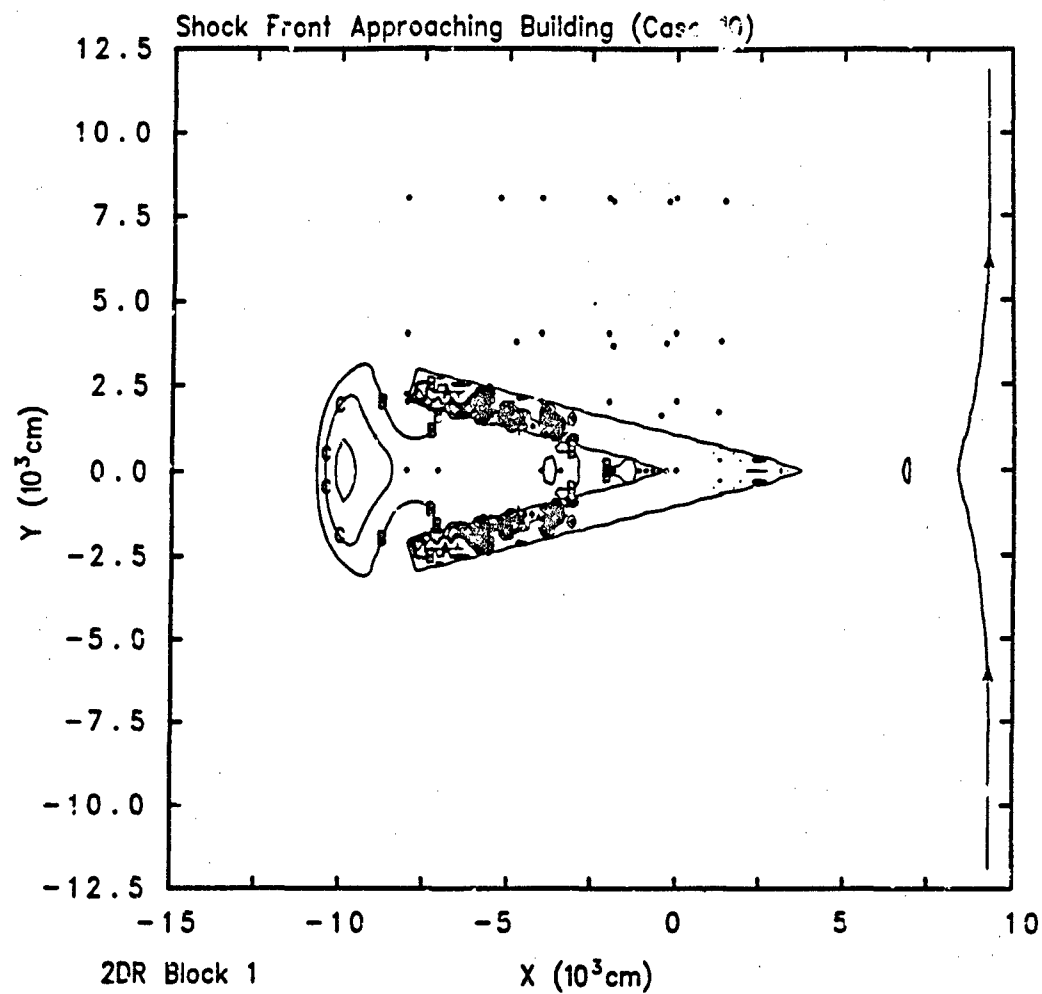
Shock generated by 2 atm in 10000 X 12000 cm (50 X 60 cells)- 2dr
LOOFES 12/15/92 18:43:35 CTH 1056 Time= 2.75062×10^{-1}



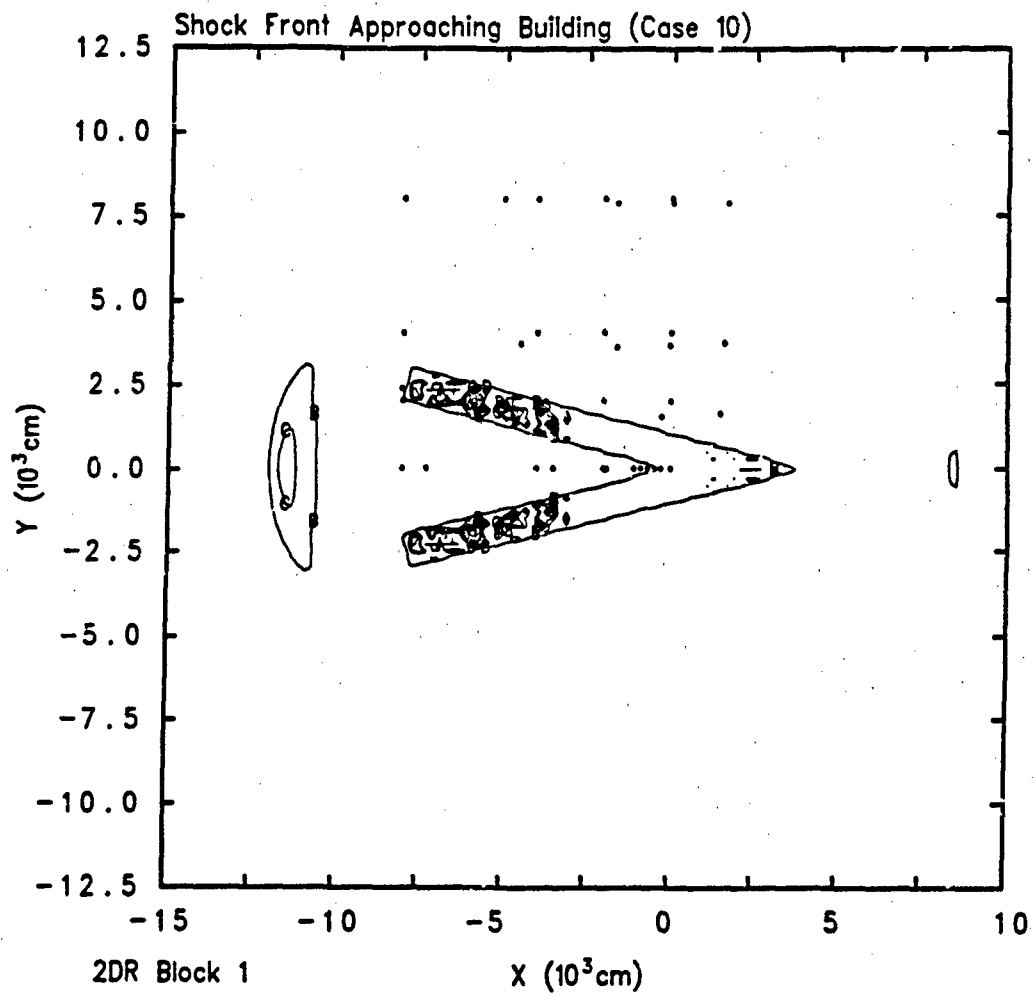
Shock generated by 2 atm in 10000 X 12000 cm (50 X 60 cells)- 2dr
 LOOFES 12/15/92 19:12:11 CTH 1171 Time= 3.00139×10^{-1}



Shock generated by 2 atm in 10000 X 12000 cm (50 X 60 cells)- 2dr
 LOOFES 12/15/92 19:41:57 CTH 1286 Time=3.25217x10⁻¹



Shock generated by 2 atm in 10000 X 12000 cm (50 X 60 cells)- 2dr
 LOOFES 12/15/92 20:11:44 CTH 1400 Time=3.50076x10⁻¹



Shock generated by 2 atm in 10000 X 12000 cm (50 X 60 cells)- 2dr
 LOOFES 12/15/92 20:42:14 CTH 1515 Time= 3.75153×10^{-1}

Vita

Captain John E. Loftis was born on 18 December 1958 at Donaldson AFB, South Carolina. He graduated from Chapman High School in Inman, South Carolina in 1976. He enlisted in the United States Air Force on 5 March 1978, and served his first tour at Myrtle Beach AFB, South Carolina. There he married Mary J. Love of Durban, South Africa on 19 April 1980. He earned his Bachelor of Science degree in Nuclear Engineering, with honors, from the University of Florida in June 1986, through the Airman's Education and Commissioning Program, managed at The Air Force Institute of Technology. After receiving his commission at Officer Training School in August 1986, Captain Loftis served his first officer tour at the Air Force Technical Applications Center, Nuclear Technology Directorate, at Patrick AFB, Florida. There he served one year as a Systems Project Officer, responsible for the directorate's program budget, and four years as a Nuclear Debris Analyst and Alert Officer. He entered the School of Engineering, Air Force Institute of Technology in August 1991. He is a member of the American Nuclear Society, the Order of the Engineer, and the Alpha Nu Sigma honor society.

Permanent address: 1687 Hudson Circle North
Melbourne, Florida 32935

REPORT DOCUMENTATION PAGE			Form Approved OMB No 0704-0188	
<small>Public reporting burden for this collection of information is estimated to average 1 hour per response, including the time for reviewing instructions, searching existing data sources, gathering and maintaining the data needed, and completing and reviewing the collection of information. Send comments regarding this burden estimate or any other aspect of this collection of information, including suggestions for reducing this burden, to Washington Headquarters Services, Directorate for Information Operations and Reports, 1215 Jefferson Davis Highway, Suite 1204, Arlington, VA 22202-4302, and to the Office of Management and Budget, Paperwork Reduction Project (0704-0188), Washington, DC 20503.</small>				
1. AGENCY USE ONLY (Leave blank)	2. REPORT DATE March 1993	3. REPORT TYPE AND DATES COVERED Master's Thesis		
4. TITLE AND SUBTITLE Amplification of Shock Overpressure by Reflection Within Concave Corners		5. FUNDING NUMBERS		
6. AUTHOR(S) John E. Loftis, Capt, USAF				
7. PERFORMING ORGANIZATION NAME(S) AND ADDRESS(ES) Air Force Institute of Technology, WPAFB OH 45433-6583		8. PERFORMING ORGANIZATION REPORT NUMBER AFIT/GNE/ENP/93M-4		
9. SPONSORING/MONITORING AGENCY NAME(S) AND ADDRESS(ES) Lt Col Mark Byers DNA/SPWE 6801 Telegraph Road Alexandria, VA 22310-3398		10. SPONSORING/MONITORING AGENCY REPORT NUMBER		
11. SUPPLEMENTARY NOTES				
12a. DISTRIBUTION/AVAILABILITY STATEMENT Approved for public release; distribution unlimited		12b. DISTRIBUTION CODE		
13. ABSTRACT (Maximum 200 words) In this study, CTH, a production hydrodynamics code developed and provided by Sandia National Laboratories, modeled the interaction of a shock wave with tall V-shaped buildings with various wall lengths and vertex angles. The purpose of this study was to determine the degree to which the length and vertex angle affect the peak overpressure at the vertex. CTH performed two-dimensional Eulerian-Lagrangian computations to obtain solutions of this problem. The models were cast in two-dimensional rectangular geometry on a horizontal plane because of the computational costs of three-dimensional calculations. This geometry simulates tall buildings exposed to a tall Mach stem blast. The free-field shock increased sharply to a peak overpressure of 6.2 psi and returned to ambient conditions after about one second. This incident shock amplified significantly in the building vertices. Peak overpressures measured as high as 8.7 times the incident free-field overpressure of 6.2 psi, or 3.9 times the peak reflected overpressure of 14 psi due to reflection at normal incidence. The amplification was greatest with narrow vertex angles, but was significant (2.7 times that at normal incidence) even with right-angle vertices. The amplification of the peak overpressure due to reflection within concave corners is important in determining the vulnerability of structures to blast damage.				
14. SUBJECT TERMS Blast, Blast Amplification, Blast Damage, Blast Reflection, Shock Amplification, and Shock Reflection		15. NUMBER OF PAGES 203		
		16. PRICE CODE		
17. SECURITY CLASSIFICATION OF REPORT Unclassified	18. SECURITY CLASSIFICATION OF THIS PAGE Unclassified	19. SECURITY CLASSIFICATION OF ABSTRACT Unclassified	20. LIMITATION OF ABSTRACT UL	

END

FILMED

DATE:

4-93

DTIC